eman ta zabal zazu

Universidad del País Vasco
Euskal Herriko Unibertsitatea

Identification of molecular mechanisms underlying frailty and successful aging in centenarians

Ander Saenz Antoñanzas

PhD thesis 2023

This thesis has been carried out at the Biodonostia Health Research Institute under the supervision of Dr. Ander Matheu. During this work, I was supported by a predoctoral fellowship from the “Instituto de Salud Carlos III” (FI17/00250) and also by an European Molecular Biology Organization (EMBO) Scientific Exchange Grant (STF_9197) to conduct an international stay and my research in the Neural Stem Cell Biology laboratory headed by Dr. François Guillemot (The Francis Crick Institute, London - United Kingdom).

biodonostia
health research institute

eman ta zabal zazu
Universidad del País Vasco
Euskal Herriko Unibertsitatea

Identification of molecular mechanisms underlying frailty and successful aging in centenarians

Ander Saenz Antoñanzas

SUPERVISOR

Ander Matheu Fernández

PhD thesis 2023

TESI ZUZENDARIAREN BAIMENA TESIA AURKEZTEKO	AUTORIZACIÓN DEL/LA DIRECTORA/A DE TESIS PARA SU PRESENTACIÓN

Zuzendariaren izen-abizenak /Nombre y apellidos del/la director/a: Ander Matheu Fernández

IFZ /NIF: 44144685A

Tesiaren izenburua / Título de la tesis: Identification of molecular mechanisms underlying frailty and successful aging in centenarians.

Doktorego programa / Programa de doctorado: Biología Molecular y Biomedicina

Doktoregaiaren izen-abizenak / Nombre y apellidos del/la doctorando/a: Ander Saenz Antoñanzas

Unibertsitateak horretarako jartzen duen tresnak emandako ANTZEKOTASUN TXOSTENA ikusita, baimena ematen dut goian aipatzen den tesia aurkez dadin, horretarako baldintza guztiak betetzen baititu.	Visto el INFORME DE SIMILITUD obtenido de la herramienta que a tal efecto pone a disposición la universidad, autorizo la presentación de la tesis doctoral arriba indicada, dado que reúne las condiciones necesarias para su defensa.

Tokia eta data / Lugar y fecha: San Sebastián, 17 de enero de 2023

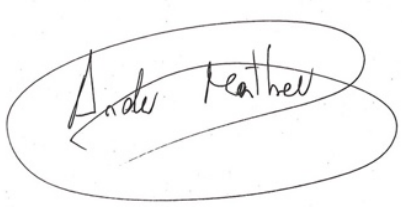

Sin. / Fdo.: Tesiaren zuzendaria / El/La director/a de la tesis

AUTORIZACION DEL TUTOR DE TESIS

PARA SU PRESENTACION

Dr. Arkaitz Carracedo Perez

como Tutor de la Tesis Doctoral: Identification of molecular mechanisms underlying frailty and successful aging in centenarians, realizada en el Programa de Doctorado Biología Molecular y Biomedicina por el Doctorando Don. Ander Saenz Antoñanzas, y dirigida por el Dr. Ander Matheu Fernández, autorizo la presentación de la citada Tesis Doctoral, dado que reúne las condiciones necesarias para su defensa.

En Bilbao, a 16 de enero de 2023

EL/LA TUTOR/A DE LA TESIS

Arkaitz Carracedo

Firmado digitalmente por Arkaitz Carracedo
Nombre de reconocimiento (DN): postalCode=48160, o=Centro de Investigación Cooperativa en Biociencias, street=Parque Tecnológico de Bizkaia edificio 801-A, st=Bizkaia, l=Derio, c=ES, cn=Arkaitz Carracedo, email=acarracedo@cicbiogune.es
Fecha: 2023.01.16 08:20:28 +01'00'

Fdo.: Arkaitz Carracedo Perez

AUTORIZACIÓN DE LA COMISIÓN ACADÉMICA DEL PROGRAMA DE DOCTORADO

La Comisión Académica del Programa de Doctorado en Biología Molecular y Biomedicina, en reunión celebrada el día 19 de enero de 2023, ha acordado dar la conformidad a la presentación de la Tesis Doctoral titulada "**Identification of molecular mechanisms underlying frailty and successful aging in centenarians**", dirigida por el Dr. Ander Matheu Fernández y presentada por Don Ander Saenz Antoñanzas adscrito al Departamento Bioquímica y Biología Molecular

En Leioa, a 19 de enero de 2023

LA RESPONSABLE DEL PROGRAMA DE DOCTORADO

LIDIA RUTH MONTES BURGOS - 45626346G

Firmado digitalmente por LIDIA RUTH MONTES BURGOS - 45626346G
Fecha: 2023.01.19 15:43:25 +01'00'

Fdo.: Lidia Ruth Montes Burgos

AUTORIZACIÓN DEL DEPARTAMENTO

El Consejo del Departamento de Bioquímica y Biología Molecular en reunión celebrada el día 19 de enero de 2023 ha acordado dar la conformidad a la admisión a trámite de presentación de la Tesis Doctoral titulada: Identification of molecular mechanisms underlying frailty and successful aging in centenarians, dirigida por el Dr. Ander Matheu Fernández y presentada por Don. Ander Saenz Antoñanzas ante este Departamento.

En Leioa a 24 de enero de 2023

VºBº DIRECTOR/A DEL DEPARTAMENTO

MIREN JOSU OMAETXEBARRIA IBARRA - 30646158S

Firmado digitalmente por MIREN JOSU OMAETXEBARRIA IBARRA - 30646158S
Nombre de reconocimiento (DN): c=ES, o=UPV - EHU, ou=Ziurtagiri Profesionala - Certificado Profesional, 2.5.4.97=VATES-Q4818001B, cn=MIREN JOSU OMAETXEBARRIA IBARRA - 30646158S, givenName=MIREN JOSU, sn=OMAETXEBARRIA IBARRA, serialNumber=30646158S
Fecha: 2023.01.24 17:43:01 +01'00'

Fdo.: Miren Josu Omaetxebarria Ibarra

SECRETARIO/A DEL DEPARTAMENTO

Izortze Santin Gomez

Firmado digitalmente por Izortze Santin Gomez
Fecha: 2023.01.24 18:09:05 +01'00'

Fdo.: Izortze Santin Gomez

ACTA DE GRADO DE DOCTOR O DOCTORA
ACTA DE DEFENSA DE TESIS DOCTORAL

DOCTORANDO/A DON/DÑA. _____

TITULO DE LA TESIS: _____

_____

_____

El Tribunal designado por la Comisión de Postgrado de la UPV/EHU para calificar la Tesis Doctoral arriba indicada y reunido en el día de la fecha, una vez efectuada la defensa por el/la doctorando/a y contestadas las objeciones y/o sugerencias que se le han formulado, ha otorgado por_____la calificación de:

unanimidad ó mayoría

SOBRESALIENTE / NOTABLE / APROBADO / NO APTO

Idioma/s de defensa (en caso de más de un idioma, especificar porcentaje defendido en cada idioma):

Castellano _____

Euskera _____

Otros Idiomas (especificar cuál/cuales y porcentaje) _____

En _____a _____de _____de _____

EL/LA PRESIDENTE/A, EL/LA SECRETARIO/A,

Fdo.: Fdo.:

Dr/a: _____ Dr/a: _____

VOCAL 1º, VOCAL 2º, VOCAL 3º,

Fdo.: Fdo.: Fdo.:

Dr/a: _____Dr/a:_____Dr/a:_____

EL/LA DOCTORANDO/A,

Fdo.: _____

A mis padres,

Acknowledgments / Agradecimientos

Cuando hecho la vista atrás, no puedo creer que ya esté terminando una etapa tan importante de mi vida. Una etapa donde he aprendido mucho a nivel profesional, pero también a nivel personal. Sin duda, me llevo muchas cosas positivas para aplicar en mi vida y también muchos amigos. Durante la tesis, hay momentos malos, con estrés, con prisas, con todo lo que uno se pueda imaginar, pero también hay momentos buenos, de risas y de disfrute que hace que todo ese proceso merezca la pena. En parte, esto es gracias a muchas de las personas a las que tengo que agradecer, ya que, de una forma u otra, han hecho que la tesis haya sido una buena experiencia. Solo espero no dejarme a nadie, porque como he dicho, han sido muchos años y ¡mucha gente!

En primer lugar, quiero agradecer a mi director de tesis Ander, por darme la oportunidad de entrar en tu grupo y realizar la tesis doctoral. Desde el primer día me acogiste en tu laboratorio donde empecé haciendo prácticas de verano hasta terminar una tesis. Siempre has confiado mucho en mí y espero haber estado a la altura de tus expectativas. A nivel profesional me has enseñado las claves de la ciencia, como gestionar tareas o resolver problemas. No todo ha quedado ahí, las innumerables comidas de grupo, celebraciones, despedidas, bienvenidas y cualquier excusa para celebrar, nunca las olvidaré. Por eso, gracias por acogerme, enseñarme y guiarme, en el que espero que sea el principio de un camino largo. También quiero agradecer a mi tutor de tesis Arkaitz, por haberme ayudado en las distintas etapas, sobre todo con el papeleo. Nos conocimos en un congreso nada más empezar y desde entonces hemos mantenido buena relación.

Sin duda, tengo que agradecer a todos los miembros del grupo de Oncología Celular, a los que estuvieron y a los que están, por ayudarme mil y una veces y por aguantar mi energía diaria en el lab. Espero que al menos os haya contagiado esa alegría a la hora de hacer las cosas para que todo fuese más ameno y trabajarais con buen ritmo, como ese que iba marcando en las mesas, bidones o sillas. Paula Aldaz, fuiste de las primeras personas que conocí y me dejaste la base de un trabajo que luego pude continuar y presentar en muchos congresos. Siempre consultaba tu tesis para aclarar dudas. Idoia, haciendo que todo estuviese organizado y que nuestro tiempo fuese productivo. Laura Garros, pequeño

Caterpie, contigo no coincidí mucho en el lab pero si en muchas celebraciones en las que lo pasamos muy muy bien. Todavía recuerdo ese martillo de Thor que me preparasteis, gracias por acogerme tan bien desde el principio y hacerme sentir uno más. Gracias también a Alejandro, que me enseñó como gestionar las miles de colonias de ratones y a lidiar con los ZSOX9… los que los conocen ¡ya saben de qué hablo! Miren, gracias por invitarnos a tu casa en Berlín, siempre recordaré ese viaje y nunca olvidaré llevarte unos pimientos la próxima vez que nos veamos. Sabrina, merci pour ces moments uniques et pour les conversations en français. María García, pura energía y buenas meriendas con aguacate, contigo eran risas aseguradas. Estefanía, muchas gracias por todos tus consejos y tu forma de hacer las cosas. Aunque alguna vez haya caído alguna bronca, siempre estaré agradecido por el tiempo que nos has dedicado para resolver dudas y que hagamos un buen trabajo. Sin duda, transmites paz y tranquilidad, espero que la gente que siga viniendo pueda aprender de todo lo bueno que tienes. Juncal, me dio mucha pena cuando dejaste el labo, eras parte del team farra, pero al menos conseguí darte un abrazo de despedida y eso ¡vale mucho! Alex Arrieta, lo poco que coincidimos fue suficiente para aprender lo que era un mocasinero y un serrinero. Leire Moreno, mi ciberami, contigo he vivido muchas cosas… Gracias por acogerme tan bien desde el primer día, por ayudarme siempre que lo he necesitado y por aguantarme en mis días más intensos. Eres la compañera perfecta de cañas y de viajes, de hecho, aún nos queda algún viajecito pendiente. Maddalen, gracias por tu paciencia y por tu trabajo. Sin duda, eres una persona trabajadora, siempre dispuesta a ayudar y que ha estado ahí para todo lo que fuera necesario. Ha sido clave poder contar contigo y compartir momentos fuera del lab. Gracias por esos arroces con leche, natillas y diversos postres caseros, ¡los mejores! Jaio, siempre mano a mano como glio team, brain team o lo que fuera. Contigo he compartido muchos buenos momentos tanto dentro como fuera del lab. Hemos sufrido, reído, rotulado, organizado, recogido, analizado… ¡de todo! Hasta hemos presentado un telediario… No olvidaré tus constantes cánticos (pa fuera lo malo) o expresiones (señores pasajeros, rata max), ¡ni tampoco tus sustos! Son demasiadas las cosas vividas contigo como para resumirlas en unas frases… Gracias por tu ayuda en el lab y por esos momentos de alegría en numerosas celebraciones, siempre entre los supervivientes. Espero que sigamos así y que coincidamos en futuros congresos como aquel de Madrid. María Álvarez Satta, escribo el nombre completo, con acentos y dos apellidos, no vaya a ser que me mandes imprimir de nuevo la tesis… pero para mí, ¡Maruxa! Contigo hemos aprendido muchas palabras nuevas, pero sobre todo hemos ampliado nuestro conocimiento de la cultura gallega. Gracias por tus

conversaciones, tu ayuda, tus consejos y esas empanadas o tartas de Santiago que te quitaban cualquier pena. Espero que nos veamos pronto en la aldea. Dieguiño, gracias por toda la ayuda que me has dado y por la paciencia que tienes, ¡mi compi de batalla! Siempre con ganas de tomar unas cañas después del trabajo y con ese espíritu de fiesta, has alegrado mucho el grupo. También me has pegado ese acento gallego… Solo espero que sigamos como hasta ahora, compartiendo buenos momentos y trabajando duro para sacar adelante todo el trabajo, en eso, somos cabezones. Vero, tu llegada al lab lo revolucionó, por eso tuvimos que mandarte al Onkologikoa… ¡broma! Gracias por tu ayuda con el confocal, la gestión del Crick, por descargar papers que nadie podía, pero sobre todo por tu alegría constante y por esas bromas tan características tuyas. Seguiré poniéndome tu colonia favorita ¡no te preocupes! Nerea, nos conocemos menos, pero desde el primer día tu actitud fue buenísima, siempre dispuesta a echar una mano con lo que fuera. Me has ayudado mucho con las famosas MTs en glio y ojalá salga un buen trabajo de ahí, seguro que lo haces y que acabas encapsulando algún compuesto. Aizpeeee, gracias por estar siempre dispuesta a ayudar, sea con lo que sea, y haciendo bien las cosas. Te deseo lo mejor en esta etapa, seguro que conseguirás buenos resultados y acabarás manejándote con ese ordenador. Joseb, compi de pasillo y también dispuesto a ayudar en temas bioinformáticos. Tu llegada al grupo solucionó muchos problemas y ahora cuantas veces es "Joseba, mírame esto… o lo otro…". Una muy buena persona, sigue así que seguro que te va a ir muy bien. Sara, equipo bioinformático y compi de ciudad, también siempre disponible para cualquier duda o análisis que se le plantee. Gracias por tu ayuda, sigue así porque te necesitaremos para futuros análisis. Olatz, las más nueva, pero con ganas e ilusión, seguro que tienes mucho que aportar a este grupo. Quiero agradecer también a todas las personas que han estado de prácticas en el grupo, han sido muchas, y de cada una de ellas también he podido aprender y llevarme buenos momentos. Manolo, nuestro patólogo por excelencia. Uno más del grupo, con mucha capacidad e ilusión por la investigación. Gracias por tu ayuda con las tinciones, con el microscopio, por tus consejos y ese aire del sur que te caracteriza. Ahora no me puedo imaginar una comida o celebración sin ti. Mikel, fuiste la primera persona que me acogió ese primer día de prácticas en Biodonostia y desde entonces me has acompañado hasta el final de esta etapa. No tengo palabras para describir todo lo que hemos vivido juntos, han sido muchísimas cosas y momentos. En el trabajo siempre me has ayudado a todo lo que se ha podido y juntos hemos sacado proyectos adelante. Pero sin duda, me quedo con toda la parte personal. Gracias por tu ayuda, tus consejos, tu paciencia, por esas fiestas, esas cenas, comidas, por acogerme en

tu casa… ¡muchas cosas! Ahora sé un poco más de flores, donde comer un buen bocatón y que es hacer una compraza. Que no se pierda la tradición de hacer viajes alrededor del mundo y que podamos seguir disfrutando de muchos momentos tan buenos como los que ya hemos vivido.

Aparte del grupo, dos personas muy importantes a lo largo de la tesis han sido los neurocirujanos Joaquín y Alex. Gracias a los dos por vuestro tiempo en el animalario y por enseñarnos a hacer una buena estereotaxia. Joaquín, tu alegría y tus bromas siempre me sacaban una sonrisa. Eres una muy buena persona y aquí siempre tendrás un batería para acompañarte con tu música. Alex, gracias por portarte siempre tan bien conmigo, por tus ánimos, por las comidas, los regalos desde Galicia (esos los puedes seguir haciendo), y sobre todo por las ganas y el esfuerzo que has puesto. Ha sido muy fácil trabajar contigo y me dio mucha pena cuando te tuviste que marchar. De todas formas, sé que tengo un buen amigo cerca y a ti también te digo, que me tienes para lo que necesites.

Muchas gracias a todos los compañeros del grupo del Oncología Molecular, Lorea, María Armesto, María Arestin, Erika, Giovanni por vuestra ayuda en las tareas diarias del lab, organización, limpieza y todas las dudas que habéis podido solucionar. Esther, gracias por tus consejos y por tu ayuda años después en Oxford y Cambrige, fuiste una muy buena guía. Carla, gracias por estar ahí siempre que lo he necesitado, por tus explicaciones sobre la digital y por esas maravillosas e intensas conversaciones en el viaje del coche desde primera hora de la mañana… Tu energía me ha ayudado mucho en todo este tiempo y tenerte detrás para distraerse de vez en cuando, siempre viene bien. Bea, June y Maitane, gracias por vuestra alegría, por vuestra predisposición a ayudar y por aguantar los innumerables sustos a lo largo de estos años.

Otra parte fundamental son todos los miembros del grupo de Bioingeniería. Vir, una de las primeras personas que me acogió como uno más. Gracias por todo lo que me has ayudado estos años y sobre todo por los consejos de vida que me has dado. Tú me conoces bien. Aparte, siempre dispuesta a tomarte un buen mojito y a aportar alegría y buen rollo con esas bromas que tanto te caracterizan. También a Araika y Hector, partes fundamentales del grupo. Ainhoa y Paula, la de Bilbo y la de Irún, vaya mezcla… Siempre disgregando tejido con alegría, con vosotras he pasado muy buenos momentos en el lab. Leire Gardeazabal, mi vecina, aplicada y con el cuaderno siempre al día. Laura Yndriago, la chama, siempre

preocupada por los demás y con una sonrisa en la cara. Has sido muy importante para resolver mis dudas de animalario y de microscopio. También Sandra, por las conversaciones tan interesantes en las largas tardes de trabajo y por tu ayuda con las técnicas de imagen. Alba, Inazio y Noelia, las últimas incorporaciones que han dado alegría extra y cotilleos variados para amenizar días de trabajo duro.

No me puedo olvidar del grupo de cáncer de Mama, cuanto os echamos de menos ahora que no estáis en el mismo lab… Gracias María Caffarel por tus consejos científicos y por tu apoyo constante, ¡nunca olvidaré esos Journal Clubs! Angela, antigua vecina de mesa, hemos compartido muchos momentos. Andrea, puro nervio y una muy buena persona, contigo era imposible aburrirse con todas las historias que me contabas sobre paipos, perros… Y también Peio y Joanna, fundamentales en el grupo, con ganas y mucha energía.

Llegamos a uno de los grandes grupos de Biodonostia, ¡Hepato! Sin duda, han sido fundamentales en toda esta etapa. Laura Izquierdo y Paula Olaizola, nos conocimos en la universidad, y desde entonces, los tres hemos llegado hasta el final del doctorado. Ya por fin me tocaba… Gracias por vuestra ayuda a lo largo de todos estos años. Desde que nos conocimos hemos compartido muy buenos momentos, celebraciones, graduaciones, cumples, doctorados… Desde los trabajos de grupo hasta los viajes en autobús de vuelta de Pamplona, meriendas, cenas y un largo etcétera de muy buenos momentos que guardo en mi memoria. Irene, también nos conocimos en la uni y desde entonces hemos pasado momentos muy buenos, desde tener que correr en el colegio mayor, hasta cenas con presentaciones de uno mismo… Ainhoa Lapitz, contigo es imposible no reírse. Eres pura energía y has aportado mucho ambiente al lab. Nos seguiremos viendo por Honyarbi para contarnos nuestra vida, seguir de fiesta y seguro que caerá alguna cerveza. Gracias también a los demás miembros del equipo, Matxus, Pedro, Javi y Nuno (o Bruno… cuantas veces te habré llamado así…), que me han dejado usar los aparatos, reactivos o me han ayudado con dudas. A los antiguos miembros de Hepato, Aitor, Ander y Álvaro, con los que también he compartido muchísimos buenos momentos. Ibone, un pilar importante en mi primera etapa de doctorado. Gracias por transmitirme esa alegría que te caracteriza, aunque a veces había algún bache, siempre sacabas una sonrisa. Me quedo con las cenas improvisadas con cualquier cosa y las tardes de música con la guitarra, seguro que esas clases han dado su fruto y ahora sabes tocar muy bien. Aloña, siempre dispuesta a ayudar y aunque un poco vergonzosa, has podido con mis bromas… ¡Eskerrik asko! Y la revolución del lab… Maider,

Irune y Anne. Con vosotras me he sentido muy a gusto y espero poder seguir compartiendo momentos como los que pasamos en las comidas del tercer piso. Siempre algún cotilleo de por medio para que no haya aburrimiento y si es con chocolate, ¡mejor!

Muchas gracias a las chicas de plataformas, siempre dispuestas a solucionar los problemas, que no han sido pocos a lo largo de estos años. Ana Aiastui, Alba y Claudia, gracias por esas miles de inmunos que habéis hecho, algunas veces en tiempo récord, por hacer que nunca falte nada en cultivos (y si faltaba, también encontrabais solución), y por intentar ayudar siempre en todo lo que os pedía. Sin duda os habéis portado muy bien y habéis estado ahí para cualquier cosa, incluso para desconectar un rato. También a Ana Gorostidi, Nanda y Carmen, buen ambiente asegurado en genómica. Gracias por vuestro buen humor y seguir mis cánticos, os seguiré visitando a menudo.

Y ahora llegamos a Neuro… Otro de los grandes grupos y con mucha gente que ha estado implicada, de una forma u otra, en todo este proceso de la tesis. Siendo sincero, siempre he tenido bastante lío con los grupos que hay en la planta 1, así que solo espero no dejarme a nadie… Sonia, alegría y siempre dispuesta a ayudar, contigo ha sido un placer hablar y poder pedirte consejos. Andrea Valls, Amaia Elicegui, Laura Mosqueira, Pablo, Alberto, Ane Rubio y Haizea, siempre dispuestos a ayudar y solucionar problemas. Gracias también a Ane Velasco por seguirme las bromas, a Oihane por esos mioblastos, a Maddi por los anticuerpos y las charlas sobre astrocitos, a Jon por la ayuda con las imágenes de microscopio y a Martxel por los últimos consejos antes de escribir la tesis. Otra parte importante ha sido Gorka Gereñu, gracias por preguntarme siempre por la tesis, por tu ayuda en aquel proyecto largo y en general por tu apoyo. Puede que quizás algún día generemos algún modelo de mosca… Andrés, Laura, Angela y Joselu, con vosotros he compartido muchos momentos en la hora de la comida. Da igual que fuesen las 4 o las 5 de la tarde, sabía que ahí estaríais para echar unas risas. Araceli y María, las chicas del sur, con vosotras me he llevado bien desde el primer día y siempre que coincidíamos, me salía ese maravilloso acento andaluz. Gracias por vuestro buen rollo. También a los que estuvieron en la planta y ya no están… Arantzazu, Haizpea, Tati, Neia, Haritz, Jaione Lasa, Garazi, Mónica y Miren. Con todos vosotros he compartido buenos momentos y aunque nos separase una planta, siempre había ocasión para charlar un rato y rellenar bidones con agua, pedir algún que otro reactivo o sellar bolsas para Western.

En la misma planta, el grupo de Esclerosis Múltiple, es otro al que también tengo que agradecer. David Otaegui, hemos trabajado en varios proyectos y espero que pronto el trabajo de sus frutos. Gracias por esos análisis bioinformáticos. Ainhoa Alberro, Maider y Andrea Iribarren, con vosotras también he compartido proyecto y aunque no ha sido fácil en algunos momentos, hemos conseguido sacar el trabajo adelante y recopilar todos los datos. Gracias por vuestra implicación y ganas por hacer las cosas bien. Lucía, siempre dispuesta a colaborar con los experimentos y encontrar muestras perdidas. A todas las demás componentes del grupo, Leire Iparaguirre, Hirune, Saioa, Miriam, también os agradezco vuestra ayuda en numerosas ocasiones y por hacer que la entrada a vuestro lab sea siempre buena. Por último, agradezco a Mikel Muñoz, Marina, Uxoa, Amaia López e Ignacio Azcue, por preguntar cómo iba la vida siempre que nos veíamos y ayudarme cuando era posible.

Tampoco me puedo olvidar de Jose, siempre dispuesto a solucionar cualquier problema, a realizar envíos allá donde sea y a traer los paquetes siempre a tiempo. Sin duda los mails de difusión no serían lo mismo sin ti, esa imaginación y forma de decir las cosas es admirable. Gracias por hacer que nunca falte de nada y por contribuir al buen ambiente del centro. Te incluyo aquí Borja, compi de la planta 0, por esos ratos de discusiones o cotilleos en las horas del café.

I would also like to thank to all the people that I met in the Crick during my short stay in London. François, thank you for giving me the opportunity for working in your lab, and for evaluating my thesis. I really had a good time in London. Although at the beginning the brexit and pandemic issue made things difficult, you always made everything easy and I felt like at home. Alice and Piero, thank you for helping me from the first day in the lab. I have learned a lot from both of you and the stay has been much easier with your help. The best, the Italian coffees, the good pasta and the panzerotto. “This, I like a lot”. I won't forget those jam session nights playing drums and guitar, and the evenings with beers after a long day at work. Thomas, with you it will always be "The last day of summer". You were a fundamental pillar in my adaptation in the lab. Thanks for your help, for showing me the good places to party and for being always with a smile on your face. With the three of you, I have made so many plans… movies, concerts, lunches, dinners... and we will always be the party people! Alexis, with you I learned that the best days to do things are Mondays. Yu Xuan and Oana, always ready to help and to teach me Korean food tricks or fashion tips. Berta, the Catalan girl of the group, you gave me a lot of tips about the life in London and the many options there are in

science. And to all the other members of the group, Sara, Michael, Christina... thank you for hosting me so well and making me feel at home.

Seguro que has leído todos los agradecimientos y estás preguntándote a ver en qué momento vas a aparecer y porque no estabas con Hepato… Te he dejado para el final porque llegaste al final de esta etapa y te has convertido en una de las personas más importantes en mi vida. Muchísimas gracias Ena por apoyarme siempre en momentos difíciles y por celebrar en momentos felices, ya sea en el trabajo o fuera de él. Has hecho que mis ganas de seguir crezcan y me has llenado de energía. Hemos vivido muchos buenos momentos juntos que no podría resumir en cuatro líneas… pero que los dos sabemos muy bien y que no vamos a olvidar. Hemos reído, llorado, celebrado, bailado, viajado, compartido… ¡de todo! Desde aquellas primeras cervezas post-trabajo, hasta hoy… donde no me veo sin ti. Gracias por tus ánimos y tu cariño, nos quedan muchas más historias por vivir.

Otro de los pilares fundamentales a lo largo de esta etapa han sido mis amigos, que me han ayudado a superar muchas veces cualquier bache en el camino y me han hecho olvidar los problemas. Tengo suerte de tener una kuadrilla como la que tengo, numerosa y con muy buena gente, amigos de verdad. Gracias a Eli y Niki, por ofrecerme vuestra casa en mis primeros días por Londres. Gracias a Nerea, Leire, Mireia, Melanie, Xabo, Amaia, Imanol, Gorka, Ander, Julia, Iñaki, Uma, Lide, Carlos y Eneko por los innumerables momentos que hemos vivido… viajes, celebraciones, bodas, cumpleaños, comidas, cenas, alegrías, penas, conciertos y un muy muy largo etcétera, que han hecho que toda esta etapa de mi vida fuera fácil y sobre todo bonita. ¡Aupa Mesubes! Tampoco me quiero olvidar de mis compañeros de Cliché, Rubén y Asier, que me han ayudado a desconectar haciendo música y a disfrutar con conciertos a lo largo de todos estos años. Sin duda, la música ha sido mi vía de escape a lo largo de la tesis.

Por último, quiero agradecer a las personas más importantes que son mi familia. A mis abuelos, que estarán orgullosos de que su nieto haya llegado hasta aquí. A mi hermano Xabi, que me ha ayudado siempre que ha podido y ha estado dispuesto a solucionar cualquier problema o avería. Cuantos apaños de coche me has hecho para poder ir a trabajar… Eres una persona muy buena y te mereces lo mejor. Gracias por aguantarme estos años de tesis y lo que te queda… Y a mis padres, Rosa y Andrés, que son los que me han dado todo lo que tengo y todo lo que soy. Vosotros me habéis enseñado a ser como soy, a luchar por lo sueños

que uno tiene cueste lo que cueste y a no rendirse nunca. Desde pequeño con todas y cada una de las cosas que hacía he sentido vuestro apoyo y en esta etapa también habéis estado siempre a mi lado para lo que he necesitado. Os debo todo y os doy las gracias por todo lo que habéis hecho por mí. Os quiero mucho.

Ahora que lo veo, quizás todo este apartado me ha quedado un poco largo… pero he tenido la gran suerte de coincidir con personas maravillosas y de conocer gente que me ha aportado mucho durante esta etapa. Sin contar con todos los que han estado a mi lado desde pequeño… Por todo lo que ya he explicado (y no me he extendido…),

¡MUCHAS GRACIAS A TODOS!

Abstract

Aging is a systemic, multifactorial and degenerative process characterized by the decline and loss of physical and mental capacities. Average life expectancy has increased considerably in last century, thus increasing the number of elderly people in the population and therefore functional limitations and age-related diseases. In this sense, frailty represents a novel geriatric syndrome that is characterized by a loss of functional capacity and a decline in the ability to respond to physiological stress, resulting in increased vulnerability of the individual and negative health outcomes. It is a dynamic condition that is becoming an important health problem that needs to be detected and intervened. Relatively little is known regarding the pathophysiology of this syndrome and the molecular mechanisms underlying frailty remain poorly understood. In order to address this issue, we analyzed the transcriptomic profile of a set of robust and frail community-dwelling individuals from the Basque Country, and we found 35 genes differentially expressed that were associated with frailty status. These included genes associated to inflammation, immune response or miRNAs, processes previously linked to frailty. Among them, 7 candidates were validated in independent cohorts and also showed a similar expression pattern in serially passaged human primary myoblasts and fibroblasts. Their expression was partially restored after different intervention programs in frail individuals. Additional analyses revealed the expression of a minimum set of 3 genes (increased *EGR1* and lower *DDX11L1* and *miR454*) robustly associated with frailty status and clinical characteristics linked to frailty such as multimorbidity and polipharmacy. Moreover, we discovered their role in cell aging and identified their activity as mediators of senescence-associated pathways, becoming potential players in the physiopathology of this geriatric syndrome. Together, our results reveal a link between frailty and senescence.

Brain aging consists of a progressive loss of functional capacities which is associated with a progressive cognitive decline and can lead to neurodegenerative diseases. Although different approaches have been used to identify biomarkers and molecular pathways underlying brain aging, they maintain largely unknown. Centenarians, display extreme longevity which is accompanied by better cognitive function, fewer comorbidities, and greater quality of life and therefore, they have been proposed as a model of healthy aging.

In our study, we performed transcriptomic analysis in hippocampus samples of human individuals of different ages, including young, elderly and centenarian individuals, in order to address the molecular mechanisms underlying brain aging. We identified a differential gene expression pattern in brain samples of centenarians compared to the other two groups. In particular, several members of the metallothioneins (*MTs*) family of genes were highly expressed in the hippocampus of centenarian individuals. These findings were validated in two additional and independent cohorts. Notably, MTs were mainly expressed by astrocytes and functional studies *in vitro* described the role of *MTs* on their viability and activity. Indeed, silencing of *MT1* or *MT3* in primary human astrocytes, resulted in decreased proliferation, increased apoptosis and senescence together with increased expression of inflammatory genes. Overall, these results show that hippocampus of centenarians dysplay high levels of MTs, which are mainly expressed in astrocytes becoming a defensive mechanism that could provide neuroprotection in the brain during aging. Further analyses, revealed a subset of 6 genes whose expression correlated with chronological aging in human hippocampus. Among them, the decline in *RAD23B* showed the strongest differences at statistical level both in human and mice. Validation in additional cohorts confirmed the decreased levels of RAD23B with age also at protein level, which were exacerbated in pathological conditions, since their levels were lower or totally absent in patients with Alzheimer´s disease. Moreover, silencing experiments in cell cultures *in vitro* showed that it was involved in astrocyte viability and activity, indicating that it is a putative biomarker and regulator of cell aging in the brain.

Resumen

El envejecimiento es un proceso sistémico, multifactorial y degenerativo caracterizado por el declive y la pérdida de capacidades físicas y mentales. La esperanza de vida ha aumentado considerablemente en el último siglo, lo que ha incrementado el número de personas mayores en la población y, por tanto, las enfermedades relacionadas con la edad. En este sentido, la fragilidad, considerada como una etapa previa a la dependencia, se caracteriza por una pérdida de la capacidad funcional y de la habilidad para responder al estrés fisiológico, lo que resulta en una mayor vulnerabilidad del individuo a eventos adversos para la salud. La prevalencia de este síndrome aumenta con la edad y se está convirtiendo en un importante problema de salud. Se sabe relativamente poco sobre la fisiopatología asociada al síndrome de la fragilidad. De hecho, el estrés oxidativo y la inflamación son los únicos procesos biológicos relacionados de manera robusta y experimental con ella. Con el fin de abordar a nivel biológico la fragilidad, estudios recientes han comenzado a utilizar enfoques ómicos. Sin embargo, estos estudios han descrito patrones moleculares y metabolómicos que no han sido analizados después de una intervención y su impacto a nivel funcional no ha sido estudiado. Por tanto, los mecanismos moleculares subyacentes a la fragilidad siguen siendo bastante desconocidos.

Teniendo todo esto en cuenta, en el primer capítulo de esta tesis doctoral, comparamos el transcriptoma de muestras de sangre de 25 individuos del País Vasco clasificados como robustos o frágiles en base a 3 escalas de fragilidad diferentes (levántate y anda, velocidad de la marcha y Tilburg). Se identificaron 35 genes expresados diferencialmente entre individuos robustos y frágiles. Entre ellos, había genes relacionados con la inflamación e hipoxia (*EGR1, CXCL8, CISH, MAPK8IP1P2* or *CD40LG*), respuesta inmunitaria (*TIA1, IGHV2-26, TRBV3-1*) y apoptosis (*G0S2*), resultados que concuerdan con estudios anteriores. La expresión de 14 genes candidatos fue estudiada mediante qRT-PCR en muestras de sangre de la cohorte completa y se confirmó un aumento estadísticamente significativo de la expresión de *G0S2*, *EGR1*, *CXCL8* y *GJB6* y una reducción de *NSF*, *DDX11L1* y *miR454*. La alteración en la expresión de este patrón de 7 genes se replicaba en dos cohortes adicionales e independientes, donde la fragilidad se midió con las 2 escalas más comúnmente utilizadas para la detección de la fragilidad (Fried y Frailty Index). Además,

evaluamos la expresión de los genes seleccionados en muestras de sangre de sujetos frágiles de 3 cohortes independientes de individuos que se sometieron a diferentes tipos de intervención durante 12 semanas. El primero fue un estudio piloto que se completó con entrenamiento físico de intensidad moderada y reveló una mejora parcial en la actividad funcional que se acompañó con la disminución en la expresión de *EGR1*. En las otras 2 intervenciones los individuos frágiles realizaron (i) un plan de intervención "multicomponente", de "doble tarea" o basado en caminar y (ii) ejercicios de natación 3 veces por semana. En ambos, los individuos mostraron una reducción estadísticamente significativa del fenotipo de fragilidad junto con una restauración parcial de la expresión génica, indicando que distintos tipos de intervención pueden recuperar la actividad funcional y revertir el patrón de expresión observado en individuos frágiles. También caracterizamos la expresión de los 7 genes seleccionados en 2 tipos de células primarias humanas mantenidas en cultivo durante un largo periodo de tiempo, lo que constituye un modelo establecido para el estudio del envejecimiento celular *in vitro*. En primer lugar, descubrimos que los fibroblastos mantenidos en cultivo durante más de 4 meses presentaban el mismo patrón de expresión observado en muestras de sangre de individuos frágiles. Además, caracterizamos si los genes identificados podrían estar relacionados con la biología muscular, un componente relevante de la fragilidad física, midiendo su expresión en mioblastos primarios humanos. Los mioblastos primarios de pase avanzado revelaron un patrón de expresión similar al de los individuos frágiles. Estos resultados indican que que la alteración del patrón molecular detectado en fragilidad se asemeja a aspectos del envejecimiento a nivel celular.

Por otro lado, se comprobó el potencial discriminatorio y diagnóstico de los 7 genes individualmente y *EGR1* mostró la mejor curva ROC individual (AUC de 0.715), indicando que podría ser un potencial biomarcador para detectar individuos frágiles. Además, intentamos encontrar un patrón mínimo de genes que pudiera permitir la identificación de individuos frágiles, por lo que realizamos curvas ROC con diferentes combinaciones de genes. Identificamos que la expresión de un grupo mínimo de 3 genes (aumento de *EGR1* y reducción de *DDX11L1* y *miR454*), predecía de forma robusta la presencia de fragilidad y mejoraba el poder predictivo de cada gen individualmente. Este grupo de 3 genes también se asoció con parámetros clínicos como la polifarmacia y la multimorbilidad, características previamente relacionadas con la fragilidad, lo que refuerza la asociación del patrón de expresión con la fragilidad. Asimismo, estudiamos la expresión de EGR1 y DDX11L1 a nivel proteico en muestras de sangre de individuos frágiles y observamos que los niveles de EGR1

estaban aumentados y los de DDX11L1 disminuidos. Estos resultados sugieren que *EGR1* solo o en combinación con *DDX11L1* y *miR454* podría ser un buen biomarcador de fragilidad.

Fuimos más allá en la comprensión del impacto del patrón de 3 genes y estudiamos el efecto funcional a nivel celular. Para ello, modulamos la expresión de estos genes en fibroblastos primarios humanos mediante transducciones lentivirales. Por un lado, la sobreexpresión del *miR454* promovió la proliferación y redujo la acumulación de marcadores de senescencia, sugiriendo una actividad anti-envejecimiento para este miRNA. Por otro lado, los experimentos de silenciamiento de *DDX11L1 y de EGR1* dieron lugar a una menor proliferación y un aumento de la senescencia, lo que les confiere un papel regulador de procesos celulares asociados al envejecimiento. Los ensayos de sobreexpresión de *EGR1* mostraron datos opuestos, con incremento de la proliferación y menor senescencia. Para corroborar el impacto de *EGR1* (gen más significativamente asociado a fragilidad) *in vivo*, realizamos un ensayo de longevidad utilizando un modelo de *C. elegans*. Se silenció el ortólogo humano de *EGR1* (*egrh-1*) y detectamos que el gusano mutante de *egrh-1* presentaba una mayor supervivencia, reforzando el papel de EGR1 en el envejecimiento y la longevidad.

También estudiamos la función y las posibles vías moleculares reguladas por este trío de genes. El análisis computacional y la bibliografía previa revelaron varias dianas de *EGR1* y *miR454* como $p21^{CIP1}$*, PTEN, C-JUN o AREG*, implicadas en vías moleculares asociadas con senescencia. De hecho, estas dianas, así como marcadores clave de senescencia como $p16^{INK4A}$ o *IL6* mostraron una mayor expresión en individuos frágiles y se restablecieron tras los diferentes planes de intervención citados anteriormente. Además, los fibroblastos de pase tardío fueron tratados con 3 compuestos senolíticos diferentes – Quercetina, Dasatinib y Navitoclax – promoviendo los 3 compuestos individualmente la disminución de marcadores de senescencia, el incremento de apoptosis y la restauración del patrón de expresión génica observado en individuos frágiles, datos que, en su conjunto, revelan la existencia de un vínculo entre fragilidad y senescencia.

Aunque el envejecimiento es un proceso biológico complejo que afecta a todos los tejidos y sistemas del organismo, el envejecimiento cerebral es especialmente distintivo y desempeña un papel central. Consiste en un deterioro cognitivo progresivo y puede conducir a la generación de enfermedades neurodegenerativas. Durante años, se han utilizado

diferentes enfoques para identificar dianas clave del envejecimiento cerebral, pero siguen siendo un campo en investigación. Por lo tanto, es necesario comprender los mecanismos moleculares fundamentales implicados como primer paso para posibles enfoques terapéuticos. En este sentido, los centenarios han sido propuestos como modelo de envejecimiento saludable, ya que su extrema longevidad parece estar acompañada de una mejor función cognitiva y menos comorbilidades. Por este motivo, son una población atractiva para desentrañar los mecanismos implicados en la longevidad humana y los genes relacionados con un envejecimiento exitoso.

En el segundo capítulo de esta tesis doctoral, abordamos la cuestión del envejecimiento cerebral a través de un enfoque biológico y realizamos un análisis transcriptómico en muestras de hipocampo de individuos humanos de diferentes edades, incluyendo individuos jóvenes, ancianos y centenarios, procedentes de una cohorte establecida en el País Vasco. El estudio transcriptómico reveló un patrón de expresión génica diferencial en centenarios con varios miembros de la familia de genes de las metalotioneínas (*MTs*) altamente expresados en el hipocampo de los centenarios. Observamos que dicho patrón de expresión génica parece ser una firma específica del nicho neurogénico hipocampal, ya que su expresión estaba enriquecida en el hipocampo y no estaba alterada en la región del córtex de los mismos individuos. Nuestros hallazgos fueron validados en dos cohortes adicionales e independientes, donde confirmamos los resultados obtenidos en el análisis transcriptómico tanto a nivel de ARNm como de proteína. Las MTs son una familia de proteínas implicadas en la homeostasis y detoxificación de metales pesados, como el zinc y el cobre, de las que se han descrito 4 isoformas (MT1, MT2, MT3 y MT4). Además, tienen una función antiinflamatoria y antioxidante con un papel en la protección contra el estrés oxidativo, la apoptosis, el daño del ADN. Por esta razón, los altos niveles de MTs observados en el cerebro de centenarios podrían ser un mecanismo defensivo que podría proporcionar neuroprotección.

Con el fin de caracterizar la función de las MTs en el envejecimiento cerebral, estudiamos su expresión en distintos tipos de células cerebrales realizando estudios de co-inmunofluorescencia con marcadores de distintos linajes celulares del cerebro. Descubrimos que las células principales que expresaban las MTs eran astrocitos, ya que las células positivas para MTs también lo eran para marcadores de astrocitos como GFAP y S100β y no expresaban marcadores neuronales como MAP2 o TUJ1. Además, observamos que los

astrocitos cultivados en pases tardíos presentaban niveles más bajos de *MTs* y que su silenciamiento provocaba una disminución de la proliferación y un aumento de la apoptosis y senescencia, lo que indica que las MTs están implicadas en la viabilidad y actividad celular de los astrocitos. Además, observamos que el silenciamiento de las *MTs* inducía un aumento en la expresión de marcadores inflamatorios que podrían estar relacionados con el fenotipo reactivo de los astrocitos neuroinflamatorios, sugiriendo que las *MTs* podrían tener un papel en la polarización de los astrocitos hacia un fenotipo protector.

En paralelo, realizamos un análisis similar al anterior comparando el grupo de los jóvenes frente al de ancianos, lo que reveló un conjunto de genes diferencialmente expresados e implicados en vías como la reparación del ADN, el metabolismo, el desarrollo, la señalización sináptica, el transporte de iones, la regulación hormonal, la secreción de proteínas y la autofagia, procesos previamente descritos como reguladores del envejecimiento. Por último, realizamos un análisis bioinformático adicional para dilucidar los mecanismos moleculares asociados al envejecimiento cronológico. Este análisis reveló cambios en la expresión de 6 genes que se correlacionaban con el envejecimiento en el hipocampo humano. En particular, *SMPD4, RASGEF1B* y *ANKRD18B* se correlacionaron positivamente con la edad, mientras que la expresión de *RAD23B*, *HYOU1* y *OR2A42* mostró un descenso con la edad. Además, se estudió la expresión de estos 6 genes tanto en fibroblastos primarios humanos como en astrocitos mantenidos en cultivo y detectamos niveles más altos de *SMPD4, RASGEF1B* y *ANKRD18B*, y menores de *RAD23B*, *HYOU1* y *OR2A42* en células "envejecidas" *in vitro*, lo que refuerza el vínculo entre este conjunto de genes y el envejecimiento celular. Entre estos 6 genes, la expresión de RAD23B, implicado en la reparación del ADN, mostró las mayores diferencias a nivel estadístico tanto en muestras humanas como de ratón con el envejecimiento fisiológico a nivel de ARNm y de proteína, lo que sugiere una menor respuesta al daño del ADN con la edad. Además, la expresión de la proteína RAD23B estaba casi ausente en pacientes con enfermedad de Alzheimer, lo que indica que está relacionado con el envejecimiento cronológico fisiológico y patológico.

Table of contents

Abbreviations

A	AD	Alzheimer´s Disease
	ADAS-Cog	Alzheimer's Disease Assessment Scale-cognitive Subscale
	AGS	Astrocyte Growth Supplement
	ALT	Alanine-aminotransferase
	ANKRD18B	Ankyrin Repeat Domain 18B
	APOE	Apolipoprotein E
	ARE	Antioxidant Response Element
	AREG	Amphiregulin
	ATCC	American Type Culture Collection
	AUC	Area Under the Curve
B	B2M	Beta-2-microglobulin
	BCA	Bicinchoninic Acid
	BCCP	Bayesian Compound Covariate Classifier
	BLAST	Basic Local Alignment Search Tool
	BSA	Bovine Serum Albumin
C	C	Celsius
	C3	Complement component 3
	CA1-4	*Cornu ammonis* areas 1-4
	CCI	Charlson Comorbidity Index
	CCP	Compound Covariate Predictor
	CD69	Cluster of Differentiation 69
	CDK	Cyclin-Dependent Kinase
	cDNA	Complementary Desoxyribonucleic Acid
	CGIC-PF	Clinical Global Impression of Change in Physical Frailty
	CHSA	Barthel Index and the Canadian Study of Health and Aging
	CNS	Central Nervous System
	CO_2	Carbon Dyoxide
	COP	Circulating Osteogenic Progenitor
	CRP	C-reactive Protein
	Cu	Cooper
	CXCL8	C-X-C Motif Chemokine Ligand 8
D	DAB	3,3'-Diaminobenzidine
	DAPI	2-(4-Amidinophenyl)-6-indolecarbamidine dihydrochloride
	DDX11L1	DEAD/H-Box Helicase 11 Like 1

	DEPC	Diethyl Pyrocarbonate
	DG	Dentate Gyrus
	DLDA	Diagonal Linear Discriminant Analysis
	DM1	Mytononic Distrophy type 1
	DMEM	Dulbecco's Modified Eagle Medium
	DMSO	Dimethyl Sulfoxide
	DNA	Deoxyribonucleic acid
	DUH	Donostia University Hospital
E	EDTA	Ethylenediaminetetraacetic Acid
	EdU	5-ethynyl-2′-deoxyuridine
	EGF	Epidermal Growth Factor
	EGR1	Early Growth Response 1
	ELISA	Enzyme-linked Immunosorbent Assay
	ER	Endoplasmic Reticulum
	EU	European Union
F	FBS	Fetal Bovine Serum
	FC	Fold Change
	FGF	Fibroblast Growth Factor
	FI	Frailty Index
	FOXO	Forkhead Box
	FWM	Forebrain White Matter
G	G0S2	G0/G1 switch 2
	G6PD	Glucose-6-phosphate Dehydrogenase
	GAPDH	Glyceraldehyde 3-phosphate dehydrogenase
	GEO	Gene Expression Omnibus
	GFAP	Glial Fibrillary Acidic Protein
	GFST	Gérontopôle Frailty Screening Tool
	γH2AX	gamma-H2A Histone Family Member X
	GJB6	Gap Junction Protein-beta 6
	GO	Gene Ontology
	GS	Gait Speed
	GWAS	Genome-wide Association Studies
H	h	Hour
	H_2O	Water
	HABCS	Healthy Aging and Biomarkers Cohort Study
	HDAC	Histone Deacetylase
	HIP	Hippocampus
	HRP	Horseradish Peroxidase
	HSP	Heat Shock Protein

	HYOU1	Hypoxia up-regulated 1
I	IF	immunofluorecence
	IGF1	Insulin-like Growth Factor 1
	IHC	Immunohistochemistry
	IL1α	Interleukin 1 apha
	IL1β	Interleukin 1 beta
	IL6	Interleukin 6
	IL8	Interleukin 8
	IL10	Interleukin 10
	IL18	Interleukin 18
	IPTG	Isopropyl β-D-1-thiogalactopyranoside
	ISH	In situ Hybridization
K	KNN	K-nearest Neighbor
L	LGP	Longevity Genes Project
	LLFS	Long Life Family Study
	LTNH	Long-term Nursing Homes
M	MAP2	Microtubule-associated Protein 2
	MAPKs	Mitogen-activated Protein Kinases
	min	Minute
	miRNA	microRNA
	MMSE	Mini-Mental State Examination
	MoCA	Montreal Cognitive Assessment test
	MOI	Multicity Of Infection
	MRE	Metal Response Element
	mRNA	Messenger Ribonucleic Acid
	MT1	Metallothionein 1
	MT3	Metallothionein 3
	MTs	Metallothioneins
N	$Na_4P_2O_7$	Tetrasodium pyrophosphate
	Na_3VO_4	Sodium orthovanadate
	NaBH4	Sodium borohydride
	NaCl	Sodium chloride
	NADPH	Nicotinamide Adenine Dinucleotide Phosphate
	NaF	Sodium fluoride
	NC	Nearest Centroid
	NCBI	National Center for Biotechnology Information
	NDS	Normal Donkey Serum

	NECS	New England Centenarian Study
	NER	Nucleotide Excision Repair
	NF-κB	Nuclear factor kappa-light-chain-enhancer of activated B cells
	NHA	Normal Human Astrocytes
	NSCs	Neural Stem Cells
	NSF	N-ethylmaleimide Sensitive Factor
O	O_2	Oxygen
	OR2A42	Olfactory Receptor family 2 subfamily A member 42
P	P/S	Penicillin/Streptomycin
	PBMCs	Peripheral Blood Mononuclear Cells
	PBS	Phosphate Buffered Saline
	PCA	Principal Component Analysis
	PCR	Polymerase Chain Reaction
	PCx	Parietal Neocortex
	PFA	Paraformaldehyde
	pH	Potential of Hydrogen
	pH3	Phospho-histone H3
	PMSF	Phenylmethylsulfonyl Fluoride
	PTEN	Phosphatase and Tensin Homolog
Q	qRT-PCR	Quantitative Real-time Polymerase Chain Reaction
R	RAD23B	RAD23 Homolog B
	RASGEF1B	Ras-GEF domain-containing Family Member 1B
	REST	RE1 Silencing Transcription Factor
	RMA	Robust Multi-array Average
	RNA	Ribonucleic Acid
	RNAi	RNA interference
	RNAseq	RNA sequencing
	ROC	Receiver Operating Characteristic
	ROS	Reactive Oxygen Species
	rpm	Revolutions per minute
	RT	Reverse Transcription
S	S100β	S100 calcium-binding Protein-beta
	SA-β-gal	Senescence-Associated beta-galactosidase
	SASP	Senescence-Associated Secretory Phenotype
	SDS	Sodium Dodecyl Sulfate
	SDS-PAGE	Sodium Dodecyl Sulphate-Polyacrylamide Gel Electrophoresis
	SEM	Standard Error of the Mean
	SGZ	Sub-granular Zone

	shRNA	Short hairpin RNA
	siRNA	Short Interference RNA
	SIRT	Sirtuin
	SLC39A12	Solute Carrier Family 39 Member 12
	SMPD4	Sphingomyelin Phosphodiesterase 4
	SNP	Single-nucleotide Polymorphism
	SPPB	Short Physical Performance Battery
	STAT3	Signal Transducer and Activator of Transcription 3
	STRING	Search Tool for the Retrieval of Interacting Genes/Proteins
	SVM	Support Vector Machines
	SVZ	Subventricular Zone
T	TBI	Traumatic Brain Injury
	TBS-T	Tris Buffered Saline-Tween
	TCx	Temporal Neocortex
	TFI	Tilburg Frailty Indicator
	TGFβ	Transforming Growth Factor-beta
	TNFα	Tumor Necrosis Factor-alpha
	TRIM3	Tripartite Motif-containing Protein 3
	Tris-Hcl	Tris hydrochloride
	TSHA	Toledo Study for Healthy Aging
	TUG	Timed Up and Go
	TUJ1	Class III beta-Tubulin
U	UBC	University of the Basque Country
W	WHO	World Health Organization
Z	ZIPs	Zinc-regulated Proteins
	Zn	Zinc
	ZnTs	Zn Transporters

Introduction

1. Aging

1.1. General description

Aging is a natural process defined as the time-dependent functional decline of organs and tissues of most living organisms that occurs due to the gradual accumulation of cellular damage [1]. It is a multifactorial process that affects all cells and tissues in the organism and it is characterised by the progressive loss of physiological integrity, which leads to impaired homeostasis and result in physical and cognitive impairment increasing the vulnerability to death [2].

Demographic aging constitutes a social and economic challenge worldwide [3], [4]. In the last century, the average life expectancy has increased considerably in most developed countries as a consequence of the combination of many factors, such as higher living standards, better lifestyle and education, and progress in healthcare and medicine [5]. Thus, the improvements in social, medical and economic conditions have resulted in reduced early mortality, better quality of life and consequent increase in life expectancy that is significantly increasing the number of elderly people in the population [6]. Indeed, it has been predicted by the year 2100, that the world demographic pyramid or population pyramid will present a block shape, with a considerable narrowing at the base and in the middle, together with an increase at the top (***Figure I1***).

Specifically in Europe, data by Eurostat (the statistical office of the European Union) have also showed an augment in life expectancy, that together with the decrease in birth rates, is shifting the current demography towards an older population throughout the European Union (EU) [7]. In his case, the EU's population is projected to continue to age and the number of elderly people will increase significantly (***Figure I2***). By 2100, the the European demographic pyramid will also take the shape of a block, where people aged 65 years or over that represented 20.8 % of the EU's population in 2021, are estimated to increase up to 31.3 % by 2100 (***Figure I2***). Thus, the median age, that provides a useful summary of the overall age profile, is expected to increase by 4.9 years, rising from 44.1 years in 2021 to 48.8 years in 2100 [7]. Moreover, between 2002 and 2020, the median lifespan of European citizens showed an increment of 3.1 years in women and 4.2 years in men, increasing from 77.7 to 81.3 years [7].

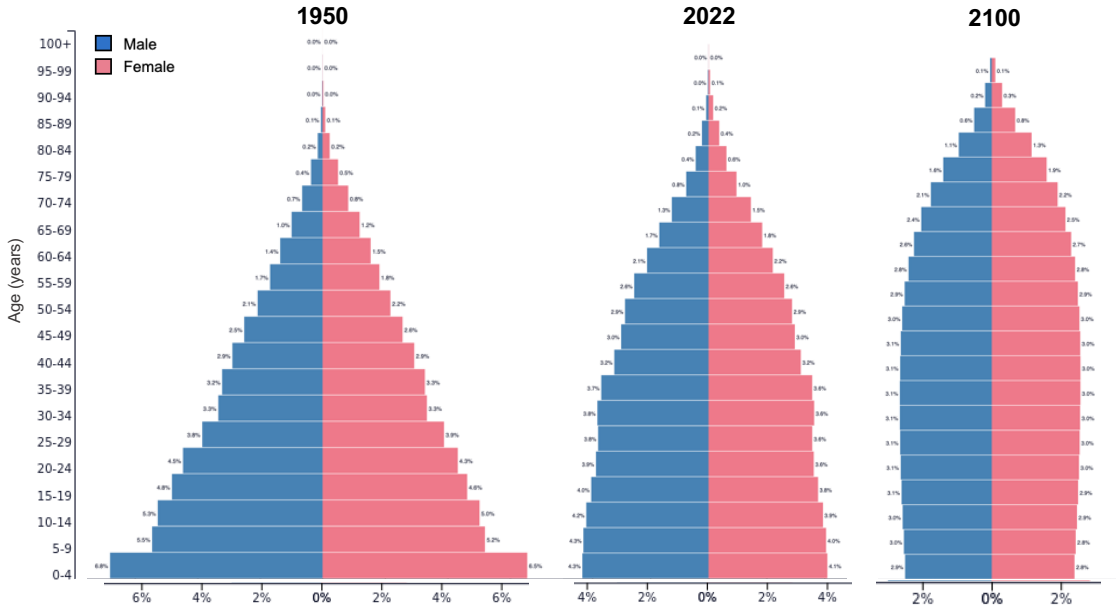

Figure I1: Demography is shifting towards an older population. World population pyramid or demographic pyramid representing data obtained in years **(A)** 1950, **(B)** 2022 and **(C)** projections for 2100. Data are shown as percentage of the total population. Adapted from https://www.populationpyramid.net.

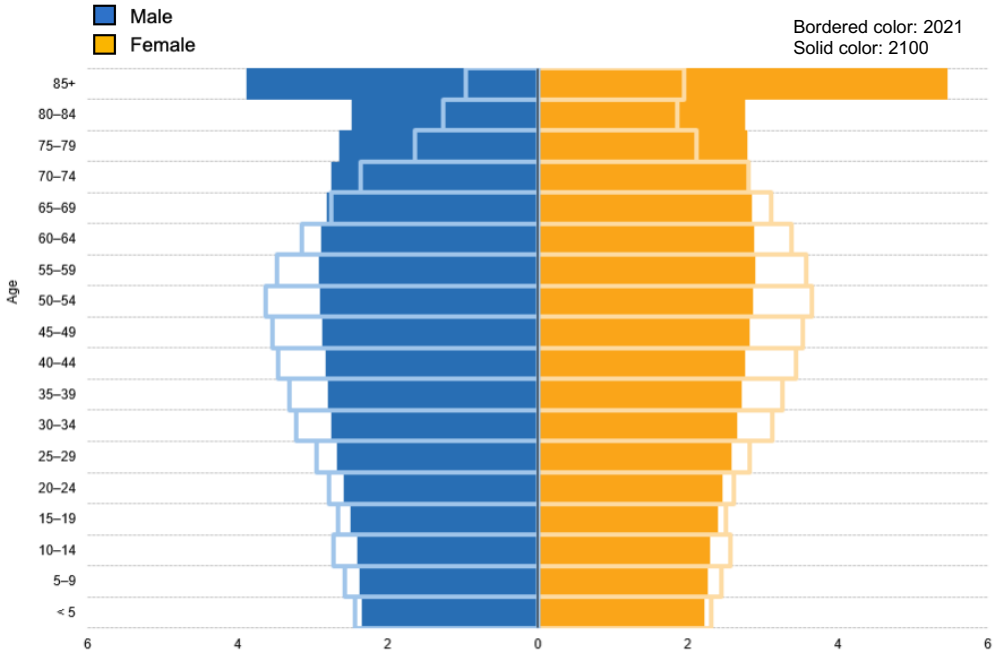

Figure I2. Comparative population pyramids representing data obtained in year 2021 (bordered) and the projections for 2100 (solid color) in the European Union. Data are shown as percentage of the total population. Adapted from Eurostat, 2022 (https://ec.europa.eu/eurostat/).

Another consequence of population aging is the progressive accumulation of the older population itself. The relative ratio of the very old is growing at a faster pace than any other age segment of the EU's population and the people aged 80 years or above is expected to double in number, from 6 % to 14.6 % (***Figure I3***).

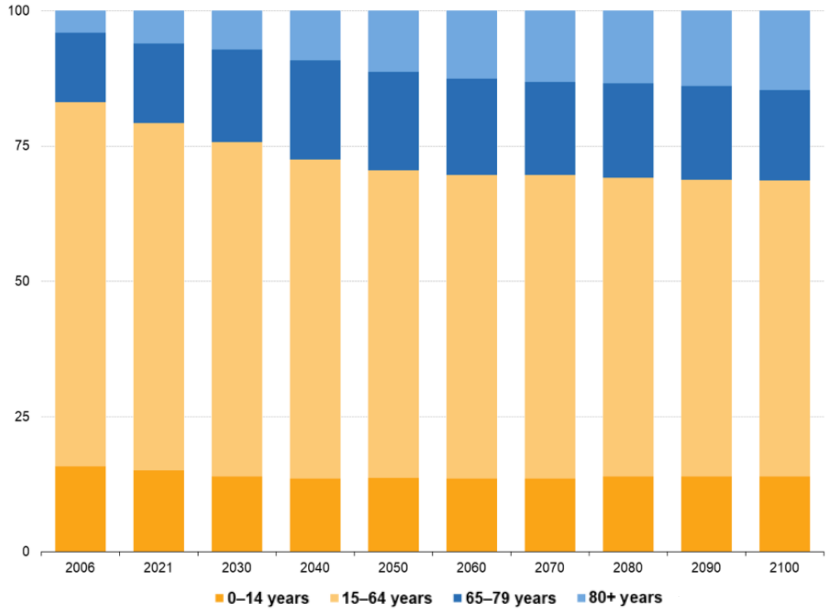

Figure I3. Population structure by major age groups from the year 2006 and the projections for the next decades until year 2100 in the European Union. The proportion of children (0- 14 years) will have only a minor decrease, while a marked decrease of the adults (15 - 64 years) and increase of elders (65 - 79 years and 80+ years) is expected. Data are shown as percentage of the total population. Adapted from Eurostat, 2022 (https://ec.europa.eu/eurostat/).

Moreover, the EU's old-age dependency ratio, defined as the ratio of the number of elderly people (aged 65 years and over) compared with the number of people of working-age (15-64 years), is projected to almost double from 32.5 % in 2021 to 57.1 % by 2100 [7]. The increase in mean lifespan has been accompanied by increased disability together with higher incidence of chronic diseases [8]. Thus, there is an increment in falls, dependency, dementia and cognitive decline as well as in diseases such as cancer, stroke, diabetes or neurodegenerative diseases [9], [10]. In consequence, the increase in aged population may jeopardize the sustainability of public health systems. Thus, the group of people older than 65 accounts for over 60 % of health care spending in developed countries. In addition, people

aged 65 years and over present a health care cost per capita five times higher than for those aged less than 65 years [11].

Human aging can be divided into two major phases, a first period of relatively healthy aging free of major chronic clinical diseases and disability, known as healthspan and a period of age-associated disability and disease [12], [13] (***Figure I4***). Several studies in animal models have slowed down the biological processes of aging and extended longevity with different pharmacological or behavioral approaches (diet and physical activity) [14]–[16]. However, living longer, is not living better and the primary objective of aging research has experimented a switch and is recently focusing in the improvement of the quality of life of the elderly, reducing disability and prolonging healthy aging [17], [18]. Thus, healthspan has become the central theme of the aging research, being its first objective the identification of biological mechanisms and strategies that will increase healthspan in order to extend the healthy period of life and delay the development of chronic diseases and disability until a brief period at the end of life [19], [20]. The general goal is living longer but with good health and quality of life, a term which has been called "optimal longevity" [21] (***Figure I4***). The major obstacle to achieve optimal longevity is the progressive decline in physiological function that occurs with aging, which causes functional limitations and is accompanied by severe comorbidities, disabilities, frailty and dependency in many cases [22], [23].

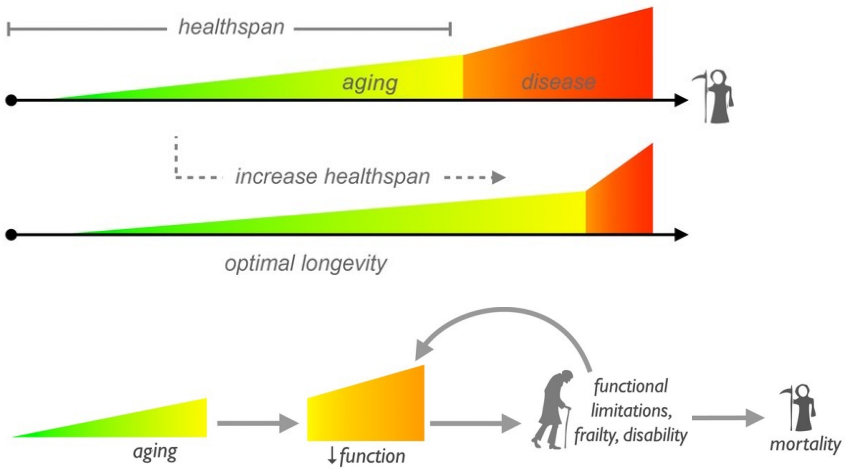

Figure I4. Impaired function with aging as a threat to healthspan and optimal longevity. Healthspan is a period of healthy aging with a modestly increasing (subclinical) chronic disease burden, followed by a period of age-related clinical disease. To achieve optimal longevity (living long, but primarily in wellness), healthspan must be significantly extended. With aging, there is a decrease in function that can lead to functional limitations, frailty or disability. Adapted from [12].

1.2. The biology of aging

Aging is a very complex biological complex that affects all the tissues and systems of the organism [24]. Physiologically, a number of changes occur such as alterations of the body composition including loss of bone, cartilage, muscle mass and strength and gain of abdominal fat [14]. Subsequently, systemic changes occur, for instance, in the endocrine system (altered hormone levels) or the cardiovascular system (changes in blood pressure and blood lipids), together with decreased lung capacity, changes in the skin (lower water content and elasticity) or vision and hearing loss among others [14]. At the molecular level, multiple studies have been carried out in the last 20 – 30 years in order to identify the cellular and molecular pathways underlying aging [8]. In this regard, López-Otín and collaborators [2], proposed ten years ago the hallmarks responsible for the aging process. They suggested 9 hallmarks and these include genomic instability, loss of proteostasis, cellular senescence, mitochondrial dysfunction, altered intercellular communication, deregulated nutrient sensing, stem cell exhaustion, epigenetic alteration and telomere attrition (***Figure I5***). At the same time, under geroscience perspective which recognizes the interplay between the biology of aging and chronic conditions (diseases, frailty or disability), Kennedy BK and collaborators postulated the pillars of aging [20]. They proposed 7, including metabolism, proteostasis, adaptation to stress, macromolecular damage, epigenetics, inflammation and stem cells and regeneration, that in the majority of cases coincide and overlap with the hallmarks of aging [20]. At the end of 2022, López-Otín and collaborators published a revised and novel version of the hallmarks of aging in which they included 3 additional hallmarks, namely disabled macroautophagy, chronic inflammation and dysbiosis [25]. Notably, they categorized and grouped them in three categories; primary, antagonistic and integrative hallmarks, that are tightly interconnected and they cannot be understood individually.

Genomic instability, telomere attrition, epigenetic alterations, loss of proteostasis and disabled macroautophagy are considered primary hallmarks since they are the primary causes of cellular damage [25]. With aging, the individual´s genes become increasingly susceptible to damage from endogenous (free radicals or replication errors) and exogenous sources (radiation, ultraviolet light and environmental chemicals) together with a deregulation of deoxyribonucleic acid (DNA) repair mechanisms [26]. In this sense, genomic damage accompanies aging and promotes mutational events. Thus, errors in DNA replication, point mutations, reactive oxygen species (ROS) generation (oxidative stress) and alterations

in DNA methylation all contribute to aging [27]. The expression of multiples genes and relevant transcription factors change with age [28], [29], however, not only the protein-coding transcripts are affected, and epigenetic changes have been described that occur during aging [2], [25], [30], [31]. Moreover, microRNAs (miRNAs) that participate in post-transcriptional regulation of gene expression are differentially expressed in individuals with different ages [32], [33].

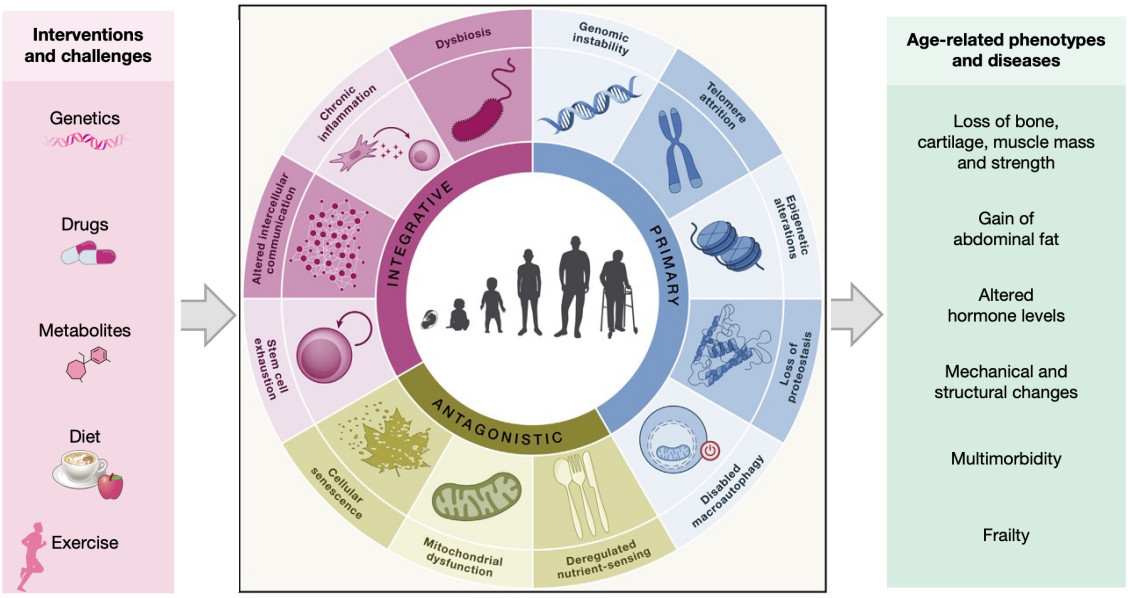

Figure I5. The hallmarks of aging. The scheme compiles the 12 hallmarks of aging proposed: genomic instability, telomere attrition, epigenetic alterations, loss of proteostasis, disabled macroautophagy, deregulated nutrient-sensing, mitochondrial dysfunction, cellular senescence, stem cell exhaustion, altered intercellular communication, chronic inflammation and dysbiosis. These hallmarks are grouped into three categories: primary, antagonistic, and integrative. Different interventions can prevent or ameliorate symptoms of aging and can affect different groups of hallmarks. Moreover, different groups of hallmarks can contribute to the etiology of specific age-related phenotypes and diseases. Adapted from [8], [25].

On the other hand, deregulated nutrient sensing, mitochondrial dysfunction and cellular senescence are part of antagonistic or compensatory responses to the damage [25]. These responses initially mitigate the damage, but eventually, if chronic or exacerbated, they become deleterious themselves [34]. In this sense, senescence is a biological process defined as a stable and permanent arrest of the cell cycle [35]–[37]. It promotes tissue remodeling during normal embryonic development and after injury, thus initiating a sequence of

processes that eliminate damaged cells and culminate in tissue regeneration, contributing to tissue homeostasis [38]. It is also a protective mechanism against cancer [34], [39], [40], however, during aging, senescence process may not be efficiently completed and the prevalent damage or the deficient clearance of senescent cells result in their accumulation [41], [42]. Senescent cells differ from other non-dividing cells by several features and morphological changes that are commonly used as senescence biomarkers, including the absence of proliferative markers, increased senescence-associated beta-galactosidase (SA-β-gal) activity and elevated expression of cell cycle inhibitors [43], [44]. Senescence can be induced by genomic instability of genes governing cell proliferation, telomere shortening, oxidative stress or inflammation accumulation [36]. The molecular mechanisms underlying cellular senescence include various signaling pathways being likely ARF/p53/$p21^{CIP1}$ or $p16^{INK4A}$/Rb the most relevant, that converge in the activation of the cyclin-dependent kinase (CDK) inhibitors and result in proliferative arrest [44]. Additionally, senescent cells present a particular secretome called senescence-associated secretory phenotype (SASP) that participate in the dissemination of a deleterious pro-inflammatory signal that can aggravate tissue dysfunction in aging [45] (***Figure I6***). The SASP includes the secretion of pro-inflammatory cytokines such as interleukin 6 (IL6) or interleukin 8 (IL8), chemokines, growth factors such as the transforming growth factor-beta (TGFβ) and proteases that creates an inflammatory microenvironment [46], [47]. These SASP components, most notably cytokines or TGFβ, can also trigger senescence in neighboring cells in a paracrine manner, through a mechanism that generates ROS and DNA damage [48], [49]. One of the targets of inflammatory cytokines is the nuclear factor kappa-light-chain-enhancer of activated B cells (NF-κB), which positively regulates many genes that encode proinflammatory cytokines and genes involved in SASP, that can result in a positive feedback loop that enhances inflammation. Furthermore, it has been described that senescence is a dynamic multistep process where the activation of $p21^{CIP1}$ is required for the onset and early stage of senescence, whereas $p16^{INK4A}$ is associated with the deep or late stage of senescence, as it is activated under persistent stress and maintains a durable growth arrest [38], [50].

Finally, stem cell exhaustion, chronic inflammation, dysbiosis and altered intercellular communication compose the integrative hallmarks. They are the end result of the previous two groups and are ultimately responsible for the functional decline associated with aging. In this sense, the decline in the regenerative potential of tissues is one of the most

obvious characteristics of aging and this ability decreases during aging due, in part, to stem cell exhaustion [51]. Stem cells are defined as undifferentiated cells that present the ability of quiescence, self-renewal capacity and multipotency, which are able to generate a wide range of differentiated progeny, preserve homeostasis and replace the dead or damaged cells for the correct maintenance of organ structure and function [52]. Usually, stem cells are tightly regulated and maintained in a quiescence state (a reversible state of temporary cell cycle arrest), that can change in response to intrinsic and extrinsic signals in order to activate them [53]. Thus, activated stem cells can perform symmetric divisions to conduct self-renewal or asymmetric divisions to allow the maintenance of quiescent cell population and give rise to daughter progenitor cells [54]. The maintenance and activation of stem cells is a complex process that involved pathways that are usually affected during organismal aging, and therefore, contribute to the age-related stem cell exhaustion [55].

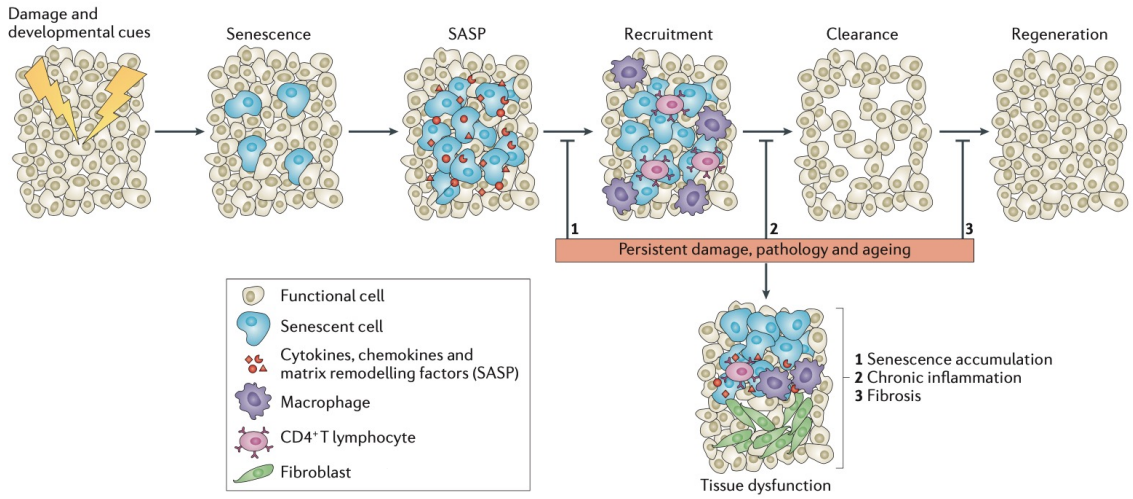

Figure I6. Proposed model of senescence. Senescence initiates a tissue remodeling process through the senescence-associated secretory phenotype (SASP) and recruitment of immune cells (macrophages), that clear the senescent cells. Then, progenitor cells repopulate and regenerate the damaged tissue. This process may be impaired upon persistent damage, pathological states or aging. In these cases, senescent cells are not efficiently cleared, the tissue is not fully regenerated and its functionality diminishes. In some cases, the resolution of the damage involves a fibrotic scar with senescent cells, inflammatory cells and fibrotic tissue. Adapted from [41].

Moreover, altered intercellular communication is another integrative hallmark that is linked to all the characteristics described previously since it encompasses the changes

that occur during aging [25]. The alteration of cellular communication can be caused by changes on the secreting cell and includes inflammatory, endocrine and neuronal signaling [56]. In this sense, inflammaging, represents the increase in proinflammatory cytokines during the aging process that is characterized by a systemic, chronic and low-grade sterile inflammatory condition, present even in the absence of acute stress such as infection [57], [58]. This state can be due to the production of inflammatory mediators by damaged cells, a dysfunction of the immune system or to the increase in the number of senescent cells that secreted proinflammatory cytokines [59]. Of note, the major regulator of inflammation are cytokines, small proteins that are secreted by a wide range of cell types and can promote or inhibit immune responses [60]. The balance between proinflammatory and anti-inflammatory cytokines needs to be firmly regulated and it has been related to healthy aging and longevity (***Figure I7***). It has been described that IL6 levels increased in an age-dependent manner, thus high levels have been found in elderly individuals [61]. Moreover, elevated levels of IL6 have been associated with disability and mortality in the elderly whereas lower levels have been associated with successful aging and longer survival [62], [63]. In addition, other inflammatory mediators such as tumor necrosis factor-alpha (TNFα) and C-reactive protein (CRP) have also present higher levels in elderly people [64], [65].

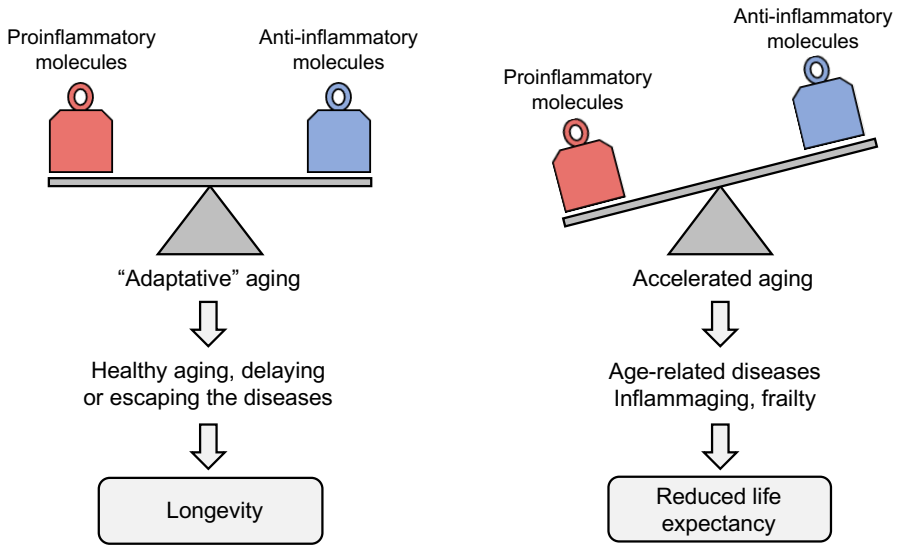

Figure I7. The benefits of maintaining balance between pro- and anti-inflammatory molecules. The importance of keeping a balanced inflammatory state favors adaptation to the conditions of life, allows avoidance or delays onset of diseases (healthy aging) and leads to longevity. When the proinflammatory molecules accumulate and the balance is lost during aging, chronic low-grade inflammation or inflammaging develops, promoting age-related diseases, frailty and finally reducing life expectancy. Adapted from [60].

2. Frailty

2.1. Definition and characteristics of frailty

The concept of frailty has evolved considerably in the literature since its original description [66] until the development of a consensus [67]. Frailty is a geriatric syndrome defined as the gradual reduction in functional reserve and resilience, as well as impaired adaptive capacity across multiple physiological systems, that increases the vulnerability against stressors and lead to deterioration and adverse health outcomes in the elderly [68], [69]. Increasing evidence is demonstrating that frailty is responsible for the transition from healthy aging towards disability [70] and it is a stage prior to dependence [71] (***Figure I8***). Thus, frail individuals show a reduced functional capacity [72] and an increased risk of adverse health outcomes such as falls, fractures, dependence, institutionalization and death [69], [73]. The opposite situation to frailty is most of the times termed robustness, when the functional capacity is conserved and phenotypic stability is also maintained after the occurrence of a stressor [74] (***Figure I8***).

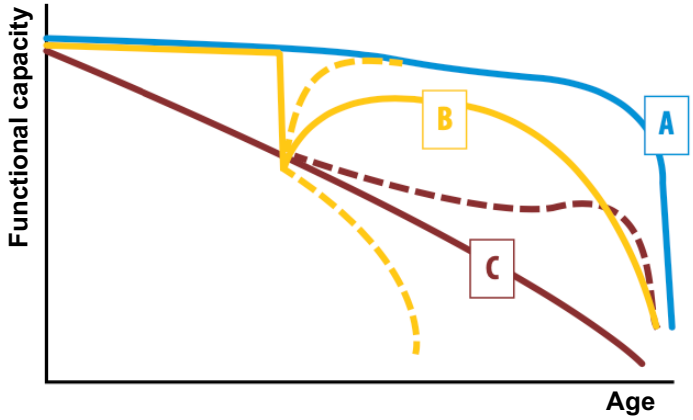

Figure I8. Representation of possible trajectories of functional capacity with age. Each line represents an individual. The subject A (robust) can be considered as having the optimal trajectory, in which functional capacity remains high until the end of life. The subject B has a similar trajectory until a point, when an event or a stressor causes a sudden fall in functional capacity (frail) followed by some amount of recovery and then a gradual deterioration. The subject C has a steady decline in function and the occurrence of another stressor in a later stage could result in a more prominent loss of functional capacity and subsequent aparition of dependence. The dashed lines represent alternative trajectories. Adapted from [72].

Frailty is a consequence of the process of aging and certainly its prevalence increases with age [75]. Thus, the prevalence of frailty ranges from 5 % to 17 % in people of 65 years from different countries and this percentage increases progresively up to almost 50 % in individuals over 85 years-old [73], [76]. Additionally, it is closely linked to multimorbidity [77]. Indeed, its distribution in aged populations and its role as a risk factor for several deleterious outcomes endorses the current consideration of frailty an emerging health challenge worldwide and a priority target for public health [78], [79].

Very close and related to frailty, the World Health Organization (WHO) has introduced the concept of intrinsic capacity which has been defined as the combination of all the physical and mental capacities of an individual, the environmental influence and the interaction between both factors, which compromise the health-related properties [80]. Five domains or components define the intrinsic capacity framework: cognition, psychological status, sensory function, vitality and locomotion, being each of them closely related to the others [81] (***Figure I9***). Thus, the functional decline that occurs with age is a consequence of the reduction of the reserves of the intrinsic capacity [79].

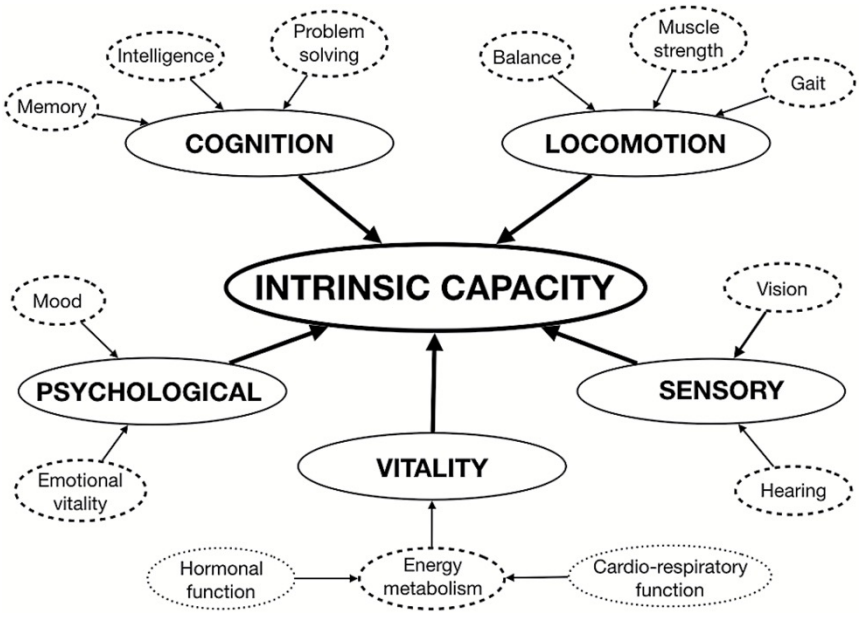

Figure I9. Schematic representation of the five domains of intrinsic capacity. The possible subdomains that have been proposed are included in the framework. Adapted from [81].

It is important to highlight that frailty represents a dynamic condition with the potential of reversibility, after an intervention therapy, which can be conducted through physical activity, dietary modification and/or multicomponent intervention (composed by strength, endurance, and balance training) [82]–[84]. Indeed, exercise- and nutrition-based interventions during 3 to 6 months, have shown to improve physical performance and frailty scores [85] and longer interventions based on dietary modification, exercise and cognitive training also improved cognitive function [86]. In this sense, intervening at an early stage is important because the process of becoming frail or dependent can be delayed, slowed [72] and even reversed by interventions in the process of functional decline [87], [88] (***Figure I10***). Key opportunities for action on trajectories of functional ability and intrinsic capacity across the life course have been highlighted by the WHO and are shown in ***Figure I10***. Thus, the identification of frail elderly subjects is highly relevant since it enables a possible intervention that could prevent frailty status, improve the functional capacity or restore cognitive function, to avoid the risk of developing dependence or premature dead [89]–[91].

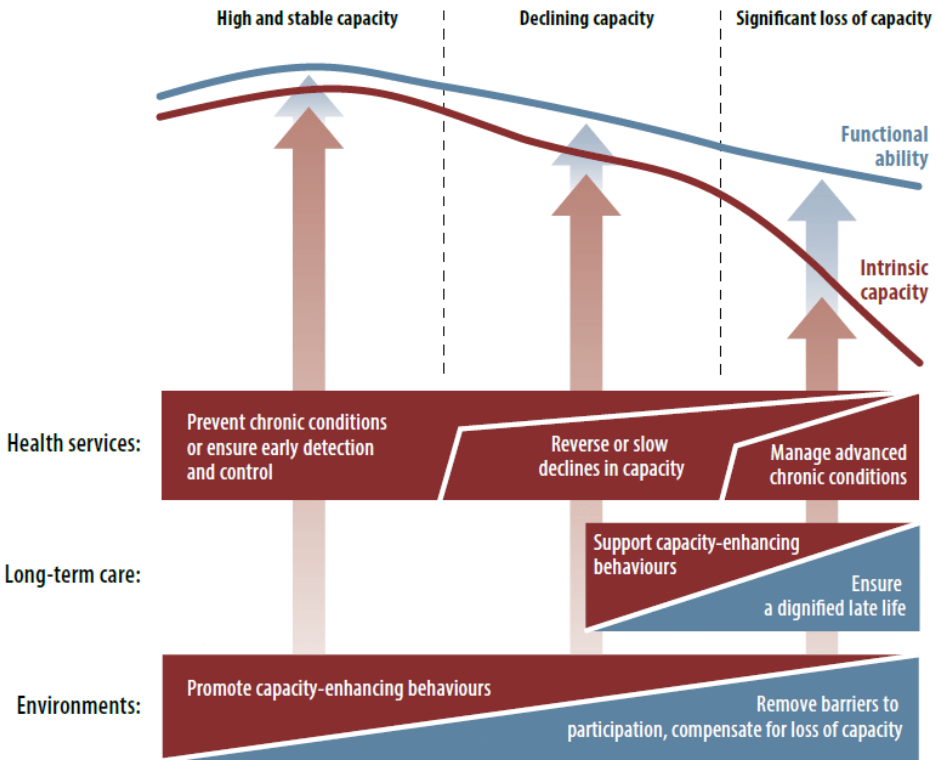

Figure I10. A public health framework for Healthy Aging: opportunities for public-health action across the life course. Intrinsic capacity and functional ability do not remain constant but decline with age as a result of underlying diseases and the aging process. The increasing decline in intrinsic capacity with time is more or less compensated by support and surroundings reflecting a person's specific environment (functional ability). Adapted from [72].

2.2. Frailty measurement and frailty scales

Since its first description at the beginning of the 20th century, numerous instruments have been proposed for the identification of frail subjects in various health care areas [92]–[94]. Frailty was first described by Fried and collaborators in 2001 [66], who established the "frailty phenotype" based on the presence or absence of a set of five criteria: weakness (low grip strength), slow walking speed, low physical activity, self-reported exhaustion and unintentional weight loss. Thus, an individual is considered as "frail" if 3 or more of these features are present, whereas it is classified as "pre-frail" if having 1 or 2 and "robust" when none is recorded [66]. The second approach most commonly used to evaluate frailty is the Frailty Index (FI), which considers the accumulation of age-related health deficits displayed by an individual [95]. The FI is calculated as the number of deficits divided by the total number of potential health deficits under consideration and high values of FI indicate a greater degree of frailty. It is important to note the FI not only takes into account physical measures but it also encompasses additional variables including cognitive and psychosocial aspects, thus assessing the multidimensionality of frailty [96]. Although they are seminal works in the frailty research field, the diagnosis of frailty using these scales is complicated in a primary care setting due to the required techniques, time or amount of information and consequenty, they are not implemented in health systems and the everyday clinics [97].

For this reason, adaptations of these scales and other easier or faster tools have been developed with the aim of identifying and screening frailty in the clinical practice. These can be grouped in accordance with their conceptual approach. One set of tools is based on the measurement of the functional performance of the individual, which could represent aspects of physical frailty, and includes Gait Speed (GS) [98], [99], Timed Up and Go (TUG) [100], [101], Barthel Index [102] and the Short Physical Performance Battery (SPPB) tests, among others [68], [103]. The SPPB test is gaining importance in the last years for the identification of frailty since is a fast and simple test that measures function in three different ways. It is composed of GS, a test of balance and a measure of the time needed to stand up from a chair 5 consecutive times [104]. Another set is composed of tools and questionnaires on the basis of clinical data, routine, and functional performance criteria that are able to predict the occurrence of adverse effects. This is the case, for instance of the "FRAIL" scale [105] or the Tilburg Frailty Indicator (TFI), a self-report user-friendly questionnaire for assessing multidimensional frailty among older people that is based in a physical, a psychological and

a social domain [106]. Finally, there is a smaller group of measures based on clinical judgment, such as the Clinical Global Impression of Change in Physical Frailty instrument (CGIC-PF) [107], Clinical Frailty Scale [96], or the Gérontopôle Frailty Screening Tool (GFST) [108]. A summary of the principple tests applied for the detection of frailty is shown in ***Table I1***. However, there is no agreement on a standard assessment instrument for identification and screening of frailty in clinical practice.

Table I1. Short description of the main tests applied to detect and measure frailty.

Frailty assessment test	Description
Fried´s frailty phenotype [66]	Presence or absence of a set of five criteria: weakness (low grip strength), slow walking speed, low physical activity, self-reported exhaustion and unintentional weight loss. An individual is considered as "frail" if 3 or more of these features are present, whereas it is classified as "pre-frail" if having 1 or 2 and "robust" when none is recorded.
Frailty Index (FI) [95]	It considers the accumulation of age-related health deficits displayed by an individual and it is calculated as the number of deficits divided by the total number of potential health deficits under consideration. High values indicate a greater degree of frailty.
Tilburg Frailty Indicator (TFI) [106]	A user-friendly questionnaire based on a multidimensional approach. It is composed of a physical, a psychological and a social domain.
Gait speed (GS) [99]	Expressed in meters per second (m/sec). Participants were asked to walk at their usual pace. The test was performed twice and GS was calculated based on the shorter time.
Timed up-and-go (TUG) [100], [101]	The time needed to stand up from a chair, walk 3 meters, turn around, walk back and sit down, with the help of their usual walking aid, if any. The individual is considered frail when it takes more than 10 seconds to complete the test.
Short Physical Performance Battery (SPPB) [104]	A functional capacity test composed of gait speed, test of balance and time needed to stand up from a chair 5 consecutive times.
Gerontopole Frailty Screening Tool (GFST) [108]	Based on clinical judgement. 6 yes/no questions that help the physician to evaluate the existence of frailty.
Barthel Index [102]	A multiparametric test measuring the performance in activities of daily living and mobility.

2.3. Multidimensionality of frailty

One of the characteristics that has reached consensus about frailty is that it represents a multidimensional syndrome [96], [109], [110]. Thus, there is a physical component as well as cognitive impairment, which has been integrated in the concept of "cognitive frailty" [111], [112]. This concept has been defined as an heterogeneous clinical condition related to age described by the simultaneous presence of cognitive impairment and physical frailty [113]. As occurs with physical frailty, there are no validated tools to accurately detect cognitive frailty in research and clinical practice. Thus the available tests such as the Mini-Mental State Examination (MMSE), the Montreal Cognitive Assessment test (MoCA), the Alzheimer's Disease Assessment Scale-cognitive subscale (ADAS-Cog) and speed processing tests explore memory performance, executive functions and other cognitive functions [90], [114]. Of note, there is an interaction among them since physical frailty could increase the risk of future cognitive impairment and that cognitive decline may increase the chances to develop frailty [115]. Under some circumstances, cognitive frailty may facilitate or become a precursor of neurodegenerative processes [116]. In addition, other additional aspects such as psychosocial or nutritional factors are gaining attention since they play a role in frailty [111].

2.4. Biomarkers and molecular mechanisms involved in frailty

Biomarkers are highly valuable tools in the diagnosis and stratification of patients as well as in the understanding of the molecular, genetic and epigenetic pathways that are dysregulated in disease [117], [118]. Aiming to complement the functional tests and questionnaires, in the last years, different studies have been conducted to identify potential biomarkers of frailty and understand at a biological level, the underlying molecular mechanisms of frailty [119]. Most of the knowledge about the physiopathology of frailty comes from independent observational studies [120], [121]. Indeed, alterations in oxidative stress and inflammation, immune response, and changes in the endocrine or vascular system have been involved in frailty [122], [123]. In particular, molecules related to oxidative stress and inflammation have been frequently described altered in frail individuals and have been postulated as potential biomarkers of frailty [122]. Thus, different studies have shown an increase of oxidative indicators and reduced levels of antioxidant molecules in frail individuals

[123]–[125]. Regarding inflammation, higher serum levels of IL6 and elevated inflammatory molecules such as CRP, factor VIII, and fibrinogen were found in frail individuals compared to robust ones [126]–[130]. In addition, individuals with cognitive frailty presented high levels of inflammatory cytokines such as IL6, TNFα, interleukin 18 (IL18), interleukin 1 beta (IL1β) and CRP [131], [132]. A very recent review has postulated that under a geroscience perspective, it is possible to conceive that molecular and cellular mechanisms leading to aging would also determine frailty onset and severity [133]. Indeed, hallmarks of aging such as senescence, nutrient sensing or inflammation, among others, may be related to frailty [133].

The relevance of inflamation and oxidative stress in frailty has been further confirmed, since there are several mouse models that have demonstrated their role in the appearance and progression of frailty. The *IL10*$^{tm/tm}$ mouse model, which display deletion of the anti-inflammatory cytokine interleukin 10 (IL10), present chronic inflammation, with increased levels of cytokines such as IL1β, IL6 or TNFα. It also includes muscle weakness, impaired cardiac and vascular functions [134]–[136], closely resembling human frail phenotypes. On the other hand, studies in a transgenic mouse model with moderate overexpression of the antioxidant glucose-6-phosphate dehydrogenase (G6PD), the enzyme responsible for Nicotinamide Adenine Dinucleotide Phosphate (NADPH) protection against oxidative damage, revealed that these mice exhibit increased resilience in response to age-associated decline of muscular and brain function [137].

One of the reasons that may explain the limited knowledge about the molecular basis of frailty is the existence of only a few omics-based studies that analyze frail and robust individuals from a global and unbiased perspective. In this sense, the FRAILOMIC Consortium [138], [139], was the first attempt to perform a multi-omic approach with the aim to unravel molecular mechanisms and identify new predictive signatures of frailty from eight European cohorts that comprise more than 75.000 individuals. This study revealed a statistical association of few biomarkers related to oxidative stress, vitamin D, and cardiovascular system, as well as some miRNAs with frailty [140]. A recent transcriptomic study in 16 middle-aged pre-frail or frail and robust individuals from the United States found pathways related to inflammation and immunity that were associated with frailty and also showed different gene expression patterns between white and black frail patients [141]. In addition, few studies performed metabolomic approaches, which revealed divergent results but several metabolites related to antioxidation, nitrogen, amino acid metabolism and Vitamin E

associated to frailty [142]–[145]. In addition to the miRNAs described by FRAILOMIC study, other studies have detected differential expression of several miRNAs associated to frailty [146]–[150]. Notably, their altered expression has been linked to alterations in critical biological processes. For instance, higher *miR21* levels in frail individuals promoted pro-inflammatory cytokines, including IL6 and TNFα and TGFβ [151]. These studies have started to unravel molecular mechanisms associated with frailty status but they still need to be further investigated in other cohorts to test their validity before they could be applied in the clinic as reliable biomarkers and predictors of frailty. In addition, no studies have been described characterizing the potential reversibility of biomarkers after an intervention plan.

3. Centenarians as models of healthy aging

3.1. Description of centenarians

Different individuals display different aging trajectories and there are groups that can give clues about the biology of aging. Even though it is a controversial topic [6], [152], [153], there is evidence postulating that the maximum age of human life is located around 115 to 120 years [6]. Centenarians are a population group that exhibits extreme longevity and that are growing exponentially in recent years, with expectations of becoming the age group with the highest growth rate in the coming decades [154]. Their extreme longevity seems to be accompanied by better cognitive function, fewer comorbidities and greater quality of life [155]. Indeed, there are two main hypotheses to explain the long life of centenarians. The first one is the "compression of morbidity" theory, which suggests that morbidity and disability would be compressed toward the end of life [156] (***Figure I11***). In this line, epidemiological and longitudinal studies in cohorts such as the Long Life Family Study (LLFS) [157], New England Centenarian Study (NECS) [158], Longevity Genes Project (LGP) [159], and Healthy Aging and Biomarkers Cohort Study (HABCS) [160], among others, have shown that centenarians are associated with better cognitive functions and need less help with the activities of daily living in comparison with the elderly [161]. Additionally, they exhibit medical histories with low incidence rates of age-associated common pathologies, such as dementia and neurodegenerative diseases including AD [162], cardiovascular diseases [163], [164],

diabetes mellitus [165], and cancer [166]. Moreover, some centenarians delay or avoid their first disease experience and present lower burden of chronic diseases, which normally cause mortality in the general population at earlier age [167], [168]. In summary, this hypothesis describe that centenarians are characterized by a remarkable compression of age-associated morbidity, to such an extent that their healthspan approximates their lifespan. On the other hand, the hypothesis of the "expansion of morbidity" [169]–[171] suggests that additional years of life are accompanied by increased rates of disease, morbidity and increasing number of years spent in poor health in long-lived individuals (***Figure I11***). In this line, centenarians have been linked with a high disease burden [172], and diminished physical and cognitive functions [173]–[177].

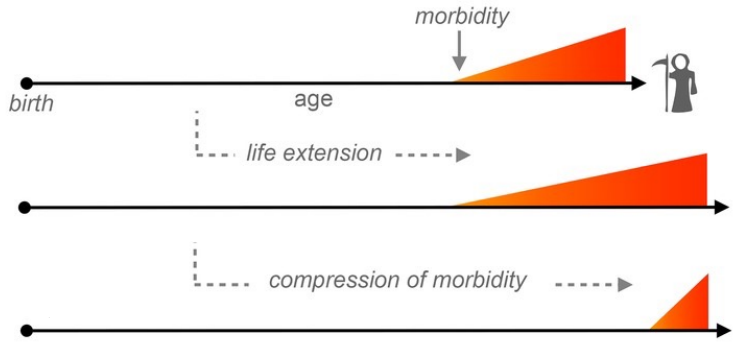

Figure I11. Expansion and compression of morbidity hypotheses in centenarians. The extended longevity that characterizes centenatians can be accompanied by increased rates of disease and morbidity, increasing number of years spent in poor health (expansion of morbidity). In contrast, the onset of chronic diseases and disability (morbidity) can be delayed, resulting in compression of the overall morbidity incurred in a lifetime. Adapted from [12].

The explanation to this putative contradiction comes from the description of three different types of centenarians, that were divided based on the age of onset for age-related diseases and categorized on "survivors" (age of onset before 80 years), "delayers" (age of onset 80 – 99 years), and "escapers" (no history of any of the common age-related diseases prior to 100 years) [178]. Of note, 80 % of centenarians belonged to "delayers" or "escapers" groups indicating that the majority of them delay their first experience of diseases, till beyond the age of 90 years or even escape these morbidities entirely [178]. Therefore, centenarians are considered examples of successful aging and they have been

postulated as a model of healthy aging [179]. Consequently, they are an attractive population for the understanding and identification of the mechanisms involved in human longevity and healthy aging pathways [179].

Significant efforts have been completed in order to understand the characteristics and reasons for the extreme longevity of centenarians and several studies have described that they are multifactorial and come from both internal and external factors [180]. In this sense, environmental factors or life habits, such as healthy diet, physical activity, healthy behaviors (avoidance of smoking or excessive alcohol consumption), active engagement and development of social networks, have been associated to centenrian populations [181], [182]. Nevertheless, biology and genetics plays also an important role. In this regard, several studies have reported that the variation in human lifespan can be attributed to genetic and molecular factors [183], [184]. This point will be detailed in the following section. Moreover, other studies have observed that individuals with exceptional familial longevity showed better lipid profiles, with lower levels of triglycerides, when compared with other elderly cohorts [157]. In addition, reduced levels of blood glucose, alanine-aminotransferase (ALT), cholesterol and platelet levels have been observed in centenarians [185]. Of note, centenarians offspring also tend to live long, present lower risk of all-cause mortality as well as age-associated diseases such as cardiovascular diseases or cancer, and exhibit better functional and cognitive status [179], [186], [187], further supporting the relevance of genetics in the extended longevity of centenarians.

3.2. Genetics and molecular mechanisms related to centenarians

Different approaches have been used to decipher the biology and genetics of centenarians in order to identify key anti-aging pathways [183], [188]. In an attempt to find genetic variants associated with human longevity, several genome-wide association studies (GWAS) have been performed in cohorts of centenarians but relatively few variants have shown genome-wide significance with longevity [189]. Of these, the most remarkable genetic findings that have been replicated across different populations were the single-nucleotide polymorphisms (SNPs) from the TOMM40/APOE/APOC1 locus [184], [190], [191]. During the last years, several genes involved in glucose metabolism (*IGF1*), oxidative stress (*SOD3*, *HSPA*), genome maintenance (*P53*), cognitive pathways (*APOE*), lipid metabolism (*CETP*), and

development (*FOXO1, FOXO3*) have been described to influence longevity in humans [192]–[195]. Of note, apolipoprotein E (*APOE*) [196], *IL6* [197], forkhead box (*FOXO*) [198]–[201] and *IGF1* [202] genes have repeatedly been associated with centenarians, becoming the so-called "longevity genes" [188].

In addition, other studies have measured genes associated with hallmarks of aging and have described alterations in markers of stem cells and senescence. Thus, a study performed in peripheral blood mononuclear cells (PBMCs) of 22 young, 32 octogenarian and 47 centenarian individuals revealed that centenarians overexpressed pluripotency and stemness-related genes such as *OCT3/4, SOX2, c-MYC, VIM, BMP4, NCAM*, and *BMPR2*, when compared with octogenarians [203], Moreover, the analysis of blood samples of individuals of different ages, indicated that lymphocytes from centenarians displayed reduced expression levels of senescence markers when compared to old donors [204]. Additionally, omic approaches have begun to be used to identify the biology associated with centenarians. A transcriptomic analysis in PBMCs of individuals of different ages, identified 1721 messenger ribonucleic acids (mRNAs) differentially expressed in centenarians when compared with septuagenarians and young people [205]. Indeed, centenarian´s pattern was more similar to young than septuagenarians. The classification of the differentially mRNAs levels revealed that the signaling pathways related to centenarians were associated with apoptosis [205]. Moreover, a recent study characterized the serum proteome of 77 centenarians and identified 1312 proteins that significantly differ between them and elderly individuals, and revealed protein signatures that are able to predict the extended survival of centenarians [206].

It has been also shown that epigenetic modifications can also contribute to the extended longevity of centenarians by three distinct principal mechanisms: DNA methylation, post-translational histone modifications and non-coding RNAs. Regarding DNA methylation levels, a significant decrease in global DNA methylation and the number of methylated CpGs with age has been reported but it has been shown to be less pronounced in centenarian indivuals [207]–[210]. Specifically, genes involved in nucleotide synthesis, metabolism and control of signal transmission were hypomethylated in centenarians, whereas DNA hypermethylation seems to occur predominantly in genes linked to the development of anatomical structures or organs and to the regulation of transcription [207]. On its part, non-coding RNAs and in particular miRNAs, have been shown to be differentially expressed

between young, older adults and centenarians [211], [212]. Indeed, it has been described that the expression pattern of miRNAs from centenarians was similar to young and vastly different than older adults [213]. These results were coherent with another study that showed that the expression of genes implictated in the miRNA biogenesis pathway were severely down-regulated in octogenarians when compared with young people and centenarians [214]. Altogether, these findings indicate that specific genetic and molecular factors are linked to centenarians, which may explain the striking maintenance of homeostasis and the healthy aging characteristic of this population group. In addition, previously described studies have shown that centenarians resemble young individuals at biological and molecular level, and that they differ from the elderly ones, which reinforces the interest in studying their biology.

The majority of the studies have been performed in blood samples and the mechanisms responsible for promoting the maintenance of cognition that characterize centenarians remain largely unknown. In this sense, there are 2 studies that were performed using human brain samples of different ages. The first one, showed that the differential gene expression pattern observed in centenarians was similar to the one of young individuals [215], further indicating that the expression pattern is altered (up-regulated or down-regulated) with aging from young to older age, but it might be maintained in centenarians. In the second and more recent study, transcriptomic analyses (RNAseq and microarray) were performed in frontal cortex samples of individuals organized in 2 different groups according to their age (≤ 80 versus ≥ 85 years) [216]. This study indicated that the ≥ 85 years group of age was associated with a distinct transcriptome signature in the cerebral cortex that was characterized by downregulation of genes related to neural excitation and synaptic function and upregulation of the RE1 Silencing Transcription Factor (*REST*) in cortical neurons [216]. *REST* is a general repressor of genes involved in neuronal excitation and synaptic function that plays a neuroprotective role against a large set of biological processes associated with aging such as premature neural stem cell depletion, neuronal hyper-excitability, oxidative stress, neuroendocrine system dysfunction and neuropathology [215], [217]–[219]. In addition, the study cited above generated a model of *Caenorhabditis elegans* (*C. elegans*) with overexpression of *spr-4* gene, which encodes a structural and functional ortholog of the mammalian *REST* that resulted in extended lifespan [216]. Notably, all these studies confirm the usefulness of take advantage of centenarian´s samples to unravel relevant pathways and processes involved in the biology of aging.

4. The impact of aging on the brain

4.1. The brain

The human brain is complex, highly organized and a key organ of the central nervous system (CNS) which commands movement, emotions, communication, thinking and memory, among others [220]. Its development starts with neurulation from the ectoderm of the embryo and it takes, on average, 20 to 25 years to mature [221]. This process involves the generation of a wide variety of specialized neural and non-neural cell types that must be produced in the correct numbers, at appropriate locations and with the right timing together with accurate connections in order to ensure the communication between distinct cell populations and the correct control for behavior, perception and higher cognitive function [220], [221].

The human brain consists of three main areas, the cerebrum, the cerebellum and the brainstem [222]. The cerebrum, which comprises grey matter (cerebral cortex) and white matter, is the largest part of the brain and takes control over motor and sensory information, (un)conscious behaviors, feelings, intelligence and memory [222]. In the other hand, the cerebellum controls the coordination of voluntary movement, posture, balance and equilibrium. Finally, the brainstem, which includes the midbrain, the pons and the medulla, connects both the cerebellum and the cerebrum with the spinal cord and contains the principal centers to perform autonomic functions such as breathing or heart rate [222]. Additionally, there are deeper structures within the brain such as the pituitary gland, hypothalamus, amygdala, pineal gland, ventricles or the hippocampus, which have different functions [220]. The hippocampus is made up of several structures called *cornu ammonis* areas (CA1-4), the dentate gyrus (DG) and the subiculum, which are collectively known as the hippocampal formation [223]. The hippocampus is part of the temporal lobe and it is responsible of memory, learning and emotion [224]. A representation of the human brain anatomy showing the main structures can be seen in the ***Figure I12***.

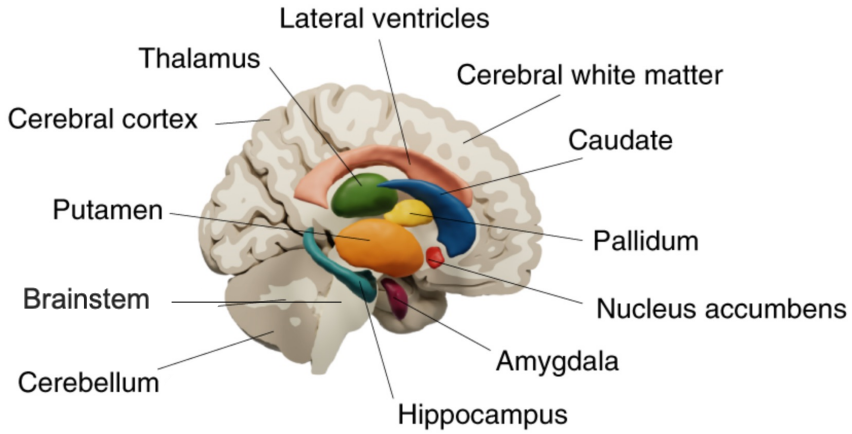

Figure I12. Representation of the main structures of the human brain. The brain consists of three main areas, the cerebrum, the cerebellum and the brainstem together with deeper structures. Addapted from [225].

4.1.1. Main characters: neurons and glial cells

The two predominant cell types in the human brain include neurons and glial cells [226]. Indeed, it contains billions of neurons and hundreds of trillions of nerve connections [227]. Moreover, these neurons are surrounded by a vast number of glial cells, whose presence in the brain, compared with neuronal amount, is equivalent or even greater [226].

4.1.1.1 Neurons

Neurons are the structural and functional unit of the CNS and they are composed of common regions that include a cell body, dendrites and an axon. They are polarized and electrically excitable cells that are responsible for the processing and transmission of nerve impulses [220]. Thus, they are responsible for receiving external sensory input, for sending motor commands to our muscles, and for transforming and relaying the electrical signals at every step in between. The neurons communicate between them and with other cells using neurotransmitters released from their synapses, and they may be inhibitory or excitatory [228]. Moreover, neuronal axons are covered with a multilamellar membrane of myelin, which facilitates rapid signal conduction and promotes insulating properties [229]. Neuronal bodies are located in the grey matter of the cerebrum, whereas myelinated axons are mainly

located in the white matter. Additionally, 3 classes of neurons can be distinguished, the sensory neurons, motor neurons and interneurons [230]. Motor neurons are responsible for transmitting nerve impulses from the CNS to the muscles to perform voluntary movements whereas sensory neurons transmit information from the sensory organs to the brain so that it processes all the information [230]. The interneurons connect with all the other neurons in order to create neurological networks. Of note, cortical interneurons play a role in modulating cortical activity, needed for cognition and many aspects of learning and memory [231], [232].

4.1.1.2 Glial cells

When glial cells were identified, they were suggested to only contribute to the structure of the brain, being the supporting cells for the neurons [233]. However, research during the following decades has demonstrated that glial cells contribute and regulate different processes such as the correct neurotransmission, neural damage repair, blood flow to the brain and even adult neurogenesis [234]. The main glial cells from CNS include on the one hand astrocytes, oligodendrocytes and ependymal cells, known collectively as macroglia and in the other hand, microglia [235]. Oligodendrocytes, are responsible for the production of myelin, which maintains the electrical impulse conduction of nerve signals and maximizes their velocity as needed [236]. Ependymal cells are ciliated-epithelial glial cells that play a critical role in cerebrospinal fluid homeostasis, brain metabolism and the clearance of waste from the brain [237]. Finally, astrocytes are the most abundant type of glial cell and occupies approximately 25 % of the total brain volume [238]. They have a structural and functional diversity; thus, they can be classified as either protoplasmic (present in the grey matter) or fibrous (present in the white matter) [239]. They have star-like shape and several branches that can interact with both synapses and blood vessels. Additionally, astrocytes are implicated in a variety of structural, metabolic, and homeostatic functions [240]. In particular, processes such as metabolic regulation, support of synaptic transmission and blood-brain barrier formation are tightly regulated by astrocytes [241]. On the other hand, microglia have also an important function in brain homeostasis through the control of neuronal proliferation and differentiation, as well as influencing formation of synaptic connections [242]. Additionally, microglia are part of the innate immune system and play a key role in detecting external signals (invading pathogens) and internal damaged or dying cells, which is why they are also known as the resident macrophages of the CNS [243].

4.1.2. Neural stem cells (NSCs) and neurogenesis

During the embryonic development, embryonic stem cells contribute to the formation of every tissue in the body as they are able to generate all cell lineages [244]. During the mammalian embryonic formation of the CNS, neuroepithelial cells-derived radial glia give rise to the different cell types of the brain [245] and other progenitors persist through adulthood giving rise to adult neural stem cells (NSCs) [246], [247]. Postnatal adult stem cells are present in all tissues, where they reside in specialized environments, called niches [248]. In the adult mammalian brain, NSCs are mainly found in the neurogenic niches, which comprehend the subventricular zone (SVZ) around the lateral ventricles and the sub-granular zone (SGZ) of the DG in the hippocampus [249], [250]. These NSCs stay dormant, in a quiescent state as a reserve pool of cells available for tissue regeneration and cell replacement [251]. In response to stimuli, NSCs get activated triggering their proliferation and giving rise to neural progenitor cells, which have the potential to differentiate into new neurons, astrocytes and oligodendrocytes [249], [252]. Moreover, a subset of astrocytes was identified as NSCs, able to generate neurons in the adult mice brain [253].

Neurogenesis is defined as the process of generating new functional neurons from neural progenitors that occurs during embryonic and perinatal stages, and continues throughout life in discrete regions of the CNS of mammals [254]. The first evidence of adult neurogenesis was obtained five decades ago in the mouse brain by using tritiated thymidine labelling, which gets incorporated into the DNA of dividing cells, where the presence of proliferating glial cells throughout the adult brain parenchyma was demonstrated [255]. Nowadays, adult neurogenesis its known to be a dynamic process that comprises the proliferation of NSCs and progenitor cells, further differentiation and maturation of the cells before being integrated into the neural networks [256], [257]. Active neurogenesis is limited to the two neurogenic niches and outside it appears to be extremely limited or non-existent in the whole adult mammalian CNS [258], [259]. In the adult hippocampus, neurogenesis could be promoted following stimuli and modulate its structural plasticity [260]. Indeed, several studies have shown the effects of new-born neurons on existing neural circuitries and their functional contribution to brain tasks under physiological and pathological conditions [261], [262]. In the DG, the newly formed neurons project to the CA2 region [263], which plays crucial roles in social memory and contextual discrimination [264]–[266] (***Figure I13***). Additionally, new neurons promote excitation of the CA3 pyramidal neurons, mossy cells and

hilar interneurons [267], which are essential for memory recovery and for delivering feedback inhibition into the mature DG neurons [268]. As mentioned above, the hippocampus governs learning and memory processes, so it is an area of particular interest in aging and cognition that is intimately linked to cognitive decline [269], [270].

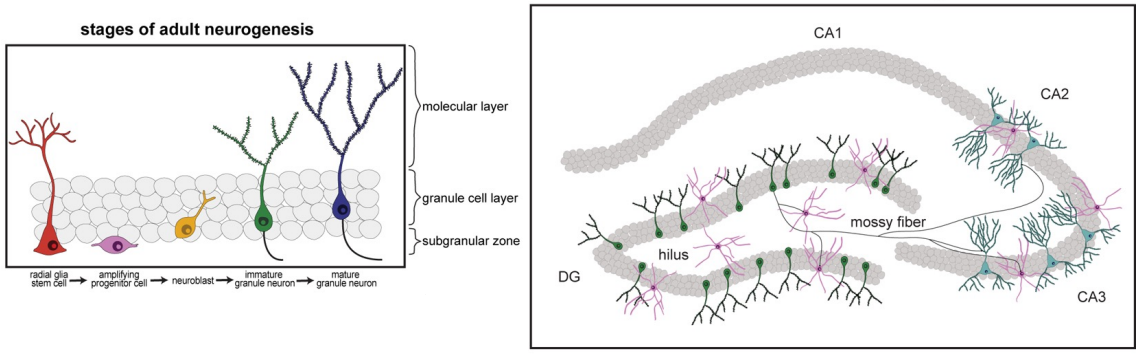

Figure I13. Overview of adult neurogenesis in the hippocampus, the circuitry into which the new cells are incorporated. In the left, different stages of adult neurogenesis in the dentate gyrus (DG) of the hippocampus are summarized. New granule neurons originate from radial glial stem cells residing in the sub-granular zone (SGZ). These stem cells give rise to amplifying progenitor cells that in turn produce neuroblasts, that migrate into the granule cell layer and develop into immature granule neurons with a single dendritic tree extending toward the molecular layer and an axon (mossy fiber) extending through the hilus toward the CA3 and CA2 subfields. In the right a schematic diagram of new neuron projections is represented, showing the different hippocampal subfields (DG, CA3, CA2, and CA1) which serve as new neuron targets. Mossy fibers from new granule neurons form connections with hilar mossy cells, pyramidal cells in the CA3 and CA2, as well as with inhibitory interneurons in the DG, hilus, and CA3. Adapted from [266].

4.2. Brain aging

4.2.1. Structural and cellular changes

Although human aging affects the entire organism, brain aging is especially distinctive. At macroscopic level, aging alters human brain structure and the whole brain volume decreases in size [271]. There is a shrinkage of grey and white matter volume and an expansion of the ventricular system [272]. At functional level, all the cognitive abilities (attention, memory, executive cognitive function, language and visuo-spatial abilities) suffer

a functional decline until they reach a point in which the individual is not able to perform the everyday functions, a physical state termed dementia [273]. At cellular level, aging promotes the loss of nerve fibers and neuron demyelination, the reduction of dendritic length and branching, and the partial loss of synapses [274]. Moreover, neuronal synapses at the hippocampus become dysregulated with age, which may be due to morphological alterations of the synapse itself, impaired neurotransmitter signaling or changes in protein or gene expression [269], [275]. Besides neurons, astrocytes lose their ability to carry out their normal functions and release detrimental factors which can affect neurons and oligodendrocytes [276], [277]. With age, there is also a decline in the number of functional NSCs within the neurogenic niches [278]–[283] and the ability of NSCs to proliferate and differentiate into new neurons decreases in a devastating manner [284], [285]. This correlates with the presence of lower neurogenesis that diminishes the production of new neurons, limits plasticity and repair capacities of the brain, which underlie age-related cognitive decline [286], [287]. The decrease in neurogenesis with age is accompanied by poorer performance on learning and memory tasks and by reduced olfactory discrimination in both hippocampus and SVZ, respectively [288]–[290]. This decreased neurogenesis involves dysregulation of intrinsic pathways crucial for NSC maintenance, such as increased NSC dormancy, decreased self-renewal, reduced neural differentiation, and induced cell death [277], [291]. Besides, external factors have been also described to have an impact on neurogenesis increasing the complexity of brain aging process [14].

The presence of adult neurogenesis in the human brain has been a theme of controversy. On the one hand, a study indicated that there is a decrease in the number of neurons in the DG during the period of life, with very few cells detected between 7 to 13 years and no new neurons in individuals of 18 to 77 years [292]. Consistent with this study, it has been observed a decrease in number of neurons during adult lifetime, confirming that generation of new neurons does not keep up with neuronal loss [293]. In the contrary, several studies have reported and described the presence of neurogenesis [294]–[296], and the existence of cells responsible for neuronal and glial production [297]. Moreover, a similar number of glia, intermediate progenitors, immature and mature neurons was found in individuals from 14 to 79 years, supporting that adult neurogenesis is preserved in healthy individuals over 65 years old [298]. Additional studies further support the idea that neurogenesis is preserved in adult humans [257], [299].

4.2.2. Biology and molecular changes of brain aging

The study of brain aging has drawn the attention of scientific community in the research of aging-associated mechanisms underlying brain dysfunction [300]. In the past years, many molecular changes relevant to brain aging have been discovered using various data types and modeling techniques [301] and they have been linked to cognition, mental health, brain structure and pathology during aging [14]. Aging alters overall intercellular communication in the brain and the different cell types, being the apparition of a chronic neuroinflammation one of the most prominent alterations that impact on brain function and may contribute to the onset of neurodegenerative diseases [302]. During aging, the different cell types of the brain display molecular alterations. For instance, astrocytes undergo changes such as increased expression levels of intermediate filament proteins (glial fibrillary acidic protein (GFAP) or vimentin), increased expression of inflammatory cytokines (IL6, IL1α or TNFα), accumulation of lipofuscin in the cytoplasm and morphological changes [303]–[305]. During aging, they also can induce a pro-inflammatory microenvironment and the apparition of SASP that may contribute to the cascade of events leading to progressive neuronal damage and impact in cognition [306]–[308]. Moreover, alterations in relevant molecular pathways of hallmarks of aging promotes mitochondrial dysfunction, disabled autophagy, loss of proteostasis, genomic instability and epigenetic alterations, among others, in brain aging [25], [309], [310]. For instance, hippocampal mitochondria dysregulation leads to the generation of ROS and activation of apoptosis [311], [312]. Related to proteostasis, the proteasome activity and autophagy have been shown to be significantly decreased in hippocampus and cerebral cortex during aging [25], [313]. Indeed, experimental amelioration of proteostasis delays the aging process. Intranasal application of recombinant human HSP70 protein to mice enhanced proteasome activity, reduced brain lipofuscin levels, improved cognitive functions, and extended lifespan [314]. Similarly, administration of the chemical chaperone 4-phenylbutyrate to aged mice reduced endoplasmic reticulum (ER) stress in the brain and improved cognition [315]. Related to epigenetic alterations, histone methylation and acetylation changes participate in the dysregulation and loss of neuronal synapses observed during aging [275]. In line with this, we have recently shown the enrichment of several histone deacetylases (HDACs) in aged human hippocampus where they correlated with microglial and senescence markers [316]. In summary, the molecular changes described during aging contribute to a decline in cognitive abilities, sensory perception, motor function and coordination [317], and the onset of neurodegenerative diseases [274]. Thus, the

identification of specific molecules and pathways that are dysfunctional or altered during aging and impact upon cognitive function, may represent good therapeutic targets.

Hypothesis and objectives

Hypothesis

In recent years, significant efforts have been made in the functional characterization of frailty and hence multiple instruments have been proposed for the screening of frailty in research or clinical practice. However, the biology underlying frailty remains relatively poorly explored. Transcriptomic analysis of peripheral blood cells of frail individuals, classified as frail by several scales that take into account the multidimensionality of frailty, could point out a molecular pattern of differentially expressed genes in frail individuals which could become potential biomarkers to detect frailty. In order to be reliable, the expression of these genes should be restored after different types of intervention plans. To be important in the pathofisiology of frailty, they should be involved in molecular pathways and biological processes related to cell aging.

Different individuals display diverse aging trajectories and there are groups that can give clues about how to display successful aging. Centenarian individuals exhibit extended longevity that is accompanied by fewer comorbidities, and better quality of life and cognitive function. Consequently, they could be an attractive population for the identification of the molecular mechanisms responsible for human longevity, successful aging and maintenance of cognition. Transcriptomic analysis of hippocampus samples of individuals of different ages, including centenarians, could identify gene expression patterns responsible for deterioration or maintenance of cognition.

Objectives

1. Identification of molecular mechanisms underlying frailty
   1.1. Unravel the molecular mechanisms underlying frailty through a transcriptomic analysis of blood samples from robust and frail individuals.
   1.2. Characterize the expression of the novel molecular mechanisms of frailty after different intervention plans.
   1.3. Determine the expression of novel molecular mechanisms of frailty in cell aging *in vitro*.
   1.4. Determine a minimun set of genes that could be used as a biomarker of frailty.
   1.5. Identify the molecular pathways and biological processes underlying the activity of the novel minimun set of genes linked to frailty.
   1.6. Characterize the function of the novel minimun set of genes in cell aging and longevity.

2. Human hippocampal transcriptome characterization with age
   2.1. Identify the molecular mechanisms underlying maintenance of cognition through a transcriptomic analysis of brain samples from centenarians.
   2.2. Determine the molecular mechanisms underlying brain aging through a transcriptomic analysis of brain samples from young and elderly individuals.
   2.3. Characterize the cell types and biological processes associated to the novel molecular mechanisms associated to maintenance or deterioration of cognition.
   2.4. Study the function of the novel molecular mechanisms linked to cognition.

Materials and methods

1. Human samples

1.1. Human samples used in the frailty study (first chapter)

In the first chapter of this doctoral thesis, the studies were performed in PBMCs, serum and plasma samples from different cohorts (***Table M1***).

Table M1. Information of human samples used in the frailty study (first chapter of this doctoral thesis).

Cohort	Material	Individuals (n)	Origin	Study used
Microarray cohort	PBMCs	25 (7 frail and 5 robust)	Basque Biobank [318], [319]	Gene expression microarray
Validation cohort 1 (extension of the microarray cohort)	PBMCs	103 robust, 17 frail	Basque Biobank [318], [319]	Validation of the array expression
Validation cohort 2	Serum	124 robust, 44 frail	Basque Biobank [320]	Validation of the array expression
Validation cohort 3	PBMCs	19 robust, 32 functionally impaired	Basque Biobank [321]	Validation of the array expression
Intervention cohort 1	PBMCs	12 (pre- and post-intervention)	Basque Biobank	Pilot intervention study
Intervention cohort 2	Plasma	95 (pre- and post-intervention)	UBC (Ageing On)	Intervention study
Intervention cohort 3	Plasma	18 (pre- and post-intervention)	Valencia Hospital (SWIMFRAIL)	Intervention study

PBMCs, Peripheral blood mononuclear cells; UBC, University of the Basque Country.

The gene expression microarray of the frailty study (first chapter of this doctoral thesis), was done in PBMCs from a cohort (microarray cohort) of community-dwelling elderly people aged 75 or older independents at inclusion, from the province of Gipuzkoa in Basque Country (Spain) [318], [319]. Frailty status was determined using three different instruments: TUG, GS and TFI. A sample of 25 individuals was selected for transcriptome screening (***Table M2***). Among these 25 participants, 7 were classified as frail and 5 as robust by the three tools

used, while the other 13 subjects did not obtain the same classification and they were classified as robust or frail only by 1 or 2 of the tests used.

Table M2. Clinical characteristics of the patients included in the gene expression microarray of the frailty study. The shading indicates subjects classified as frail in each scale.

Biobank code	Sex	Age (years)	TUG	GS	Tilburg
HD53D140039	F	79	Frail	Frail	Frail
HD53D140018	F	82	Frail	Frail	Frail
HD53D140021	M	83	Frail	Frail	Frail
HD53D140011	F	85	Frail	Frail	Frail
HD53D140002	M	86	Frail	Frail	Frail
HD53D140026	M	86	Frail	Frail	Frail
HD53D140037	M	86	Frail	Frail	Frail
HD53D140010	F	79	Robust	Robust	Frail
HD53D140013	F	79	Robust	Frail	Robust
HD53D140035	F	79	Robust	Robust	Frail
HD53D140044	M	79	Frail	Robust	Robust
HD53D140054	F	79	Robust	Frail	Robust
HD53D140004	M	79	Robust	Robust	Robust
HD53D140005	M	80	Robust	Robust	Robust
HD53D140015	M	81	Frail	Frail	Robust
HD53D140009	F	82	Frail	Frail	Robust
HD53D140006	F	82	Robust	Robust	Robust
HD53D140008	F	82	Robust	Robust	Robust
HD53D140012	M	83	Robust	Frail	Robust
HD53D140033	F	85	Robust	Frail	Robust
HD53D140003	F	86	Frail	Robust	Robust
HD53D140007	M	89	Frail	Robust	Robust
HD53D140016	F	90	Robust	Frail	Robust
HD53D140014	M	91	Robust	Robust	Robust
HD53D140050	F	92	Robust	Robust	Frail

F, Female; M, Male;

An extension of subjects from the cohort cited above, were included for the experimental validation of candidate genes (validation cohort 1) [318], [319]. Here too, only the individuals that were classified as frail (n = 17) or robust (n = 103) by TUG, GS and TFI were included. Additionally, the expression of the selected genes was studied in two

additional and independent cohorts. In the validation cohort 2 [320], frailty was assessed by Fried´s frailty phenotype, TUG and GS tests and only robust (n = 124) or frail (n = 44) individuals considering the three scales were selected. In the validation cohort 3 [321], frailty was assessed by the Frailty Index, the Barthel Index and the Canadian Study of Health and Aging (CSHA) Clinical Frailty scale and robust (n = 19) and functionally impaired individuals (n = 32) of advanced age were compared.

Finally, the expression of the selected genes was studied in 3 additional cohorts of individuals who underwent different types of interventions. The first cohort (intervention cohort 1), was composed of 12 frail subjects from Gipuzkoa (Basque Biobank) which participated in a 12 weeks duration pilot intervention plan consisting of a personalized physical training. The participants received 36 sessions of training including strength, flexibility and aerobic exercises, which was performed in groups at the sport and leisure facilities of the municipality. The impact of the intervention on individual physical activity was measured with TUG as well as SPPB tool. This study is coordinated by Itziar Vergara responsible of primary care group in the Biodonostia Health Research Institute and the detailed methodology and results are being described in an ongoing article. The intervention cohort 2 from the Ageing On group in the UBC, was composed of 95 individuals classified as pre-frail or frail based on Fried´s frailty phenotype. The participants performed 3 different types of intervention plans (dual task, walking and multicomponent) during 12 weeks. The impact of the intervention on individual physical activity was measured with Fried´s frailty phenotype. The intervention cohort 3 was composed of 18 frail individuals (frailty assessed by Fried´s frailty phenotype) from the Valencia Hospital and belonging to the project SWIMFRAIL. In this case, a physical intervention based on swimming exercises was carried out 3 times per week for a total of 12 weeks. The impact of the intervention on individual physical activity was measured with Fried´s frailty phenotype. In all cases, blood samples were collected before and after the intervention plan from all participants. We used PBMCs in the case of intervention cohort 1 and plasma samples in the case of intervention cohort 2 and 3.

1.2. Human samples used in the brain aging study (second chapter)

In the second chapter of this doctoral thesis, we used different human samples that are summarized in the ***Table M3***. Inclusion criteria for selection of patients included the

absence of diagnosis of neurodegenerative disorders as well as the lack of neuropathological injuries in the regions analyzed (except for the additional cohort 2 where the expression in healthy individuals was compared with patients with Alzheimer´s disease (AD)).

Table M3. Information of human samples used in the brain aging study (second chapter of this doctoral thesis).

Cohort	Material	Individuals (n)	Origin	Study used
Microarray cohort	RNA*	16	Basque Biobank	Gene expression microarray
Validation cohort 1	RNA*	120	UBC	Validation of the array expression
Additional cohort 1	Paraffin sections	23	Navarra Biomed	Protein expression
Additional cohort 2	Paraffin sections	20	DUH	Protein expression in healthy individuals and patients with AD

*The RNA was extracted from frozen samples of human hippocampus; UBC, University of the Basque Country; DUH, Donostia University Hospital; AD, Alzheimer´s disease.

The gene expression microarray of the aging study (second chapter of this doctoral thesis), was performed in human hippocampal samples from 16 individuals from the Basque Country (***Table M4***). In particular, this cohort comprises young individuals ranged from 27 to 49 years old (n = 5), elderly people from 58 to 88 years old (n = 8) and centenarian people from 97 to 100 years old (n = 3).

The validations were done in frozen human hippocampal samples of 120 individuals from a larger cohort of the UBC (Vitoria, Spain), provided by Marian Martínez de Pancorbo (head of DNA Bank of the UBC). This cohort comprises young individuals ranged from 27 to 49 years old (n = 78), elderly people from 65 to 88 years old (n = 38) and nonagenarian people from 92 to 96 years old (n = 4) [322]. Protein expression studies were performed in two different cohorts. On the one hand, paraffin sections of human hippocampus samples of 23 individuals from the cohort of Navarra Biomed (Pamplona, Spain), that comprises samples from young individuals ranged from 26 to 43 years old (n = 7), elderly people from 65 to 80 years old (n = 14) and nonagenarian/centenarian individuals

of 90 and 103 years old (n = 2). Secondly, we used paraffin sections of hippocampus and cortex samples from 20 individuals divided in 12 healthy individuals (young, from 36 to 47 years old (n = 3) and elderly, from 58 to 87 years old (n = 9)) and 8 patients with AD (from 62 to 82 years old (n = 8)), provided by the pathology service of the Donostia University Hospital (DUH) [323], [324]. This human brain samples were collected from autopsies conducted at DUH. In all cases, postmortem interval was limited to 12 h due to its effects on brain proteins. Brains were kept in a fixative solution (4 % paraformaldehyde) for a period of 24 h and embedded in paraffin.

Table M4. Information of human hippocampus samples used for the gene expression microarray of the brain aging study.

Group	Sex	Age (years)
Young	M	27
	M	30
	M	33
	M	35
	F	49
Old	M	58
	M	62
	M	70
	M	75
	M	76
	M	77
	M	79
	F	88
Centenarian	F	97
	F	99
	M	100

F, Female; M, Male.

In addition to the cohorts mentioned above, public available datasets were also used. RNAseq data from white matter of forebrain, hippocampus, parietal neocortex and temporal neocortex from aged individuals were obtained from "Aging, Dementia and Traumatic Brain Injury (TBI) Study" (https://aging.brain-map.org/rnaseq/search) [325]. This cohort encompasses 54 participants from 78 to 100+ years old (female n = 22, male n = 32), among which 24 presented dementia (AD, vascular dementia, multiple etiologies, or other

medical dementia), while other 30 did not present any of these disorders. For the studies in microglia, RNAseq data originated from the bulk human dorsolateral prefrontal cortex (n = 540) and from purified human microglia (n = 10) from the same brain region were studied (http://shiny.maths.usyd.edu.au/Ellis/MicrogliaPlots/) [326]. Transcriptomic data in the brain and different human tissues (endocrine tissues, respiratory system, proximal digestive tract, gastrointestinal tract, liver, gallbladder, pancreas, kidney, muscle tissues, connective and soft tissue, skin, bone marrow and lymphoid tissues, male and female reproductive systems) was extracted from "The Human Protein Atlas" (http://www.proteinatlas.org) using the consensus dataset consisting on the normalized expression (nTPM) levels, combining the HPA and GTEx transcriptomic datasets. Moreover, single cell RNAseq data from the brain was analyzed in the same public available data sets.

1.3. Blood sample extraction and PBMCs isolation

For the frailty study performed in the array cohort and the validation cohort 1, peripheral blood was collected from all participants by experienced nurses by venipuncture with a 21-gage needle in 8 mL serum separator tubes and 4 mL ethylenediaminetetraacetic acid (EDTA) tubes (Vacutainer, BD Biosciences) and directly deposited in the Basque Biobank for their processing and storage (https://www.biobancovasco.org/).

For the isolation of PBMCs from healthy individuals a standard procedure using a Ficoll gradient was performed. The blood was diluted 1:1 in phosphate buffered saline (PBS), added to a conical tube containing 15 mL of Ficoll and then centrifuged at 400 g for 30 min at 20 ^{o}C without braking mechanism. The interphase containing the mononuclear cell fraction was carefully isolated, washed twice with PBS and centrifuged at 100 g for 10 min at 20 ^{o}C. The samples were kept at -80 ^{o}C until use and processed according to their final use depending on whether protein or total RNA extraction was performed.

1.4. Ethical considerations

The present studies were approved by the Clinical Research Ethics Committee of the DUH and the Basque Country and complies with Law 14/2007 on biomedical research and the ethical principles of the Declaration of Helsinki. The ethical codes of the projects are

as follows: PI2021023 (Validation of molecular pattern for the diagnosis and stratification of frailty) and PI2020206 (Comprehensive approach to centenarians: a model of healthy aging?).

2. Animal models

2.1. Mouse model

The C57BL/6J mouse strain was used for the correlation study of gene expression with chronological aging and was obtained from The Jackson Laboratory (Stock. No. 000664). All mice were housed in specific pathogen-free barrier areas of the Biodonostia Health Research Institute and handled in compliance with the animal research regulations specified in the European Union Directive [2010/63/EU]. All studies were approved by Biodonostia Institute Animal Care and Use Committee in accordance with the Spanish Royal Decree 53/2013. Mice were maintained in ventilated racks under controlled humidity, light cycle, temperature, food and water, always fulfilling the criteria established for this species. For the experiments that require aged mice, animals were left to grow old up until they reach at least 18 - 20 months. For brain extraction, mice were anesthetized with isoflurane (8803934HO, Abbvie) and culled by decapitation.

Together with these experimental models, *in situ* hybridization and expression data were obtained from sagittal sections of P56 male adult C57BL6 mice from Allen Brain Atlas data portal (https://mouse.brain-map.org/) [327].

2.2. *Caenorhabditis elegans* lifespan analysis

The generation of the *C. elegans* model with knockdown for the ortholog of Early Growth Response 1 (*EGR1*) human gene (*egrh-1*) and lifespan analysis were performed in collaboration with Nuria Flames PhD, head of the developmental neurobiology unit in the Biomedicine Institute of Valencia.

C. elegans strains were maintained as described [328]. *C. elegans* eggs were isolated from N2 gravid adults by bleaching (NaOCl 10 - 50 %, KOH 5 M, H_20). Eggs were then placed in M9 1X medium overnight to obtain a synchronized population of L1 worms that were then plated and fed *E. coli* OP50. RNA interference (RNAi) feeding experiments were performed following standard protocols [329]. Briefly, at L4 larval stage, 300 worms per RNAi treatment group (L4440 empty vector as control and sjj_C27C12.2 plasmid for *egrh-1* RNAi) were transferred onto 20 freshly seeded RNAi plates (15 worms/plate) at day 0, and changed to new plates every other day. Isopropyl β-D-1-thiogalactopyranoside (IPTG) 0.6 M was added to the plates in addition to their normal NGM composition. Worms were scored every day as dead or alive by observing spontaneous movement or gently tapping with an eyelash. Lifespan is defined as the time elapsed from when worms were put on plates (adult lifespan = 0) to when they were scored as dead. Worms that died of protruding/bursting vulva, bagging, or crawling off the agar were censored.

3. Cell culture

3.1. Isolation and culture of primary fibroblasts

For the isolation of human primary fibroblasts from healthy donors, punch skin biopsies were obtained in the Neurology Department of the DUH. 5 skin biopsies (***Table M5***) were obtained from healthy individuals aged from 27 to 49 years old and fibroblasts were isolated by mechanical dissection and enzymatic digestion with 0.05 % trypsin-EDTA (25300054, Gibco). Briefly, the skin biopsies were cut into 2–3 mm^3 fragments and placed on a surface moistened with modified Eagle's medium, containing 13 % newborn calf serum, 0.4 % penicillin/streptomycin (P/S, 15140122, Gibco) and 2 mM L-glutamine (25030024, Gibco). Flasks were incubated vertically for 3-6 h in standard culture conditions at 37 ^oC, 95 % humidity, 21 % O_2 and under 5 % CO_2 in a Steri-Cycle incubator (Thermo Scientific) and then returned to the horizontal position. Human fibroblasts were cultured in Dulbecco's modified Eagle medium (DMEM, 41966029, Gibco) supplemented by 10 % Fetal Bovine Serum (FBS, 10270106, Gibco), 2 mM L-Glutamine, 100 U/mL and 100 µg/mL P/S.

Table M5. Information of primary fibroblasts derived from skin and used in this doctoral thesis.

Skin biopsie	Age (years)	Sex
1	27	Male
2	29	Male
3	46	Male
4	48	Female
5	49	Male

3.2. Isolation and culture of primary myoblasts

Proximal muscle biopsies of two healthy individuals (male of 26 years and female of 36 years) were obtained from the Neurology Department of the DUH. Donors were healthy individuals that underwent surgery for bone fractures and the muscle biopsies were obtained during this surgery. The samples were obtained from proximal limb muscles (biceps, deltoids and triceps), they were processed and cultured to isolate primary myoblasts (***Table M6***). To obtain highly purified myoblasts, primary cultures were sorted by immunomagnetic selection based on the presence of the early cell surface marker CD56 (separator and reagents from Miltenyi Biotec). Myoblasts were maintained in previously treated culture flasks with 0.5 % gelatin and with 7 mL of a specific culture medium composed of 65 % DMEM and 21 % M-199 (BE12-117F, Lonza), supplemented with 10 % FBS, 1% insulin, 1% L-glutamine, 100 U/mL and 100 µg/mL P/S, 10 µg/mL Epidermal growth factor (EGF), and 25 µg/mL Fibroblast growth factor (FGF).

3.3. Culture of normal human astrocytes

Normal Human Astrocytes (NHA) from cerebral cortex were purchased in ScienCell (***Table M6***). This cell line was cultured in adhesion in culture plates pre-treated with 15 µg/mL poly-L-lysine (0413, ScienCell) for 1 h. Astrocyte medium kit (1801, ScienCell) was employed, which contains supplements such as FBS, P/S and astrocyte growth supplement (AGS).

3.4. Culture of HEK293T cell line

The embryonic kidney cell line HEK293T was obtained from the American Type Culture Collection (ATCC) (***Table M6***). This adherent cell line was cultured in treated culture plates (130182, Thermo Scientific) with DMEM, supplemented by 10 % FBS, 2 mM L-Glutamine, 100 U/mL and 100 µg/mL P/S. For cell splitting, 0.05 % trypsin-EDTA was used, with incubations of 4 min at 37 °C. Phosphate-buffered saline (PBS) was used for cell wash and cells were centrifuged at 1.500 rpm for 5 min.

All cell lines were maintained in standard culture conditions, at 37 °C, 95 % humidity, 21 % O_2 and under 5 % CO_2 pressure. All cell culture procedures were performed in class II security laminar flow hoods (Class II Biohazard Safety Cabinets, ESCO). Cell lines were tested regularly for Mycoplasma (90021, Biotools). A summary of the main characteristics of cell lines used in this docotral thesis can be found in the ***Table M6***.

Table M6. Main characteristics of cell lines used in this doctoral thesis.

Cell line	Origin	Culture medium	Reference
Primary human fibroblasts	Skin biopsie	DMEM + 10 % FBS	Donostia University Hospital
Primary human myoblasts	Muscle biopsie	Specific myoblast medium	Donostia University Hospital
Normal human astrocytes (NHA)	Cerebral cortex	Specific astrocyte medium	ScienCell 1800
HEK293T	Embryonic kidney	DMEM + 10 % FBS	ATCC® CRL-1573™

4. Gene expression modulation

4.1. Transfections and lentiviral infections

In order to modulate the expression of the genes studied in this work, lentiviral infections were performed. Main characteristics of the plasmids used are summarized in

Table M7. We took advantage of ampicillin resistance of the plasmids to amplify them by transforming DH5α™ competent *E. coli* (18265017, Thermo Fisher). Plasmid extraction was then performed using NucleoBond Xtra Midi Plus kit (740412.50, Macherey-Nagel). Prior to lentivirus generation, all the plasmids were verified by restriction enzyme cut-off digestion. The Restriction Mapper v3 platform (Blaiklock, 2018) was used for the digestion design.

Lentiviruses were generated by transfection of the HEK293T cell line with third generation lentiviral packaging plasmids. Herein, 3.10^6 HEK293T cells were seeded in 100 mm diameter culture plates (130182, Thermo Fisher). After 24 h, transfection mix was prepared with 0.7 mL DMEM medium, 10 µg of the plasmid of interest, 2.55 µg MDL, 1.37 µg VSV-g, 0.98 µg REV and 18 µL transfection agent TurboFect (R0531, Thermo Fisher), and incubated at room temperature for 20 min. HEK293T medium was replaced by 7 mL of fresh DMEM medium and transfection cocktail was added dropwise. HEK293T cells were transduced for 6 h at 37 °C and 5 % CO_2, and consecutively, medium was replaced by 4 mL DMEM + 10 % FBS. After 48 h, the HEK293T supernatant was filtered with 0.45 µm filters (17598K, Sartorius), supplemented by 2 µg/mL polybrene and transferred to the cells of interest (20.10^4 fibroblasts or NHA) plated 24 h before in 75 cm^2 type culture flasks. Lentiviral infections were performed with a multicity of infection (MOI) of 10 overnight at 37 °C and 5 % CO_2 in DMEM complete medium supplemented with 2 µg/mL polybrene (H9268, Sigma-Aldrich). After 48 h, infected cells were selected in the presence of 2 µg/mL puromycin (Sigma-Aldrich) for 48-72 h.

4.1.1. Lentiviral infections of fibroblasts

For *EGR1* downregulation, the short hairpin RNA (shRNA) technique was employed. Primary fibroblasts were transduced with lentiviral vectors containing a plasmid with two different silencing sequences (*shEGR1*, ***Table M7***). We selected two short hairpin sequences (TRCN0000273910 and TRCN0000013837 from Sigma-Aldrich) and *pLKO.1 puro* empty vector (a gift from Dr. Bob Weinberg; Addgene plasmid #8453) was used as control.

For the overexpression of *EGR1,* primary fibroblasts were transduced with lentiviral vectors containing the *pLKO.1 puro* plasmid with the coding sequence of *EGR1* (*EGR1*, ***Table M7***) and for the *miR454* overexpression *(miR454)*, full-length *miR454* cDNA was

cloned into the plasmid *pLKO.1 puro* (***Table M7***). In both cases, *pLKO.1 puro* empty vector was used as control.

4.1.2. Lentiviral infections of NHA

For metallothionein 1 (*MT1*), metallothionein 3 (*MT3*) and RAD23 Homolog B (*RAD23B*) down-regulation in NHA, we used the shRNA technique. NHA were transduced with lentiviral vectors containing a plasmid with silencing sequence of *MT1* (*shMT1*, TRCN0000243009, Sigma-Aldrich), *MT3* (*shMT3*, TRCN0000072602, Sigma-Aldrich) or *RAD23B* (*shRAD23B*, TRCN0000003955, Sigma-Aldrich) and the plasmid *pLKO.1 puro* was used as control (***Table M7***). The viral supernatants were generated following the same protocol previously described

Table M7. Information of plasmids used in this doctoral thesis.

Name of the plasmid	Transgene	Selection (bacteria/cells)	Reference and origin
pLKO.1 puro (pLKO)	Control, empty vector	Ampicillin / Puromycin	Dr. Bob Weinberg Addgene plasmid #8453
pLKO-shEGR1 (sh1 and *sh2)*	Silencing of *EGR1*	Ampicillin / Puromycin	TRCN0000273910, TRCN0000013837 Sigma Aldrich
pLKO-EGR1 (EGR1)	Overexpression of *EGR1*	Ampicillin / Puromycin	coding sequence of *EGR1* cloned in *pLKO*
pLKO-miR454 (miR454)	Overexpression of *miR454*	Ampicillin / Puromycin	full-length *miR454* cDNA cloned in *pLKO*
pLKO-shMT1 (shMT1)	Silencing of *MT1*	Ampicillin / Puromiycin	TRCN0000243009 Sigma-Aldrich
pLKO-shMT3 (shMT3)	Silencing of *MT3*	Ampicillin / Puromiycin	TRCN0000072602 Sigma-Aldrich
pLKO-shRAD23B (shRAD23B)	Silencing of *RAD23B*	Ampicillin / Puromiycin	TRCN0000003955 Sigma-Aldrich

4.2. Short interference siRNAs

For DEAD/H-Box Helicase 11 Like 1 (*DDX11L1*) knockdown, we used two independent short interference siRNAs (*siRNA1*, n262368 and *siRNA2*, n262369, Thermo-Fisher) and the negative control #1 siRNA (*Control*, #4390843, Thermo-Fisher). Lipofectamine RNAiMAX (#13778-075, Invitrogen) and 30 nM siRNAs were combined in OptiMEM (#11058021, Gibco) and incubated for 20 min. The mixture was added dropwise to primary fibroblasts and transfection was maintained for 24 h. Then, transfection medium was changed to DMEM medium supplemented with 10 % FBS, L-Glutamine and P/S for another 24 h.

5. Treatments with senolytic compounds

Several compounds have been used, whose main characteristics are summarized in ***Table M8.*** Quercetin (Q4951, Sigma-Aldrich), Navitoclax (S1001, Selleckchem), and Dasatinib (SML2589, Sigma-Aldrich) were dissolved in Dimethyl sulfoxide (DMSO, D2650, Sigma-Aldrich) and were used to treat fibroblasts. Treatments were done 14-16 h after seeding the cells and the doses employed were 10 μM of Quercetin, 15 μM of Navitoclax and 0.5 nM of Dasatinib for 48 h.

Table M8. List of compounds used in this doctoral thesis and their main characteristics.

Compound	Solvent	Dose	Time (hours)	Function	Reference
Quercetin	DMSO	10 μM	48h	Oxidative stress and inflammation inhibitor	Q4951 Sigma-Aldrich
Navitoclax (ABT-263)	DMSO	15 μM	48h	BCL-XL, BCL2 and BCL-W inhibitor	S1001 Selleckchem
Dasatinib	DMSO	0.5 nM	48h	Src/Bcr-Abl inhibitor	SML2589 Sigma-Aldrich

DMSO, Dimethyl sulfoxide.

6. Functional assays

6.1. Cell growth assay

To assess cell growth, primary fibroblasts or NHA were plated in duplicate in 6-well treated plates (3506, Corning™) in 2 mL of the appropriate culture medium (***Table M6***), in a density of 10^4 cells per well. Total number of fibroblasts for each condition was determined at days 2, 6 and 12 days after seeding using a Neubauer counting chamber (717805, Brand) and an inverted optical microscope. In the case of NHA, total number of cells for each condition was determined at days 1, 4 and 8. For cell dissociation 0.05 % trypsin-EDTA was used and data were represented indicating the total number of cells per experimental condition in each time point.

6.2. Serial passage experiments

Primary human fibroblasts were cultured for serial passages and each passage was performed every 6-8 days. For cell splitting, 0.05 % trypsin-EDTA was used, with incubations of 5 min at 37 °C. PBS (14190094, Gibco) was used for cell wash, and cells were centrifuged at 1.500 rpm for 5 min. The expression of candidate genes was studied at early (5 - 10) and late (35 - 40) passages after total RNA extraction from cell cultures.

Primary human myoblasts were cultured for serial passages and the subculture was performed every 7-10 days using 0.25 % trypsin for 5 min at 37 °C. PBS was used for cell wash, and cells were centrifuged at 1.500 rpm for 5 min. The expression of candidate genes was studied at early (2 - 3) and late (10 - 12) passages after total RNA extraction from cell cultures.

NHA were cultured for serial passages and the subculture was performed every 4-5 days. For cell splitting, 0.05 % trypsin-EDTA was used, with incubations of 3 - 4 min at 37 °C. PBS was used for cell wash, and cells were centrifuged at 1.000 rpm for 5 min. The expression of candidate genes was studied at early (2 - 3) and late (15 - 17) passages after total RNA extraction from cell cultures.

6.3. Senescence assay

Senescence assay was performed by measuring SA-β-gal activity using the *Senescence β-Galactosidase Staining Kit* (#9860, Cell Signaling) according to the manufacturer's guidelines. This kit detects the β-galactosidase activity of cells at pH 6, which is a distinctive characteristic of senescent cells. Thus, the substrate X-Gal is metabolized by senescent cells, generating a blue and insoluble product (5,5'-dibromo-4,4'-di-chloro-indigo) that is visible in the cells by light microscopy. Briefly, 10^4 primary fibroblasts or NHA were seeded in 8-well immunofluorescence chambers (154534, LabTek Thermo-Scientific) in 0.5 mL of appropriate culture medium (***Table M6***). After 24 - 48 h, cells were washed with PBS fixed and stained according to the manufacturer's instructions. The staining was done keeping cell plates overnight with the pH 6-adjusted-staining-reagent in a non-CO_2 incubator at 37 °C. Finally, the blue cells positive for β-Galactosidase were observed using and inverted optical microscope and quantified to obtain the number of positive or senescent cells for each experimental condition. In the case of assays with treatments, the compound was applied for 72 h at the indicated doses, 24 h after seeding.

6.4. 5-ethynyl-2´-deoxyuridine (EdU) staining

To assess the ability of the cell to proliferate, the technique based on the detection of 5-ethynyl-2´-deoxyuridine (EdU) incorporation was used. EdU is an analog of the thymine nucleotide and therefore, it will be incorporated into the DNA molecule when it replicates. Subsequently, the incorporated EdU was detected using fluorescence. The commercial *Click-iT™ EdU Cell Proliferation Kit for Imaging, Alexa Fluor™ 488 dye* (C10337, Invitrogen) was used according to the manufacturer's instructions. For this purpose, 10^4 primary fibroblasts were seeded in 8-well immunofluorescence chambers with 0.5 mL of their appropriate culture medium (***Table M6***). After cell adhesion, fresh culture medium containing 10 µM of EdU was added and the cells were incubated in standard culture conditions for 24 h. Then, fibroblasts were fixed with 4 % paraformaldehyde (PFA, 158127, Sigma-Aldrich) for 15 min at room temperature. Cells were then washed 3 times with 3 % Bovine Serum Albumin (BSA) in PBS (3 % BSA in PBS), pH 7.4 and blocked and permeabilized with 1X PBS-0.5 % Triton X-100 (T8787, Sigma-Aldrich) for 20 min at room temperature. After 2 washes with 3 % BSA in PBS, they were incubated with the reaction cocktail (***Table M9***) for 30 min. The chromatin

was stained with 5 µg/mL of Hoechst (33342, Invitrogen) supplied by the kit for 10 min and slides were mounted with mounting medium Fluoro-Gel (17985, Aname). The slides were evaluated on a Nikon Eclipse 80i microscope or a Zeiss LSM 900 confocal microscope and processed with *NIS Elements Advances Research* software or *Zen Blue* software, respectively.

Table M9. Composition of the reaction cocktail for EdU staining.

Component	Quantity used/well
1X Click-IT reaction buffer	172 µL
$CuSO_4$	8 µL
Alexa Fluor 488 picolyl azide	0.48 µL
Reaction buffer additive	20 µL

7. Protein analysis

7.1. Protein extraction and quantification

For protein extraction, cells were collected in conical centrifuge tubes, centrifuged at 8.000 g for 5 min and washed with PBS. Resulting cell pellets were lysed in 80-100 µL of lysis buffer (1% NP-40, 150 mM NaCl, 5 mM EDTA, 50 mM NaF, 30 mM $Na_4P_2O_7$, 1 mM Na_3VO_4, 50 mM Tris-HCl pH 7.4), supplemented by 100 µM protease inhibitor cocktail (P8340, Sigma-Aldrich), 100 µM phosphatase inhibitor mix (P5726, Sigma-Aldrich) and 100 µM serine protease inhibitor phenylmethylsulfonyl fluoride (PMSF, P7626, Sigma-Aldrich), for 20 min on ice. After that, cell lysates were centrifuged at 12000 g for 10 min at 4 °C in order to precipitate cell debris. Supernatants containing whole cell protein extracts were then collected and placed in new tubes.

For protein quantification, colorimetric bicinchoninic acid (BCA) assay (Pierce BCA Protein Assay 23227, Thermo Fisher) was used. This process combines the reduction of cooper (Cu) Cu^{++} to Cu^{+} by proteins in an alkaline medium with the highly sensitive colorimetric detection of the Cu^{+} by BCA. Thus, following manufacturer's instructions, 1 µL of whole protein extract was incubated with BCA for 20 min at 37 °C and colorimetric intensity

was measured at 560 nm in a Halo LED 96 microplate reader (Dynamica). In parallel, a calibration line was performed with five known concentrations of BSA provided by the kit in order to extrapolate protein concentration of the samples of interest. Protein samples were stored at -80 °C until use.

7.2. Western Blot

In western blot experiments 20 ng protein were usually used. Thus, the appropriate sample volume was collected, to which one fifth loading buffer 5X (312.5 mM Tris pH 6.8, 10 % sodium dodecyl sulfate (SDS), 50 % glycerol, 0.5 % bromophenol blue and 5 % β-mercaptoethanol) was added. For protein denaturation, samples were then heat-shocked by incubating them 5 min at 95 °C and immediately after placed on ice.

For protein separation by their molecular weight, sodium dodecyl sulphate-polyacrylamide gel electrophoresis (SDS-PAGE) technique was performed. Herein, 1.5 mm thick polyacrylamide gels were used, composed by stacking gel (4.5 % polyacrylamide) and separating gel (10-20 % polyacrylamide, depending on the molecular weight of the protein of interest). Electrophoresis was performed using electrophoresis buffer (Tris 20 mM, glycine 0.2 M, SDS 0.1 %, pH 8.3) and buckets (Mini-PROTEAN® Tetra Cell Precast, Bio-Rad). The power supply BioRad HC Power Pac was run first for 10 min at 90 V and then, for 60-90 min at 120 V at room temperature, depending on the molecular weight of the protein of interest.After this process, proteins were transferred into a nitrocellulose membrane using pre-cast 0.2 µm nitrocellulose transfer packs (1704158, Bio-Rad). For this, a semi-dry transfer was performed using the Trans-Blot Turbo Transfer System (Bio-Rad) at 1.3 A, 25 V in 7 min. For verification of the efficiency of the protein transfer, Ponceau staining was used (P7170, Sigma-Aldrich).

In order to avoid unspecific bindings of primary antibodies, membranes were incubated with blocking solution (Tris Buffered Saline 0.1 M-0.01 % Tween 20 (TBS-T), 5 % powder milk) for 1 h in agitation at room temperature. Once membranes were blocked, they were incubated overnight at 4 °C with primary antibodies (***Table M10***) diluted in blocking solution and following manufacturer recommendations. After this incubation, the membranes were washed 3 times with TBS-T solution for 5 min in agitation and then, horseradish peroxidase (HRP)-conjugated secondary antibodies (***Table M10***) were applied for

1 h in blocking solution at room temperature. After this incubation, the membranes were washed 3 times with TBS-T solution for 5 min in agitation.

Proteins were finally detected by chemiluminescence. In particular, NOVEL ECL Chemi Substrate (WP20005, Thermo Fisher) was used for highly expressed proteins, Luminata Crescendo Western HRP substrate (WBLUR0100, Merck Millipore) was used for the detection of medium expressed proteins and SuperSignal West Femto Maximum Sensitive Substrate (34096, Thermo Fisher) was employed for the detection of low expressed proteins. Signal was captured and recorded by iBrightFL1000 imaging system (Invitrogen).

Table M10. Primary and secondary antibodies used in western blot technique.

Type of antibody	Recognized antigen	Working dilution	Produced in	Supplier	Reference
Primary antibody	EGR1	1/200	Rabbit	Cell Signaling	#4153
	DDX11L1	1/250	Mouse	Santa Cruz	sc-271711
	$p16^{INK4A}$	1/250	Rabbit	Abcam	ab108349
	$p21^{CIP1}$	1/250	Goat	Santa Cruz	sc-397
	RAD23B	1/250	Mouse	Novus	H00005887
	MT1	1/250	Rabbit	Abcam	ab12228
	MT3	1/250	Mouse	Sigma	HPA004011
	β-actin	1/100000	Mouse	Sigma	A5441
Secondary antibody	anti-rabbit HRP	1/1000	Goat	Cell Signaling	7074S
	anti-mouse HRP	1/1000	Horse	Cell Signaling	7076S
	anti-goat HRP	1/1000	Donkey	Santa Cruz	Sc-2020

7.3. Cell immunofluorescence (IF)

10^4 primary fibroblasts or NHA were seeded in 8-well immunofluorescence (IF) chambers using their culture medium, and after cell adhesion or treatment completion, cells were fixed with 4 % PFA for 15 min at room temperature. Cells were then washed 3 times with 1X PBS (44592, BioSystems) and blocked and permeabilized with 1X PBS-0.3 % Triton X-

100 supplemented by 5 % FBS for 1 h at room temperature. Later on, they were incubated with primary antibodies (***Table M11***) diluted in 1X PBS 0.3 % Triton X-100 overnight at 4 °C. Afterwards, 3 washes with 1X PBS were done and cells were incubated with fluorophore-conjugated secondary antibodies (***Table M11***) diluted in 1X PBS 0.3 % Triton X-100 for 1 h in darkness at room temperature. After other three washes as previously described, chromatin was stained with 1 µg/mL 2-(4-Amidinophenyl)-6-indolecarbamidine dihydrochloride (DAPI, D9542, Sigma-Aldrich) for 2-3 min. Next, two washes with 1X PBS and a final wash with distilled water were performed. Finally, slides were mounted with mounting medium Fluoro-Gel. Immunofluorescence was evaluated with a Nikon Eclipse 80i microscope or a Zeiss LSM 900 confocal microscope and processed with *NIS Elements Advances Research* software or *Zen Blue* software, respectively. In the case of assays with treatments, the compound was applied for 72 h at the indicated doses, 24 h after seeding.

Table M11. Primary and secondary antibodies used in cell immunofluorescence.

Type of antibody	Recognized antigen	Working dilution	Produced in	Supplier	Reference
Primary antibody	Phospho-histone H3 (pH3)	1/2000	Mouse	Abcam	ab14955
	Ki67	1/500	Rabbit	Abcam	ab15580
	Cleaved-caspase 3	1/500	Rabbit	R&D Systems	AF835
Secondary antibody	Alexa Fluor® 555 Goat anti-mouse IgG (H+L)	1/500	Goat	Invitrogen	A21422
	Alexa Fluor® 555 Goat anti-rabbit IgG (H+L)	1/500	Goat	Invitrogen	A32732
	Alexa Fluor® 488 Goat anti-rabbit IgG (H+L)	1/500	Goat	Invitrogen	A32731

7.4. Tissue IF

In order to characterize the expression of proteins of interest, tissue IF was performed in formalin fixed brain samples. The sections were deparaffinized in xylene (2 washes of 5 min) and rehydrated in a series of graded alcohols (2 washes of 2 min with 100

% ethanol and 2 washes of 2 min with 70 % ethanol). Then, they were incubated with 0.5 % sodium borohydride (NaBH4, #213462, Sigma) for 30 min and heated in citrate buffer (S/3320/53, Fisher) at pH6 for 20 min for antigen retrieval. After incubation of the sections in 100 % ethanol for 3 min, the H-4000 *Vector ImmEdge*® Hydrophobic pen was used to delineate the tissues. The sections were permeabilized and blocked for 2 h with 2 % normal donkey serum (NDS, 017-0000-121, Jackson) in PBS 0.2 % Triton X-100 (blocking solution) and they were incubated at 4 °C overnight with primary antibodies (***Table M12***) diluted in blocking solution. Then, sections were washed 3 times for 15 min with PBS and incubated for 2 h at room temperature in darkness with secondary antibodies (***Table M12***) diluted in blocking solution. After 2 washes of 10 min with PBS, nuclear DNA was stained with 1/5000 of 10 mg/mL DAPI (40043, Biotium) for 20 min at room temperature. Finally, the sections were submerged in 70 % ethanol for 5 min and incubated with autofluorescence eliminator reagent (2160, Millipore) for 3-4 min for background removal. The preparation was mounted with *Prolong™ Gold antifade* mounting media (P36930, Invitrogen) and IF was evaluated with SP5 laser scanning confocal microscope (TCS SP5, Leica) and with SP8 laser scanning inverted confocal microscope (TCS SP8 MP, Leica). Controls with secondary antibodies without primary antibody were used to account for unspecific interactions and discard autofluorescence contribution.

Confocal images of tissue sections were acquired at different planes in Z (z-stack). Processing and analysis were performed on the maximal intensity projection of the z-stack using Fiji software, the open-source platform for biological image analysis [330]. The quantification of the staining or positive cells for the different markers was measured and categorized based on each protein positive signal percentage respect to the counting of the total nuclei that was achieved using DAPI channel.

These experiments were performed during the international stay done in the Neural Stem Cell Biology Laboratory, headed by Dr. François Guillemot and located in The Francis Crick Institute (London, United Kingdom).

Table M12. Primary and secondary antibodies used in tissue immunofluorescence.

Type of antibody	Recognized antigen	Working dilution	Produced in	Supplier	Reference
Primary antibody	RAD23B	1/300	Mouse	Novus	H00005887
	MT1	1/100	Rabbit	Abcam	ab12228
	MT3	1/200	Mouse	Sigma	HPA004011
	GFAP	1/300	Rat	Invitrogen	13-0300
	S100β	1/200	Rabbit	Abcam	ab196175
	S100β	1/200	Mouse	Sigma	S2657
	MAP2	1/200	Mouse	Sigma	M4403
	TUJ1	1/500	Rabbit	Biolegend	802001
	TUJ1	1/500	Mouse	Biolegend	801201
Secondary antibody	anti-rat 488	1/500	Donkey	Jackson	712-546-150
	anti-rabbit Cy3	1/500	Donkey	Jackson	711-166-152
	anti-rabbit 647	1/500	Donkey	Jackson	711-606-152
	anti-mouse Cy3	1/500	Donkey	Jackson	715-166-151
	anti-mouse 647	1/500	Donkey	Jackson	715-605-151

7.5. Tissue immunohistochemistry (IHC)

Tissue immunohistochemistry (IHC) was performed in paraffin embedded brain samples by the Pathology department of the DUH following standard protocols. Briefly, 5 µm sections were done using a microtome (HM355S, Thermo Scientific) were deparaffined in xylene and rehydrated in a series of graded alcohols. Heat-induced antigen retrieval with citrate buffer was performed and subsequently, PBS 0.3 %-Triton X-100 5 % FBS (blocking solution) was applied to the sections. Next, the sections were incubated overnight at 4 °C with the primary antibody anti-RAD23B (1/300, H00005887, Novus). After this time, sections were washed and secondary antibody MACH 3 Mouse HRP-Polymer (1/2000, M3M530, BioCare Medical) was applied, incubating it for 1 h at room temperature. Finally, 10 min

incubation with 3,3'-Diaminobenzidine (DAB, ab64238, Abcam) was performed at room temperature, so that DAB got oxidized and could be visualized by its brown color. Staining was visualized using the Eclipse 80i light microscope, scanned with scanned with *Virtuoso v.5.6.1* software (Roche) and processed by the *NIS Elements Advances Research* software.

7.6. Enzyme-linked immunosorbent assay (ELISA)

We used serum samples from cohort 2 of the frailty study (robust, n = 41; frail, n = 17) to study the expression of EGR1 (EH167RB, Invitrogen) and DDX11L1 (RAB1365, Millipore) using Enzyme-linked immunosorbent assay (ELISA) kits and following manufacturer´s instructions.

8. Gene expression

8.1. RNA extraction and quantification

Total RNA was extracted from PBMCs, cell lysates and brain tissues. RNA from PBMCs was isolated using QIAamp RNA Blood Mini Kit (52304, Qiagen) following manufacturer's instructions. RNA from plasma and serum samples was extracted using Maxwell® RSC miRNA Plasma and Serum Kit (AS1680, Promega) following manufacturer's instructions. In the case of tissues, samples were firstly homogenized by a tissue-lyser tissue dissociation apparatus (Qiagen Retsch MM300) with 1 mL TRI Reagent Solution (AM9738, Life Technologies) and using stainless steel beads. In the case of cellular pellets, 1 mL TRI Reagent Solution was added as a first step. Once cell lysis was performed, the same protocol was applied for both cases. First, 200 µM chloroform (C2432, Sigma-Aldrich) were added, and after gently mixing the samples, they were incubated 10 min at room temperature. Samples were then centrifuged at 12000 rpm for 10 min at 4 °C, so that three phases were separated. Thus, aqueous phase was collected in a new tube and 500 µL 2-propanol (I9516, Sigma-Aldrich) and 1 µL 5 µg/µL glycogen (AM9510, Ambion) were added. Samples were gently mixed, incubated for 10 min at room temperature and centrifuged at 12.000 rpm for 22 min at 4 °C for RNA precipitation. Supernatants were discarded and two washes with 75

% ethanol (Scharlau) were done to increase purity of the sample. Finally, RNA pellet was dried at room temperature and resuspended in H_2O DNase/RNase free (10977035, Invitrogen). All procedures with RNA were performed in tubes treated for 24 h with diethyl pyrocarbonate (DEPC, 159220, Sigma-Aldrich) for inhibiting RNases.

RNA concentration and purity were determined by measuring absorbance at 260 nm on a Nanodrop-100 spectrophotometer (Thermo Fisher). RNA samples were stored at -80 °C until use.

8.2. Gene expression microarrays

In this doctoral thesis, two different gene expression microarrays were performed. The microarray of the frailty study (first chapter of this doctoral thesis), was done in RNA samples from PBMCs of 25 individuals from the cohort cited above (***Table M2***). Among these 25 participants, 7 were classified as frail and 5 as robust by the three tools used (TUG, GS and Tilburg) for frailty status determination. Whole-transcriptome analysis was performed from 300 ng of RNA using HuGene-2_0-st-v1 expression array (Affymetrix) which covers 48.226 transcripts. Raw data were first checked for quality purposes through the Affymetrix® Expression Console™ Software v1.4.1 and TAC software v4.0. Then, data were normalized using the Robust Multi-array Average (RMA) and analyzed by TAC and BRB-array tools. We used univariate parametric tests to find genes that were differentially expressed between the studied groups. The inclusion criteria were the p-value (< 0.05) and the fold change (FC) (> |1.5|) between the analyzed groups. A class prediction analysis was also performed. The objective of this analysis is the construction of predictors for classifying experiments into phenotype classes based on expression levels. Using the BRB-array tools package, six methods of prediction have been employed: compound covariate predictor (CCP), diagonal linear discriminant analysis (DLDA), k-nearest neighbor (using k=1 and 3) (KNN), nearest centroid (NC), Bayesian compound covariate classifier (BCCP) and support vector machines (SVM). The data that support this study have been deposited in NCBI´s Gene Expression Omnibus (GEO) and are accessible through GEO series accession number GSE140358.

The microarray of the brain aging study (second chapter of this doctoral thesis), was done in RNA samples from human hippocampus of 16 individuals from the cohort cited

above (***Table M4***). Whole-transcriptome analysis was performed from 300 ng of RNA using ClariomTM S array (Affymetrix), which accurately measure gene level expression from more than 20.000 well-annotated genes. Raw data were first checked for quality purposes through the Affymetrix® Expression Console™ Software v1.4.1and then analyzed in Transcriptome Analysis Console software v4.0. Data were normalized using RMA and batch effects detected due to sample processing were eliminated using batch effect module of the TAC software. Then, studied groups were compared with Limma differential expression analysis to find differentially expressed genes. Differentially expressed genes with p-value < 0.05 and FC ≥ |2| were selected. Functional enrichment on Gene Ontology (GO) biological process analysis in centenarians vs. elderly and young individuals was performed in RStudio software (version 4.2.1, https://www.R-project.org/), using *clusterProfiler* package [331] with a p-value cutoff of 0.05. GO analysis between elderly and young individuals was performed using PANTHER GO-Slim Biological Process (http://www.pantherdb.org/panther/goSlim.jsp) [332]. Terms with an FDR-corrected p-value < 0.05 were treated as significantly enriched. Additionally, we performed correlation studies of gene expression with age and Pearson's correlation was calculated between the expression and age of the individual for each transcript.

8.3. Reverse transcription

For the obtention of complementary desoxyribonucleic acid (cDNA) from RNA samples, reverse transcription (RT) was performed by *Maxima First Strand cDNA Synthesis Kit* (K1671, Thermo Fisher), which comprises a first step for double strand DNA degradation by DNase to avoid contamination with genomic DNA. The employed protocol was based on manufacturer's instructions, and BioRad C1000 thermocycler was used to perform the next incubation steps: 10 min at 25 °C, 30 min at 50 °C and 5 min at 85 °C. For miRNA analysis, miRNA-specific reverse transcription was performed using 20 ng of RNA and the *miRCURY LNA RT kit* (339340, bioNova), following manufacturer's instructions and the next protocol: 60 min at 42 ^{o}C, and 5 min at 95 ^{o}C. Immediately after, samples were placed on ice and diluted to final concentration of 2-4 ng/µL in DNase/RNase free H_2O. cDNA samples were stored at -20 °C until use.

8.4. Quantitative real-time PCR (qRT-PCR)

In order to measure the expression level of the genes of interest, quantitative real-time polymerase chain reaction (qRT-PCR) was used. Herein, an initial amount of 10 - 20 ng cDNA as reaction template, 10 mM of each gene-specific forward and reverse primers and 6 µL Power SYBR® Green Master Mix (4368706, Applied Biosystem) were included per reaction. For the study of *miR454*, *miRCURY LNA SYBR Green PCR* kit (339347, bioNova) was used following manufacturer´s instructions. Human and mice primer sequences were obtained from PrimerBank database (https://pga.mgh.harvard.edu/primerbank/), from previously published research articles or designed using NCBI´s primer basic local alignment search tool (BLAST) software (http://www.ncbi.nlm.nih.gov/tools/primer-blast/) (***Table M13 and M14***).

Table M13. Human primer sequences used in qRT-PCR reactions.

Gene	Forward primer sequence (5' → 3')	Reverse primer sequence (5' → 3')	Tm
CSNRP1	CCCCTGTCTATCCTGAAGCG	CCATACCCAGAGTACAGCCA	136
CLDN12	CTGTGTGGAATCGCCTCAGTA	GTCAGGTTCTTCTCGTTTCTGTT	104
CNTNAP3	ACCTTTCAGTTATCCTCGCCA	TGTTTCTTTGCGCTCTGGTTA	184
CISH	TTCGGGAATCTGGCTGGTATT	GAACGTGCCTTCTGGCATCT	83
RLN1	AGAGGCAACCATCATTACCAGA	AAACAGTGCCACGTAGGGTC	194
TIA	GATGCCCGAGTGGTAAAAGAC	CCCATCTGTTGAATGGCGTTT	104
GCNT4	TCCCTAAGTACCTCGCCTTTT	TCCCTAAGTACCTCGCCTTTT	193
TRIM3	GCGACCTGGAGACCATTTGT	GCTACTGCCGATGTGTTCCTG	92
$p14^{ARF}$	CCCTCGTGCTGATGCTACTG	CATCATGACCTGGTCTTCTAGGAA	72
$p16^{INK4A}$	GGGGGCACCAGAGGCAGT	GGTTGTGGCGGGGGCAGTT	159
$p21^{CIP1}$	GACACCACTGGAGGGTGACT	CAGGTCCACATGGTCTTCCT	172
$p27^{KIP1}$	GCAACCGACGATTCTTCTAC	CTTCTGAGGCCAGGCTTCTT	119
IL6	CCAGGAGCCCAGCTATGAAC	CCCAGGGAGAAGGCAACTG	64
MT1A	TGCGCCTTATAGCCTCTCAAC	AGTTGGGGTCCATTTCGAGC	71
MT1B	CTGATGTTGGGAGAGCCCTG	GCAAACCGGTCAGGGTAGTT	89
MT1E	TGGGCTTTCTTTGCCCTCAT	TAGGGGGTACAGTTGGGGTT	117
MT1F	TCGCTTCTCTCTTGGAAAGTCC	AGGAGCAGCAGCTCTTCTTG	147
MT1G	CTTCCACGTGCACCCACT	CTTTGCACTTGCAGGAGCTG	132
MT1H	CATCTGCAAAGGGGCGTCAG	GTTTTCATCTGACAGCAGGGC	74
MT1M	TGTGTCTGCAAAGGGACGTT	TCCAGGTTGTGCAGCTTGTT	98
MT1X	CTGCTTCTCCTTGCCTCGAA	TGTCTGACGTCCCTTTGCAG	186
MT2A	AGCTTTTCTTGCAGGAGGTG	GCAACCTGTCCCGACTCTA	135

Table M13 (continued). Human primer sequences used in qRT-PCR reactions.

Gene	Forward primer sequence (5' → 3')	Reverse primer sequence (5' → 3')	Tm
MT3	CTGCTCTCCTCGACATGGAC	AGGAGCAGCAGCTCTTCTTG	123
MT4	CACTGGAGCCTTTCGGACAC	TGCAGATTCCTCCAGACATGC	70
REST	ACTCAGCGTCGTAGAACCTCA	CGAAAGGGTTTGGTCTTCGAG	135
TNFα	CCCAGGCAGTCAGATCATCTTC	AGCTGCCCCTCAGCTTGA	85
IL1α	AGATGCCTGAGATACCCAAAACC	CCAAGCACACCCAGTAGTCT	147
STAT3	ATCACGCCTTCTACAGACTGC	CATCCTGGAGATTCTCTACCACT	176
C3	AAAAGGGGCGCAACAAGTTC	GATGCCTTCCGGGTTCTCAA	224
TGFβ	GGCCAGATCCTGTCCAAGC	GTGGGTTTCCACCATTAGCAC	204
CHI3L1	GAAGACTCTCTTGTCTGTCGGA	AATGGCGGTACTGACTTGATG	108
SERPINA3	TGCCAGCGCACTCTTCATC	TGTCGTTCAGGTTATAGTCCCTC	167
ANKRD30B	CCTTCAGCGAACGGGTCTAC	CAGGTTGACGGGCTTCTTCC	140
MRAP2	AACAGCTTTGTGTCAGACTTTGG	TGTAGCAGTGAAAGAGAGACCT	97
CERCAM	CACATCCCAACTACACTTGGC	ATGTACCCATAACGGTGCTCA	109
CHI3L2	TCAGCAGGTTCCCTACGCA	GCAGGATTTGCCAGTGAAGTC	154
HSD11B1	TGGCTTATCATCTGGCGAAGA	AGGCAGTGGGATACCACCT	88
MS4A6A	TGTGGCATGATGGTATTGAGC	AGGGTCCTATGAATGGGTAAGC	115
KCNAB1	CATGGAAGCCTATTCTGTAGCAA	CGCCAACACCTATTTTGTGGTAG	134
DLGAP1	GCTACTCAGCCATCCCTTACA	GCCCTCAGGTAACTATGACTCC	95
CAPN3	GATTGCGCTCATGGATACAGA	GCATCTCGTAGCTGTTGATGGT	143
PDE1C	GATGTGGACAAGTGGTCCTTTG	GGGGATCTTGAAACGGCTGA	123
BEST1	CTGGGCTTCTACGTGACGC	TTGCTCGTCCTTGCCTTCG	117
MOG	ACCAGGCACCTGAATATCGG	CAGGGCTCACCCAGTAGAAAG	195
LGI3	AGAGATCCAGGATGGAGCGTT	GGATAGTGCCCAGATGTCATTG	154
GRK4	CCCCTGGCAGAATGAGATGA	GGTCTGGAAACCGGGGTATG	117
EYA1	GGACTATCCGTCTTATCCCAGT	GCTGCTGGTCATATAATGTGCTG	91
RAD21	GGATAAGAAGCTAACCAAAGCCC	CTCCCAGTAAGAGATGTCCTGAT	119
SWI5	GAGTCTCTGCACCTTGACATTC	GCCTTCAGATACGAACTGGGAG	84
OSR1	CGGTGCCTATCCACCCTTC	GCAACGCGCTGAAACCATA	117
CHRNA6	GGCAGGGATTCCTTCATGGG	GCCTCTCCTCAGTTGCACAG	93
TSPAN18	GCTGTTACACGGTGATCCTCA	CATGGCGAAAAGCTCGATGG	95
SSTR2	TGGCTATCCATTCCATTTGACC	AGGACTGCATTGCTTGTCAGG	98
PPP1R1B	CAAGTCGAAGAGACCCAACCC	GCCTGGTTCTCATTCAAATTGCT	111
LPAR3	GCTGCCGATTTCTTCGCTG	AGCAGTCAAGCTACTGTCCAG	126
CREM	ACAGTACGCAGCACAATCAG	CTGGTAAGTTGGCATGTCACC	136
ZBTB10	CGGCTCCACGAACAATAACG	CAGGCCCTCCAATTCCACTT	145
MTIF2	GGAATGACTATTGAGGAACTGGC	CCTGCCTTCGTTATCACTTCTTT	152
SLC22A8	CCAGAGTCCATACGCTGGTTG	TCACTTGCGGTGTACTTGGC	179

Table M13 (continued). Human primer sequences used in qRT-PCR reactions.

Gene	Forward primer sequence (5' → 3')	Reverse primer sequence (5' → 3')	Tm
ZIC1	CACGCGGGACTTTCTGTTC	TGCCCGTTGACCACGTTAG	198
EFEMP2	AAGAGCCCGACAGCTACAC	AGGGATGGTCAGACACTCGTT	95
HLF	CCCTCGGTCATGGACCTCA	ACTTGGTGTATTGCGGTTTGC	126
NNAT	ACTGGGTAGGATTCGCTTTTCG	ACACCTCACTTCTCGCAATGG	63
SMPD4	GACAGTCCTCTGTACCACAACA	CGAACGGATTCAGGGCCAA	79
RASGEF1B	TTTGCCACTTATGTGTTGAGCA	TCCATTCCGTGAGGAGTTGAA	105
ANKRD18B	TTGGGCCCTTGCTCCTATCT	CTGTTGGGGACTAGTGAGCG	107
RAD23B	AGCAACTGACAGTACATCGGG	CTCGTTCATAGCCCATTGACAT	128
HYOU1	CGAGCTGACTTTCGACCCAC	TGAGAACCATGCCCAACACTT	95
OR2A42	CCTTCTCTGGGCCTCATGAA	CGAGTAGGAGACAAGCACCA	158
GAPDH	ATGGGGAAGGTGAAGGTCGG	GACGGTGCCATGGAATTTGC	180

Table M14. Mouse primers sequences used in qRT-PCR reactions.

Gene	Forward primer sequence (5' → 3')	Reverse primer sequence (5' → 3')	Tm
Smpd4	CACACTAGCCTCTTGAAGCGA	TGTAGAACCTCCAACTTGGCAT	182
Rasgef1b	TCTGGAAGCCCTTATCCAACA	GTGGCAAACCTTAGCCATGAG	130
Rad23b	ACCTTCAAGATCGACATCGACC	ACTTCTGACCTGCTACCGGAA	103
Hyou1	GAGGATCTTCGGGTATTTGGC	TGCCTTTGGACTCATAGTCGG	100
β-actin	GGCACCACACCTTCTACAATG	GTGGTGGTGAAGCTGTAGCC	152

In all cases, primer specificity was verified first by primer-BLAST tool and by melting curve analysis in each qRT-PCR experiment. The primers were designed against sequences between exons in order to avoid amplification of genomic DNA. We also used commercial gene-specific primer assays that were used in the frailty study (***Table M15***).

Reactions were performed in triplicate in CFX384 Touch Real-Time PCR Detection System (BioRad), following the next protocol: 1 cycle of 2 min at 50 °C, 1 cycle of 10 min at 95 °C, 41 cycles of 15 seconds at 95 °C and 1 min at 60 °C, and a last cycle of 10 seconds at 95 °C followed by 1 min at 60 °C and 1 second at 97 °C. As internal control to correct possible variations in cDNA levels, *glyceraldehyde 3-phosphate dehydrogenase* (*GAPDH*) and *beta-2-microglobulin* (B2M) housekeeping genes were used in the case of

human samples, whereas *β-actin* was used in mice samples. For *miR454* study we used the next protocol: 1 cycle of 2 min at 95 °C and 40 cycles of 10 seconds at 95 °C. In this case, as internal control *miR191* housekeeping was used. Relative quantification was calculated using the $2^{-\Delta\Delta Ct}$ formula, which is based on the normalization of the expression of the gene of interest with respect to the expression of the housekeeping gene and the sample of reference. Results were represented as FC.

Table M15. Information of commercial gene-specific primer assays used in qRT-PCR reactions.

Gene	Commercial name	Supplier	Reference
G0S2	G0S2 PrimePCR™ SYBR® Green Assay	Bio-Rad	qHsaCED0044000
GJB6	GJB6 PrimePCR™ SYBR® Green Assay	Bio-Rad	qHsaCED0043916
NSF	NSF PrimePCR™ SYBR® Green Assay	Bio-Rad	qHsaCID0021934
CXCL8	CXCL8 PrimePCR™ SYBR® Green Assay	Bio-Rad	qHsaCED0046633
C-JUN	Hs_CJUN_1_SG QuantiTect Primer Assay	Qiagen	QT00242956
CD69	Hs_CD69_1_SG QuantiTect Primer Assay	Qiagen	QT00043155
PTEN	Hs_PTEN_1_SG QuantiTect Primer Assay	Qiagen	QT00086933
AREG	Hs_AREG_1_SG QuantiTect Primer Assay	Qiagen	QT00030772
EGR1	Hs_EGR1_2_SG QuantiTect Primer Assay	Qiagen	QT00999964
DDX11L1	Hs_DDX11L1_SG QuantiTect Primer Assay	Qiagen	QT01339310
miR454	Hs_mir-454_PR_1_miScript Primer Assay	Qiagen	MP00002324
miR454	hsa-miR-454 miRCURY LNA miRNA PCR Assay	bioNova	YP00205663
miR191	hsa-miR-191 miRCURY LNA miRNA PCR Assay	bioNova	YP00204306
B2M	Hs_B2M_1_SG QuantiTect Primer Assay	Qiagen	QT00088935

9. Statistical analysis

The data shown in the present study represent mean values ± standard error of the mean (SEM) with the number of independent experiments (n) in the figure legends. Unless otherwise indicated, statistical significance (p-values) were calculated using a two-tailed Student´s t-test where $p \leq 0.1$, $p \leq 0.05$, $p \leq 0.01$, $p \leq 0.001$ and $p \leq 0.0001$ are represented as #, *, **, *** and ****, respectively. Statistical analyses and graphics were performed using Microsoft Office Excel, IBM SPSS Statistics 20 and GraphPad Prism 8

software (GraphPad Software, Inc. CA, USA). The statistical significance in the *C. elegans* lifespan analysis was assessed with Gehan-Breslow-Wilcoxon test. For correlation analysis, we first performed a Kolmogorov Smirnov test for the assessment of normality and then we used Pearson's coefficient when samples were normally distributed or Spearman's coefficient when they were not normally distributed. Receiver Operating Characteristic (ROC) curves with sensitivity and specificity values were calculated as part of the class prediction analysis by BRB-array tool package.

Results

FIRST CHAPTER

Identification of molecular mechanisms underlying frailty

Whole-transcriptome analysis reveals a pattern of 35 genes differentially expressed between frail and robust individuals.

We performed a gene expression microarray in PBMCs samples from 25 individuals (microarray cohort) classified as robust and frail based on TFI, TUG and GS test. The first analysis showed a great heterogeneity in expression profiles according to the individual frailty scale employed (***Figure R1A***). So, in order to be more accurate with the analysis and the definition of frailty, only those individuals classified as frail or robust by the 3 scales were selected (***Figure R1B***). Therefore, the comparative gene expression analysis was performed in 7 frail and 5 robust individuals. Applying a class prediction approach to obtain the best genes that were able to discriminate between frail and robust individuals, 35 genes were identified (***Figure R2A***). This set of 35 genes includes a variety of protein-coding genes, pseudogenes and regulatory noncoding RNAs, mainly encompassing miRNAs (***Table R1***).

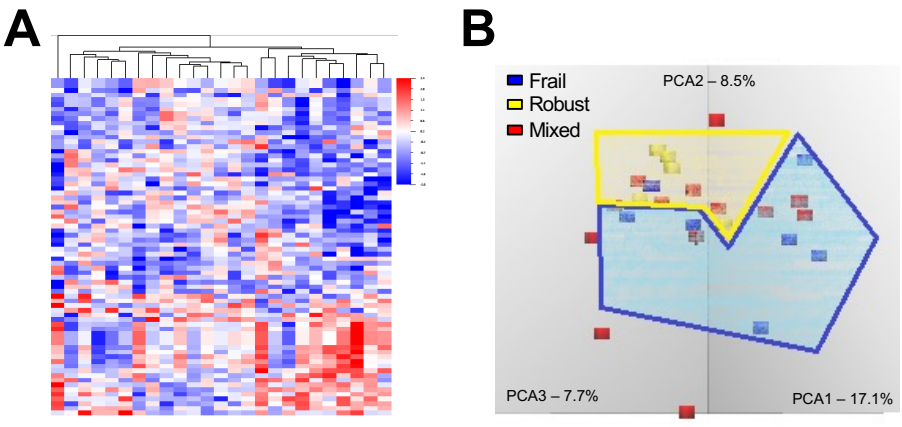

Figure R1. Transcriptomic studies reveal heterogeneity at molecular level depending on the frailty scale used. (A) Hierarchical clustering of the 25 subjects selected for microarray screening which reveals heterogeneity at molecular level depending on the frailty scale employed (TUG, GS or TFI). **(B)** Principal Component Analysis (PCA) of the 25 subjets selected for microarray screening. Blue (frail) and yellow (robust) squares represent individuals classified as frail or robust by the 3 scales used. In red, samples that diverge in at least one of the classification scales.

Table R1. List of the 35 genes differentially expressed between robust and frail individuals classified by the 3 scales used (TUG, GS and TFI).

Gene symbol	Gene name	Fold change	p-value
Up-regulated genes in frail individuals			
G0S2	G0/G1 switch 2	2.69	0.031
EGR1	early growth response 1	2.66	0.001
CXCL8	C-X-C motif chemokine ligand 8	2.15	0.019
GJB6	gap junction protein beta 6	2.12	0.005
CSRNP1	cysteine and serine rich nuclear protein 1	2.10	0.030
Down-regulated genes in frail individuals			
DDX11L1	DEAD/H-box helicase 11 like 1	-4.11	0.001
NSF	N-ethylmaleimide sensitive factor, vesicle fusing ATPase	-3.59	0.000
DDX11L10	DEAD/H-box helicase 11 like 10	-3.01	0.003
TRAV16	T cell receptor alpha variable 16	-2.98	0.017
TRAV8-3	T cell receptor alpha variable 8-3	-2.71	0.000
LOC101929775	C-Jun-amino-terminal kinase-interacting protein 1-like	-2.62	0.000
MAPK8IP1	mitogen-activated protein kinase 8 interacting protein 1	-2.62	0.000
TRAJ17	T cell receptor alpha joining 17	-2.62	0.001
CLDN12	claudin 12	-2.60	0.015
CNTNAP3	contactin associated protein family member 3	-2.60	0.047
LINC01765	long intergenic non-protein coding RNA 1765	-2.56	0.033
LINC02520	long intergenic non-protein coding RNA 2520	-2.45	0.022
miR3941	microRNA 3941	-2.40	0.005
CNTNAP3B	contactin associated protein family member 3B	-2.39	0.031
MTRNR2L2	MT-RNR2 like 2	-2.39	0.033
IGHV2-26	immunoglobulin heavy variable 2-26	-2.38	0.029
miR487A	microRNA 487a	-2.29	0.027
TRBV3-1	T cell receptor beta variable 3-1	-2.26	0.005
CISH	cytokine inducible SH2 containing protein	-2.25	0.003
CTSLP8	cathepsin L pseudogene 8	-2.16	0.026
miR626	microRNA 626	-2.11	0.024
TRAJ19	T cell receptor alpha joining 19 (non-functional)	-2.11	0.003
TRAJ48	T cell receptor alpha joining 48	-2.09	0.018
RLN1	relaxin 1	-2.08	0.009
TIA1	TIA1 cytotoxic granule associated RNA binding protein	-2.05	0.046
TRAJ14	T cell receptor alpha joining 14	-2.04	0.012
GCNT4	glucosaminyl (N-acetyl) transferase 4	-2.02	0.021
CD40LG	CD40 ligand	-2.01	0.009
TRAJ16	T cell receptor alpha joining 16	-2.01	0.030
miR454	microRNA-454	-1.63	0.000

A number of these genes are linked to inflammation- and hypoxia-related pathways (*EGR1, CXCL8, CISH, MAPK8IP1* or *CD40LG*), immune response (*TIA1, IGHV2-26, TRBV3-1* and several members of the T cell receptor alpha locus at 14q11.2 chromosome location), apoptosis (*G0S2*) and neuropeptides (*CNTNAP3, CNTNAP3B, MTRNR2L2*), processes previously associated to frailty [133] (***Table R1***). From these 35 genes, 14 of them were

chosen for experimental validation in an extension of subjects from the cohort cited above, including 103 robust and 17 frail individuals for the 3 scales (validation cohort 1), based on the highest FC and p-value. qRT-PCR confirmed a statistically significant increase of *G0S2, EGR1, CXCL8*, and *GJB6* expression (***Figure R2B***) and a reduction of *NSF*, *DDX11L1* and *miR454* expression in PBMCs of frail individuals compared to robust individuals (***Figure R2C***). Thus, these 7 differentially expressed genes (4 up-regulated and 3 down-regulated) were selected to perform further validations

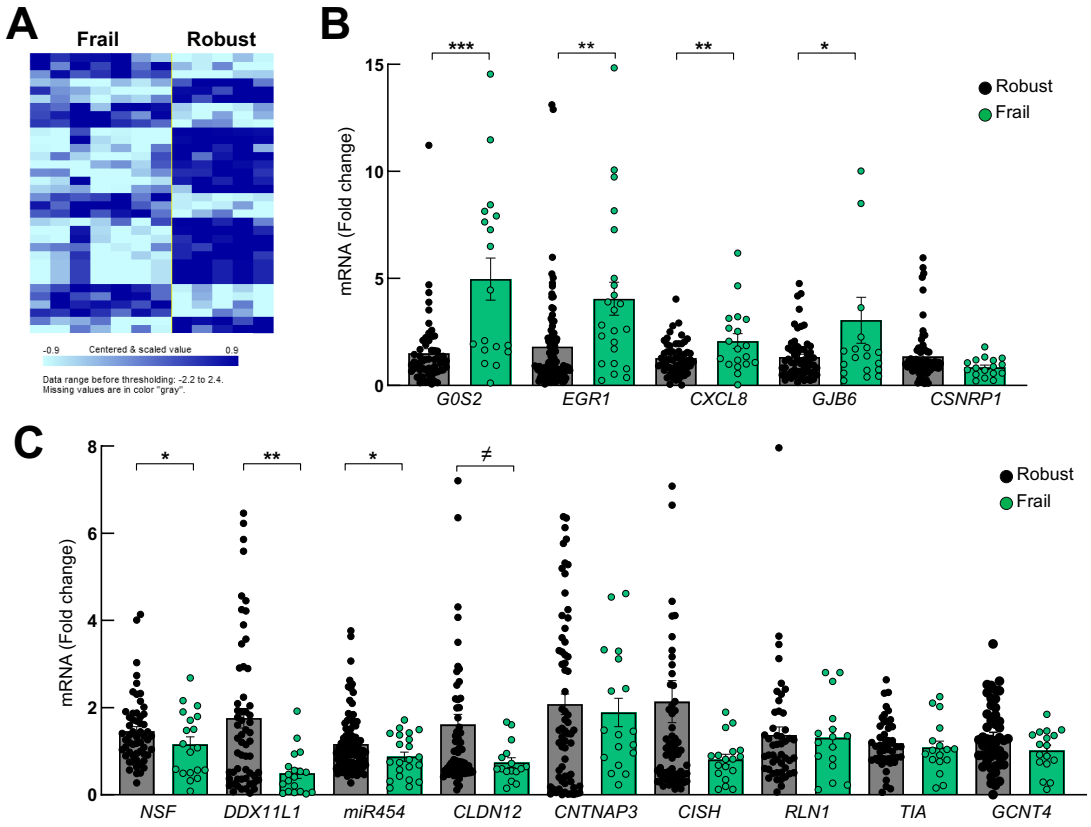

Figure R2. Transcriptomic studies reveal a differential expression pattern of 35 genes between robust and frail individuals. (A) Hierarchical clustering of robust (n = 5) and frail (n = 7) individuals classified by the three frailty scales (TUG, GS and TFI) based in the expression of the 35 selected genes. **(B, C)** mRNA levels of the 14 genes chosen for experimental validation (based on the highest FC and p-value) in PBMCs samples of the whole validation cohort 1 that includes robust (n = 108) and frail (n = 24) individuals for the 3 scales. **(B)** *G0S2, EGR1, CXCL8, GJB6* and *CSNRP1* were up-regulated and **(C)** *NSF, DDX11L1, miR454, CLDN12, CNTNAP3, CISH, RLN1, TIA* and *GCNT4* were down-regulated in frail individuals (n = 24) compared to robust ones (n = 108). The statistical significance was assessed with the Student's t-test ($^{\neq}$ $p < 0.1$, * $p < 0.05$, ** $p < 0.01$, *** $p < 0.001$).

The pattern of expression of the 7 selected genes is replicated in additional cohorts.

In order to further validate the differential expression of the 7 selected genes and link them to the most common scales used in frailty research, we studied their expression in 2 additional and independent cohorts. In the first one (validation cohort 2), frailty was assessed by Fried´s frailty phenotype, TUG and GS tests and only robust (n = 124) or frail (n = 44) individuals considering the three scales were selected. In this group, the increased levels of *G0S2, EGR1* (***Figure R3A***) and the reduced expression of *DDX11L1* and *miR454* (***Figure R3B***) in serum samples were statistically significant. In the second one (validation cohort 3), frailty was assessed by the FI, the Barthel Index and the CSHA Clinical Frailty scale, and robust (n = 19) and functionally impaired individuals (n = 32) were compared. In this context, statistically significant higher levels of *G0S2*, *EGR1*, and *GJB6* (***Figure R3C***) and reduced expression of *NSF* and *miR454* (***Figure R3D***) was detected in PBMCs of functionally impaired individuals compared to robust ones.

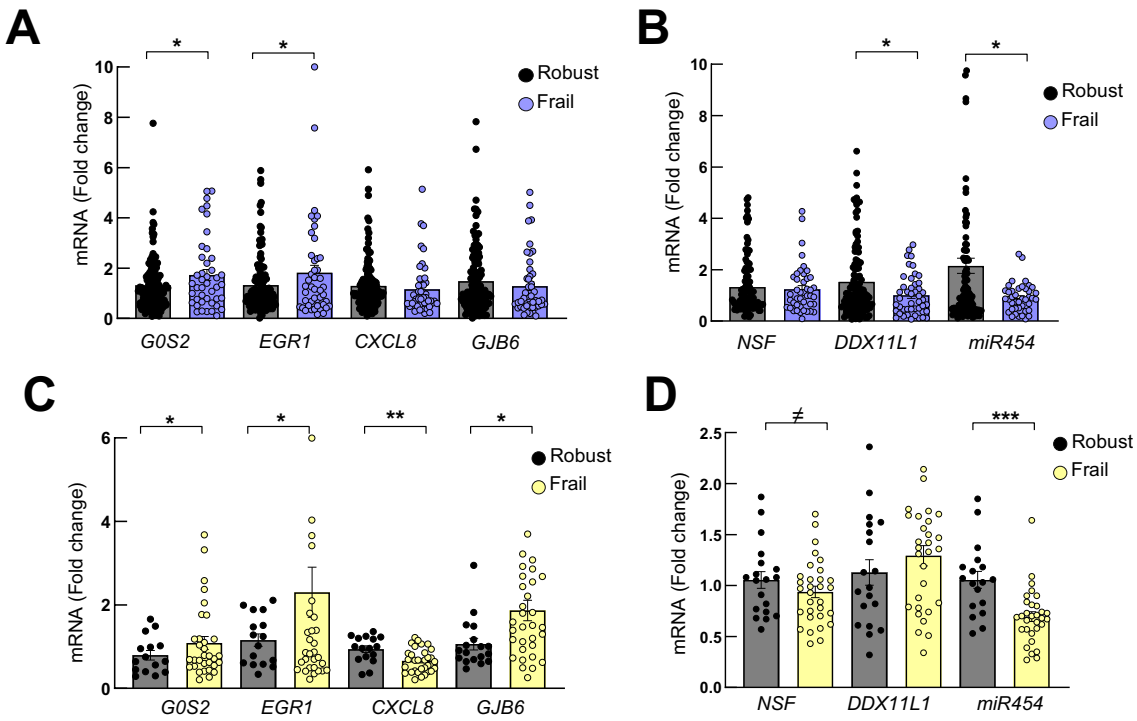

Figure R3. The pattern of expression of the 7 selected genes is replicated in additional cohorts using different frailty scales. (A, B) mRNA levels of the 7 selected genes in the validation cohort 2 where **(A)** *G0S2* and *EGR1* were up-regulated and **(B)** *NSF, DDX11L1* and *miR454* were down-regulated in serum samples of frail individuals (n = 44) compared to robust ones (n = 124). **(C, D)** mRNA levels of the 7 selected genes in the validation cohort 3 where **(C)** *G0S2, EGR1* and *GJB6* were up-regulated and **(D)** *NSF* and *miR454* were down-regulated in PBMCs of functionally impaired individuals (n = 32) compared to robust ones (n = 19). The statistical significance was assessed with the Student's t-test (≠ $p < 0.1$, * $p < 0.05$, ** $p < 0.01$, *** $p < 0.001$).

Intervention plans reverse the expression of the selected genes.

Then, the expression of the selected genes was studied in 3 cohorts of individuals who underwent different types of interventions. The first intervention plan, based on physical training during 12 weeks developed by 12 frail subjects from Gipuzkoa (intervention cohort 1), reduced the time of TUG in 7 out of 12 cases, with the mean time passing from 10.54 ± 0.60 seconds to 9.90 ± 0.39 seconds in pre- and post-intervention stages, respectively (***Figure R4A***). Similarly, SPPB was also improved in 8 out of 12 cases with values increasing from 7.15 ± 0.52 seconds to 8.08 ± 0.51 seconds after the intervention (***Figure R4B***). This implies a moderate success in partially recovering functional activity in the majority of individuals. Blood samples were collected before and after the intervention to determine the expression level of the 7 selected genes by RT-qPCR. The reversion was obtained with *EGR1*, since its expression levels were significantly reduced after the intervention (***Figure R4C***).

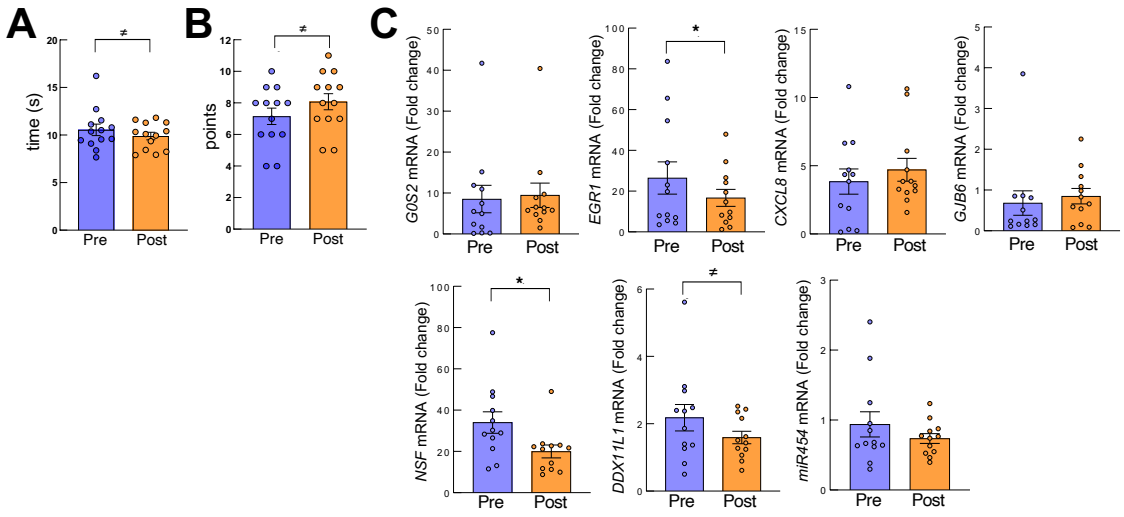

Figure R4. Physical intervention modulates the expression of the selected candidate genes. Evolution of **(A)** TUG and **(B)** SPPB performance after the intervention plan performed in the individuals from the intervention cohort 1 (n = 12). **(C)** mRNA levels of the 7 candidate genes determined in PBMCs of individuals pre- and post-intervention from the intervention cohort 1 (n = 12). The statistical significance was assessed with the Student's t-test (≠ $p < 0.1$, * $p < 0.05$).

Moreover, association studies showed that the better performance on TUG or SPPB tests correlated with a reduction in *EGR1* levels in more than 80% of the cases (6 out of 7 and 7 out of 8, respectively) (***Table R2***). Slightly lower percentages were obtained with the additional candidate genes (***Table R2***).

Table R2. Correlation studies between SPPB or TUG and the expression of the 7 candidate genes.

Expression	SPPB (performance)		TUG (performance)	
	Improvement	Equal or deterioration	Improvement	Equal or deterioration
G0S2 Higher	3/12 (25 %)	3/12 (25 %)	4/12 (33 %)	3/12 (25 %)
G0S2 Lower	5/12 (42 %)	1/12 (8 %)	3/12 (25 %)	2/12 (17 %)
EGR1 Higher	1/12 (8 %)	2/12 (17 %)	1/12 (8 %)	2/12 (17 %)
EGR1 Lower	7/12 (58 %)	2/12 (17 %)	6/12 (50 %)	3/12 (25 %)
CXCL8 Higher	4/12 (33 %)	2/12 (17 %)	4/12 (33 %)	2/12 (17 %)
CXCL8 Lower	4/12 (33 %)	2/12 (17 %)	3/12 (25 %)	3/12 (25 %)
GJB6 Higher	4/12 (33 %)	3/12 (25 %)	5/12 (42 %)	2/12 (17 %)
GJB6 Lower	4/12 (33 %)	1/12 (8 %)	2/12 (17 %)	3/12 (25 %)
NSF Higher	1/12 (8 %)	1/12 (8 %)	1/12 (8 %)	1/12 (8 %)
NSF Lower	7/12 (58 %)	3/12 (25 %)	6/12 (50 %)	4/12 (33 %)
DDX11L1 Higher	3/12 (25 %)	2/12 (17 %)	2/12 (17 %)	3/12 (25 %)
DDX11L1 Lower	5/12 (42 %)	2/12 (17 %)	5/12 (42 %)	2/12 (17 %)
miR454 Higher	4/12 (33 %)	1/12 (8 %)	3/12 (25 %)	2/12 (17 %)
miR454 Lower	4/12 (33 %)	3/12 (25 %)	4/12 (33 %)	3/12 (25 %)

SPPB, Short Physical Performance Battery test; TUG, Timed Up and Go.

Furthermore, we studied the expression of the 7 genes of interest in an additional cohort of individuals that performed 3 different types of intervention plans (dual task, walking and multicomponent) during 12 weeks (intervention cohort 2). These interventions showed a statistically significant reduction in Fried´s frailty phenotype (***Figure R5A***). The expression of the 7 selected genes was determined by qRT-PCR in plasma samples and we found a statistically significant reduction of *G0S2*, *EGR1*, *CXCL8* and *GJB6* expression (***Figure R5B***) and a statistically significant increase of *miR454* in post-intervention plasma samples (***Figure R5C***). In the other hand, frail individuals from the Valencia Hospital (intervention cohort 3) that performed swimming exercises 3 times per week for a total of 12 weeks also exhibited a statistically significant reduction in Fried´s frailty phenotype (***Figure R5D***). In this case, we observed a statistically significant reduction of *EGR1* and *CXCL8*, together with lower expression of *G0S2* and *GJB6* (***Figure R5E***) and higher levels of *miR454* (***Figure R5F***) in post-intervention plasma samples. These data suggest that after different types of intervention plans, the frailty phenotype is reverted and the expression of some genes is restored.

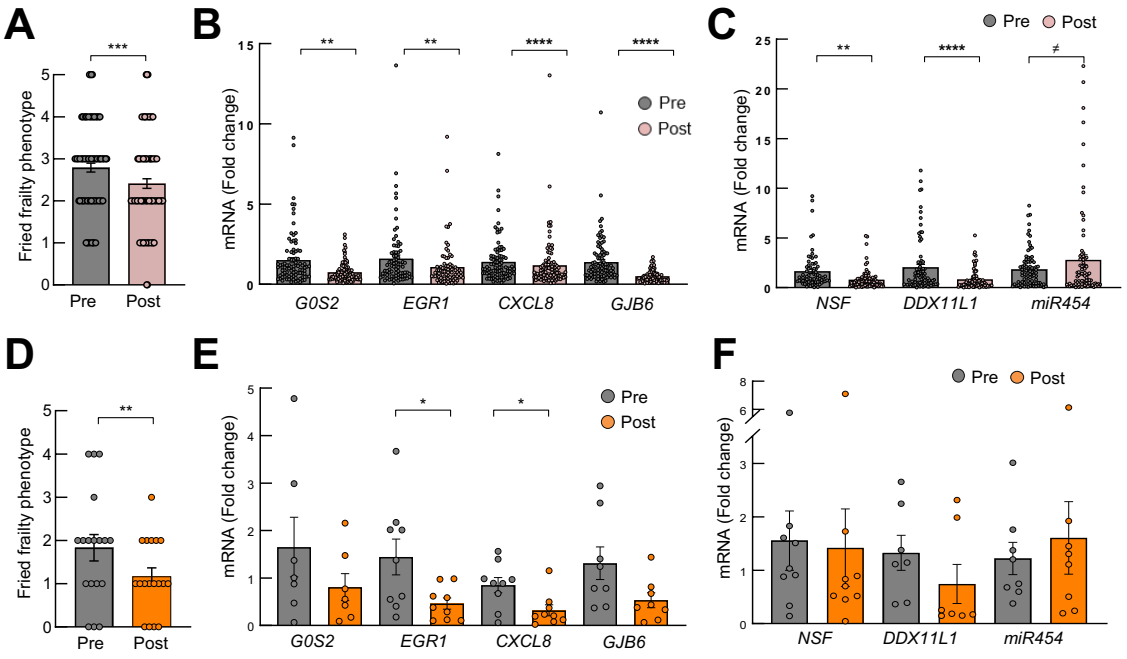

Figure R5. The pattern of expression of the 7 selected genes is restored after different intervention plans. **(A)** Evolution of Fried´s frailty phenotype after the intervention plan performed in the individuals from the intervention cohort 2 (n = 95). **(B, C)** mRNA levels of the 7 candidate genes determined in plasma samples of individuals pre- and post-intervention from the intervention cohort 2 (n = 95) where **(B)** *G0S2, EGR1, CXCL8* and *GJB6* were down-regulated and **(C)** *miR454* was up-regulated in post-intervention plasma samples. **(D)** Evolution of Fried´s frailty phenotype after the intervention plan performed in the individuals from the intervention cohort 3 (n = 18). **(E, F)** mRNA levels of the 7 candidate genes determined in plasma samples of individuals pre- and post-intervention from the intervention cohort 3 (n = 18) where **(E)** *G0S2, EGR1, CXCL8* and *GJB6* were down-regulated and **(F)** *miR454* was up-regulated in post-intervention plasma samples. The statistical significance was assessed with the Student's t-test ($^{\neq}$ $p < 0.1$, * $p < 0.05$, ** $p < 0.01$, *** $p < 0.001$, **** $p < 0.0001$).

Serial passage-cultured human primary cells display a similar pattern of expression as frail individuals.

Frailty and aging share some biomarkers and underlying molecular mechanisms [120], [122]. The maintenance of cells for several passages under culture conditions creates a stress context that induces phenotypic and molecular changes in cells that resemble physiological aging *in vivo* [333]. Consequently, the expression of the 7 selected candidate genes was determined by RT-qPCR in human primary myoblasts isolated from muscle biopsies of healthy individuals and cultured for several passages. We found that the expression of *EGR1* and *GJB6* was significantly elevated (***Figure R6A***) and that the levels of *NSF*, *DDX11L1* and *miR454* were significantly decreased (***Figure R6B***) in late passage

myoblasts compared to early ones. Further analyses showed that late passage cells presented statistically significant higher levels of *p16*^{INK4A} and *IL6* (***Figure R6C***), the well-known biomarkers of aging and senescence, providing further validation of the experimental setting.

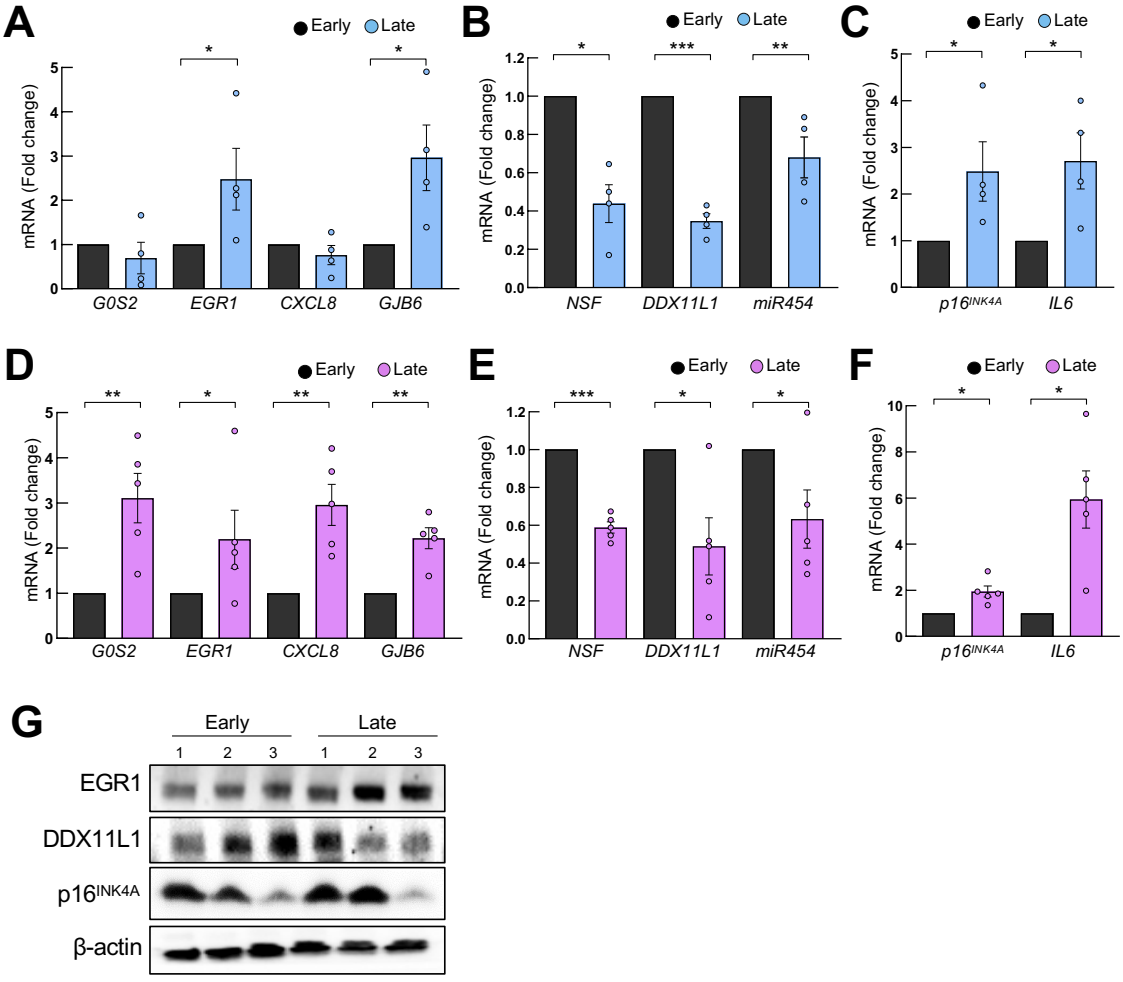

Figure R6. The expression pattern of the 7 selected genes is maintained in serial passage-cultured human primary fibroblasts and myoblasts. (A, B) Relative mRNA levels of the 7 candidate genes in human primary myoblasts obtained from muscle biopsies of healthy individuals and cultured at early (2 – 3) and late (10 – 12) passages (n = 4) where **(A)** *EGR1* and *GJB6* were up-regulated and **(B)** *NSF, DDX11L1* and *miR454* were down-regulated in late passage primary myoblasts compared to early passage ones (n = 5). **(C)** *p16*^{INK4A} and *IL6* relative mRNA expression in early and late passage human primary myoblasts (n = 4). **(D, E)** Relative mRNA levels of the 7 candidate genes in human primary fibroblasts obtained from skin biopsies of 5 individuals and cultured at early (5 – 10) and late (35 – 40) passages (n = 5) where **(D)** *G0S2, EGR1, CXCL8* and *GJB6* were up-regulated and **(E)** *NSF, DDX11L1* and *miR454* were down-regulated in late passage primary fibroblasts compared to early passage ones (n = 5). **(F)** *p16*^{INK4A} and *IL6* relative mRNA expression in early and late passage human primary fibroblasts (n = 5). Data were relativized to the expression in early passage cultures. The statistical significance was assessed with the Student's t-test (* $p < 0.05$, ** $p < 0.01$, *** $p < 0.001$). **(G)** Protein levels of EGR1, DDX11L1 and p16^{INK4A} in early and late passage human primary fibroblast (n = 3).

Additionally, the expression of the 7 selected candidate genes was determined in human primary fibroblasts derived from adult individuals at early and late passages. In line with the results obtained in myoblasts, an increase of *G0S2*, *EGR1*, *CXCL8* and *GJB6* expression (***Figure R6D***), as well as lower levels of *NSF*, *DDX11L1* and *miR454* in late passage fibroblasts compared to early ones was detected (***Figure R6E***). Late passage fibroblasts also displayed higher $p16^{INK4A}$ and *IL6* expression (***Figure R6F***). We also observed a higher expression of EGR1 and a lower expression of DDX11L1 at protein level by western blot in late passage fibroblasts from 3 different individuals compared to early ones (***Figure R6G***).

A reduced pattern of 3 genes (EGR1, DDX11L1 and miR454) identifies frail individuals and is associated with adverse health outcomes.

The discriminating and diagnostic potential of the 7 genes selected was checked through the construction of individual ROC curves for each gene in the whole validation cohort 1 (robust, n = 108 and frail, n = 24). Among them, *EGR1* was especially remarkable as it showed the best individual ROC curve with an area under the curve (AUC) of 0.715, followed by *G0S2* (AUC = 0.703), *DDX11L1* (AUC = 0.623), *NSF* (AUC = 0.594), *GJB6* (AUC = 0.582), *miR454* (AUC = 0.538) and *CXCL8* (AUC = 0.469) (***Figure R7A***). Next, we tried to obtain the minimum number of candidate genes that could allow the identification of frail individuals. Thus, we performed the same strategy and we made ROC curves with combinations of genes. A group of only three genes, *EGR1*, *DDX11L1* and *miR454*, could predict the status of frailty with an AUC of 0.869 improving the predictive power of each gene individually (***Figure R7B***). These results point out that *EGR1* alone or in combination with *DDX11L1* and *miR454* could be a good biomarker of frailty.

With the aim to further characterize the link between *EGR1*, *DDX11L1* and *miR454* with frailty, we studied the association of their expression with clinical characteristics of the individuals of the whole validation cohort 1. Notably, the expression of the 3 genes in combination significantly correlated with the burden of comorbidity measured as Charlson Comorbidity Index and with polypharmacy (***Table R3***). These results show the association of *EGR1*, *DDX11L1* and *miR454* expression with relevant adverse health outcomes related to frailty syndrome.

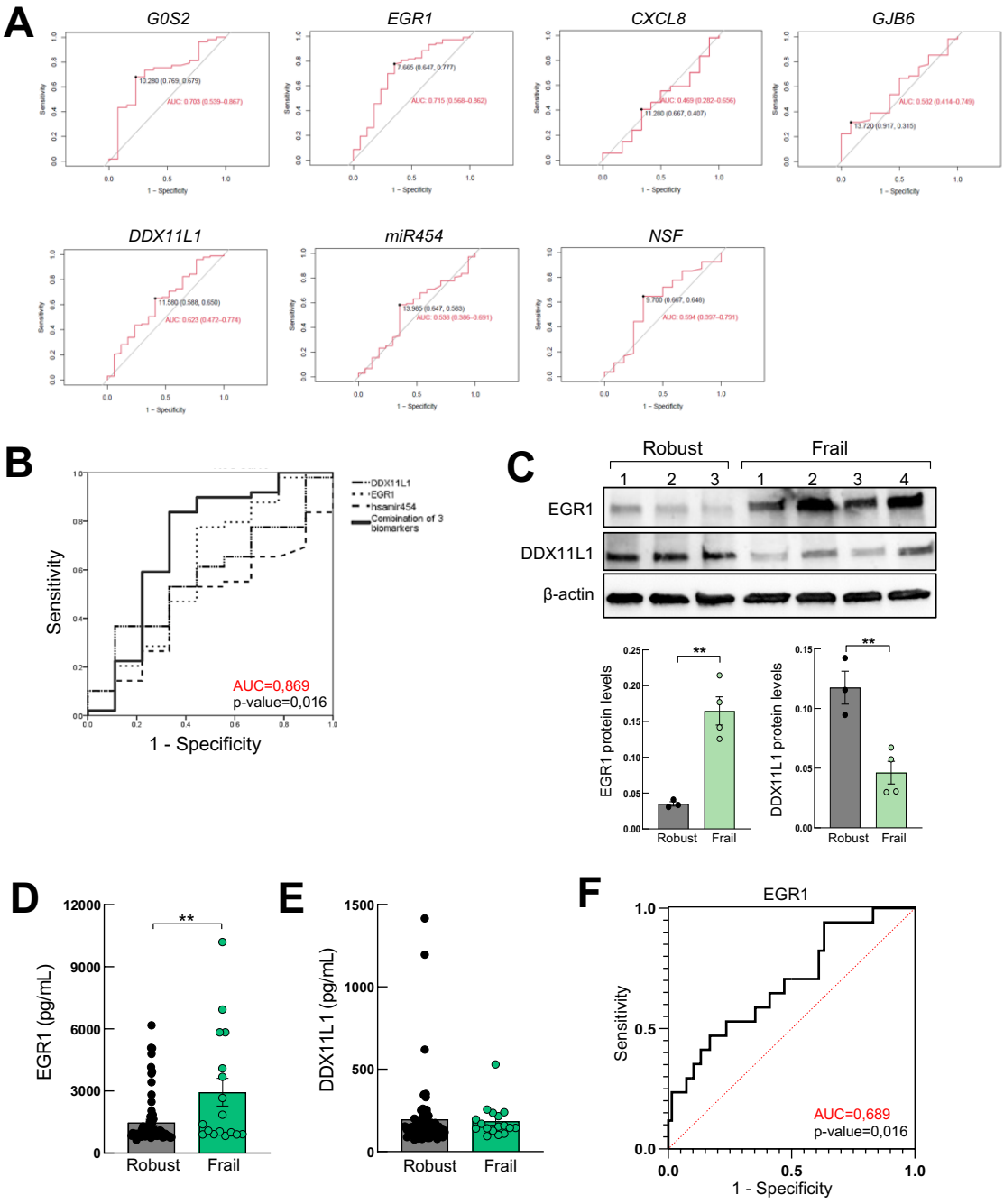

Figure R7. A reduced pattern of 3 genes (*EGR1*, *DDX11L1* and *miR454*) identifies frail individuals. (A) Individual ROC curves of the 7 selected genes performed with the information of individuals from the whole validation cohort 1 that includes robust (n = 108) and frail (n = 24) individuals: *G0S2* (AUC = 0.703), *EGR1* (AUC = 0.715), *CXCL8* (AUC = 0.469), *GJB6* (AUC = 0.582), *DDX11L1* (AUC = 0.623), miR454 (AUC = 0.538) and *NSF* (AUC = 0.594). **(B)** ROC curve with the combination of *EGR1, DDX11L1* and *miR454* (AUC = 0.869) performed with the information of individuals from the same cohort. **(C)** Representative western blot and protein quantification of *EGR1* and *DDX11L1* in PBMCs of robust (n = 3) and frail (n = 4) individuals from the array cohort. **(D)** ELISA assay of EGR1 and **(E)** DDX11L1 in robust (n = 41) and frail (n = 17) serum samples of individuals from the validation cohort 2. **(F)** ROC curve of EGR1 (AUC = 0.689) performed with the information of protein levels in serum of individuals from the validation cohort 2 that includes robust (n = 41) and frail (n = 17) individuals. The statistical significance was assessed with the Student´s t-test (** $p < 0.01$).

Table R3. Description and comparison between the clinical data and the expression of *EGR1*, *DDX11L1* and *miR454* in the whole validation cohort.

		Expression of *EGR1*, *DDX11L1* and *miR454*			
	Total	None	At least one	All	p-value
Sample Size	234	95 (41 %)	134 (57 %)	5 (2 %)	
Age, mean (SD)	80.6 (4.2)	80.9 (4.1)	80.4 (4.3)	80 (3.1)	0.568
CCI, mean (SD)	1 (1.2)	0.7 (0.8)	1.1 (1.4)	2 (1.6)	0.011
median (Q1, Q3)	1 (0.1)	0.5 (0.1)	1 (0.2)	2 (1.5, 2.5)	0.055
Number of drugs	5.6 (3.5)	5.1 (3.8)	5.8 (3.2)	8.4 (3.2)	0.051
median (Q1, Q3)	5 (3.7)	4 (2.7)	6 (4.7)	8 (6.1)	0.012
Polypharmacy (>5 drugs)	132 (57 %)	84 (63 %)	43 (45 %)	5 (100%)	0.003
SPPB score, mean (SD)	9 (1.7)	9.5 (1.3)	8.8 (1.9)	7.8 (0.5)	0.008
median (Q1, Q3)	9 (8.1)	10 (9.1)	9 (7.1)	8 (7.8, 8)	0.006
Frail by SPPB	105 (58 %)	33 (45 %)	68 (65 %)	4 (100 %)	0.004

CCI, Charlson Comorbidity Index.

Next, we carried out the study of EGR1 and DDX11L1 at protein level. For this, we first checked the expression levels of these genes by western blot between robust and frail individuals in the protein extracted from the PBMCs used for the gene expression microarray. We observed a statistically significant increase of EGR1 and decrease in DDX11L1 protein levels in frail individuals compared to robust ones (***Figure R7C***). We also performed ELISA assays of both proteins in robust (n = 41) and frail (n = 17) serum samples of individuals from the validation cohort 2. We observed a statistically significant increase of EGR1 levels in frail individuals compared to robust ones (***Figure R7D***) but no differences between the groups in the case of DDX11L1 levels (***Figure R7E***). Moreover, we build a ROC curve using the information of this assay and EGR1 showed a strong predictive potential for the detection of frail individuals with an AUC of 0.689 (***Figure R6F***). In summary, our results correlate the expression of EGR1, DDX11L1 and *miR454* with frailty syndrome.

miR454 overexpression rejuvenates cellular activity.

Next, we studied the cellular effects of modulating *miR454*, *EGR1* and *DDX11L1* expression in human primary fibroblasts. First, we performed the overexpression of *miR454*

through lentiviral infections after cloning full-length *miR454* cDNA into the control plasmid *pLKO*. We detected statistically significant higher levels of *miR454* in the fibroblasts with *miR454* overexpression (*miR454*) compared to control cells (*pLKO*), thus validating our model (***Figure R8A***). Then, we analyzed the cellular effects of increasing *miR454* activity. In this case, *miR454*-overexpressing fibroblasts displayed a statistically significant higher cell growth compared to control fibroblasts measured by cell counting (***Figure R8B***). The increased cell growth observed in the *miR454* fibroblasts, was complemented by the quantification of EdU, Ki67 and pH3 positive cells, as markers of proliferation, which were also significantly increased in approximately 2.5-fold in comparison to control fibroblasts (***Figure R8C - E***). In addition, cellular senescence, measured as the number of SA-β-gal positive cells, was significantly reduced in *miR454*-overexpressing fibroblasts (***Figure R8F***). This functional analysis correlated at the molecular level with lower protein levels of $p16^{INK4A}$ and $p21^{CIP1}$ in *miR454*-overexpressing fibroblasts (***Figure R8G***). These data suggest that *miR454* plays a positive role in delaying aging-associated phenotypes in human primary fibroblasts.

DDX11L1 silencing alters cell activity.

Then, we performed *DDX11L1* downregulation using two independent short interference siRNAs constructs (*siRNA1* and *siRNA2*). We detected statistically significant lower levels of *DDX11L1* in the *siRNA1* and *siRNA2* fibroblasts compared to control ones (*Control*) (***Figure R9A***). Furthermore, we observed a statistically significant reduction in cell growth measured by cell counting in the *DDX11L1*-silenced fibroblasts (***Figure R9B***). We also found a significantly lower number of positive cells for EdU, Ki67 and pH3 markers (***Figure R9C - E***), indicating that cell proliferation was impaired in *DDX11L1*-silenced cells. In addition, cellular senescence, measured as the number of SA-β-gal positive cells, was significantly increased in *siRNA1* and *siRNA2* fibroblasts compared to *Control* ones (***Figure R9F***). These data correlated at the molecular level, with higher protein levels of $p16^{INK4A}$ and $p21^{CIP1}$ in fibroblasts with silencing of *DDX11L1* (***Figure R9G***). These results indicates that *DDX11L1* silencing reduces cell proliferation and increases senescence in human primary fibroblasts suggesting that *DDX11L1* could play a regulatory role in aging-associated processes.

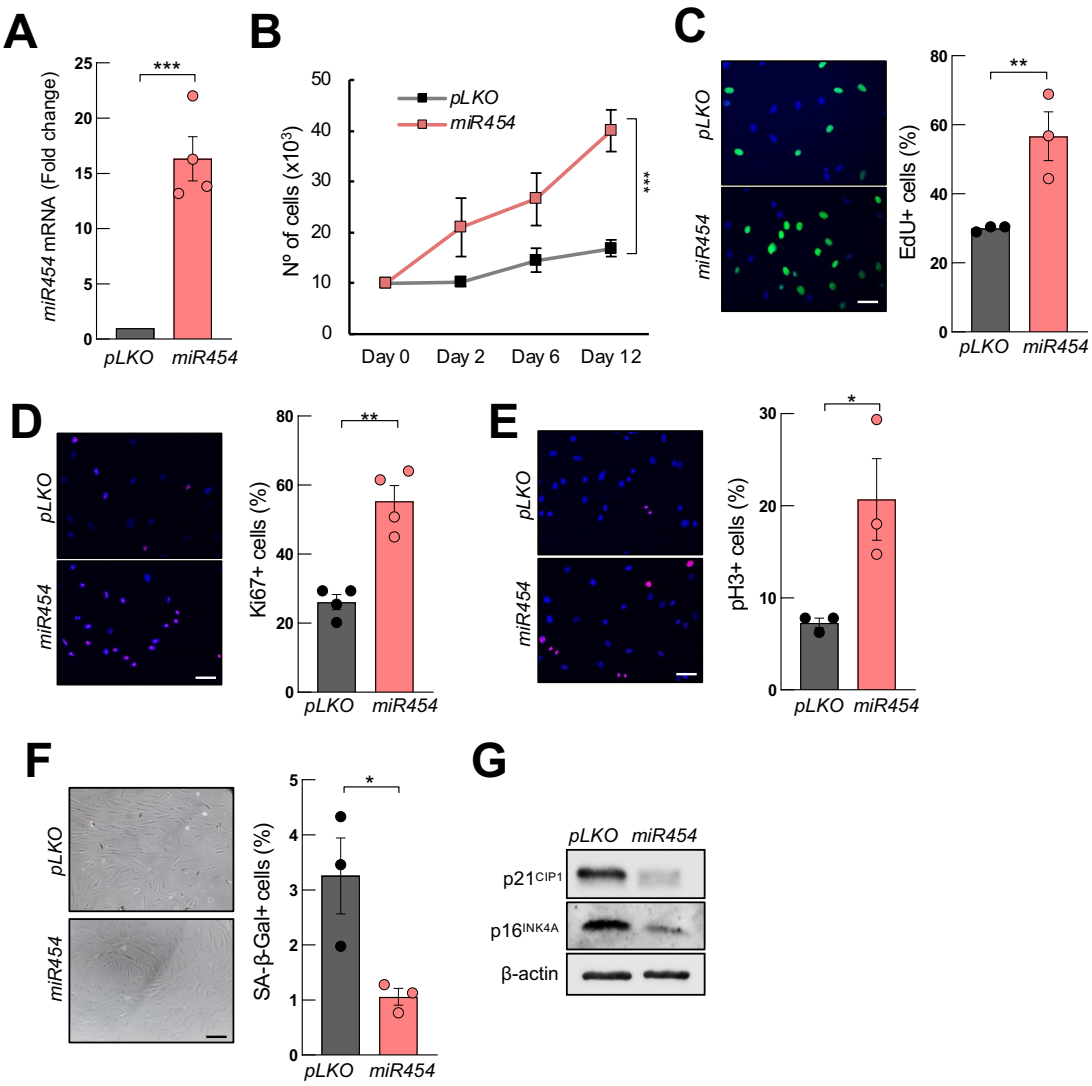

Figure R8. *miR454* overexpression rejuvenates cellular activity. Human primary fibroblasts were lentivirally-infected with a construct expressing full-length *miR454*. **(A)** Relative mRNA levels of *miR454* in overexpressing (*miR454*) and control (*pLKO*) primary fibroblasts (n = 4). Data were relativized to the expression in *pLKO* fibroblasts. **(B)** Cell growth at indicated time points in *miR454* fibroblasts compared to *pLKO* ones (n = 3). Representative images (scale bar = 50 µm) and percentage of **(C)** EdU positive cells (n = 3), **(D)** Ki67 positive cells (n = 4), **(E)** pH3 positive cells (n = 3) and **(F)** SA-β-gal activity (n = 3) in *miR454* fibroblasts compared to *pLKO* ones. **(G)** Representative western blot of $p21^{CIP1}$ and $p16^{INK4A}$ in *miR454* fibroblasts compared to *pLKO* ones (n = 3). The statistical significance was assessed with the Student's t-test (* $p < 0.05$, ** $p < 0.01$, *** $p < 0.001$).

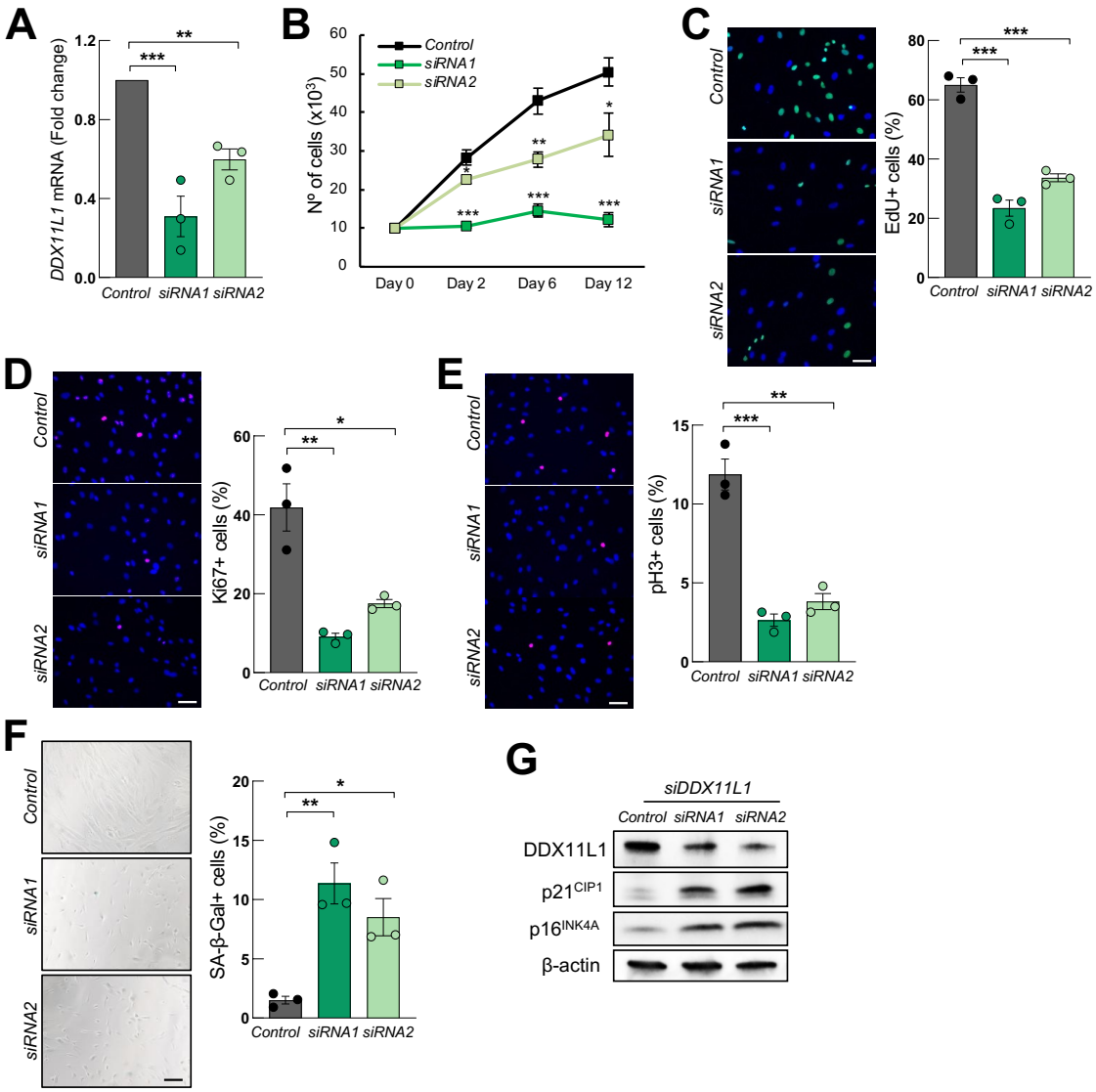

Figure R9. *DDX11L1* silencing alters proliferation and senescence. For *DDX11L1* downregulation, we used two independent short interference siRNAs constructs (*siRNA1* and *siRNA2*). **(A)** Relative mRNA levels of *DDX11L1* in primary fibroblasts with *DDX11L1* downregulation (*siRNA1* and *siRNA2*) compared to control fibroblasts (*Control*) (n = 4). Data were relativized to the expression in *Control* fibroblasts. **(B)** Cell growth at indicated time points in *siRNA1* and *siRNA2* fibroblasts compared to *Control* ones (n = 3). Representative images (scale bar = 50 µm) and percentage of **(C)** EdU positive cells (n = 3), **(D)** Ki67 positive cells (n = 3), **(E)** pH3 positive cells (n = 3) and **(F)** SA-β-gal activity (n = 3) in *siRNA1* and *siRNA2* fibroblasts compared to *Control* ones. **(G)** Representative western blot of DDX11L1, $p21^{CIP1}$ and $p16^{INK4A}$ in *siRNA1* and *siRNA2* fibroblasts compared to *Control* ones (n = 3). The statistical significance was assessed with the Student's t-test (* $p < 0.05$, ** $p < 0.01$, *** $p < 0.001$).

EGR1 modulation (silencing and overexpression) alters cellular activity.

Additionally, we studied the effects of modulating *EGR1* expression in human primary fibroblasts and we performed silencing and overexpression experiments. First, we achieved *EGR1* downregulation through lentiviral infections using two independent shRNA (*sh1* and *sh2*). We detected statistically significant lower levels of *EGR1* in the fibroblasts with *EGR1* downregulation (*sh1* and *sh2*) compared to control fibroblasts (*pLKO*) (***Figure R10A***). Moreover, we observed a statistically significant reduction of cell growth (***Figure R10B***) as well as in cell proliferation in *EGR1*-silenced cells, measured as the number of positive cells for EdU, Ki67 and pH3 markers (***Figure R10C - E***). Moreover, senescence was increased as the number of SA-β-gal positive cells (***Figure R10F***) and the protein expression of $p16^{INK4A}$ and $p21^{CIP1}$ was elevated in cells with silencing of *EGR1* compared to control ones (***Figure R10G***).

Secondly, we performed the overexpression of *EGR1* and primary fibroblasts were transduced with lentiviral vectors containing the coding sequence of *EGR1* (*EGR1*) or the empty vector (*pLKO*). In this case, *EGR1*-overexpressing fibroblasts (***Figure R11A***) displayed significantly higher cell growth (***Figure R11B***) and higher number of positive cells for EdU, Ki67 and pH3 markers (***Figure R11C - E***), indicating that the fibroblasts with overexpression of *EGR1* exhibit greater proliferation than control fibroblasts. Besides, cellular senescence, measured as the number of SA-β-gal positive cells, was significantly reduced in *EGR1*-overexpressing fibroblasts (***Figure R11F***).

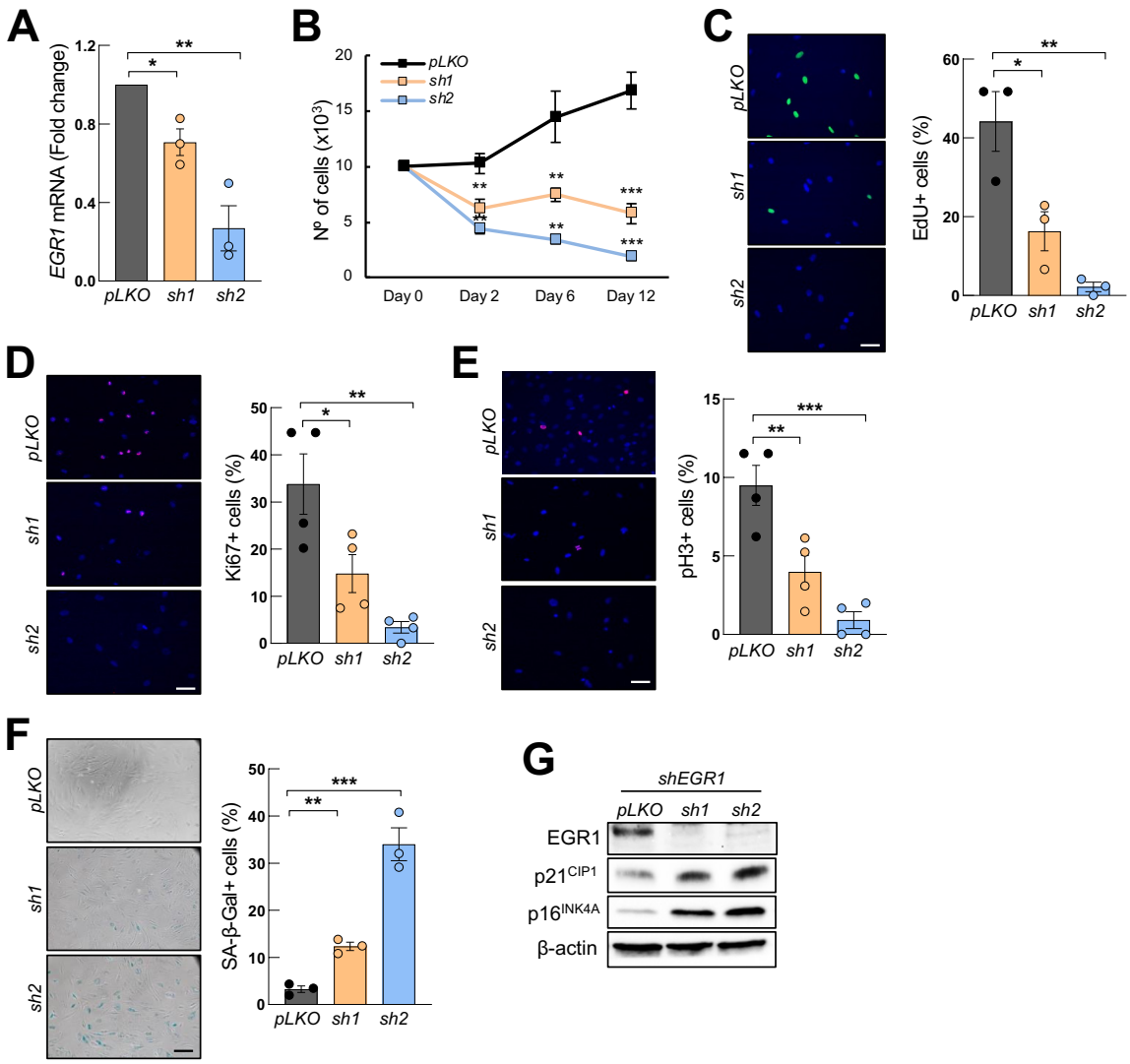

Figure R10. Silencing of *EGR1* alters cellular activity. For *EGR1* downregulation, we performed lentiviral infections using two independent shRNA (*sh1* and *sh2*). **(A)** Relative mRNA levels of *EGR1* in primary fibroblasts with *EGR1* downregulation (*sh1* and *sh2*) compared to control fibroblasts (*pLKO*) (n = 3). Data were relativized to the expression in *pLKO* fibroblasts. **(B)** Cell growth at indicated time points in *sh1* and *sh2* fibroblasts compared to *pLKO* ones (n = 3). Representative images (scale bar = 50 µm) and percentage of **(C)** EdU positive cells (n = 3), **(D)** Ki67 positive cells (n = 4), **(E)** pH3 positive cells (n = 4) and **(F)** SA-β-gal activity (n = 3) in *sh1* and *sh2* fibroblasts compared to *pLKO* ones. **(G)** Representative western blot of EGR1, $p21^{CIP1}$ and $p16^{INK4A}$ in *sh1* and *sh2* fibroblasts compared to *pLKO* ones (n = 3). The statistical significance was assessed with the Student's t-test (* $p < 0.05$, ** $p < 0.01$, *** $p < 0.001$).

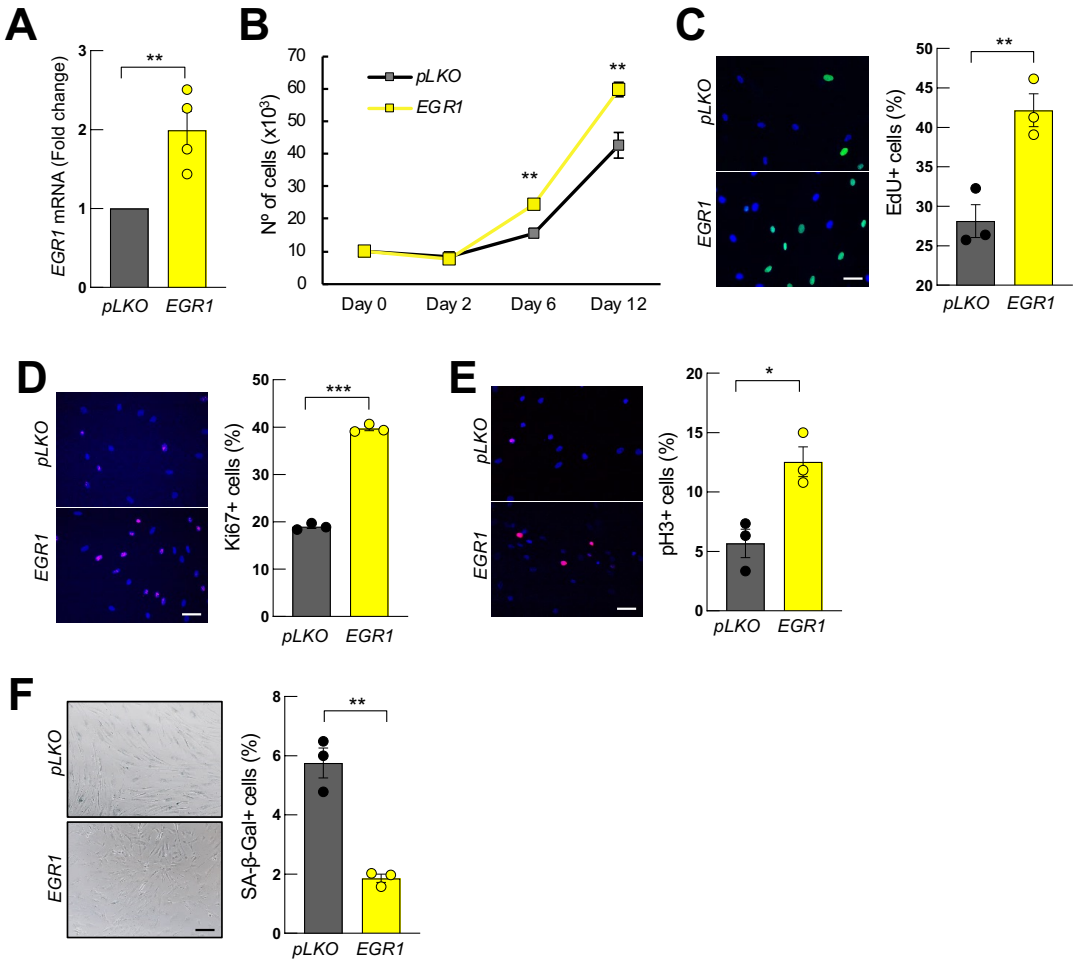

Figure R11. *EGR1* overexpression alters cellular activity. Human primary fibroblasts were lentivirally-infected with a construct expressing the coding sequence of *EGR1*. **(A)** Representative mRNA levels of *EGR1* in overexpressing (*EGR1*) and control (*pLKO*) primary fibroblasts (n = 4). Data were relativized to the expression in *pLKO* fibroblasts. **(B)** Cell growth at indicated time points in *EGR1* fibroblasts compared to *pLKO* ones (n = 3). Representative images (scale bar = 50 µm) and percentage of **(C)** EdU positive cells (n = 3), **(D)** Ki67 positive cells (n = 3), **(E)** pH3 positive cells (n = 3) and **(F)** SA-β-gal activity (n = 3) in *EGR1* fibroblasts compared to *pLKO* ones. The statistical significance was assessed with the Student's t-test (* $p < 0.05$, ** $p < 0.01$, *** $p < 0.001$).

Finally, we perform a longevity assay for the determination of lifespan using a *C. elegans* model with knockdown for the ortholog of *EGR1* human gene (*egrh-1*). Thus, *egrh-1* was silenced in an adult model of *C. elegans* using RNAi (*egrh-1 RNAi*). We observed higher survival in the *egrh-1*-silenced model compared to wild type one (***Figure R12A***). Altogether, these data point out that *EGR1* plays a regulatory role in aging-associated processes *in vitro* and longevity *in vivo.*

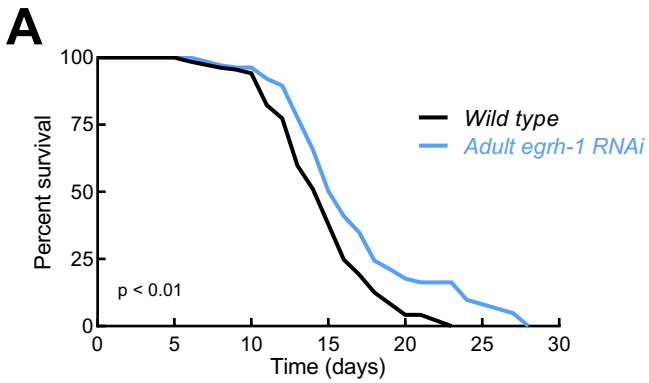

Figure R12. Knockdown of the human ortholog of *egrh-1* in *C. elegans* increases survival. (A) Survival curve in adult *C. elegans* model with knockdown for the human *EGR1* ortholog (*Adult egrh-1 RNAi*) compared to control model (*Wild type*) (n = 2). The statistical significance was assessed with Gehan-Breslow-Wilcoxon test ($p < 0.01$).

Analysis of downstream targets of EGR1 and miR454 identifies senescence-associated pathways potentially involved in frailty.

The data presented so far highlight the expression and potential role that *EGR1*, *DDX11L1* and *miR454* can play in cell aging and frailty. Therefore, we went deeper in the study of their potential downstream targets. For *EGR1*, a protein-protein interaction network was completed by Search Tool for the Retrieval of Interacting Genes/Proteins (STRING) (https://string-db.org/), which revealed predicted targets such as *C-JUN*, *FOS*, *PTEN AREG*, *CD69* or several mitogen-activated protein kinases (MAPKs) (***Figure R13A***). In the case of *miR454*, previous literature suggested *PTEN*, $p21^{CIP1}$ and *TRIM3* as potential targets of its activity [334]–[336]. Moreover, *DDX11L1* belongs to a transcript family located in sub-telomeric region, which can modulate various processes of telomere activity [337]. Of note, all these genes have been related to maintenance of cell homeostasis and senescence [38], [338]–[340]. Their expression was studied in frail and robust individuals from the whole validation cohort (validation cohort 1), wherein an elevation in *C-JUN, CD69, PTEN,* $p21^{CIP1}$ and *TRIM3*, was observed in frail individuals, although in the later 3 the differences were not statistically significant (***Figure R13B and C***). In the case of *AREG*, its levels were decreased in frail individuals compared to robust ones (***Figure R13B***). Altogether, these results suggest that the pattern of 3 genes could be associated with senescence related pathways.

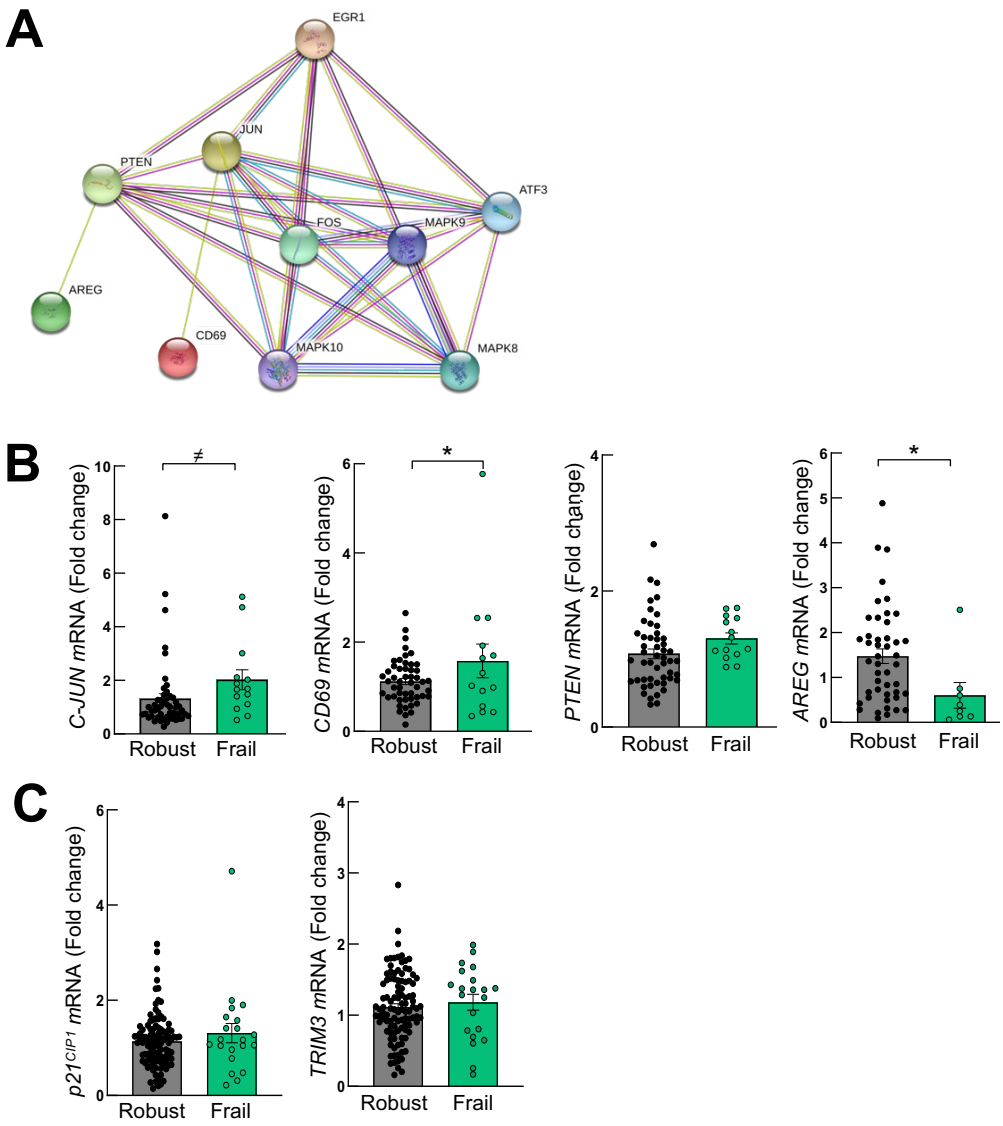

Figure R13. Downstream targets of *EGR1* and *miR454* are deregulated in frail individuals. (A) Protein-protein interaction network of *EGR1* predicted by STRING tool (https://string-db.org/). **(B)** *C-JUN, CD69, PTEN* and *AREG* mRNA levels in PBMCs of robust (n = 51) and frail (n = 14) individuals from the validation cohort 1. **(C)** $p21^{CIP1}$ and *TRIM3* mRNA levels in PBMCs of robust (n = 105) and frail (n = 22) individuals from the same cohort. The statistical significance was assessed with the Student's t-test ($^{\neq}$ $p < 0.1$, * $p < 0.05$).

Frail individuals present higher expression of cellular senescence genes and their levels are reverted after different intervention plans.

With the aim of reinforce the link between the processes of frailty and senescence, we studied some of the well-known senescence markers involved in cell cycle arrest and SASP [341], [342] such as $p16^{INK4A}$, $p21^{CIP1}$ and *IL6*, in the different cohorts of the study. First, we observed that the protein levels of $p16^{INK4A}$ and $p21^{CIP1}$ were significantly increased in the

PBMCs of frail individuals from the microarray cohort (***Figure R14A***). Then, we evaluated the expression of these genes at RNA level in the additional and independent validation cohorts (***Figure R14B - D***). In the validation cohort 2 we detected an increase of $p16^{INK4A}$, $p21^{CIP1}$ and *IL6* expression in serum samples that was statistically significant in the case of $p16^{INK4A}$ and $p21^{CIP1}$ (***Figure R14C***) and in the validation cohort 3, we observed significantly higher levels of $p16^{INK4A}$, $p21^{CIP1}$ and *IL6* in PBMCs of functionally impaired individuals (***Figure R14D***). These data suggest that frail individuals present increased expression of cellular senescence genes. Additionally, we checked the levels of these 3 genes in blood samples from the individuals that performed different types of intervention during 12 weeks (intervention cohort 1 and 2). Due to a sample limitation, the levels of these genes in intervention cohort 3 could not be tested. In the case of the intervention cohort 1, we found a statistically significant lower expression of $p16^{INK4A}$, $p21^{CIP1}$ and *IL6* in post-intervention PBMCs samples (***Figure R14E***). In the intervention cohort 2, the expression of the 3 genes was reverted in plasma samples after the intervention, being the decrease statistically significant in the case of $p21^{CIP1}$ and *IL6* (***Figure R14F***). These data indicate that different types of intervention with physical activity reverse the expression of the genes associated with senescence.

The treatment of late passage fibroblasts with senolytic compounds restores the expression pattern observed in frail individuals.

Taking into account the link between senescence and frailty obtained in the analysis of expression in different cohorts and in the functional assays, late passage fibroblasts were treated with senolytic compounds and we studied whether there was a reversion in the expression of the 7 identified genes. We used 3 different senolytic compounds, the anti-apoptotic protein inhibitor Navitoclax [343], [344], the tyrosine kinase inhibitor Dasatinib [345] and Quercetin [346]. We observed a statistically significant reduction of senescence measured as the number of SA-β-gal positive cells in treated fibroblasts compared to control ones (***Figure R15A***) together with a statistically significant increase of apoptosis measured as the number of Caspase 3 positive cells by IF (***Figure R15B***). At the molecular level, we noticed a statistically significant lower expression of EGR1 and higher levels of DDX11L1 and *miR454* at both RNA (***Figure R15C and D***) and protein levels (***Figure R15E***) in treated fibroblast compared to control ones. In addition, the expression of *G0S2*, *CXCL8*, *GJB6* was significantly

reduced (***Figure R15C***) and the levels of *NSF* were higher in treated fibroblasts (***Figure R15D***). These data suggest that the treatment with senolytics can reverse the expression pattern observed in frail individuals, which reinforces the link between the frailty and senescence.

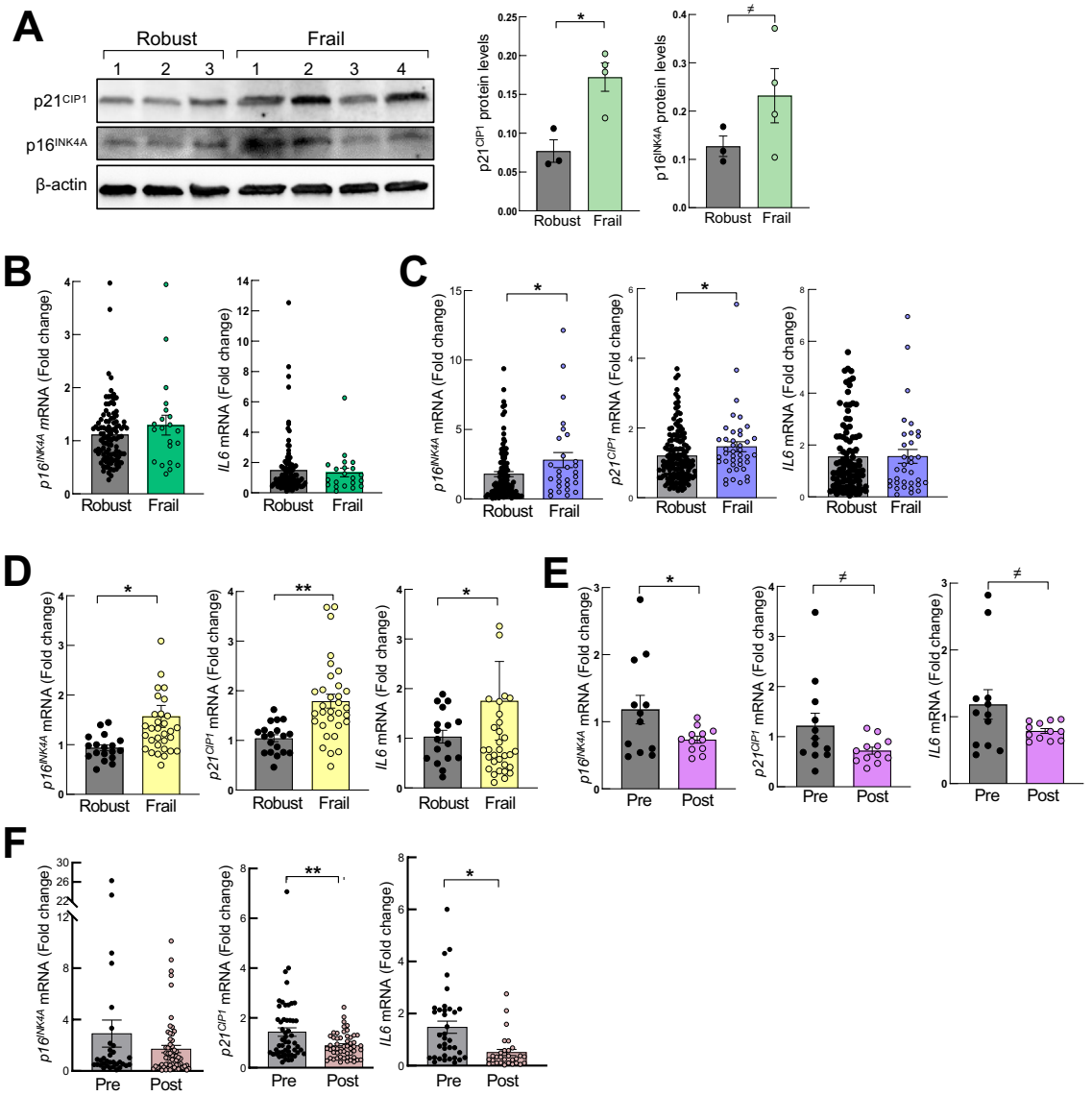

Figure R14. Frail individuals present higher expression of cellular senescence-specific genes and it is reverted after physical intervention plans. (A) Representative western blot and protein quantification of $p21^{CIP1}$ and $p16^{INK4A}$ in PBMCs of robust (n = 3) and frail (n = 4) individuals from the array cohort. **(B)** mRNA levels of $p16^{INK4A}$ and *IL6* in PBMCs of robust (n = 105) and frail (n = 22) individuals from the validation cohort 1. **(C)** mRNA levels of $p16^{INK4A}$, $p21^{CIP1}$ and *IL6* in serum samples of frail individuals (n = 44) compared to robust ones (n = 124) from the validation cohort 2. **(D)** mRNA levels of $p16^{INK4A}$, $p21^{CIP1}$ and *IL6* in PBMCs of functionally impaired individuals (n = 32) compared to robust ones (n =19) from the validation cohort 3. **(E)** mRNA levels of $p16^{INK4A}$, $p21^{CIP1}$ and *IL6* determined in PBMCs of individuals pre- and post-intervention from the intervention cohort 1 (n =12). **(F)** mRNA levels of $p16^{INK4A}$, $p21^{CIP1}$ and *IL6* determined in plasma samples of individuals pre- and post-intervention from the intervention cohort 2 (n ≥ 32). The statistical significance was assessed with the Student's t-test ($^{\neq}$ $p < 0.1$, * $p < 0.05$, ** $p < 0.01$).

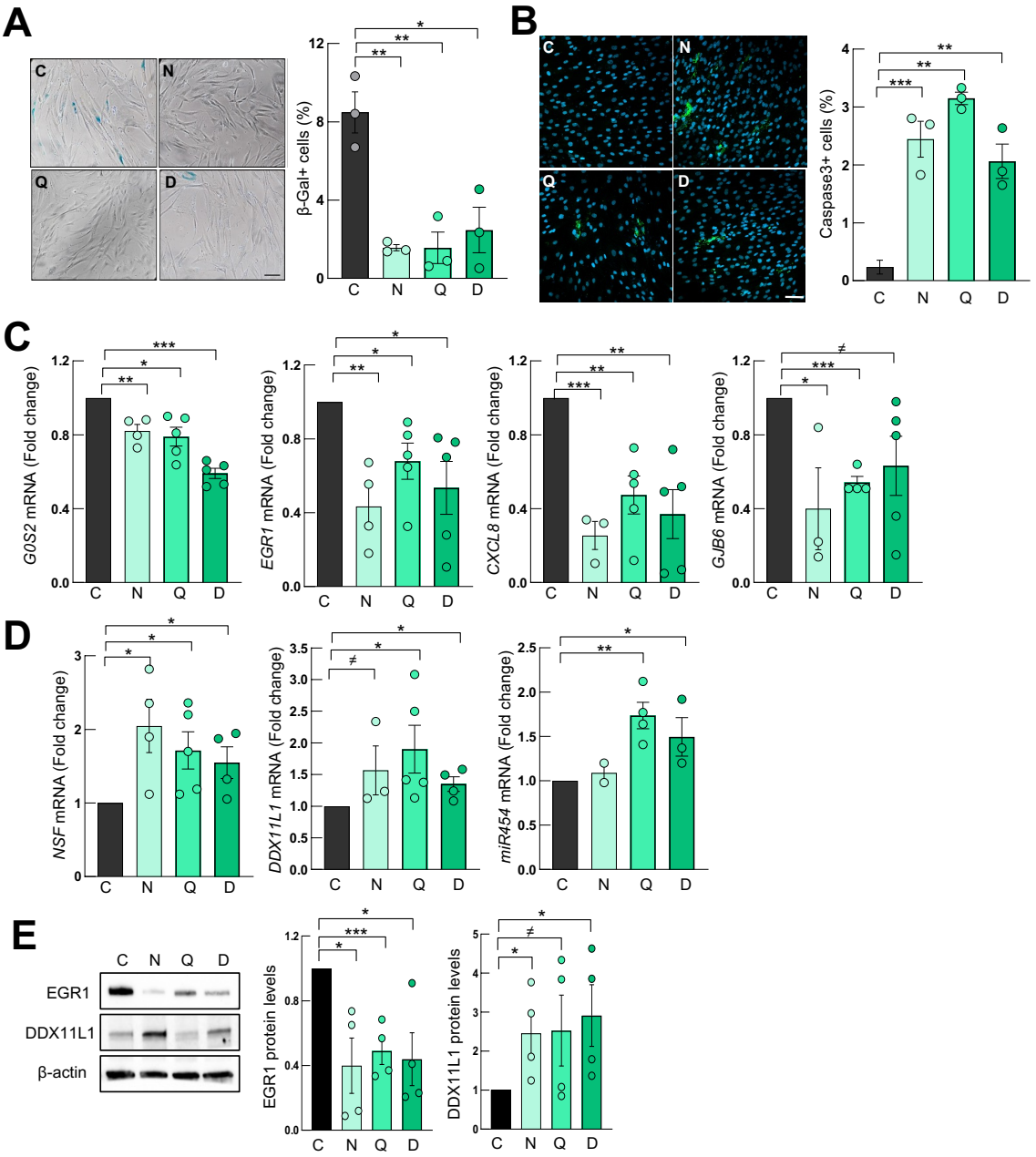

Figure R15. The treatment of fibroblasts with senolytics reduces senescence, promotes apoptosis and restores the expression pattern observed in frail individuals. Representative images (scale bar = 50 µm) and percentage of **(A)** SA-β-gal positive cells (n = 3) and **(B)** Caspase 3 positive cells (n = 3) in late passage primary fibroblasts treated for 48 h with the senolytic compounds 15 µM Navitoclax (N), 10 µM Quercetin (Q) or 0.5 nM Dasatinib (D) compared to non-treated fibroblasts (Control, C). **(C)** Relative mRNA levels of *G0S2, EGR1, CXCL8, GJB6* and **(D)** *NSF, DDX11L1* and *miR454* in treated fibroblasts compared to control ones (n ≥ 3). Data were relativized to the expression in control fibroblasts. **(E)** Representative western blot and quantification of the protein levels of EGR1 and DDX11L1 in treated fibroblasts compared to control ones (n = 4). The statistical significance was assessed with the Student's t-test ($^{\neq}$ $p < 0.1$, * $p < 0.05$, ** $p < 0.01$, *** $p < 0.001$).

SECOND CHAPTER

Gene expression is altered in human hippocampus with age

For this second chapter of the doctoral thesis, we performed a gene expression microarray in RNA samples from human hippocampus of 16 individuals of different ages and without diagnosis of neurodegenerative diseases from the Basque Country. In particular, the study was divided in young individuals ranged from 27 to 49 years old (n = 5), elderly people from 58 to 88 years old (n = 8) and centenarian individuals from 97 to 100 years old (n = 3). In the first part (**PART A**) of this second chapter, different comparisons were made between the 3 established groups. First, we focused on the centenarian group and compared them to young and elderly groups in order to identify the molecular mechanisms that could be differentially expressed in centenarians and associated with the extended longevity of this group. Then, we studied the differentially expressed genes between elderly and young individuals. In the second part (**PART B**) of this second chapter, we performed a correlation study with chronological aging.

PART A. Study of the differentially expressed genes between young, elderly and centenarian individuals in human hippocampus.

Transcriptome analysis in human hippocampal RNA samples reveal differentially expressed genes in centenarians.

After performing the transcriptomic assay, we focused on the centenarian group and studied the differentially expressed genes between centenarians (n = 3) vs. young (n = 5) and old individuals (n = 11). In this context, transcriptome analysis showed a differential gene expression pattern in centenarian people compared to old (***Figure R16A***) and to young individuals (***Figure R16B***) including genes with p-value < 0.05 and FC ≥ |2|. In particular, we

identified 255 genes, among which 190 were up-regulated and 65 down-regulated in centenarian individuals compared to elderly ones and 209 differentially expressed genes, among which 135 were up-regulated and 74 down-regulated compared to young individuals (***Figure R16C***). The complete list of differentially expressed genes can be found in the ***Appendix 1 (Table A1-4)***. GO analysis revealed heavy metal and zinc (Zn) related biological processes associated to up-regulated genes in centenarians (***Figure 17A***), and axon extension or cell growth processes associated to down-regulated genes (***Figure 17B***). Among the differentially expressed genes, several members of the metallothioneins (*MTs*) family of genes were significantly overexpressed in the hippocampus of centenarians compared to the other groups (*MT1M*, p = 0.0001; *MT1E*, p =0.0001; *MT1X*, p = 0.0001; *MT1F*, p = 0.001; *MT1A*, p = 0.001; *MT1G*, p = 0.004, *MT1L*, 0.008; *MT1B*, p = 0.01; *MT3*, 0.04).

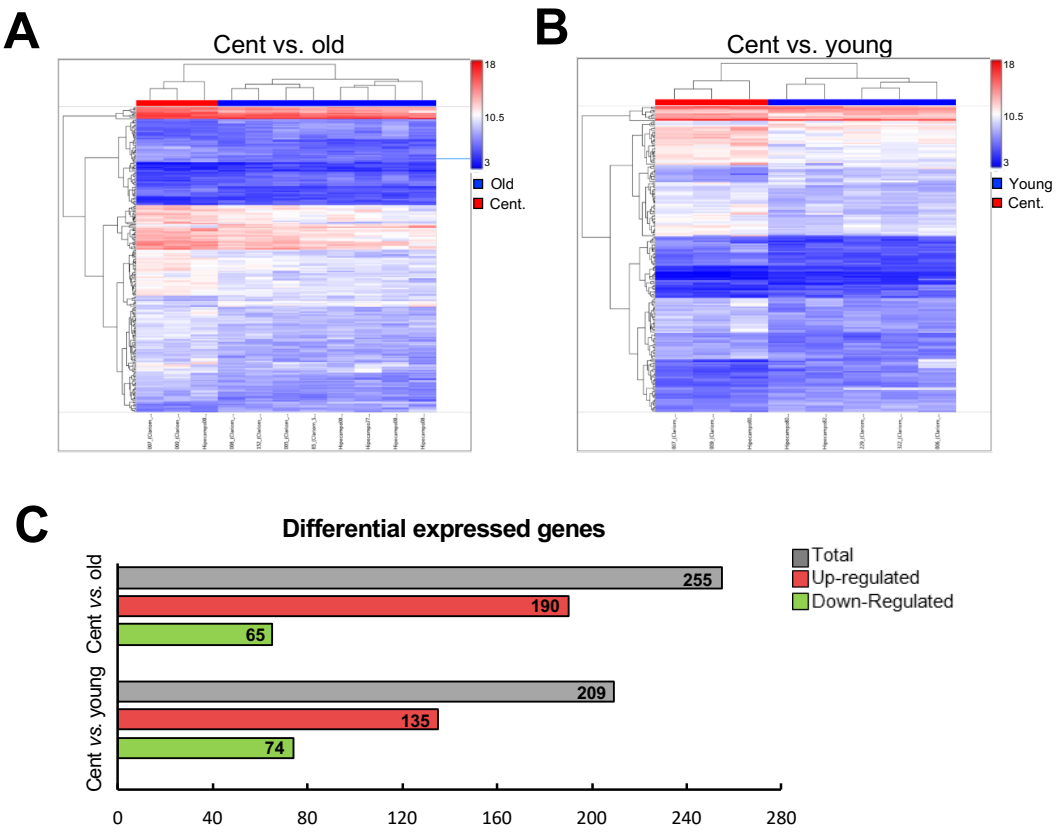

Figure R16. Transcriptome analysis in human hippocampal RNA samples reveal differentially expressed genes in centenarians. Hierarchical clustering of **(A)** centenarian (n = 3) and old (n = 8) individuals, and **(B)** centenarian (n = 3) and young (n = 5) individuals selected for array screening. **(C)** Representative figure of up-regulated and down-regulated genes in the microarray analysis of centenarian (n = 3) vs. old (n = 8) or young (n =5) human hippocampus samples. All genes selected presented p-value < 0.05 and FC ≥ |2| in the microarray.

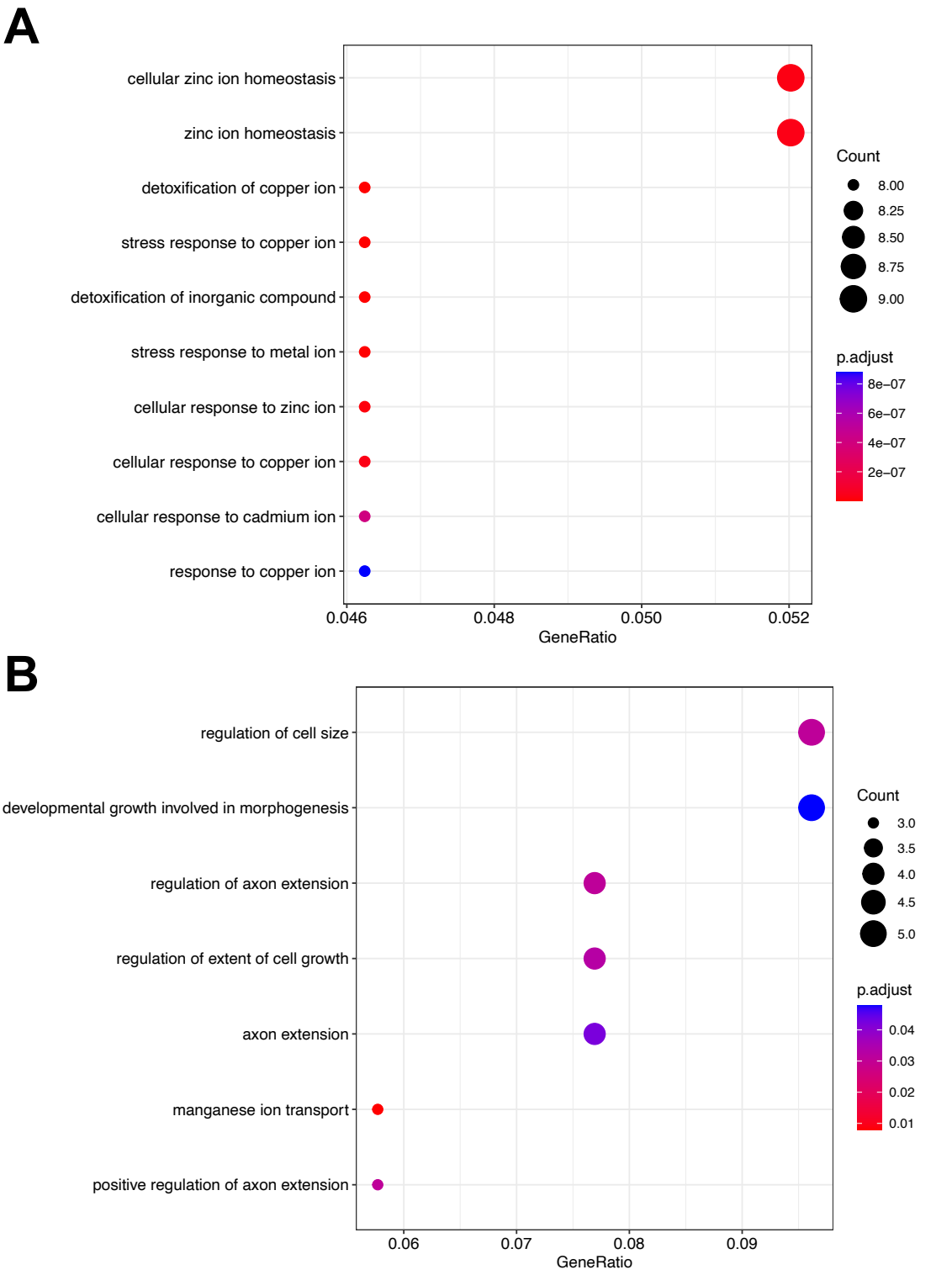

Figure R17. Gene ontology analysis of differentially expressed genes shows altered pathways such as heavy metal and zinc related pathways. (A) Representative dotplot of the main altered biological processes associated to up-regulated and **(B)** down-regulated genes in centenarian (n = 3) vs. old (n = 11) human hippocampus samples after GO analysis of microarray study. GO analysis was performed using *clusterProfiler* package in RStudio software (version 4.2.1, https://www.R-project.org/).

MTs are highly expressed in the hippocampus of centenarians.

Next, we measured the expression of the *MTs* family of genes in hippocampus samples used for the microarray and in an additional cohort from the UBC (validation cohort 1). In general, we detected higher levels of MTs isoforms in nonagenarian/centenarian individuals compared to young and old individuals, validating the results obtained in the transcriptome analysis. Specifically, we observed a statistically significant higher expression of the MT1 subtypes *MT1A*, *MT1E*, *MT1F*, *MT1G*, *MT1H*, *MT1M* and *MT1X* in nonagenarian/centenarians compared to old or young individuals (***Figure R18A***). Similarly, the brain-specific *MT3* isoform was significantly increased in very old individuals (***Figure R18B***). *REST* transcription factor has been described as an important player of extreme longevity and cognitive activity [216]. Additionally, its levels were significantly elevated in hippocampus samples of centenarian individuals (***Figure R18C***). These results confirm that *MTs* are overexpressed in the hippocampus of centenarians.

Moreover, we analyzed the expression of *MT1* subtypes in cortex samples of individuals from the microarray cohort and we did not observe differences between the expression of *MT1A*, *MT1B*, *MT1E*, *MT1F*, *MT1G*, *MT1M* and *MT1X* in centenarians compared to elderly individuals (***Figure R19A***). Making use of data from RNAseq studies in public available datasets (https://aging.brain-map.org), we further characterized the expression of *MTs* in different brain regions of aged individuals. In general, the expression of all *MTs* appeared to be higher in the hippocampus than in the white matter of the forebrain or the parietal and temporal neocortex (***Figure R19B***). These results indicate that the high levels of *MTs* observed in centenarians could be a specific signature of the hippocampal neurogenic niche.

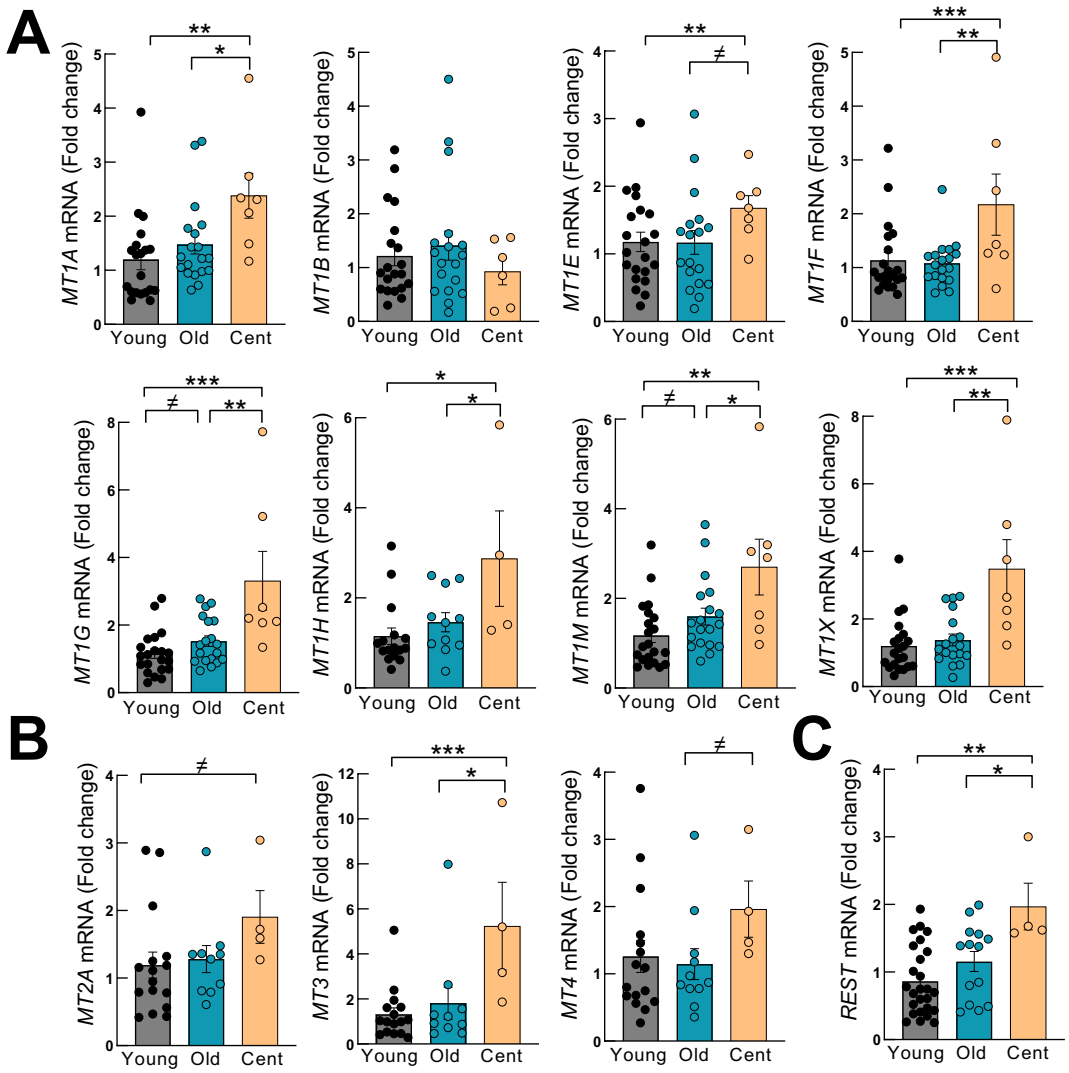

Figure R18. *MTs* are highly expressed in the hippocampus of centenarians. (A) mRNA expression levels of *MT1A, MT1B, MT1E, MT1F, MT1G, MT1H, MT1M, MT1X*, **(B)** *MT2A, MT3, MT4* and **(C)** *REST* by qRT-PCR in hippocampus samples of young (n ≥ 16), old (n ≥ 10) and centenarian individuals (n ≥ 4) from the UBC cohort (validation cohort 1). The statistical significance was assessed with the Student's t-test (≠ $p < 0.1$, * $p < 0.05$, ** $p < 0.01$, *** $p < 0.001$).

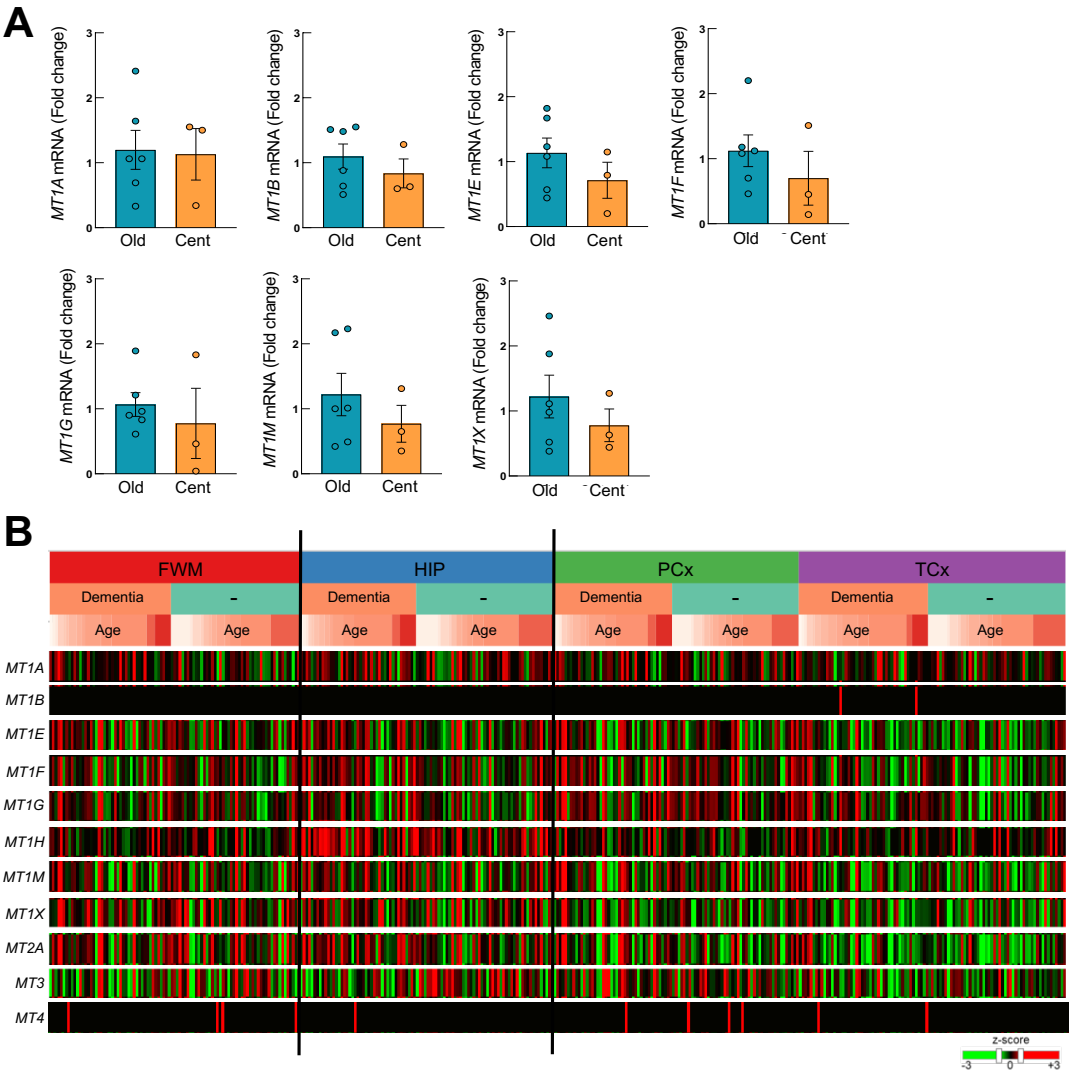

Figure R19. ***MTs*** **are not expressed in the cortex and their expression is enriched in the hippocampus. (A)** mRNA expression levels of *MT1A, MT1B, MT1E, MT1F, MT1G, MT1M* and *MT1X* by qRT-PCR in cortex samples of old (n = 6) and centenarian individuals (n = 3) from the microarray cohort. **(B)** Expression of *MT1A, MT1B, MT1E, MT1F, MT1G, MT1H, MT1M, MT1X, MT2A, MT3* and *MT4* represented by z-score in white matter of forebrain (FWM), hippocampus (HIP), parietal neocortex (PCx) and temporal neocortex (TCx) of aged human individuals ranged between 78-100+ years old (n = 30 healthy, n = 24 dementia). Dementia was presented as vascular, multiple etiologies, Alzheimer´s disease or other medical form. Data obtained from https://aging.brain-map.org.

The protein levels of MTs are increased in the DG of centenarians.

In order to validate the results obtained at transcriptional level, we studied the expression of MT1 and MT3 isoforms at protein level through IF in paraffin sections of human hippocampus samples of 23 individuals from the cohort of Navarra Biomed (additional cohort 1) that comprises samples from young, old and nonagenarian/centenarian individuals. We found a significantly higher expression of MT1 (***Figure R20A***) and MT3 (***Figure R20B***) in the

DG of centenarians compared to the other two groups. These results confirm that the expression of MT1 and MT3 is high in the DG of very old individuals.

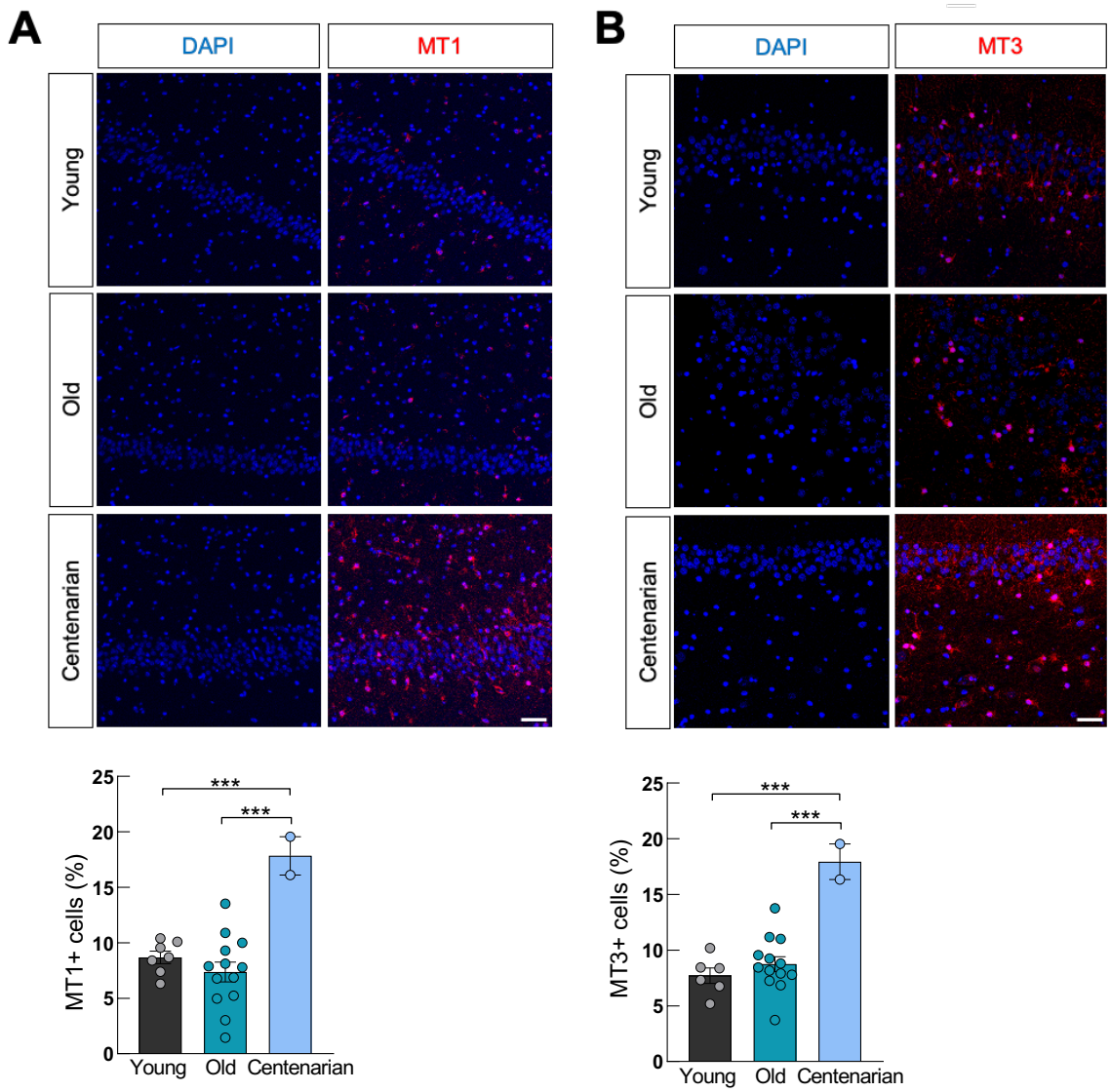

Figure R20. The protein levels of MTs are increased in the DG of centenarians. (A) Representative IF images of MT1 (red) in the dentate gyrus (DG, scale bar = 50 µm) and quantification of MT1 protein levels in the DG of young (n = 7), old (n = 14) and centenarian individuals (n = 2) from the cohort of Navarra Biomed (additional cohort 1). **(B)** Representative IF images of MT3 (red) in the DG (scale bar = 50 µm) and quantification of MT3 protein levels in DG samples of the same cohort. The protein levels were represented as the percentage of MT1 or MT3 positive cells with respect to total nuclei stained with DAPI. The statistical significance was assessed with the Student's t-test (*** $p < 0.001$).

The expression levels of MTs correlate positively with age.

An additional analysis was performed to identify a possible correlation between MTs expression with age in the hippocampus samples from the microarray cohort and validation

cohort 1. For this correlation studies, we first performed a Kolmogorov Smirnov test for the assessment of normality and then we used Spearman's coefficient since the samples followed a non-normal distribution. Herein, we found that the expression of *MT1A, MT1F, MT1G, MT1H, MT1M, MT1X* (***Figure R21A***) *and MT3* (***Figure R21B***) correlated positively with age. In the same way, we observed a positive correlation between the expression of *REST* with age (***Figure R21C***).

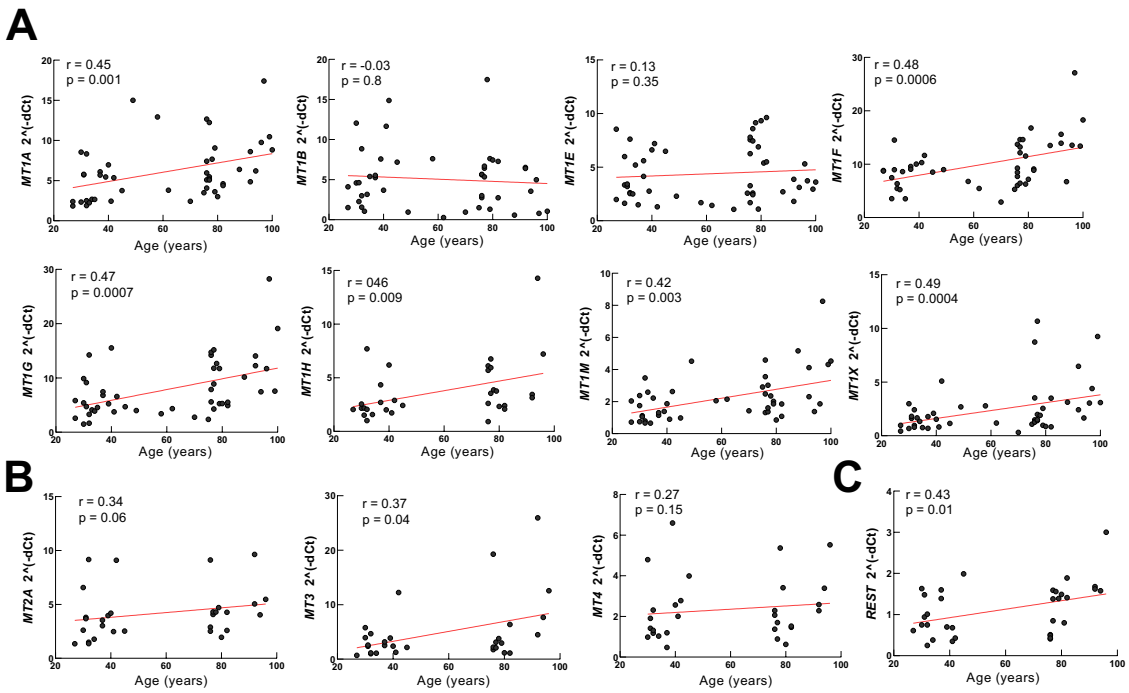

Figure R21. The expression of *MTs* correlate positively with age. (A) Correlation studies of *MT1A, MT1B, MT1E, MT1F, MT1G, MT1H, MT1M, MT1X*, **(B)** *MT2A, MT3, MT4* and **(C)** *REST* with chronological aging in hippocampus samples from the validation cohort 1 (n ≥ 30) using Spearman correlation coefficient (r). The samples do not followed a normal distribution (checked by Kolmogorov Smirnov test).

Similarly, we performed additional correlation studies between MT1 and MT3 protein levels with age. The normality was checked with Kolmogorov Smirnov test and we used the Pearson correlation coefficient since the samples followed a normal distribution. The correlation analysis revealed that there was not statistically significant correlation between MT1 (***Figure R22A***) and MT3 (***Figure R22B***) protein expression with age when all samples including the 3 groups were evaluated. However, when only the samples of old and very old individuals were included in the analysis, we found a positive correlation of both MT1 (***Figure***

R22C) and MT3 (*Figure R22D*) expression with age that was statistically significant ($p < 0.0001$).

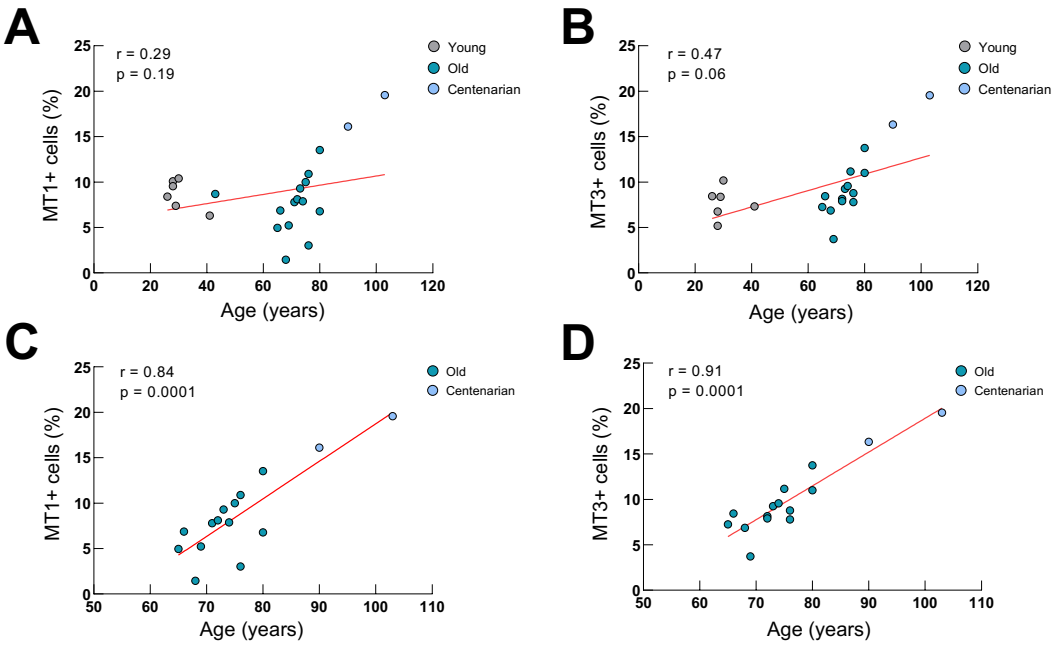

Figure R22. Protein levels of MTs correlate positively with age. (A) Correlation studies of MT1 and **(B)** MT3 protein levels (percentage of MT1 positive cells respect to total cells) with age in hippocampus samples of young (n = 7), old (n = 14) and centenarian individuals (n = 2) from the additional cohort 1. **(C)** Correlation studies of MT1 and **(D)** MT3 protein levels in hippocampus samples of old (n = 14) and centenarian individuals (n = 2) from the additional cohort 1. For all the correlation analyses Pearson correlation coefficient (r) was used since the samples followed a normal distribution (checked by Kolmogorov Smirnov test).

MT1 and MT3 are mainly expressed in astrocytes.

In order to take a further step in the characterization of the expression and function of MTs in aging and cognition, we studied in detail their expression in different brain cell types. We performed co-staining studies of MT1 and MT3 with markers of cell types of the brain such as neurons or astrocytes and we also checked their expression in microglia.

We first performed co-IF of both MT1 and MT3 with microtubule-associated protein 2 (MAP2), a neuron-specific cytoskeletal protein that promotes the assembly and stability of the microtubule network in neurons [347], [348] and with Class III β-Tubulin (TUJ1) that is expressed in differentiated neurons of the CNS and contributes to microtubule stability in neuronal cell bodies and axons [349], [350]. We found that only 1 – 2 % of the cells that were positive for MT1 were also positive for MAP2 independently of the age of the groups (*Figure*

R23A and B). Similarly, less than 1 % of the cells positive for MT3 showed a positive signal for MAP2 (***Figure R24A and B***).

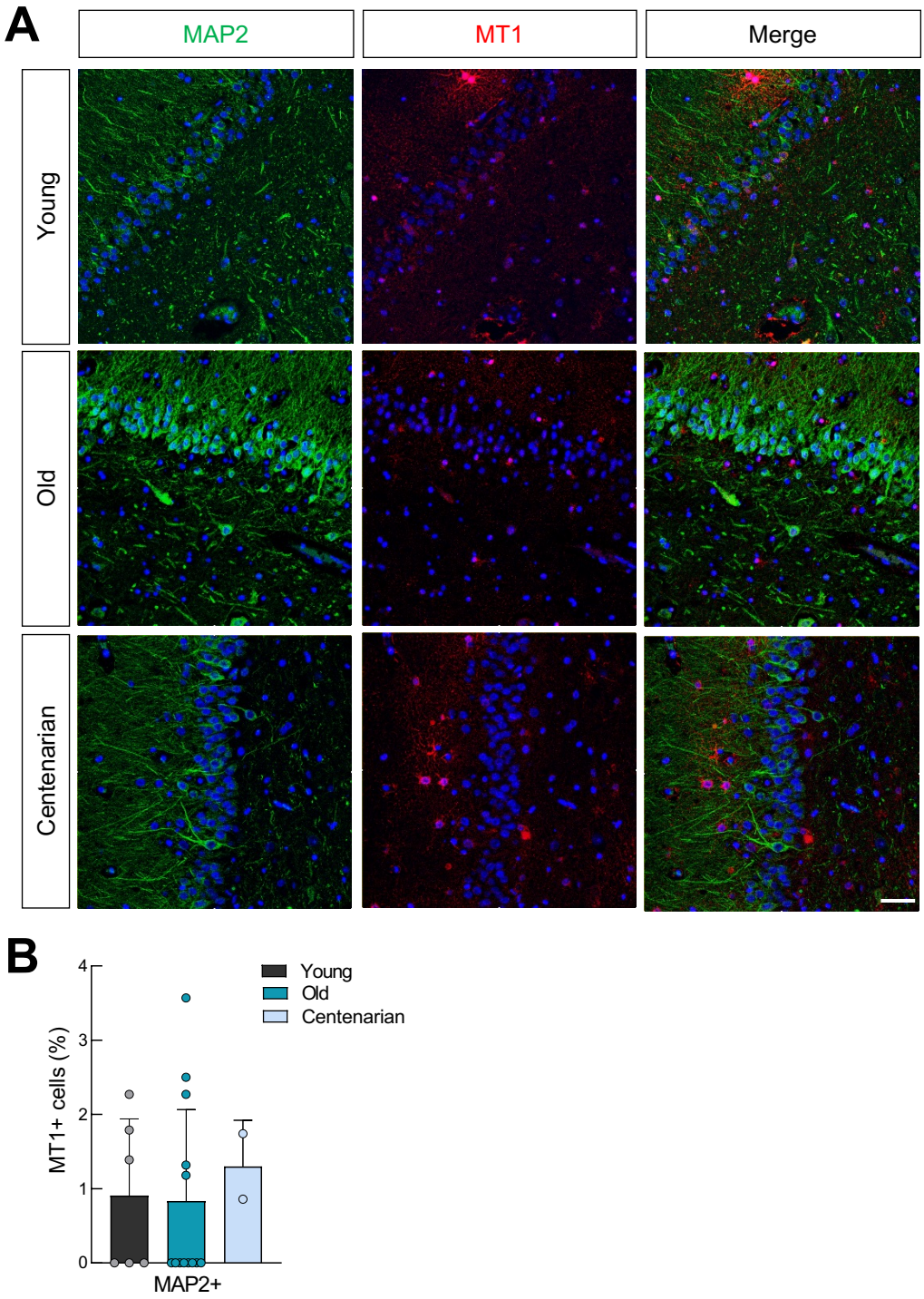

Figure R23. MAP2+ cells do not express MT1. (A) Representative IF images of MAP2 (green) and MT1 (red) in the dentate gyrus (DG, scale bar = 50 µm) of hippocampal coronal sections of young (n = 7), old (n = 14) and centenarian individuals (n = 2) from the additional cohort 1. **(B)** Quantification (percentage) of MT1 positive cells that are also positive for MAP2 (MT1+/MAP2+ cells) respect to total nuclei stained with DAPI in the DG of the same samples (n = 23).

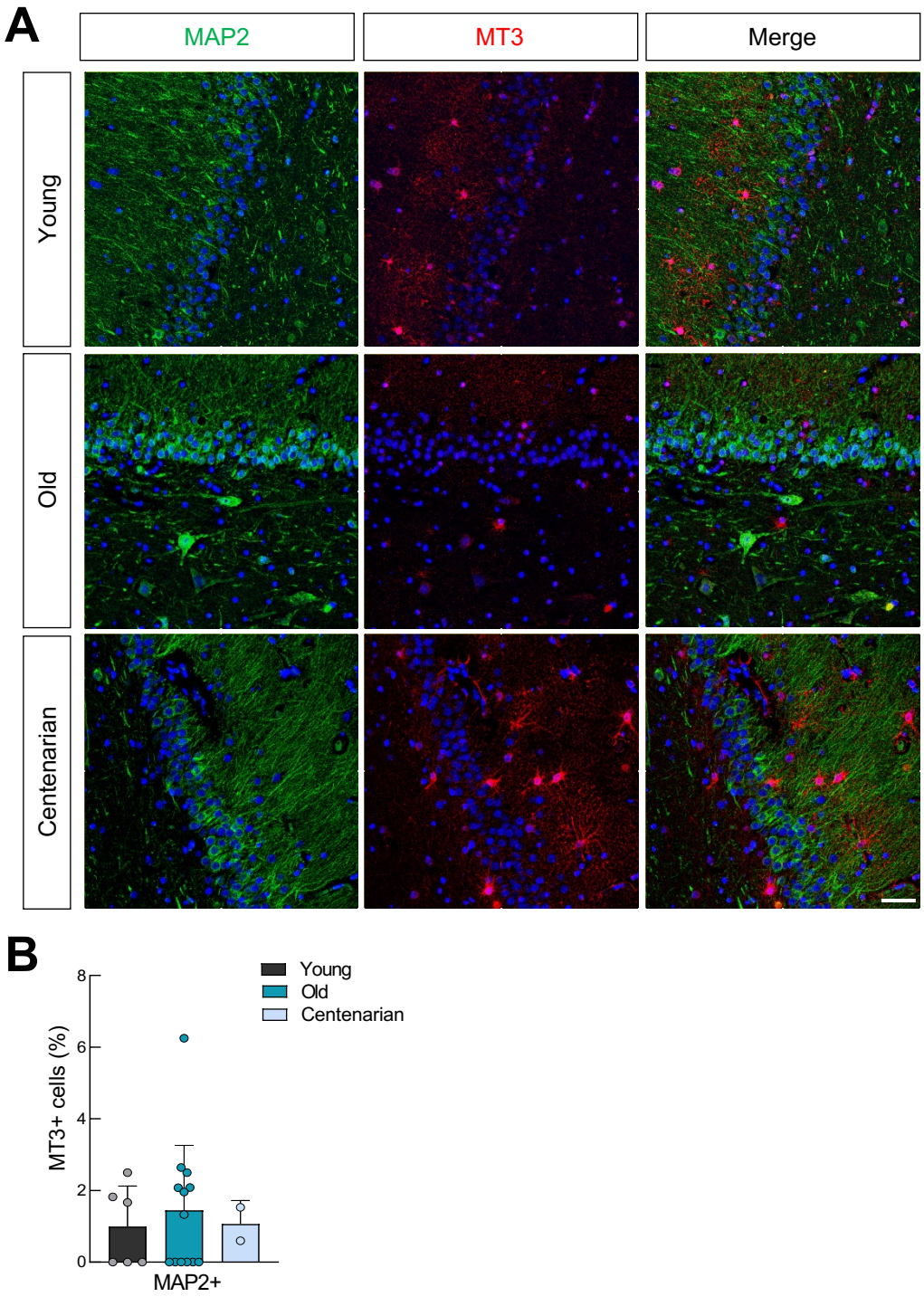

Figure R24. MAP2+ cells do not express MT3. (A) Representative IF images of MAP2 (green) and MT3 (red) in the dentate gyrus (DG, scale bar = 50 µm) of hippocampal coronal sections of young (n = 7), old (n = 14) and centenarian individuals (n = 2) from the additional cohort 1. **(B)** Quantification (percentage) of MT3 positive cells that are also positive for MAP2 (MT3+/MAP2+ cells) respect to total nuclei stained with DAPI in the DG of the same samples (n = 23).

In the case of TUJ1, we observed similar results than the ones obtained with MAP2, and less than 1 – 2 % of the cells that were positive for MT1 or MT3 were also positive for

TUJ1 in the 3 groups of age (***Figure R25A, B and R26A, B***). These results indicate that neurons do not express MTs.

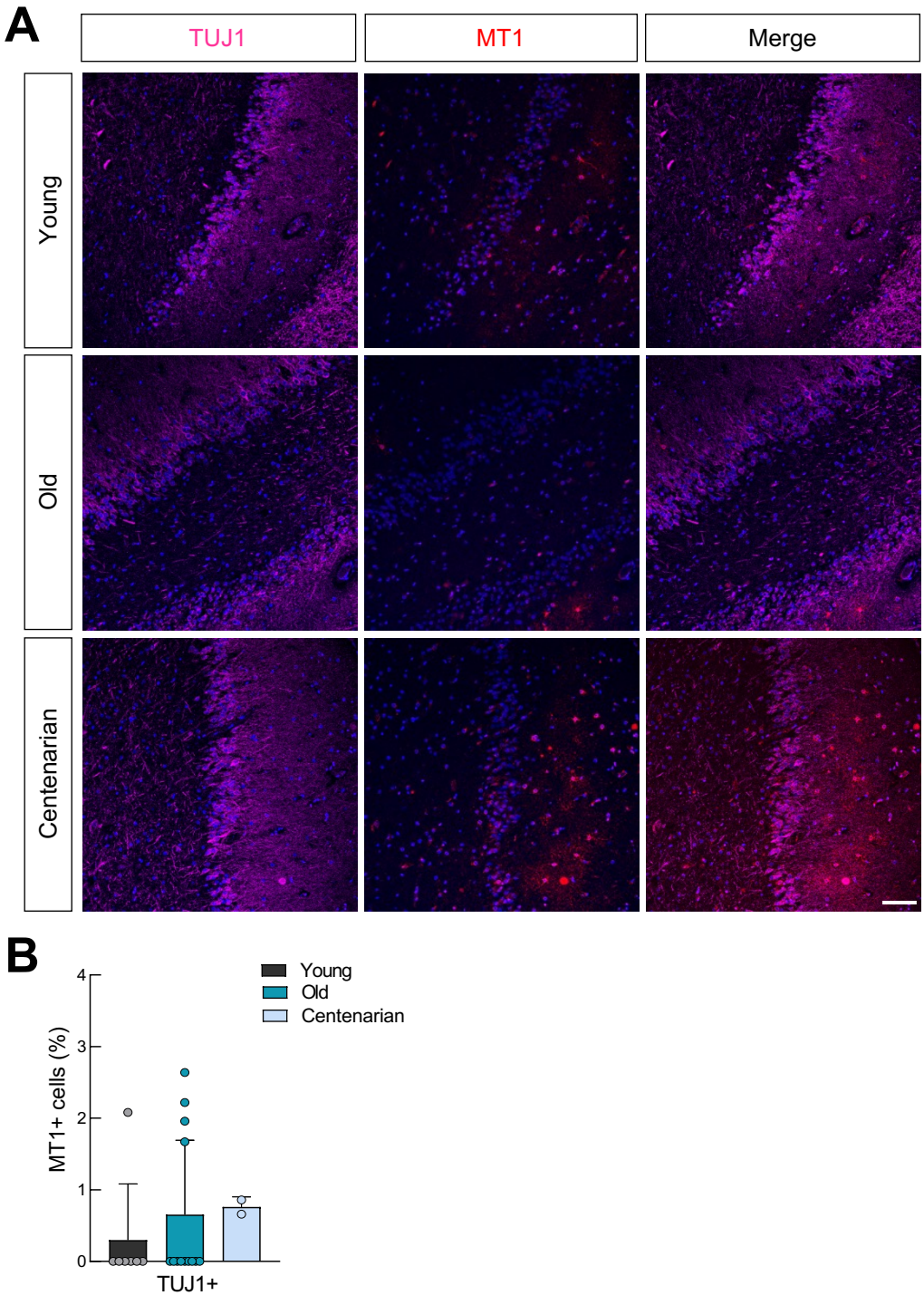

Figure R25. TUJ1+ cells do not express MT1. (A) Representative IF images of TUJ1 (far red) and MT1 (red) in the dentate gyrus (DG, scale bar = 50 µm) of hippocampal coronal sections of young (n = 7), old (n = 14) and centenarian individuals (n = 2) from the additional cohort 1. **(B)** Quantification (percentage) of MT1 positive cells that are also positive for TUJ1 (MT1+/TUJ1+ cells) respect to total nuclei stained with DAPI in the DG of the same samples (n = 23).

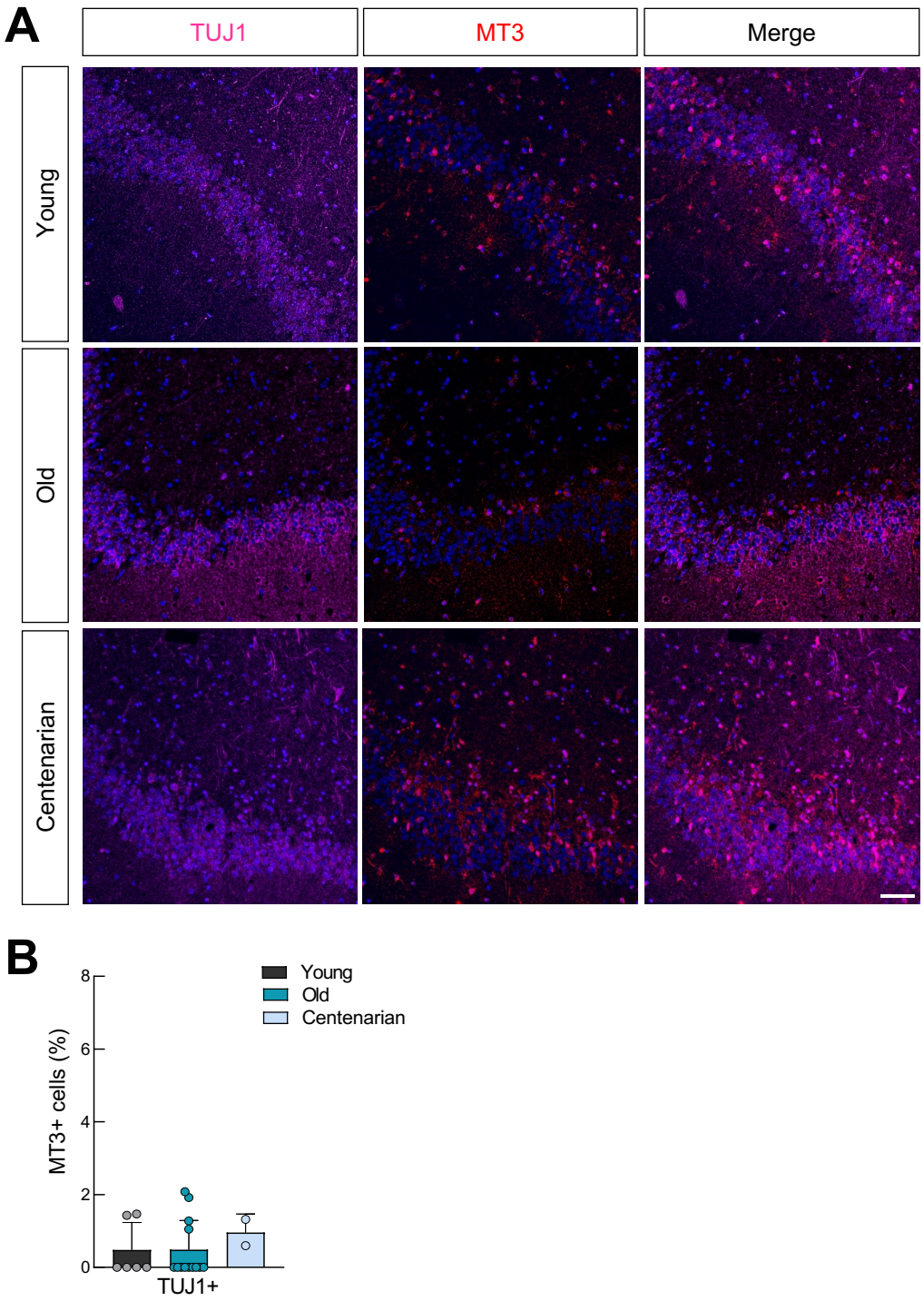

Figure R26. TUJ1+ cells do not express MT3. (A) Representative IF images of TUJ1 (far red) and MT3 (red) in the dentate gyrus (DG, scale bar = 50 µm) of hippocampal coronal sections of young (n = 7), old (n = 14) and centenarian individuals (n = 2) from the additional cohort 1. **(B)** Quantification (percentage) of MT3 positive cells that are also positive for TUJ1 (MT3+/TUJ1+ cells) respect to total nuclei stained with DAPI in the DG of the same samples (n = 23).

Next, we decided to check the expression of all the *MTs* directly in microglia. For that, we took advantage of RNAseq data from aged human bulk dorsolateral prefrontal cortex samples and purified microglia from the same region (http://shiny.maths.usyd.edu.au/Ellis/MicrogliaPlots/). We observed that none of the *MTs* were enriched in microglia compared to bulk cortex (***Figure R27A and B***), which indicate that there is not an association of *MTs* with microglia.

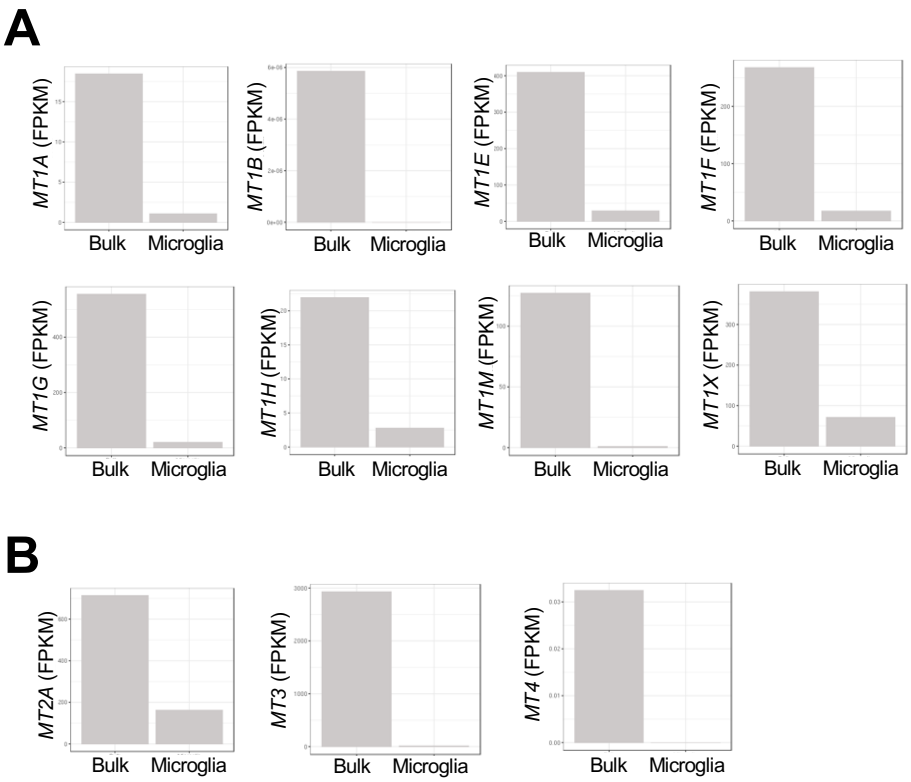

Figure R27. Microglia do not express *MTs*. (A) RNAseq data for the expression of *MT1A, MT1B, MT1E, MT1F, MT1G, MT1H, MT1M, MT1X* and **(B)** *MT2A, MT3* and *MT4* in bulk dorsolateral prefrontal cortex (n = 540) vs. purified microglia from the same region (n = 10). Data obtained from http://shiny.maths.usyd.edu.au/Ellis/MicrogliaPlots/.

Finally, we moved to the study of astrocytes. For this, we first performed co-IF of both MT1 and MT3 with GFAP, majorly expressed in astrocytic glial cells [351]. We found that 70 – 80 % of the cells that were positive for MT1 in the samples of different ages were also positive for GFAP (***Figure R28A and B***). Similarly, 70 – 80 % of the cells positive for MT3 showed a positive signal for GFAP (***Figure R29A and B***).

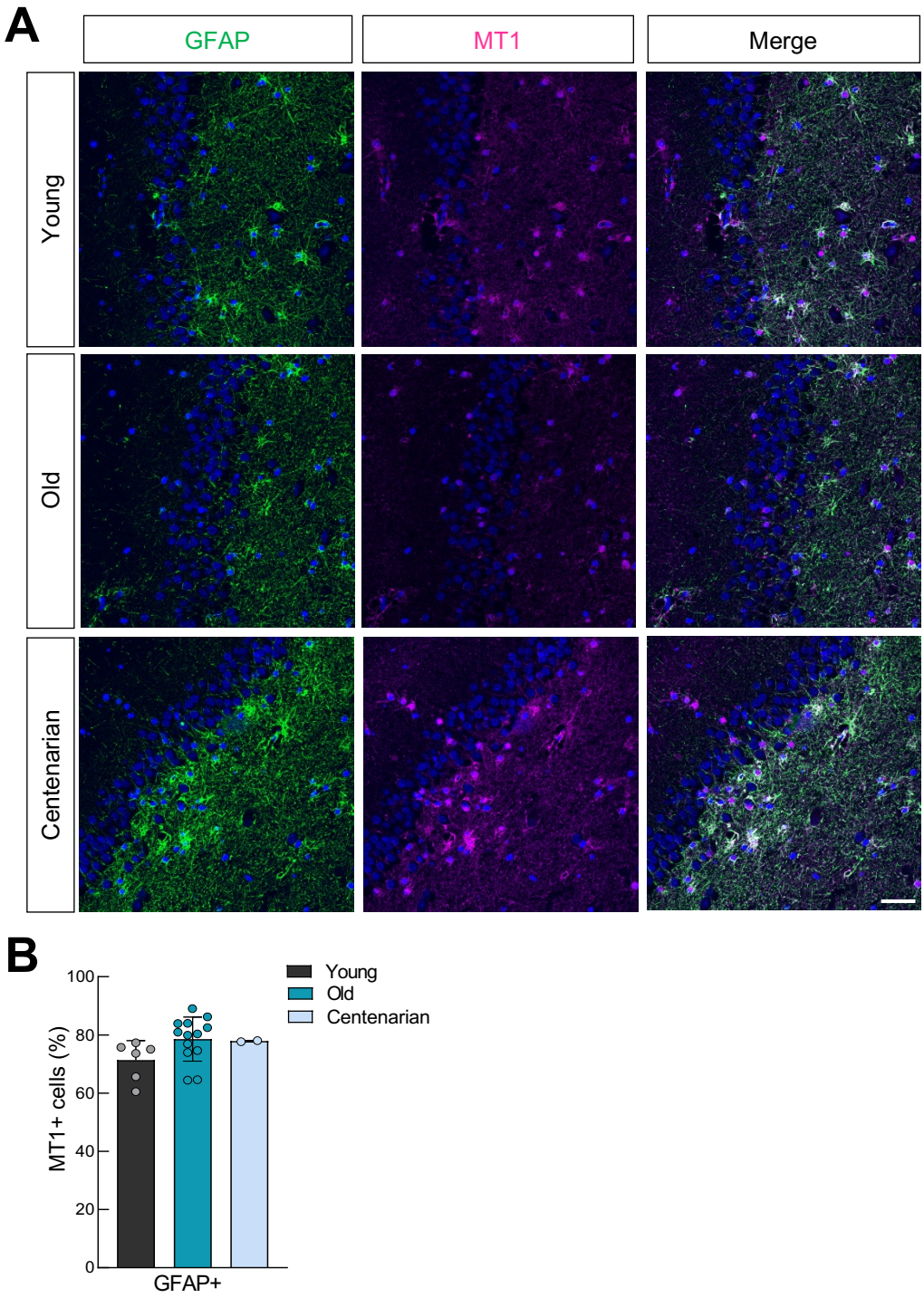

Figure R28. GFAP+ cells express MT1. (A) Representative IF images of GFAP (green) and MT1 (far red) in the dentate gyrus (DG, scale bar = 50 µm) of hippocampal coronal sections of young (n = 7), old (n = 14) and centenarian individuals (n = 2) from the additional cohort 1. **(B)** Quantification (percentage) of MT1 positive cells that are also positive for GFAP (MT1+/GFAP+ cells) respect to total nuclei stained with DAPI in the DG of the same samples (n = 23).

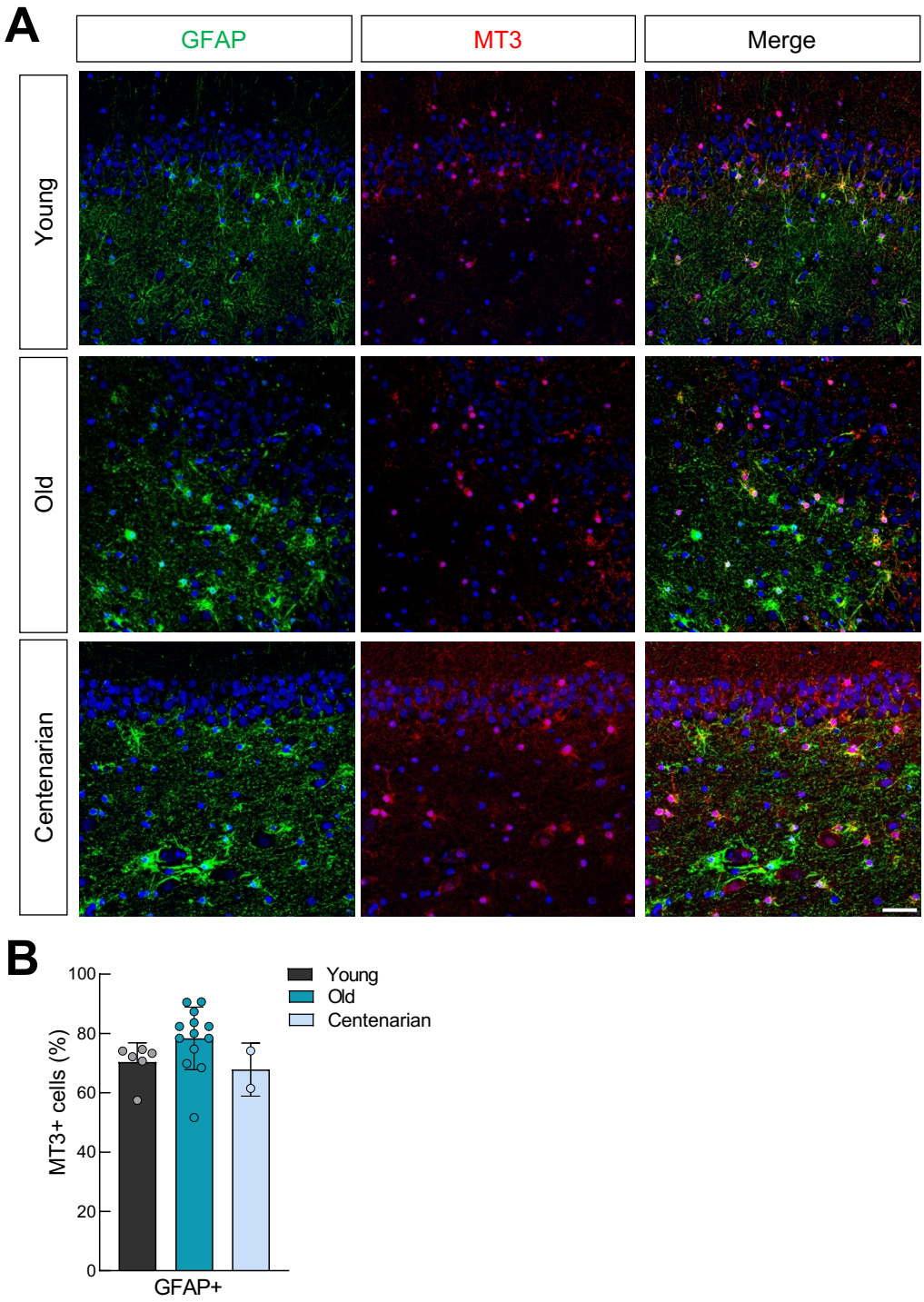

Figure R29. GFAP+ cells express MT3. (A) Representative IF images of GFAP (green) and MT3 (red) in the dentate gyrus (DG, scale bar = 50 µm) of hippocampal coronal sections of young (n = 7), old (n = 14) and centenarian individuals (n = 2) from the additional cohort 1. **(B)** Quantification (percentage) of MT3 positive cells that are also positive for GFAP (MT3+/GFAP+ cells) respect to total nuclei stained with DAPI in the DG of the same samples (n = 23).

Furthermore, we performed co-IF of both MT1 and MT3 with S100 calcium-binding protein-beta (S100β), the glial-specific protein that is primarily expressed by mature

astrocytes [351]. We found that almost 90 % of the cells that were positive for MT1 were also positive for S100β (***Figure R30A and B***). Likewise, 90 – 95 % of the cells positive for MT3 presented a positive signal for S100β (***Figure R31A and B***). Altogether, these results show that there is a strong co-localization between MT1 or MT3 and both GFAP and S100β and confirm that astrocytes express high levels of MTs in the brain.

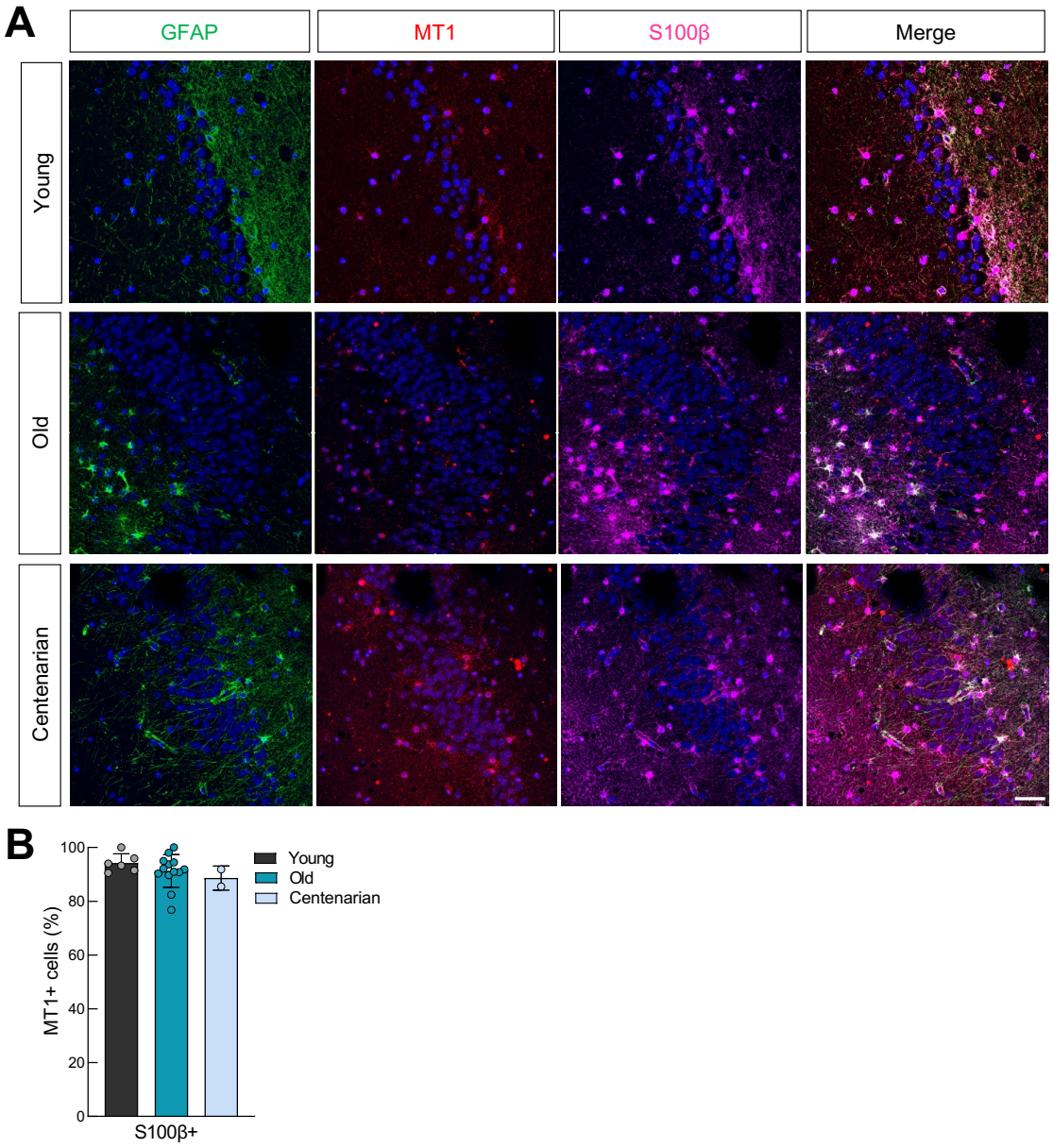

Figure R30. S100β+ cells express MT1. (A) Representative IF images of GFAP (green), MT1 (red) and S100β (far red) in the dentate gyrus (DG, scale bar = 50 µm) of hippocampal coronal sections of young (n = 7), old (n = 14) and centenarian individuals (n = 2) from the additional cohort 1. **(B)** Quantification (percentage) of MT1 positive cells that are also positive for S100β (MT1+/ S100β+ cells) respect to total nuclei stained with DAPI in the DG of the same samples (n = 23).

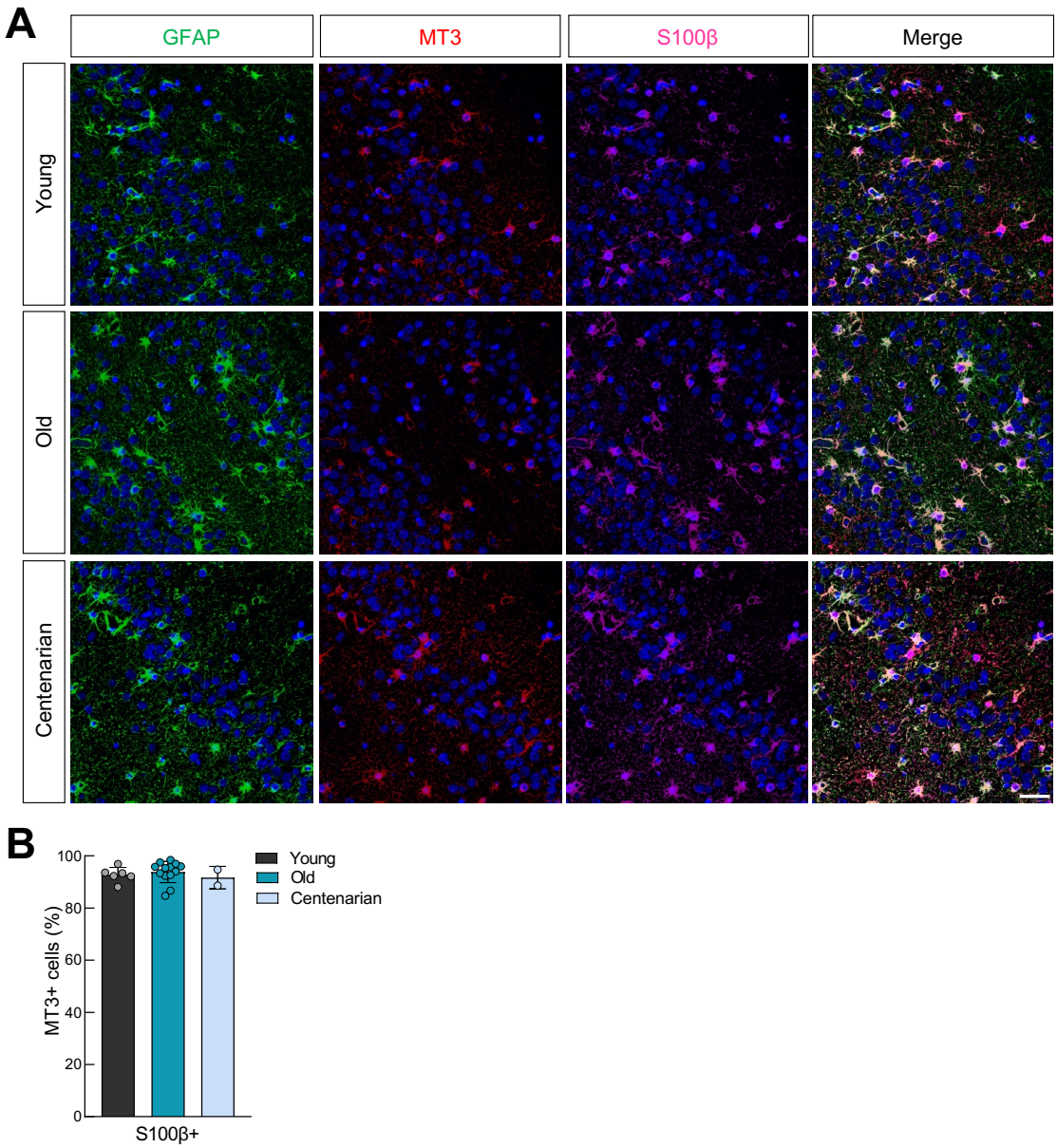

Figure R31. S100β+ cells express MT3. (A) Representative IF images of GFAP (green), MT3 (red) and S100β (far red) in the dentate gyrus (DG, scale bar = 50 µm) of hippocampal coronal sections of young (n = 7), old (n = 14) and centenarian individuals (n = 2) from the additional cohort 1. **(B)** Quantification (percentage) of MT3 positive cells that are also positive for S100β (MT3+/ S100β+ cells) respect to total nuclei stained with DAPI in the DG of the same samples (n = 23).

To further study the link of MTs with different cell types, we analyzed single cell RNAseq studies performed in human brains from publicly available data set (The Human Protein Atlas, http://www.proteinatlas.org). In this case, we observed that all the *MTs* were expressed almost exclusively by astrocytes, an effect detected mostly in the case of *MT1E*, *MT1F*, *MT1G*, *MT1M*, *MT1X*, *MT2A* and *MT3* (***Figure R32A and B***).

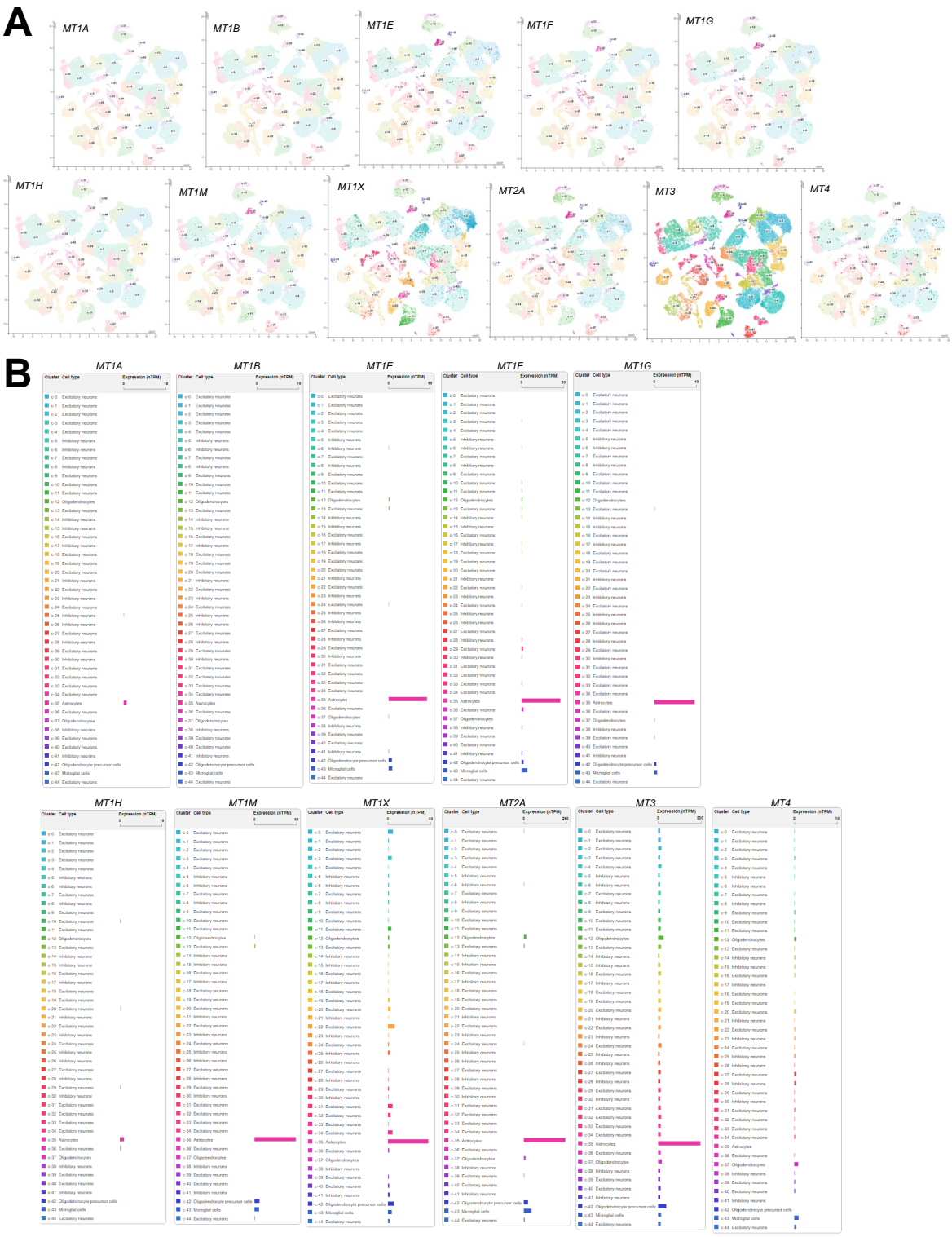

Figure R32. MTs are expressed mainly by astrocytes and not by neuronal cells. (A) Single cell RNAseq data from whole brain for the expression of *MT1A, MT1B, MT1E, MT1F, MT1G, MT1H, MT1M, MT1X, MT2A, MT3* and *MT4* obtained from "The Human Protein Atlas" (http://www.proteinatlas.org). **(B)** Normalized expression (nTPM) levels of the selected genes in neurons and glial cells from the same single cell RNAseq study.

Serial passage-cultured NHA have lower levels of MTs.

Since the expression of MTs is enriched in astrocytes, we studied the expression of *MTs* in NHA at early (2 - 3) and late (15 - 17) passages. In the case of *MT1* subtypes, their expression was mainly decreased in late passage NHA and it was statistically significant in the case of *MT1A*, *MT1E*, *MT1F* and *MT1X* (***Figure R33A***). Similarly, the levels of the other *MTs* isoforms were significantly lower in late passage NHA compared to early passage ones (***Figure R33B***).

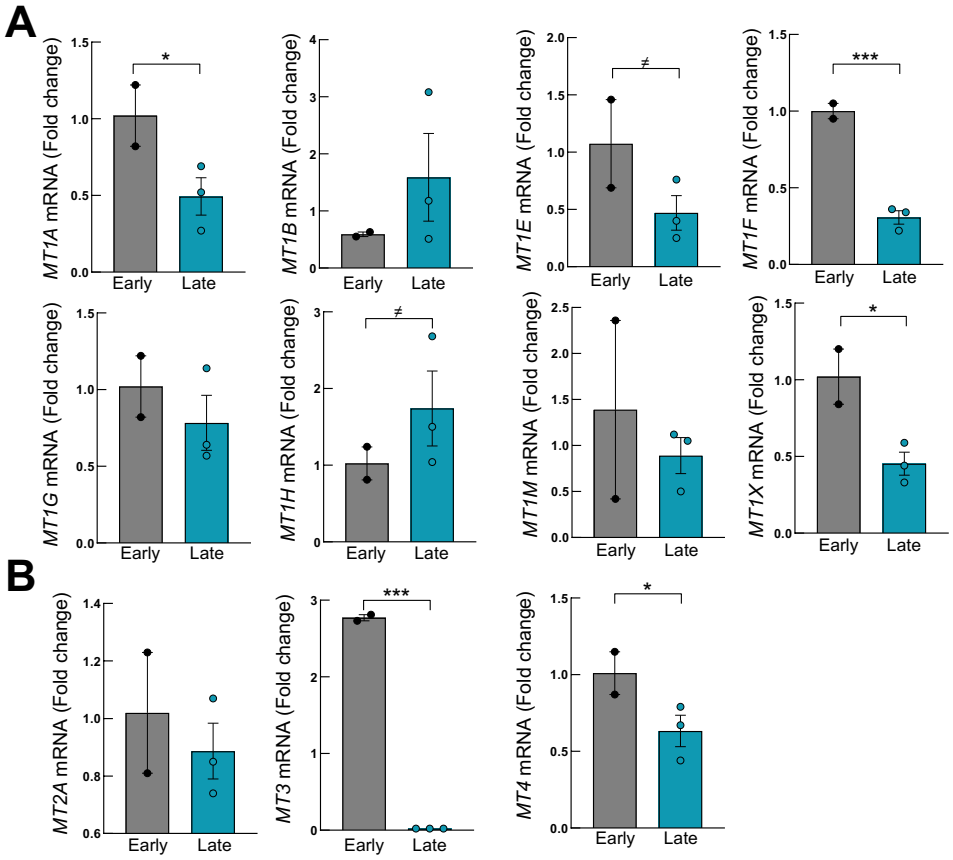

Figure R33. Serial passage-cultured NHA have lower levels of *MTs*. (A) mRNA levels of *MT1A, MT1B, MT1E, MT1F, MT1G, MT1H, MT1M, MT1X* and **(B)** *MT2A, MT3* and *MT4* in NHA cultured at early (2 – 3) and late (15 – 17) passages (n ≥ 2). The statistical significance was assessed with the Student's t-test (≠ $p < 0.1$, * $p < 0.05$, *** $p < 0.001$).

MT1 and MT3 silencing alters proliferation, apoptosis and senescence.

We finally studied the possible effects of the modulation of *MTs* in NHA in order to unravel the possible role that *MTs* might have in astrocytes. For this, we first silenced *MT1* in

astrocytes using lentiviral infections and a specific *shRNA* construct. First, we validated the infection and we detected statistically significant lower protein levels of MT1 measured by western blot (***Figure R34A***) and by IF (***Figure R34B***) in NHA with *MT1* downregulation (*shMT1*) compared to control ones (*pLKO*). Moreover, we checked mRNA expression of all the *MT1* subtypes and we observed statistically significant lower levels of *MT1A*, *MT1B*, *MT1E*, *MT1F*, *MT1G*, *MT1H*, *MT1M* and *MT1X* in *shMT1* astrocytes compared to control ones (***Figure R34C***). Then, we analyzed the cellular effects of decreasing *MT1* and we detected that *MT1*-silenced NHA displayed a statistically significant lower cell growth compared to control astrocytes measured by cell counting (***Figure R34D***). In addition, we observed lower proliferation in *shMT1* astrocytes by the quantification of Ki67 positive cells, which were significantly lower in comparison to control ones (***Figure R34E***). Furthermore, silencing of *MT1* significantly increased apoptosis measured as the number of positive cells for Caspase 3 marker (***Figure R34F***) and also cellular senescence, measured as the number of SA-β-gal positive cells (***Figure R34G***). Finally, the expression of some proliferation and senescence markers were analyzed to confirm the data obtained at molecular level. We found a statistically significant higher expression of $p16^{INK4A}$, $p21^{CIP1}$, $p27^{KIP1}$ and *IL6* in *shMT1* astrocytes compared *pLKO* ones (***Figure R34H***). These data indicate that *MT1* could be involved in astrocyte cell viability, activity and aging.

We then focus on the brain-specific isoform and we silenced *MT3* in astrocytes using the same strategy. We detected statistically significant lower protein levels of MT3 measured by western blot (***Figure R35A***) and by IF (***Figure R35B***) together with a lower mRNA expression of *MT3* (***Figure R35C***) in astrocytes with *MT3* down-regulation (*shMT3*) compared to control ones (*pLKO*), thus validating our model. Then we performed different functional assays and we observed a very significant decrease of cell growth in *MT3* knockdown astrocytes compared to control ones (***Figure R35D***). Additionally, the silencing of *MT3* significantly reduced the number of positive cells for Ki67 (***Figure R35E***) whereas significantly increased apoptosis (***Figure R35F***) and senescence (***Figure R35G***), measured as the number of Caspase 3 positive cells and SA-β-gal positive cells respectively. Finally, we found a statistically significant higher expression of $p14^{ARF}$, $p16^{INK4A}$, $p21^{CIP1}$, $p27^{KIP1}$ and *IL6* in *shMT3* astrocytes compared *pLKO* ones (***Figure R35H***), confirming the data previously obtained at molecular level. These results indicate that *MT3* could have a role in astrocyte cell viability, activity and aging.

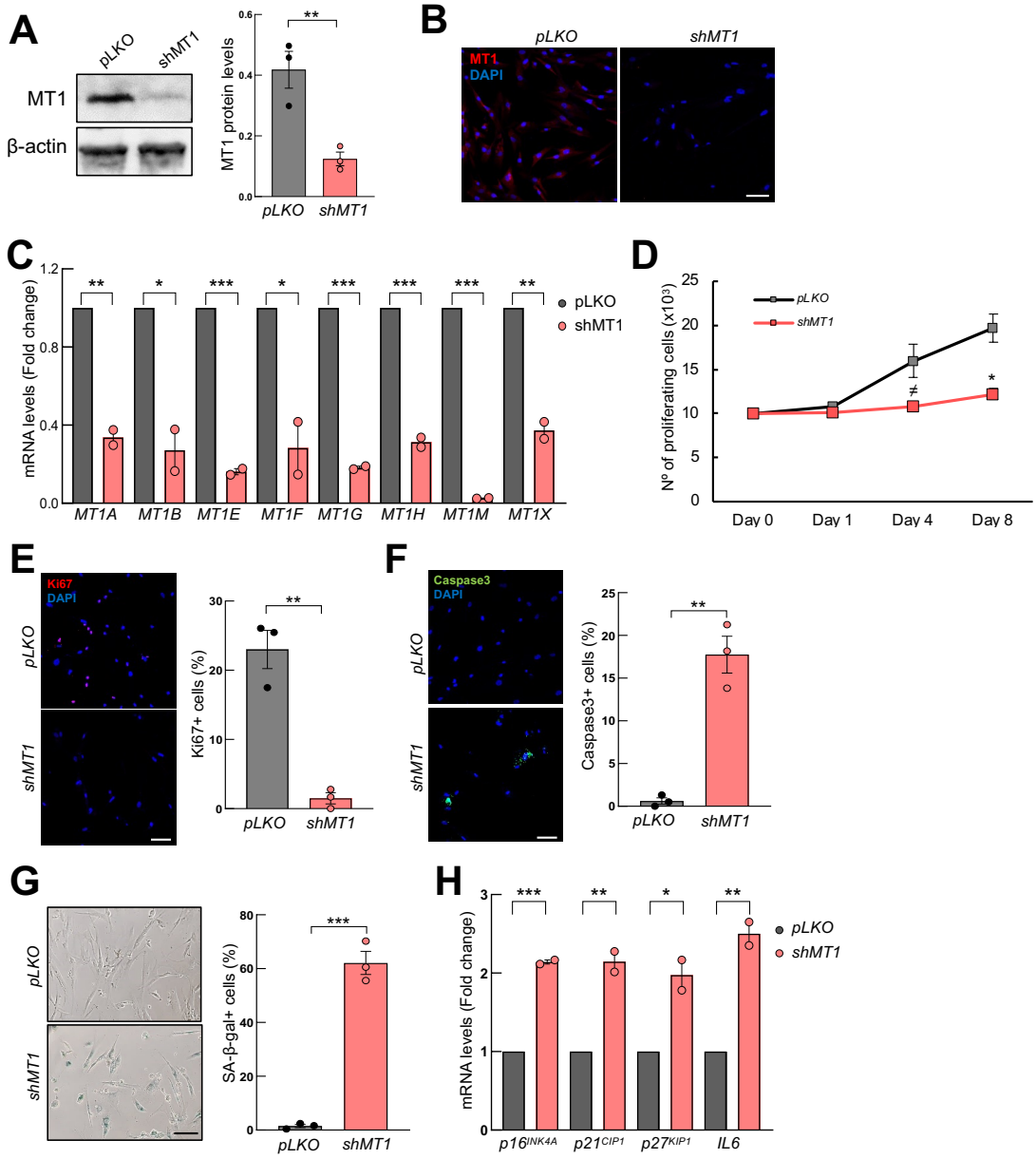

Figure R34. *MT1* silencing alters proliferation, apoptosis and senescence. *MT1* silencing was done in NHA using lentiviral infections and the shRNA technique. **(A)** Representative western blot and quantification of MT1 protein levels in NHA with MT1 downregulation (*shMT1*) compared to control astrocytes (*pLKO*) (n = 3). **(B)** Representative IF images of MT1 in *shMT1* and *pLKO* astrocytes (scale bar = 50 µm). **(C)** mRNA levels of *MT1A, MT1B, MT1E, MT1F, MT1G, MT1H, MT1M* and *MT1X* in *shMT1* astrocytes compared to *pLKO* ones (n = 2). **(D)** Cell growth at indicated time points in *shMT1* astrocytes compared to *pLKO* ones (n = 3). **(E)** Representative images (scale bar = 50 µm) and percentage of Ki67 positive cells (n = 3), **(F)** Caspase 3 positive cells (n = 3) and **(G)** SA-β-gal activity (n = 3) in *shMT1* astrocytes compared to *pLKO* ones. **(H)** mRNA levels of $p16^{INK4A}$, $p21^{CIP1}$, $p27^{KIP1}$ and *IL6* in *shMT1* astrocytes compared to *pLKO* ones (n = 2). The statistical significance was assessed with the Student's t-test (≠ $p < 0.1$, * $p < 0.05$, ** $p < 0.01$, *** $p < 0.001$).

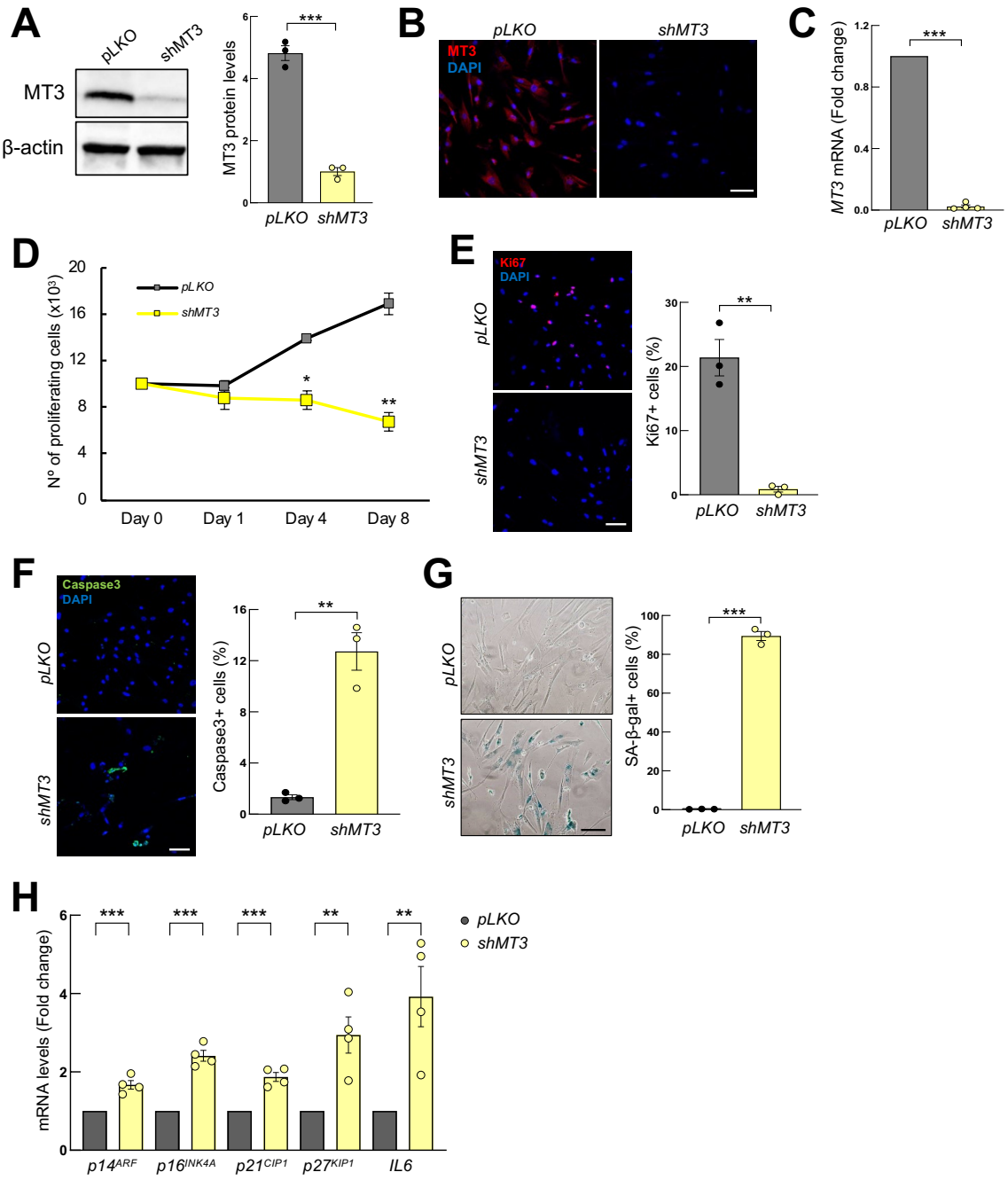

Figure R35. *MT3* silencing alters proliferation, apoptosis and senescence. *MT3* silencing was done in NHA using lentiviral infections and the shRNA technique. **(A)** Representative western blot and quantification of MT3 protein levels in NHA with MT3 downregulation (*shMT3*) compared to control astrocytes (*pLKO*) (n = 3). **(B)** Representative IF images of MT3 in *shMT3* and *pLKO* astrocytes (scale bar = 50 µm). **(C)** mRNA levels of *MT3* in *shMT3* astrocytes compared to *pLKO* ones (n = 4). **(D)** Cell growth at indicated time points in *shMT3* astrocytes compared to *pLKO* ones (n = 3). **(E)** Representative images (scale bar = 50 µm) and percentage of Ki67 positive cells (n = 3), **(F)** Caspase 3 positive cells (n = 3) and **(G)** SA-β-gal activity (n = 3) in *shMT3* astrocytes compared to *pLKO* ones. **(H)** mRNA levels of $p14^{ARF}$, $p16^{INK4A}$, $p21^{CIP1}$, $p27^{KIP1}$ and *IL6* in *shMT3* astrocytes compared to *pLKO* ones (n = 4). The statistical significance was assessed with the Student's t-test (* $p < 0.05$, ** $p < 0.01$, *** $p < 0.001$).

In addition, we studied some inflammatory markers in *MT1* and *MT3* silencing models. We observed statistically significant high levels of *TNFα*, *IL1α*, *STAT3* and *C3* and low levels of *TGFβ* in both *shMT1* (***Figure 36A***) and *shMT3* NHA *(**Figure 36B***). These results indicate that silencing of *MTs* increases the expression of inflammatory genes.

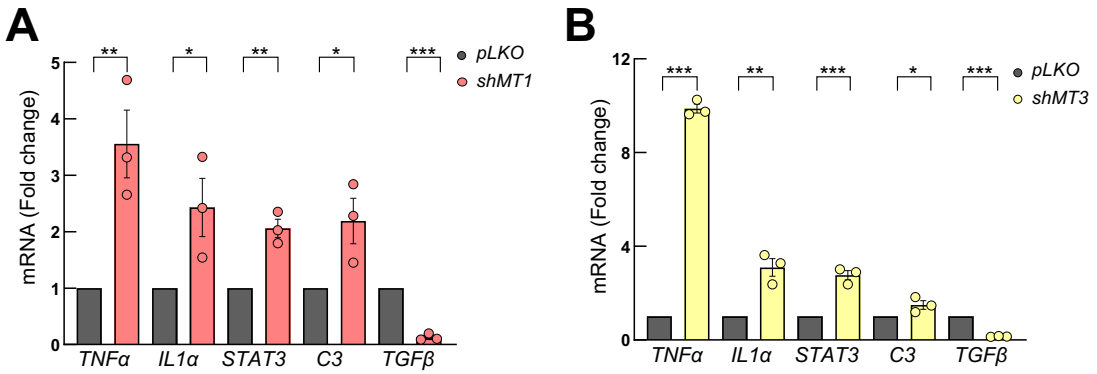

Figure R36. *MT1* or *MT3* silencing increases markers of inflammation. (A) mRNA levels of *TNFα*, *IL1α*, *STAT3*, *C3* and *TGFβ* in NHA with MT1 downregulation (*shMT1*) or with **(B)** MT3 downregulation (*shMT3*) compared to control astrocytes (*pLKO*) (n = 3). The statistical significance was assessed with the Student's t-test (* $p < 0.05$, ** $p < 0.01$, *** $p < 0.001$).

Transcriptome analysis in human hippocampal RNA samples reveal differentially expressed genes with age.

In addition to the study of centenarians, we also analyzed the differentially expressed genes between young (up to 50 years old, n = 5) and old individuals (over 50 years old, n = 11). For this specific part of the study, the 3 centenarians were considered in the old group. In this context, transcriptome analysis showed a differential expression pattern in old people compared to young individuals (***Figure R37A***). In particular, 73 genes, among which 45 were down-regulated and 28 up-regulated , were differentially expressed with p-value < 0.05 and FC ≥ |2| in old individuals compared to young ones (***Figure R37B***). The complete list of differentially expressed genes can be found in the ***Appendix 1 (Table A5*** and ***A6)***.

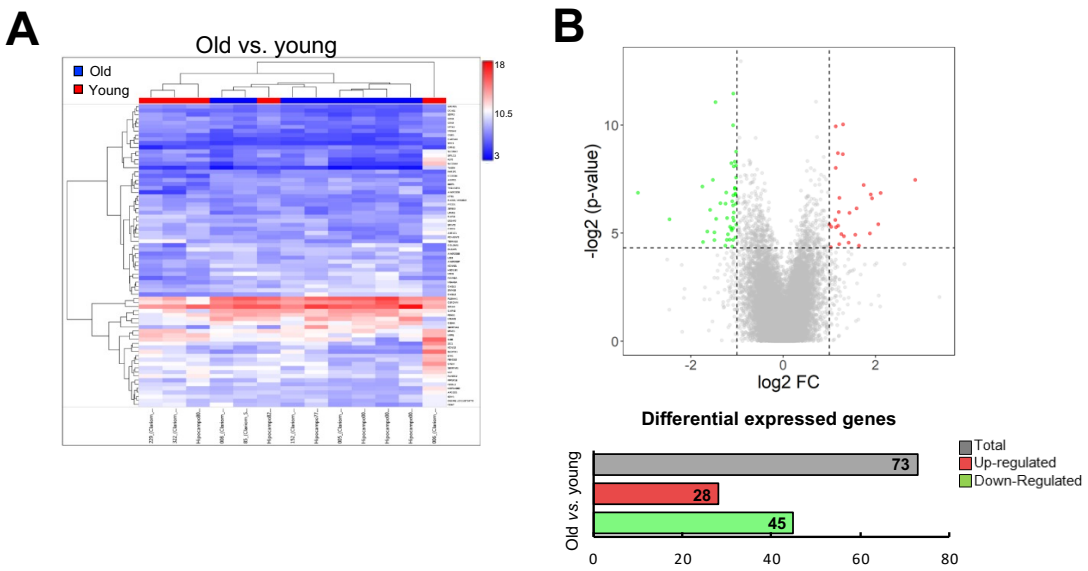

Figure R37. Transcriptome analysis in human hippocampal RNA samples reveals a pattern of genes differentially expressed with age. (A) Hierarchical clustering of young (n = 5) and old (n = 11) individuals selected for array screening. **(B)** Volcano plot of up-regulated and down-regulated genes in the microarray analysis of old vs. young human hippocampus samples. All genes selected presented p-value < 0.05 and FC ≥ |2| in the microarray.

Gene ontology analysis of differentially expressed genes shows altered pathways such as metabolism or transport, among others.

For getting a general landscape of altered pathways we carried out a GO analysis of significantly altered genes between old and young individuals. Interestingly, the top canonical biological processes of down-regulated genes were associated with metabolism, hormone regulation, protein secretion, autophagy, hypoxia, DNA repair, apoptosis, transport and others (***Figure R38A***). On the contrary, among up-regulated genes, processes associated with metabolism, synaptic signaling, ion transport and others were found (***Figure R38B***).

Next, we measured the expression of a selection of identified genes in samples of an additional and larger cohort from the UBC (validation cohort 1) of individuals ranging from 27 to 96 years. In line with the array cohort, young individuals were considered from 27 to 50 years, whereas old individuals were from 65 to 96 years. Interestingly, 33 genes (18 down-regulated and 15 up-regulated) were chosen for experimental validation based on the FC, p-values and the pathways in which they participate. In particular, we selected down-regulated

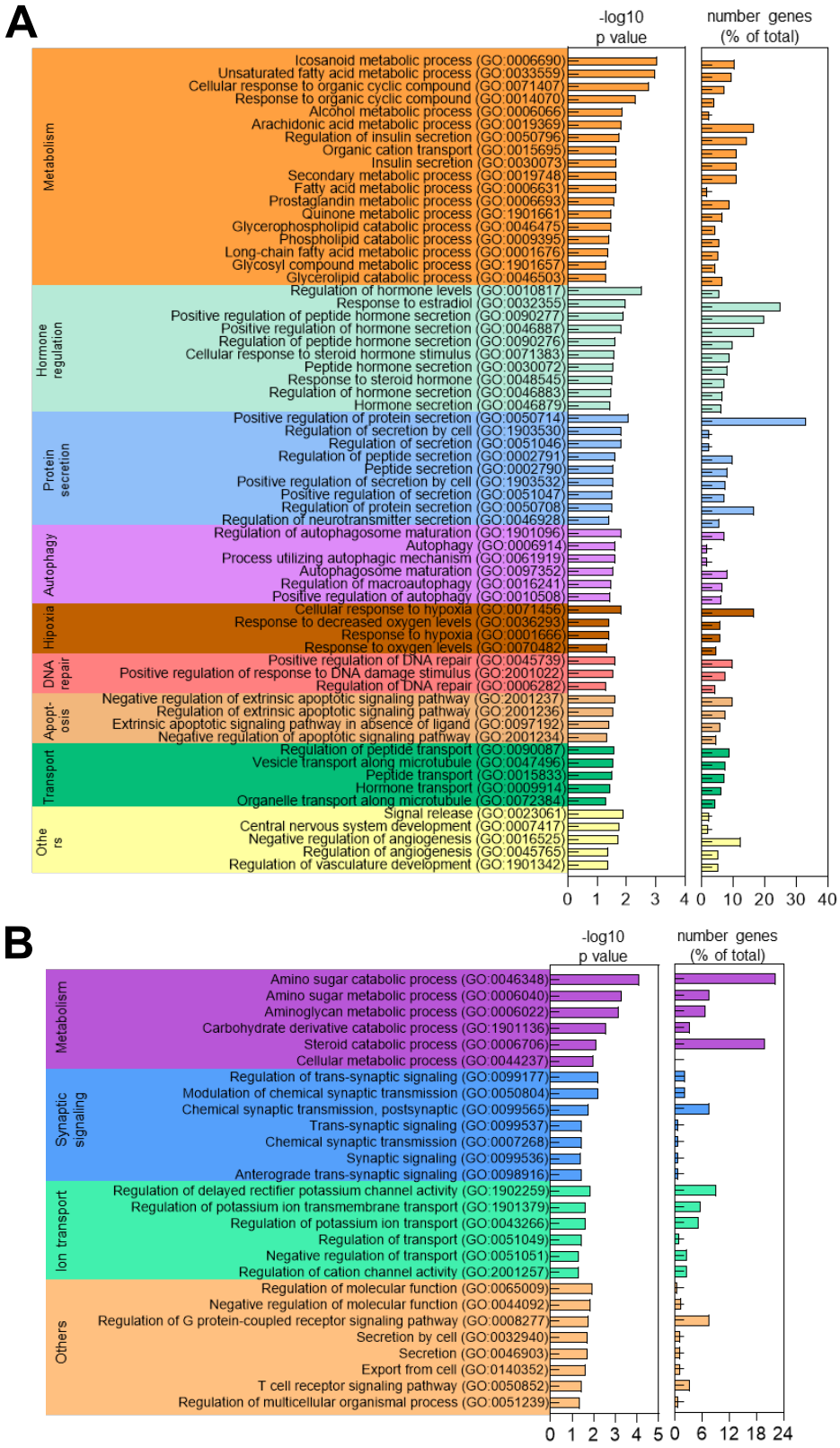

Figure R38. Gene ontology analysis of differentially expressed genes shows altered pathways such as metabolism or transport, among others. (A) Representative bar plots of biological processes associated with down-regulated and **(B)** up-regulated genes in old (n = 11) vs. young (n = 5) human hippocampus samples after GO analysis of microarray results. All genes selected for gene ontology analysis presented p-value < 0.05 and FC ≥ |2| in the microarray. GO analysis was performed using PANTHER GO-Slim Biological Process (http://www.pantherdb.org/panther/goSlim.jsp).

genes linked to metabolism or transport pathways (*GRK4*, *TSPAN18*, *SSTR2*, *PPP1R1B*), DNA repair (*EYA1*, *RAD21*, *ZBTB10*), development (*OSR1*, *CREM*, *ZIC1*, *EFEMP2*, *NNAT*) and neurotransmitter release or activity (*CHRNA6*), and up-regulated genes mainly linked to inflammation or immune system pathways (*CHI3L1*, *CHI3L2*, *SERPINA3*, *CERCAM*, *MOG*) and metabolism (*MRAP2*, *CAPN3*, *PD1E1C*, *BEST1*). 13 genes (*GRK4*, *EYA1*, *RAD21*, *OSR1*, *CHRNA6*, *TSPAN18*, *SSTR2*, *PPP1R1B*, *CREM*, *ZBTB10*, *ZIC1*, *EFEMP2* and *NNAT*) presented statistically significant lower expression levels (***Figure R39A***) and 9 genes (*CHI3L1*, *SERPINA3*, *ANKRD30*, *MRAP2*, *CERCAM*, *CHI3L2*, *MS4A6A*, *CAPN3* and *PD1E1C*) a higher expression in the hippocampus of old individuals compared to young ones (***Figure R39B***). These results reveal a set of genes differentially expressed in hippocampus neurogenic niche with aging.

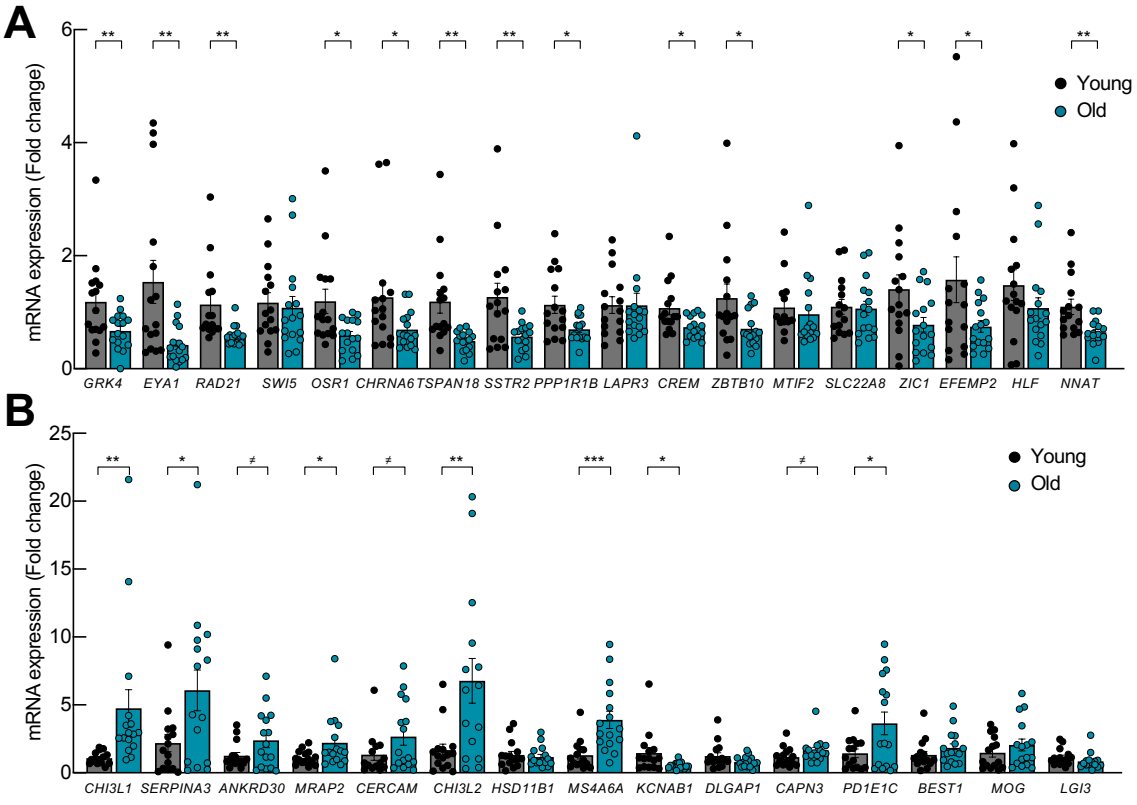

Figure R39. Gene expression in a larger validation cohort. mRNA expression levels of **(A)** the down-regulated genes (*GRK4, EYA1, RAD21, SWI5, OSR1, CHRNA6, TSPAN18, SSTR2, PPP1R1B, CREM, ZBTB10, MTIF2, SLC22A8, ZIC1, EFEMP2, HLF* and *NNAT*) and **(B)** up-regulated genes (*CHI3L1, SERPINA3, ANKRD30, MRAP2, CERCAM, CHI3L2, HSD11B1, MS4A6A, KCNAB1, DLGAP1, CAPN3, PD1E1C, BEST1, MOG* and *LGI3*) validation by qRT-PCR in hippocampus samples of young individuals (ranging from 27 to 50 years, n = 16) and old individuals (ranging from 65 to 96 years, n = 16) from the UBC cohort (validation cohort 1). The statistical significance was assessed with the Student's t-test (≠ $p < 0.1$, * $p < 0.05$, ** $p < 0.01$, *** $p < 0.001$).

PART B. Study of the correlation of gene expression with chronological aging in human hippocampus.

The expression of 6 genes correlates positively or negatively with chronological aging.

Apart from the study of the differentially expressed genes between the 3 groups of the study, we performed an additional analysis to identify the molecular mechanisms that were associated with chronological aging. Thus, correlation studies between gene expression and age were done in the hippocampus samples from the microarray cohort. The normality was checked with Kolmogorov Smirnov test and we used the Pearson correlation coefficient since the samples followed a normal distribution. Only genes with p-value < 0.001 and correlation coefficient < |8| with age were selected. Notably, this analysis revealed 6 genes whose expression was positively or negatively correlated with chronological aging in human hippocampus samples (***Table R4***).

Table R4. Correlation between gene expression and chronological aging in human hippocampus samples from the microarray cohort (n = 16).

Gene symbol	Gene name	Correlation coefficient*	p-value
SMPD4	Sphingomyelin phosphodiesterase 4	0.822	< 0.001
RASGEF1B	RasGEF domain family member 1B	0.836	< 0.001
ANKRD18B	Ankyrin repeat domain 18B	0.837	< 0.001
RAD23B	RAD23 homolog B, nucleotide excision repair protein	-0.841	< 0.001
HYOU1	Hypoxia up-regulated 1	-0.835	< 0.001
OR2A42	Olfactory receptor, family 2, subfamily A, member 42	-0.822	< 0.001

*Correlation studies between age and candidate genes was done using Pearson correlation coefficient since the samples followed a normal distribution (checked by Kolmogorov Smirnov test).

Among them, the expression of Sphingomyelin Phosphodiesterase 4 (*SMPD4*), Ras-GEF domain-containing family member 1B (*RASGEF1B*) and Ankyrin Repeat Domain 18B (*ANKRD18B*) correlated positively with aging (***Figure R40A***). On the other hand, the expression of RAD23 homolog B nucleotide excision repair protein (*RAD23B*), Hypoxia up-

regulated 1 (*HYOU1*) and Olfactory Receptor family 2 subfamily A member 42 (*OR2A42*) decreased with age in the hippocampus (***Figure R40B***). Next, the validations were done in the validation cohort 1 and the expression of the 6 identified genes was measured by qRT-PCR. In this context, the expression of *SMPD4*, *RASGEF1B* and *ANKRD18B* was significantly higher (***Figure R40C***) whereas the expression of *RAD23B* and *HYOU1* was significantly lower in hippocampus samples from aged individuals compared to young ones (***Figure R40D***). Moreover, we performed correlation studies between gene expression and age in the same samples of the validation cohort 1 and we observed that the expression of *SMPD4*, *RASGEF1B* and *ANKRD18B* correlated positively with age showing a statistical significance of p = 0.04, p = 0.02, p = 0.03 respectively (***Figure R40E***). On the other hand, decline in *RAD23B* expression with age presented the strongest Pearson correlation coefficient (r = -0.2, p-value = 0.03), whereas *HYOU1* did not reach statistical significance (***Figure R40F***). Altogether, these data reveal that there is a correlation between the expression of some of the identified genes with age in human hippocampus.

Serial passage-cultured human primary fibroblasts and NHA display a similar pattern of expression as old individuals.

The expression of the 6 selected candidate genes was determined by RT-qPCR in human primary fibroblasts derived from adult individuals at early and late passages. Thus, the expression of *SMPD4* and *RASGEF1B* increased significantly in late passage primary fibroblasts (***Figure R41A***), whereas the levels of *RAD23B* were significantly lower (***Figure R41B***). Additionally, we characterized the expression of these genes in NHA at early and late passages. In this case, late passage NHA presented a statistically significant higher expression of *SMPD4* and *ANKRD18B* (***Figure R41C***), but a significant lower expression of *RAD23B*, *HYOU1* and *OR2A42* compared to early passage ones (***Figure R41D***). These results extend the link of identified genes to cellular aging.

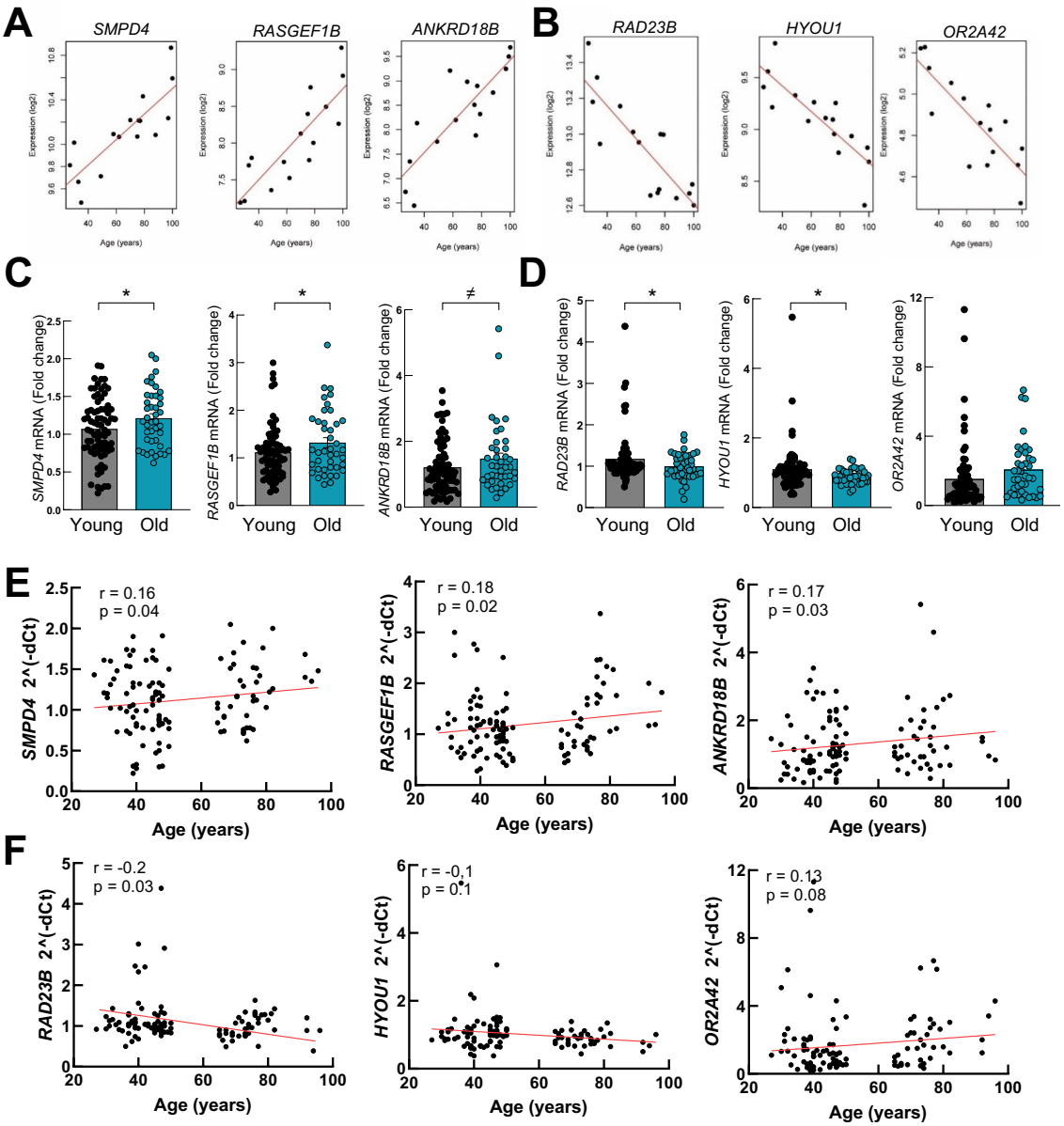

Figure R40. The expression of 6 genes correlates positively or negatively with chronological aging. (A) Correlation studies of *SMPD4*, *RASGEF1B*, *ANKRD18B* and **(B)** *RAD23B*, *HYOU1* and *OR2A42* with chronological aging in hippocampus samples used for the microarray (n = 16) using Pearson correlation coefficient. **(C)** mRNA expression levels of *SMPD4*, *RASGEF1B*, *ANKRD18B* and **(D)** *RAD23B*, *HYOU1* and *OR2A42* by RT-qPCR in hippocampus samples of young individuals (ranging from 27 to 50 years, n = 78) and old individuals (ranging from 65 to 96 years, n = 42) from the from the UBC cohort (validation cohort 1, n = 120). The statistical significance was assessed with the Student's t-test (≠ $p < 0.1$, * $p < 0.05$). **(E)** Correlation studies of *SMPD4*, *RASGEF1B*, *ANKRD18B* and **(F)** *RAD23B*, *HYOU1* and *OR2A42* with chronological aging in hippocampus samples from the validation cohort 1 (n = 120) using Pearson correlation coefficient (r). The samples followed a normal distribution (checked by Kolmogorov Smirnov test).

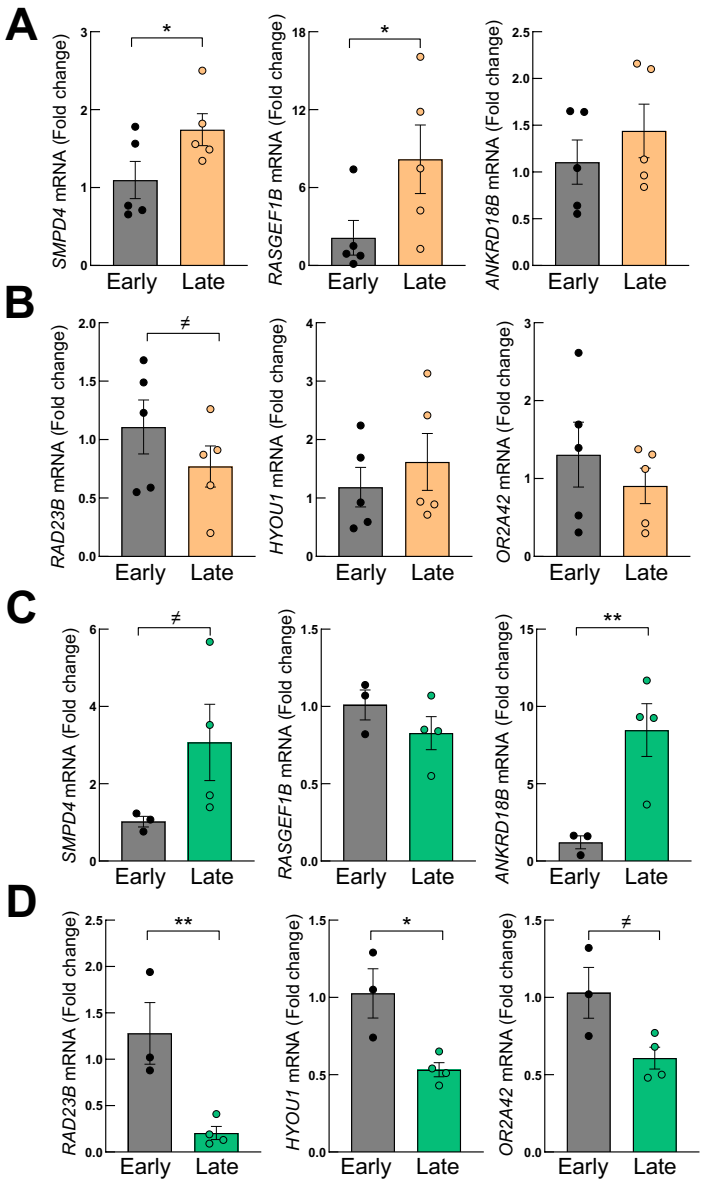

Figure R41. The expression pattern of the selected genes in serial passage-cultured human primary fibroblasts and NHA is similar to the one observed in old individuals. (A) mRNA levels of *SMPD4*, *RASGEF1B*, *ANKRD18B* and **(B)** *RAD23B*, *HYOU1*, *OR2A42* in human primary fibroblasts obtained from skin biopsies of 5 individuals and cultured at early (5 – 10) and late (35 – 40) passages (n = 5). **(C)** mRNA levels of *SMPD4, RASGEF1*, *ANKRD18B* and **(D)** *RAD23B, HYOU1, OR2A42* in NHA cultured at early (2 – 3) and late (15 – 17) passages (n = 4). The statistical significance was assessed with the Student's t-test (≠ $p < 0.1$, * $p < 0.05$, ** $p < 0.01$).

The identified genes are highly expressed in the brain and enriched in different regions.

Taking advantage of transcriptomic studies in available public datasets from "The Human Protein Atlas" (http://www.proteinatlas.org), we further characterized the expression of the 6 genes of interest in different human samples. Herein, we observed that

their expression pattern was variable among the different organs and tissues and that they were expressed in the brain to a greater or lesser extent (***Figure R42A and B***).

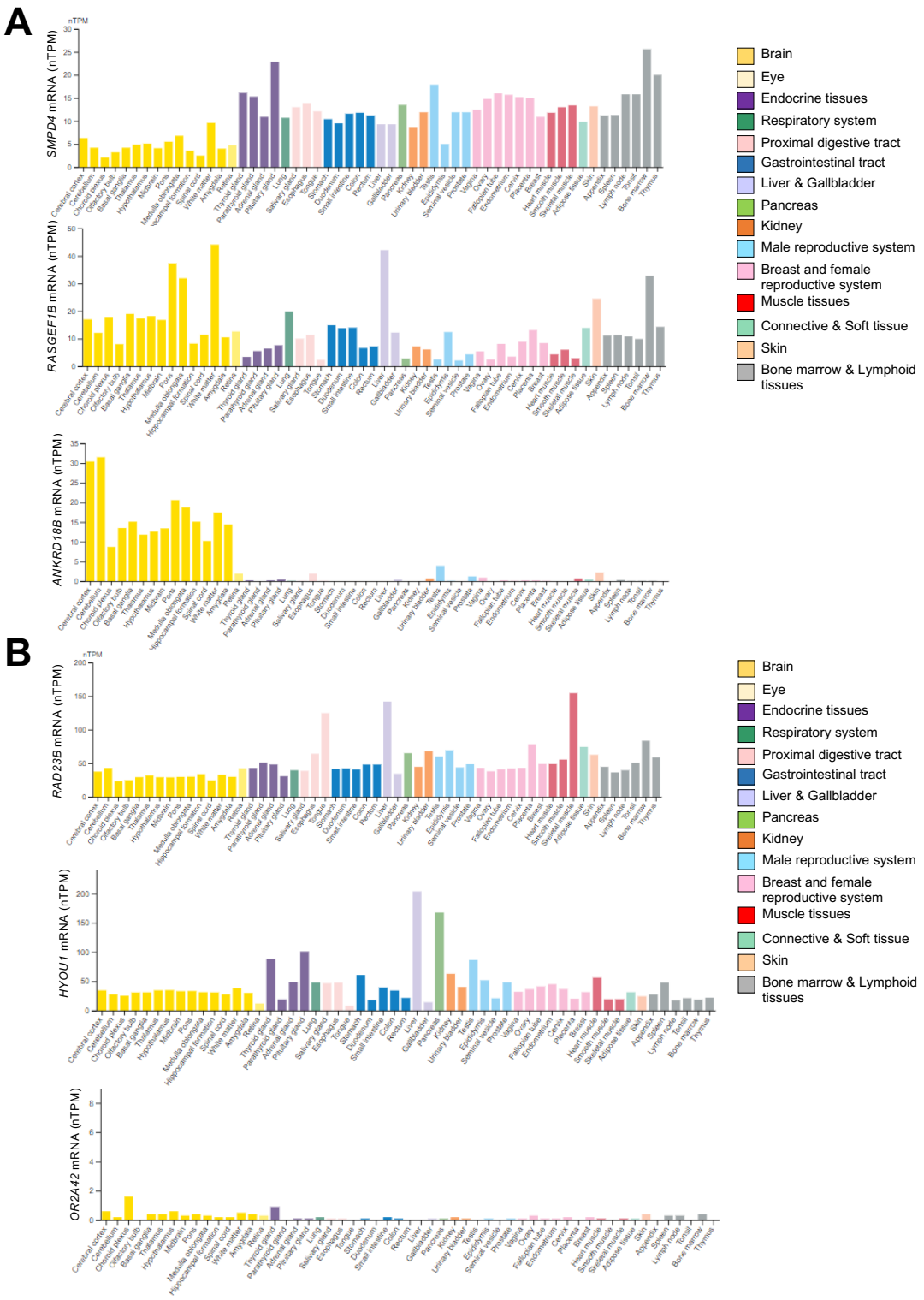

Figure R42. The expression of the selected genes is variable among human tissues. (A) Normalized expression (nTPM) levels of *SMPD4, RASGEF1B, ANKRD18B* and **(B)** *RAD23B, HYOU1, OR2A42* in the indicated tissue types created combining the HPA and GTEx transcriptomic datasets from "The Human Protein Atlas" (http://www.proteinatlas.org).

We further characterized the expression of the candidate genes in different brain regions of aged individuals, from additional RNAseq studies in publicly available datasets (https://aging.brain-map.org). Notably, the expression of *SMPD4* and *RASGEF1B* appeared to be higher in the white matter of the forebrain, whereas the levels of *ANKRD18B* were more elevated in the parietal and temporal neocortex (***Figure R43A***). In contrast, the expression of *RAD23B* was higher in the hippocampus compared to additional brain regions (***Figure R43B***). Similarly, *HYOU1* expression appeared to be enriched also in this brain region and less clearly in other regions (***Figure R43B***).

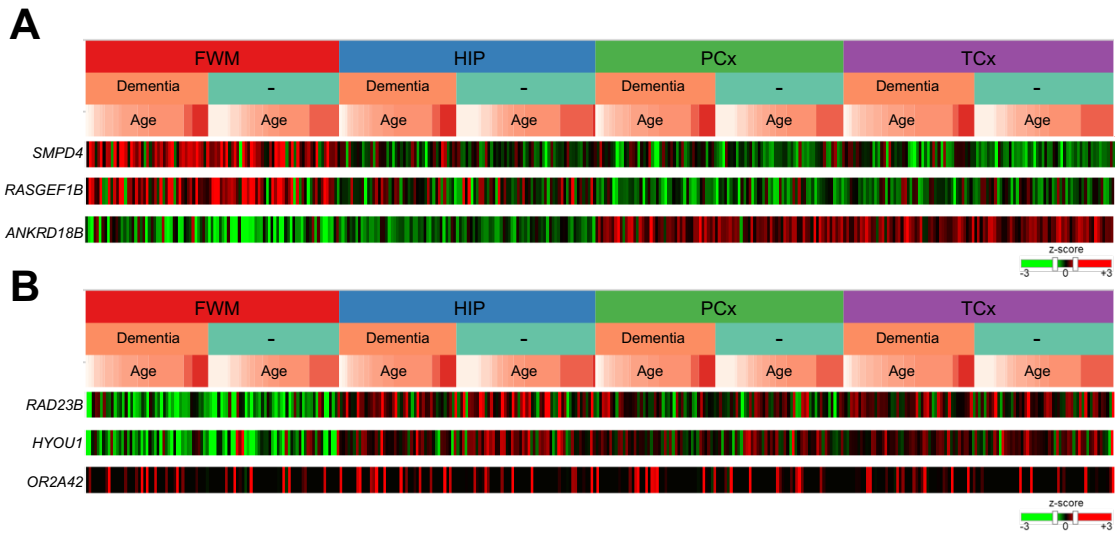

Figure R43. The expression of identified genes is enriched in different human brain regions. (A) Expression of *SMPD4, RASGEF1B, ANKRD18B* and **(B)** *RAD23B, HYOU1, OR2A42* represented by z-score in white matter of forebrain (FWM), hippocampus (HIP), parietal neocortex (PCx) and temporal neocortex (TCx) of aged human individuals ranged between 78-100+ years old (n = 30 healthy, n = 24 dementia). Dementia was presented as vascular, multiple etiologies, Alzheimer´s disease or other medical form. Data obtained from https://aging.brain-map.org.

Next, we studied the expression of the selected genes in adult C57BL6 mice brain sections using "Allen Mouse Brain Atlas" (https://mouse.brain-map.org). Indeed, *Smpd4*, *Rasgef1b, Rad23b* and *Hyou1* were detected in different regions of the brain (***Figure R44A and B***), with the last 2 being highly expressed in the DG from adult mice (***Figure R44B***). Furthermore, we studied the expression of the ortholog genes in DG samples from a set of young and aged C57BL6 mice. We did not detected changes in the expression of *Smpd4* and *Rasgef1b* (***Figure R44C***) but we found significantly lower levels of *Rad23b* and a tendency for decreased expression of *Hyou1* in old mice compared to young ones (***Figure R44D***).

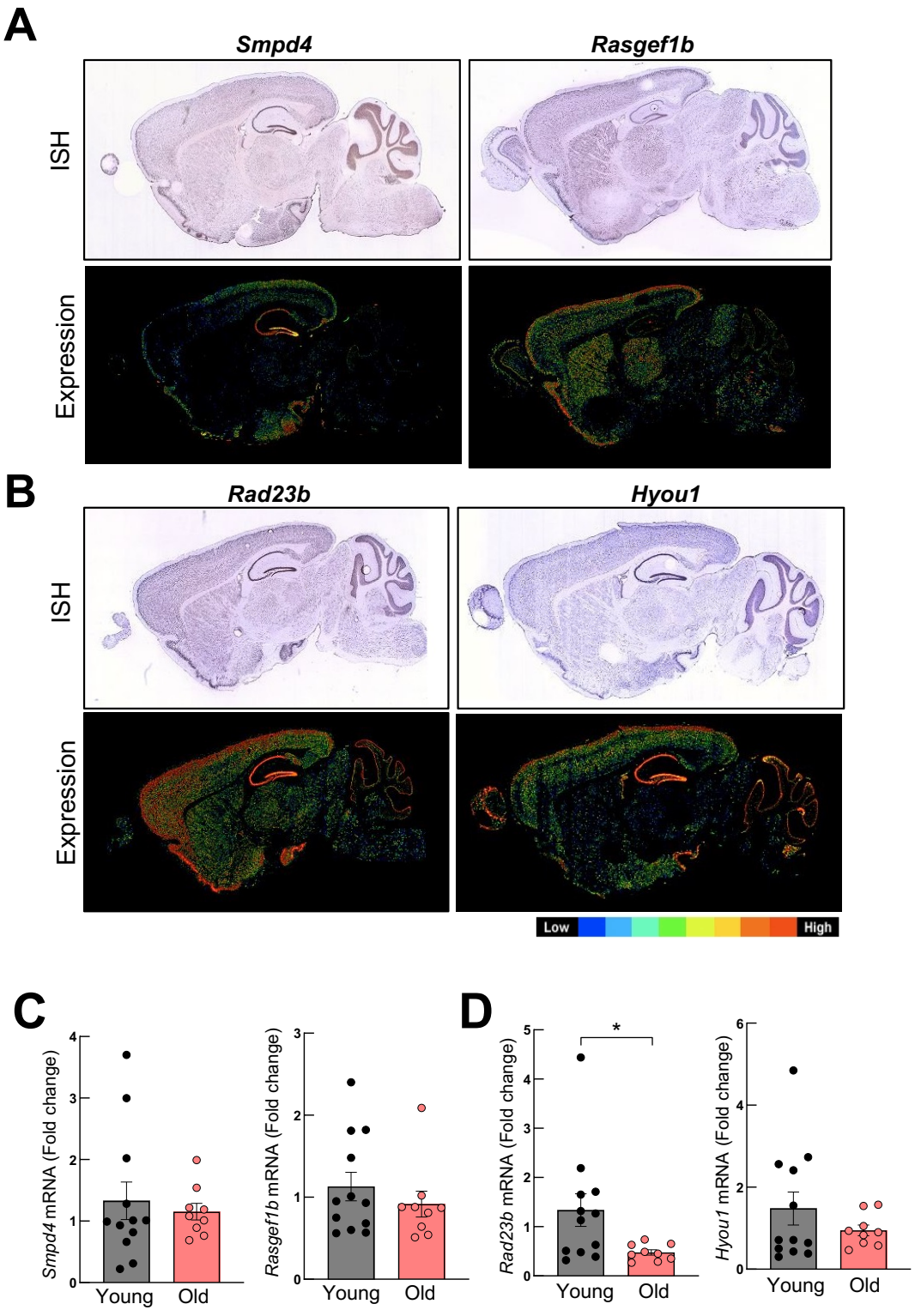

Figure R44. The expression of identified genes is enriched in different mice brain regions and altered in the DG of C57BL6 aged mice. (A) Images of in situ hybridization (ISH, up) and expression (down) of *Smpd4, Rasgef1b* and **(B)** *Rad23b* and *Hyou* in brain sections from adult (P56) C57BL6 mice obtained from "Allen Mouse Brain Atlas" (https://mouse.brain-map.org). **(C)** mRNA expression levels of *Smpd4, Rasgef1b* and **(D)** *Rad23b* and *Hyou1* in the dentate gyrus (DG) of young (2 months, n = 12) and old (over 20 months, n = 9) C57BL6 mice. The statistical significance was assessed with the Student's t-test (* $p < 0.05$).

The expression of the 6 genes is similar between different cell types of the brain.

Moreover, single cell RNAseq data from the brain was analyzed in the same available public data set. In this case, we observed that the expression of the 6 genes presented a homogeneous expression pattern between the different cell types of the brain, with the exception of *RASGEF1B*, which appeared to be expressed mostly by glial cells (***Figure R45A and B***).

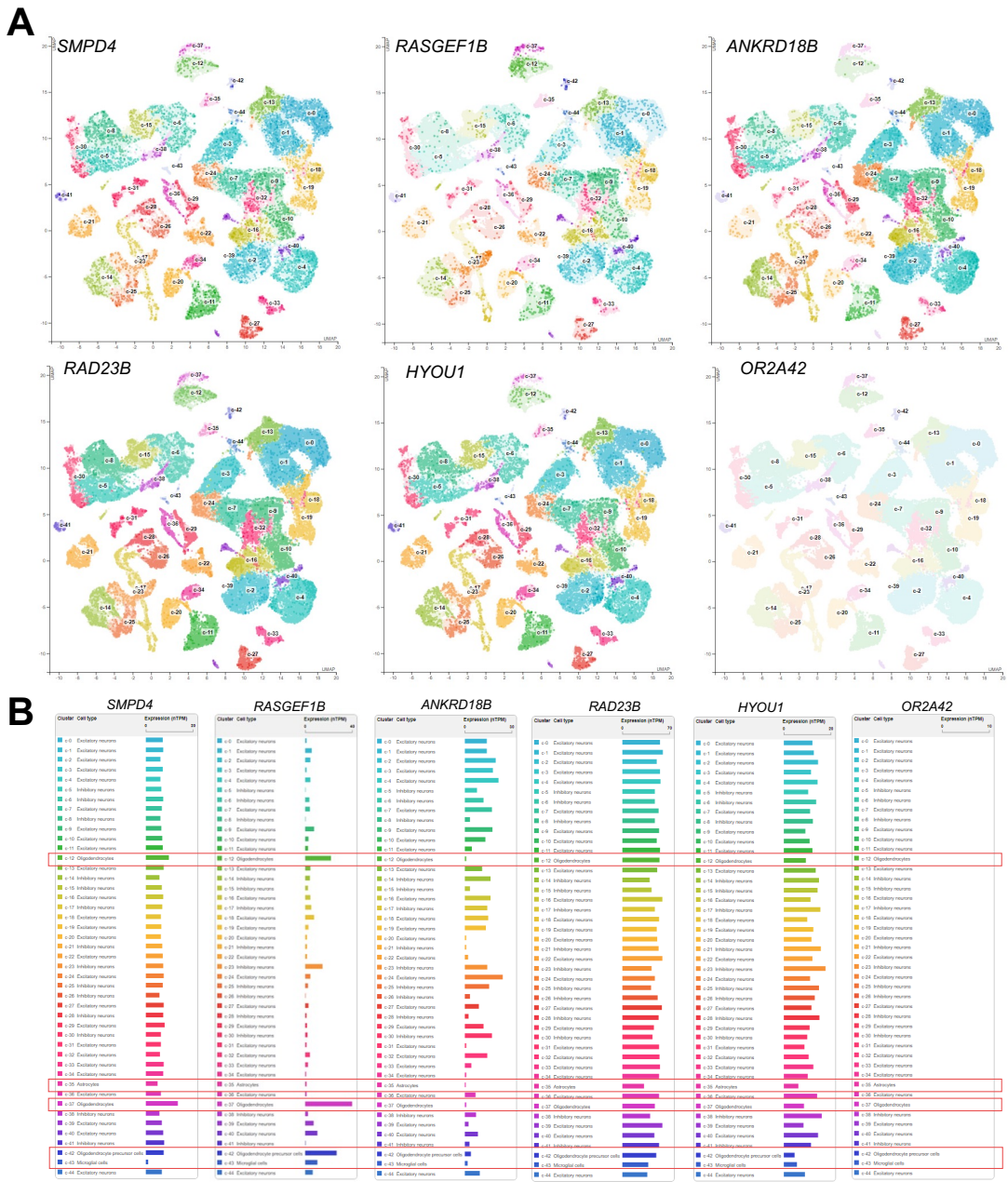

Figure R45. The expression of the 6 genes is similar in neurons and glial cells. (A) Single cell RNAseq data from whole brain for the expression of *SMPD4, RASGEF1B, ANKRD18B, RAD23B, HYOU1* and *OR2A42*, obtained from "The Human Protein Atlas" (http://www.proteinatlas.org). **(B)** Normalized expression (nTPM) levels of the selected genes in neurons and glial cells (marked with a red square) from the same single cell RNAseq study.

We also check the expression of the 6 genes directly in aged microglia. For that, we took advantage of RNAseq data (http://shiny.maths.usyd.edu.au/Ellis/MicrogliaPlots/) from aged human bulk dorsolateral prefrontal cortex samples and purified microglia from the same region. We observed that none of the genes studied were enriched in microglia compared to bulk cortex with the exception of *RASGEF1B* and *OR2A42* that were clearly enriched in microglia (***Figure R46A and B***), which could indicate an association with microglial aging.

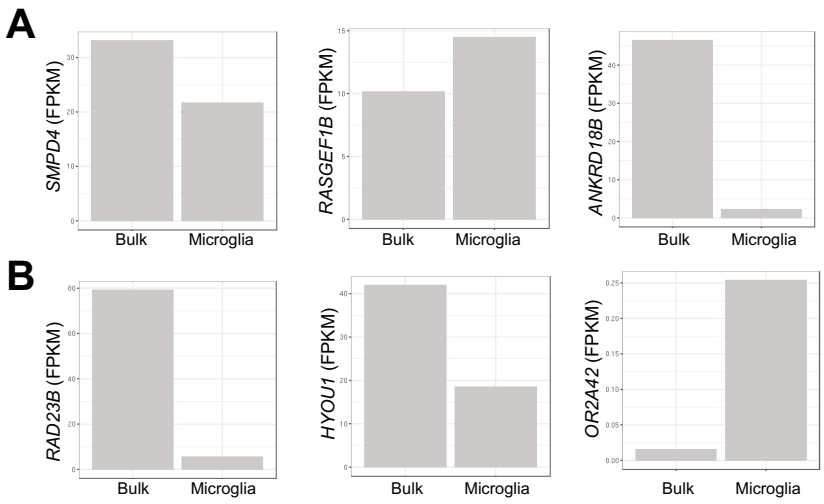

Figure R46. The expression of the 6 genes in microglia. (A) RNAseq data for the expression of *SMPD4, RASGEF1B, ANKRD18B* and **(B)** *RAD23B, HYOU1, OR2A42* in bulk dorsolateral prefrontal cortex (n = 540) vs. purified microglia from the same region (n = 10). Data obtained from http://shiny.maths.usyd.edu.au/Ellis/MicrogliaPlots/.

RAD23B protein expression diminishes with age and with AD.

RAD23B is implicated in DNA repair, which has been described to have a relevant role in aging and in neurodegeneration [352]. Since it is probably the gene that shows the strongest association with age and it is more intensively expressed in the hippocampal neurogenic niche, we focused on its characterization. Thus, we studied RAD23B protein expression by IHC in human brain samples from the pathology service of the DUH (additional cohort 2), including hippocampus and cortex regions of healthy individuals of different ages and patients with AD. Notably, we observed a marked decrease in the staining of RAD23B in the DG of old compared to young individuals that was less remarkable in the cortex of these individuals (***Figure R47A***). The quantification of RAD23B expression in the DG (high staining,

value = 3; moderate staining, value = 2 and low or absent staining, value = 1) confirmed that the levels of RAD23B were decreased in old individuals compared to young ones *(**Figure R47B***). Moreover, the expression in AD patients was even lower or absent in comparison with old and young healthy individuals (***Figure R47B***). Similarly, the IF performed in samples of the additional cohort 1 revealed that the levels of RAD23B were significantly lower in the DG of old individuals compared to young ones and further confirmed the marked reduction of RAD23B in AD patients *(**Figure R47C and D**)*. Altogether, these results reveal a significant decrease in the expression of RAD23B in the hippocampal neurogenic niche with physiological aging that is exacerbated in pathological conditions.

RAD23B silencing alters proliferation, apoptosis and senescence.

With these results in mind, we studied the possible effects of the down-regulation of *RAD23B* in NHA. For this, *RAD23B* was silenced in NHA using lentiviral infections and a specific *shRNA* construct. We detected statistically significant lower protein levels of RAD23B (***Figure R48A***) and lower mRNA expression of *RAD23B* (***Figure R48B***) in astrocytes with *RAD23B* down-regulation (*shRAD23B*) compared to control ones (*pLKO*), thus validating our model. Moreover, the expression of proliferation and senescence markers were analyzed and we found a statistically significant higher expression of $p16^{INK4A}$, $p21^{CIP1}$, $p27^{KIP1}$ and *IL6* in *shRAD23B* NHA compared *pLKO* ones (***Figure R48C***). These data were consistent with the reduction of cell growth observed in *RAD23B* knockdown cells measured by cell counting (***Figure R48D***). Additionally, we found a significantly lower number of positive cells for Ki67 marker (***Figure R48E***), indicating that cell proliferation was impaired in *RAD23B*-silenced NHA. Furthermore, silencing of *RAD23B* significantly increased apoptosis measured as the number of positive cells for Caspase 3 marker (***Figure R48F***) and also cellular senescence, measured as the number of SA-β-gal positive cells (***Figure R48G***). These data indicate that *RAD23B* could be involved in astrocyte viability, activity and aging.

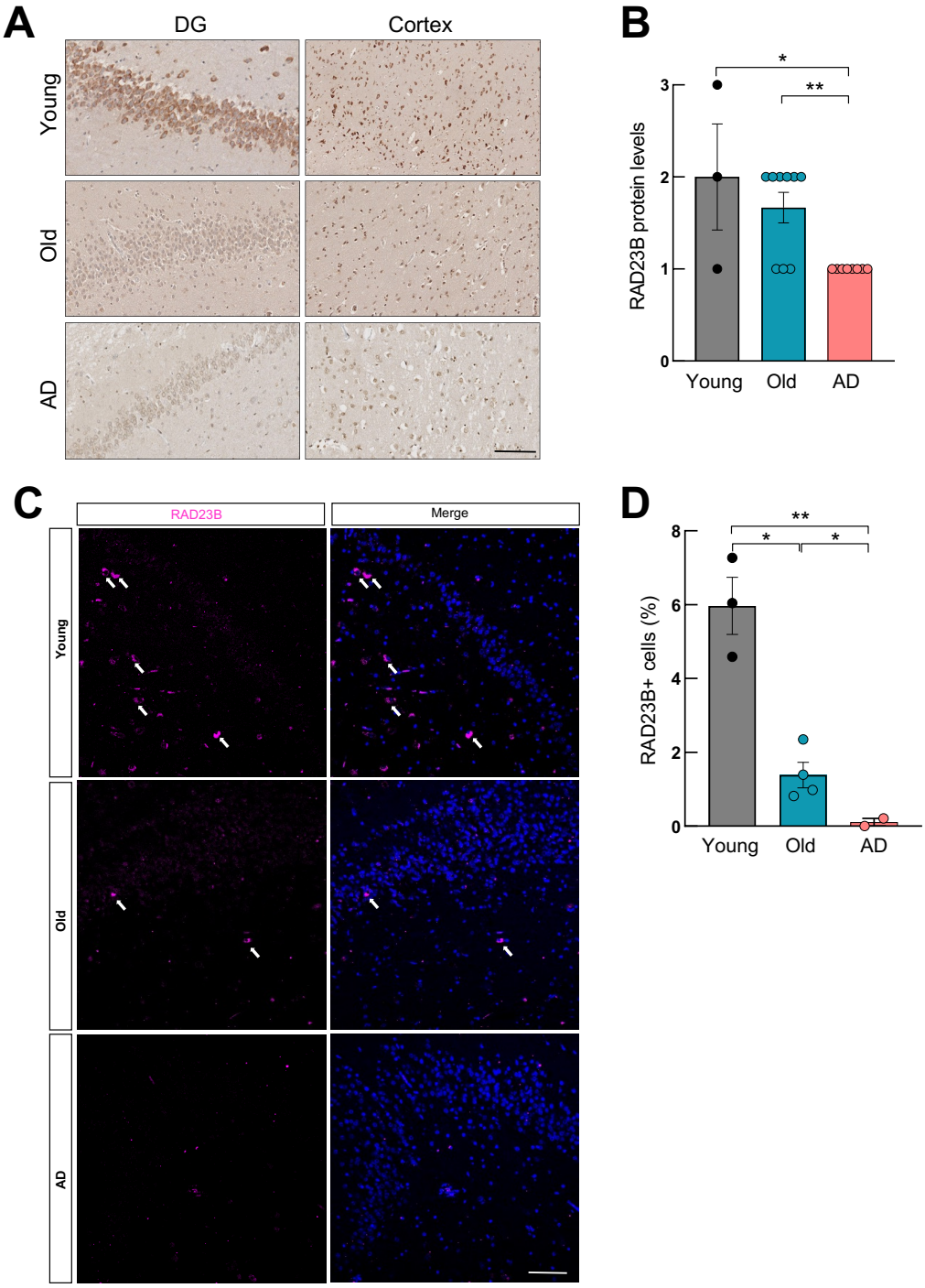

Figure R47. Reduction of RAD23B protein levels with physiological and pathological aging. (A) Representative immunohistochemistry images of RAD23B (scale bar = 100 µm) in human dentate gyrus (DG) and cortex samples of young (n = 3), old (n = 9) and Alzheimer´s disease (AD) individuals (n = 8) from the pathology service of the DUH (additional cohort 2). **(B)** RAD23B protein quantification in DG samples of the same cohort (young, n = 3; old, n = 9 and AD, n = 8). The protein levels were classified as high (value = 3), moderate (value = 2), low or absent expression (value = 1). The statistical significance was assessed with the Chi-squared test (* $p < 0.05$, ** $p < 0.01$). **(C)** Representative immunofluorescence images of RAD23B in the DG (scale bar = 100 µm) and **(D)** protein quantification of RAD23B in the DG of young (n = 3) and old individuals (n = 9) from the cohort of Navarra Biomed (additional cohort 1) and patients of AD (n = 2) from the pathology service of the DUH (additional cohort 2). The statistical significance was assessed with the Student's t-test (≠ $p < 0.1$, * $p < 0.05$, ** $p < 0.01$).

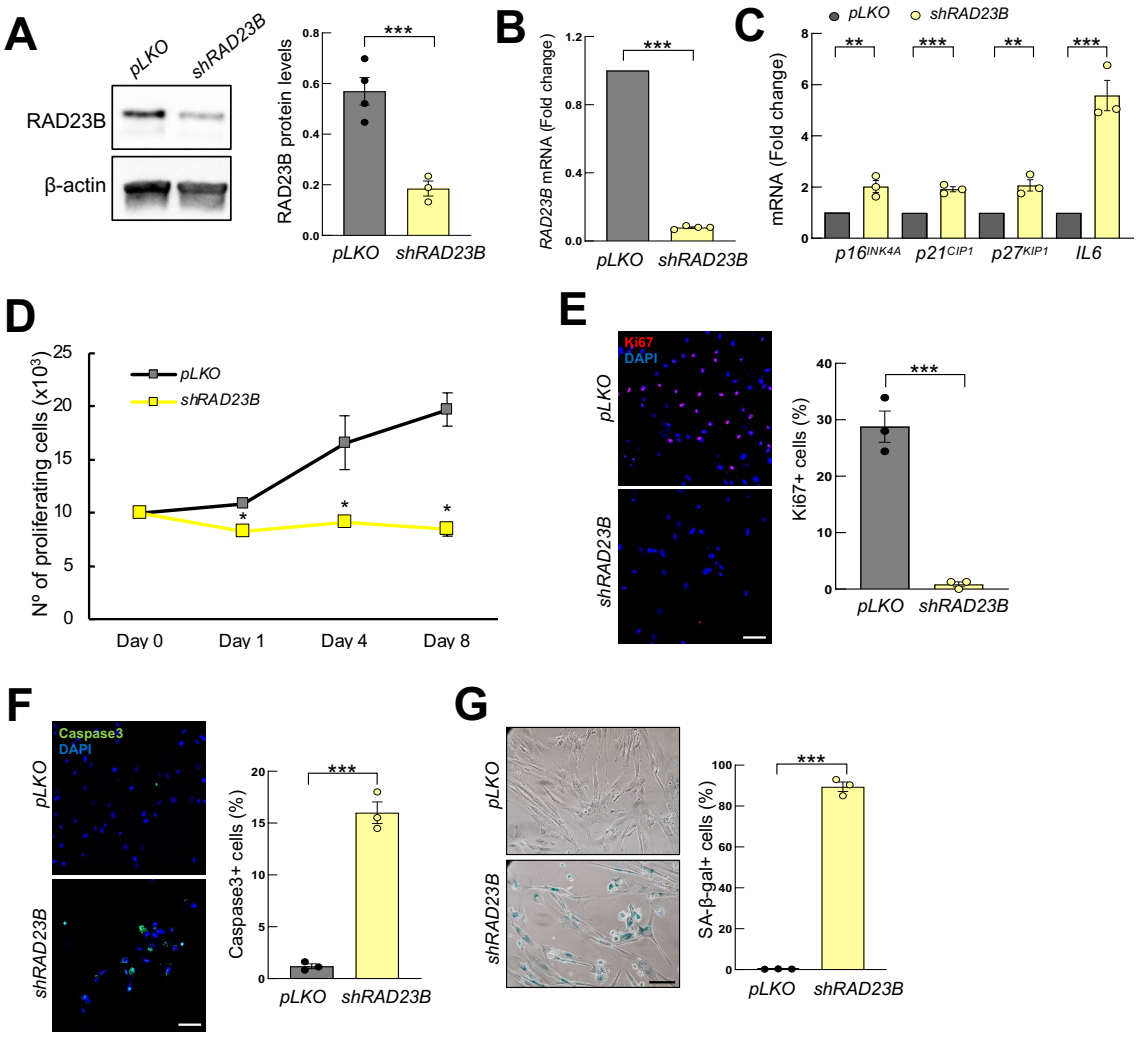

Figure R48. *RAD23B* silencing decreases proliferation and increases apoptosis and senescence. *RAD23B* silencing was done in NHA using lentiviral infections and the shRNA technique. **(A)** Representative western blot and quantification of RAD23B protein levels in NHA with RAD23B downregulation (*shRAD23B*) compared to control astrocytes (*pLKO*) (n ≥ 3). **(B)** mRNA levels of *RAD23B* (n = 4) and **(C)** $p16^{INK4A}$, $p21^{CIP1}$, $p27^{KIP1}$ and *IL6* in *shRAD23B* astrocytes compared to *pLKO* ones (n = 3). **(D)** Cell growth at indicated time points in *shRAD23B* astrocytes compared to *pLKO* ones (n = 3). **(E)** Representative images (scale bar = 50 µm) and percentage of Ki67 positive cells (n = 3), **(F)** Caspase 3 positive cells (n = 3) and **(G)** SA-β-gal activity (n = 3) in *shRAD23B* astrocytes compared to *pLKO* ones. The statistical significance was assessed with the Student's t-test (* $p < 0.05$, ** $p < 0.01$, *** $p < 0.001$).

Discussion

Average life expectancy has increased considerably in last century, thus increasing the number of elderly people in the population and therefore functional limitations and age-related diseases [353]. Aging is a systemic, degenerative and multifactorial process characterized by the decline and loss of physical and mental capacities [2]. In this sense, the cumulative decline in multiple physiological systems gives rise to a geriatric syndrome, named frailty, that represents a state of vulnerability with increased risk of negative health outcomes [67]. It is considered a stage prior to dependency, characterized by a loss of functional capacity and the ability to respond to physiological stress that is becoming an important health problem. It is a dynamic condition with potential of reversibility through the application of intervention programs [82], [354]. Threfore, the identification of the biology underlying frailty can give important clues for its detection as well as for intervention.

Although aging affects all tissues and systems of the organism, brain aging is especially distinctive and play a central role in the degenerative process [8]. Indeed, brain aging promotes a progressive loss of mental capacities which drives a progressive cognitive decline and functional individual deterioration, that can also lead to neurodegenerative diseases [300]. In previous years, different approaches have been used to identify biomarkers and molecular pathways underlying brain aging [301], however, they are not clearly characterized yet. Therefore, an understanding of the fundamental molecular mechanisms involved in brain aging is still necessary as a first step to therapy approaches. Different individuals display diverse aging trajectories and there are groups that can give clues about how to display successful aging. Centenarian individuals exhibit extended longevity that is accompanied by better cognitive function, greater quality of life and fewer comorbidities [155]. Therefore, they might be a good model to understand brain aging.

1. Identification of molecular mechanisms underlying frailty

Relatively little is known regarding the pathophysiology associated to frailty syndrome. Indeed, oxidative stress and inflammation are the only biological processes robustly and experimentally linked to frailty. In this regard, recent studies have started to use omics approaches in order to recognize frail individuals at biological or molecular level [139], [140], [142], [144]. However, the potential for reversibility after an intervention of the

identified genes or metabolites and their impact at functional level has not been studied. In addition, very few omics studies have been performed in community-dwelling individuals and the molecular mechanisms underlying frailty remain poorly understood. Taking all these into account, we analyzed the transcriptomic profile of a set of robust and frail community-dwelling individuals from the Basque Country, we validated their expression in different cohorts as well as after different types of interventions, and in different cell types under culture stress, that resemble physiological aging. Moreover, we performed functional studies in cell cultures with the most promising candidates overall revealing senescence related pathways as novel mechanisms underlying the pathobiology of frailty.

1.1. Identification of a molecular pattern associated to frailty

In the first chapter of this doctoral thesis, we compared the transcriptome of PBMCs samples of 25 individuals from the Basque Country classified as robust or frail based on TFI, TUG and GS tests individually. These scales are based on different conceptual approaches: TUG and GS, based on the measurement of functional activity and TFI, which considers an integral model of frailty [355], [356]. The first analysis, taking into account individual scales used for frailty analysis, revealed significant heterogeneity at molecular level. Therefore, our results extend to the biological level the heterogeneous clinical manifestations of frailty, which we have already observed in our population [357]. In order to be more accurate with the analysis of frailty, only those individuals classified as frail or robust by the 3 scales were selected and the comparative gene expression analysis was performed in 7 frail and 5 robust individuals. We identified 35 differentially expressed genes between robust and frail individuals. Among them, there were genes linked to inflammation and hypoxia-related pathways, immune response and apoptosis, results which are in line with previous studies that described alterations in inflammation, immunity and oxidative stress as the main biological processes associated with frailty status [120], [121], [141]. The expression of 14 candidate genes (based on the highest FC and p-value) was studied in samples of an extension of subjects from the original cohort [357], and we validated a statistically significant increase of *G0S2, EGR1, CXCL8*, and *GJB6* and a reduction of *NSF*, *DDX11L1* and *miR454* expressio by qRT-PCR.

These pattern of 7 differentially expressed genes was selected for further validations in 2 additional and independent cohorts. We observed, that the molecular pattern was replicated to some extent, in both cohorts. In particular *G0S2*, *EGR1* and *miR454* gene expression was replicated in both cohorts. In these cases, frailty was measured with Fried´s frailty phenotype or the FI. The differences between cohorts might be explained by the different origin of the samples (PBMCs or serum) and the scale used to measure frailty. However, given that Fried´s frailty phenotype and the FI are the most commonly used scales for screening frailty in humans [97] and that we observed differences in the expression of identified genes with them, the pattern of expression reported in our study can be considered to be associated with the multidimensionality of frailty and might be useful to detect frail individuals. In support of this, we detected elevated levels of *CXCL8* (also known as IL8), which have been observed in additional studies that considered both Fried´s frailty phenotype and FI [149], [358]. Additionally, omics studies in European and American cohorts revealed differences in expression of *miR454* and *EGR1* between robust and frail individuals [140], [141]. In the FRAILOMIC study, that assessed both frailty and disability in four large European cohorts, *miR454* was decreased in frail samples from Toledo Study for Healthy Aging (TSHA) cohort [140]. In the American study, higher levels of *EGR1* in a subset of frail individuals based on FRAIL scale were reported [141]. In this case, they found elevation of *EGR1* in black but decrease in white frail individuals of middle age. The age could be the cause of this difference, since their study was done on middle age samples and our study was performed on individuals over 75 years of age. These similarities reinforce the methodology of selecting only robust and frail individuals considering all the frailty scales employed and strengthen the results obtained in our study.

Next, we evaluated the expression of the selected genes in blood samples of frail subjects from 3 independent cohorts of individuals who underwent different types of interventions with physical activity during 12 weeks. Physical interventions were selected since it has been described that old adults that adopt a more active lifestyle and perform exercise training can prevent frailty, and delay dependency as well as other age-related diseases such as sarcopenia or AD [354], [359]. Thus, a recent study performed in old adults living in long-term nursing homes (LTNH), has shown a better handgrip strength, improvement of TUG, and a smaller number of falls after a multicomponent exercise program during 3 months [360]. Moreover, a study that analyzed the effects of multicomponent exercise program focused on strength, balance and walking recommendations during 6

months, appeared to be effective in preventing cardiorespiratory fitness decline in older adults living in long-term care settings [361]. Similar studies have shown improvements in physical performance, improvements in SPPB and GS [362], [363], a reduced Fried frailty score and maintenance of cognitive function [363], [364] after multicomponent interventions in LTNH residents. The first intervention was completed with physical training of moderate intensity and revealed an improvement of functional activity measured by TUG and SPPB performances and a decrease in the expression of *EGR1*. In the second intervention, frail individuals performed 3 different types of intervention plans (dual task, walking and multicomponent) whilst the third intervention included individuals who performed swimming exercises 3 times per week. The individuals completing the latest interventions exhibited a statistically significant reduction in Fried´s frailty phenotype together with a partial gene expression restoration, including decreased *EGR1* and *CXCL8* in both studies and lower *G0S2*, *GJB6* and higher *miR454* in the first one. These results indicate that different types of physical intervention plans can recover functional activity and revert the expression pattern observed in frail individuals. Notably, our study is the first one to combine the characterization of frail individuals through omic approach and validation in several cohorts as well as with different interventions.

We also characterized the expression of the 7 selected genes in different human primary cell types maintained for an extensive period of time in culture, which constitutes a well-established model for the study of cellular aging *in vitro* [333]. First, we found that advanced passage primary myoblasts presented a similar pattern of expression than frail individuals in 5 out of 7 candidate genes including elevation of *EGR1*, *GJB6* and reduction of *NSF*, *DDX11L1*, *miR454* expression. These results link the identified genes to muscle biology, a relevant component of physical frailty [68], [365], [366]. Additionally, fibroblasts maintained in culture for over 4 months revealed the same expression pattern observed in blood samples of frail individuals, including the elevation of *G0S2*, *EGR1*, *CXCL8* and *GJB6* levels and the reduction of *NSF*, *DDX11L1* and *miR454* expression. Altogether, our results suggest that these *in vitro* models resemble aspects of frailty, at least at molecular level, and link our transcriptomic data to muscle physiopathology. However, the use of these cell cultures is also a limitation of our work since even if they are well characterized models to study cellular activities and resemble several aspects of physiological aging, it is not known to what extent they are related to frailty.

The results of expression obtained in the different frailty cohorts, the reversion observed after different interventions plans and the replication of this pattern in cellular models, suggest that these genes could be potential biomarkers of frailty. In this sense, the discriminating and diagnostic potential of the 7 genes individually was checked and *EGR1* showed the best individual ROC curve. Moreover, protein levels of EGR1 were increased in serum samples of frail individuals measured by ELISA, a method that is applied in the clinic. Notably, using the information of this assay, EGR1 showed a strong predictive potential for the detection of frail individuals. However, it is now evident that efforts in the search of suitable frailty biomarkers should be directed to a panel of blood biomarkers rather than an assessment of individual molecules, since this would contribute to better reflect the accumulation of damage in frail individuals [367]. In this sense, we identified the expression of a minimum group of 3 genes (increased *EGR1* and reduced *DDX11L1* and *miR454*), that robustly predicted the presence of frailty and improved the predictive power of each gene individually. Additionally, this group of 3 genes was associated with clinical parameters related to frailty such as polypharmacy and multimorbidity. Taking into account these results and since other omic studies have already reported changes in *miR454* and *EGR1* levels in frail individuals [140], [141], we propose that *EGR1* alone or in combination with *DDX11L1* and *miR454* could be a good biomarker of frailty.

1.2. *miR454*, *DDX11L1* and *EGR1* are implicated in cell homeostasis and aging

We went further in understanding the impact of the pattern of 3 genes and we studied the cellular effects of modulating *miR454*, *DDX11L1* and *EGR1* expression in human primary fibroblasts. On the one hand, the overexpression of *miR454* promoted proliferation and reduced the accumulation of senescence markers, suggesting an anti-aging activity for this miRNA. On the other hand, knockdown experiments of *DDX11L1* resulted in impaired proliferation and enhanced senescence, results that are in line with the data in frail individuals and suggest that maintenance of high levels of *miR454* and *DDX11L1* are associated with cell and tissue homeostasis. The downregulation of *EGR1* reduced proliferation and promoted senescence, whereas overexpression assays showed opposite data, higher proliferation and lower levels of senescence. These results are not in line with the data in frail individuals but they are in agreement with other studies, where knockdown of this gene correlated with decreased proliferation and induction of apoptosis in different

cell types and contexts [368]–[370]. Moreover, *Egr1*-deficient mice displayed a reduced locomotor activity, an altered temperature regulation and a disturbed circadian clock regulation in the brain [371]. On the contrary, the deletion of Egr1 in a murine model of lung ischemia/reperfusion, diminished the expression of mediators of vascular injury, enhanced animal survival and organ function [372]. Consistent with this, our longevity assay using a model of *C. elegans* with knockdown of the ortholog of *EGR1* human gene (*egrh-1*) showed higher survival in the *egrh-1*-silenced model, reinforcing the role of *EGR1* in aging. Of note, *EGR1* is a transcription factor activated in response to a broad range of extracellular stimuli, which subsequently participates and modulates multiple cellular processes such as mitogen response, growth, proliferation, apoptosis or differentiation of several cell types and tissues [373], [374]. Moreover, it can affect directly or indirectly the expression of multiple signaling pathways and tumor suppressor genes such as *PTEN* or *P53* [373], [375]. Thus, its role in cell aging might be complex and depend on the choice of *EGR1* function and target genes, which are likely to be context-dependent. Our results indicate that these 3 genes are implicated in the maintenance of cellular homeostasis and the regulation of processes related to cellular aging, postulating them as genes involved in frailty physiopathology.

1.3. *miR454*, *DDX11L1* and *EGR1* are linked to senescence

We went deeper in the study of the function and potential downstream pathways of this trio of genes. Computational analysis revealed several predicted targets of *EGR1* such as *PTEN* and *C-JUN* that have been involved in relevant senescence pathways [338], and MAPKs and *AREG*, which have been linked to SASP [376]–[379], a process consisting in the secretion of several pro-inflammatory cytokines including IL6 [46]. Moreover, *EGR1* has an important role during the development in programmed senescence [41] and has been shown to be regulator of the ARF/p53/p21^{CIP1} signaling pathway in different contexts [380]–[382]. Similarly, previous bibliography revealed *p21^{CIP1}* and *TRIM3*, also involved in senescence, as downstream targets of *miR454* [383]. In addition, *DDX11L1* belongs to a transcript family located in sub-telomeric region which can modulate various processes of telomere activity [337], such as the control of the replicative capacity of cells and their entry into replicative senescence [384]. These results with the above described functional studies in cell cultures, suggest that *EGR1*, *DDX11L* and *miR454* could be associated with senescence related pathways. In line with this, we described that the expression of several of these downstream

targets and important senescence markers was elevated in frail individuals from different cohorts. In particular, *CD69* and *C-JUN* expression together with $p16^{INK4A}$ and $p21^{CIP1}$ protein levels were increased in PBMCs of frail individuals from the microarray and validation cohort 1. In addition, we detected higher levels of $p16^{INK4A}$, $p21^{CIP1}$ and *IL6* in the 2 additional cohorts of frail individuals. Consistent with these, it has been described that elevated expression of $p16^{INK4A}$ is associated with lower physical function measured by walk time, GS and grip strength [385]. Moreover, serum IL6 levels were negatively correlated with physical function, measured by GS test [386]. In addition, several studies where frailty was measured by Fried´s frailty phenotype or Rockwood frailty scale among others, have reported that higher serum levels of IL6 are associated with frailty status [387]–[390], reinfoircing the data observed in our cohorts. Notably, we tested the expression of senescence markers in individuals that underwent the different intervention plans and we observed a decreased expression of $p16^{INK4A}$, $p21^{CIP1}$ and *IL6* on them.

Senotherapy is a novel therapeutic strategy that selectively remove senescent cells, clear immune-mediated senescent cells, and neutralize the SASP [391], [392]. Remarkably, the pharmacological elimination of senescent cells have gained attention in the field of aging research, since the elimination of accumulated senescent cells has allowed to recover tissue function and restored tissue homeostasis, for instance of muscle, eye, kidney or adipose tissue, in aged mice [393], [394]. Combined treatment with Quercetin and Dasatinib, probably the most used and effective senolytics, improved the health and lifespan of aged mice [395] and reverted the accelerated or premature aging phenotype observed in Mytononic Distrophy type 1 (DM1) both, *in vitro* and *in vivo* [396]. Moreover, some studies have shown that Quercetin and Dasatinib are effective in elderly individuals and that their use alleviated physical dysfunction in patients with idiopathic pulmonary fibrosis [397] and decreased the senescent cell burden in individuals with chronic kidney disease [398]. With this information in mind and knowing that the genes of interest have been associated with senescence programs, we tested whether different senolytics could have any effect on their expression. Our results showed that the 3 tested senolytic compounds, Quercetin, Dasatinib and Navitoclax individually, eliminated senescent cells and restored the expression of the minimum trio of genes as well as the molecular pattern of 7 genes described in frail individuals. These data further support the identified link between frailty and senescence and postulate the interest and potential benefit of senotherapy for the treatment of frail individuals in the preclinical setting.

In summary, our results show that the minimum pattern of 3 genes regulates senescence-related downstream pathways, linking frailty and senescence programs. Additionally, our results allow us to speculate that the pattern of expression of the 3 genes could be associated with advanced stages of frailty since (i) at clinical level it is associated with processes that are more common in people of advanced age and poorer health and (ii) at molecular level it is associated with senescence.

2. Gene expression is altered in human hippocampus with age

Centenarians are an attractive population to unravel the mechanisms involved in human longevity and genes related to successful aging and maintenance of cognition. In this direction, several genes and molecular pathways have been associated to centenarians with majority of studies mostly performed on blood samples [399]. Notably, a study recently published used brain samples (specifically from cortex) of individuals divided in two groups of age (≤ 80 versus ≥ 85 years) and described a novel molecular mechanism related to brain aging and extended longevity [216]. Following the approach of using brain samples, in our study we performed transcriptomic analysis in hippocampus samples of human individuals of different ages, including young, elderly and centenarian individuals, from a cohort established in the Basque Country.

2.1. MTs are highly expressed in the hippocampus of centenarians

First, we compared the expression pattern of centenarians with young and elderly groups. The transcriptomic study revealed a differential gene expression pattern in centenarians compared to the other two groups and GO analysis showed heavy metal and Zn related pathways as highly enriched in centenarians. Among the differentially expressed genes, we identified Solute Carrier Family 39 Member 12 (*SLC39A12)* also known as *ZIP12*, which is a zinc transporter with an important role in nervous system development and in neurite extension of neuronal cells [400], [401], and that its mutations or lower levels have been associated with several brain-related diseases including schizophrenia [402], [403] and

autism [404]. Similarly, several members of the *MTs* family of genes were also highly expressed in the hippocampus of centenarians. MTs are a family of cysteine-rich proteins involved in the homeostasis and detoxification of heavy metals, specifically they bind divalent metals such as Zn and Cu [405], [406]. They are not limited to the homeostasis or detoxification of heavy metals and they have been described as having cytoprotective effects that promote cell survival and tissue regeneration [407]–[409]. Indeed, they have been also reported as anti-inflammatory and anti-oxidants with a role in the protection against oxidative stress, apoptosis and DNA damage [410]–[413]. In mammals, there are 4 isoforms (*MT1, MT2, MT3* and *MT4*), encoded by a group of closely related family of genes, which in humans are located on chromosome 16q13 [414], [415]. Different *MT1* subtypes have been described (A, B, E, F, G, H, M and X) which, together with *MT2A*, are found ubiquitously in a broad range of organs in contrast to *MT3* which is a brain-specific isoform expressed in the CNS, or *MT4* that is specifically expressed in the stratified squamous epithelia [216], [416], [417]. We confirmed the high expression of several *MT1* subtypes and *MTs* isoforms together with high protein levels of MT1 and MT3 in two independent cohorts. In addition, we detected higher *REST* levels, a gene that has been associated with cognition and successful aging, and linked to centenarian population in brain samples [216]; thus, validating our experimental and methodological models. We noted that such differential gene expression pattern could be a specific signature of the hippocampal neurogenic niche since their expression was enriched in the hippocampus and not altered in the cortex region of same individuals.

An European study focused on aging (MARK-AGE project), analyzed MTs induction after Zn treatment in PBMCs in centenarian's offspring and in individuals from general population showing that centenarian´s offspring displayed increased basal expression of some *MTs* and Zinc transporter 1 (*ZNT1*) genes in comparison to the general population but lower Zn-induced MTs [418]. In addition, *MTs* levels were found to be inversely related with oxidative stress markers [418]. Our results, together with these ones, indicate that centenarians and their offspring have a better control of Zn homeostasis that provides them protection against stress stimuli over the whole lifespan. The concentration of Zn needs to be tightly controlled since it plays an important role in cellular and molecular processes, enzymatic activity and regulation of transcription factors [419]. Of note, the concentration of Zn in the brain surpasses that of the body by ten-fold and it is essential for its normal functioning [420]. Indeed, in the brain, the majority of Zn tightly binds to macromolecules

such as proteins or amino acids and only 10 to 15 % exist as free Zn [419]. Thus, MTs, Zn transporters family (ZnTs), presenilins, and zinc-regulated and iron-regulated proteins (ZIPs) are responsible for the homeostasis of Zn in the brain [421], [422]. There is a link between Zn levels in the brain and cognitive function [423], and the decline in cognitive performance observed during aging or the apparition of neurodegenerative diseases such as AD, has been linked to the dysregulation of Zn homeostasis [421]. For instance, reduced zinc transporter-3 (ZnT3) expression or mutations of this gene, which has shown to be responsible for loading zinc into presynaptic vesicles in the hippocampus [424], have been associated to the onset of cognitive decline and accelerated brain aging, ultimately impairing learning and memory functions [424]–[427]. Additional metals to Zn such as iron and Cu, have been also involved in brain aging since they have been shown to trigger oxidative stress, accumulation of damaging molecules, DNA damage and neuroinflammation [428], [429].

The impact of MTs in the brain aging process has been further described in mouse models. Thus, a study performed in *Mt1*/*Mt2*-null mice reported that *MTs* are also important in learning and memory, since mice with deletions of *MTs* showed a poorer rate of learning during the training period on a maze and less choice accuracy than the parental strain [430]. Additionally, a study performed in *Mt1*, *Mt2* or *Mt3*-null mice models described that MTs have a role in CNS homeostasis since they are induced in the aging brain as a defensive mechanism to attenuate oxidative stress, ROS production and inflammation [431], [432]. Indeed, after damage caused by a focal cryolesion in the cortex, mice with deletions of *MTs* showed increased oxidative stress, apoptosis, astrogliosis and secretion of several inflammatory cytokines including TNFα, IL1α, IL6 [431]. Moreover, the protective role of high levels of MTs in aging and longevity has been documented in different animal models [433]. Thus, several studies have indicated that high levels of MTs prevent diabetic complications [434], attenuate cardiac dysfunction [435], protect against organ damages during inflammation [436] and against DNA and lipid metabolic damages [437], which are common age-related disorders. Regarding longevity, Mt1-overexpressing mice model displayed increased lifespan [438]. Consistently, cardiac-specific MT transgenic mice, also presented increased longevity together with an attenuation of oxidative stress [439]. Moreover, in *C. elegans*, increased expression of *MTs* (*CeMT-1* and *CeMT-2*) promoted extension of lifespan in insulin receptor-like protein (daf-2) mutant model [440]. By contrast, *Mt1* and *Mt2* knockout mice displayed shorter lifespan than wild type mice [441]. The link between MTs

and longevity has been extended to humans and a study performed in Italian centenarian females showed that a specific SNP corresponding to an Adenine/Cytosine (Asparagine/Threonine) transition at +647 nucleotide position in the *MT1A* coding region is associated with longevity since it was present in nonagenarian and centenarian females [442]. In addition, it was associated with lower inflammatory status since lower levels of circulating IL6 in plasma of these individuals was observed [442].

2.2. MTs are mainly expressed by astrocytes and participate in their viability and activity

We went further in the characterization of the expression and function of MTs in the brain. First, we studied their expression in different brain cell types performing co-staining studies of MT1 and MT3 with markers of specific cell types of the brain. We found that MTs were expressed mainly by astrocytes, since MT1 and MT3 positive cells were also positive for GFAP and S100β astrocytic markers. On the contrary, they did not colocalize with the neuronal markers MAP2 or TUJ1, and their expression was not enriched in isolated microglia. These IF results were completed with publicly available datasets from single cell RNAseq (The Human Protein Atlas, http://www.proteinatlas.org) [443], which showed that *MTs* were mainly expressed by astrocytes. Astrocytes, are the cells involved in the response to stress signals or inflammation in the CNS [305]. In particular, physiological aging triggers astrocyte activation in order to respond to stress signals and astrocyte dysfunction contribute to cognitive decline in aging [276]. Then, in order to unravel the possible role that *MTs* could have in astrocytes, we studied their expression in serial passage-cultured NHA and we performed different functional experiments in NHA with modulation of *MTs*. We found that late passage cultured NHA presented lower levels of *MTs* and that silencing of *MT1* or *MT3* in NHA, resulted in (i) decreased proliferation and (ii) increased apoptosis and senescence, indicating that *MTs* are involved in astrocyte cell viability and activity. These results are in agreement with other studies performed in mice models where the upregulation of *Mt3* in glial cells provided neuroprotective effect after brain damage acting as a growth inhibitory factor [444]. Moreover, studies performed in *Mt1/Mt2*-transgenic mice, have shown that both *Mt1* and *Mt2* are expressed in response to brain damage and protect the CNS [430]. In addition, mice overexpressing *Mt1* were protected against mild focal cerebral ischemia, showing lower infarcts and better functional recovery than the controls [445] and the opposite was observed in *Mt1*/*Mt2*-null mice [446]. Following these results, MTs deficiency

increases oxidative stress and cell death, worsening recovery in traumatic injuries or in neurodegenerative pathologies [447]–[450]. For instance, the downregulation of *MT3* has been associated with AD, since silencing of *MT3* in cortical astrocytes reduced amyloid beta uptake and contributed to its accumulation [451].

Our results also showed that *MT1* or *MT3* silencing induced an increase in the expression of inflammatory genes such as *TNFα, IL1α, STAT3* and *C3*, all of them linked with reactive phenotype of neuroinflammatory astrocytes [276]. Consistent with our data, additional studies have shown that MTs regulates the expression of inflammatory factors mainly cytokines such as IL6, TNFα and interferons in the brain of mice [452], [453]. On the other hand, transgenic mice expressing high IL6 or TNFα in astrocytes, exhibited a specific phenotype of cytokine-induced damage which increased Mt1 and Mt2 expresion in response to the damage [454]–[456]. Reactive astrocytes are astrocytes that are "activated" in response to various physiological and pathological states that causes their morphological, molecular, and functional remodeling, that along with cellular proliferation give rise to astrogliosis [457], [458]. In this state, astrocytes are also a source of inflammatory factors that cooperate with microglia, proliferate and increase their number in the affected region [459], [460]. Recently, a preliminary division of activated astroglia into two subtypes has been proposed, based on their structure, proliferative state, the types of cells they interact with, and the tissue architecture to which they contribute [461], [462]. Astroglia polarized towards A1 phenotype are considered as cytotoxic or inflammatory and may lead to cellular damage, an issue that appears often in the context of neurodegenerative diseases. On the other hand, the phenotype leading to A2 polarization (protective) is related to the promotion of synaptic formation, growth of neurites and production of anti-inflammatory factors [351], [462]. A recent single cell RNAseq study in mice has associated high levels of *Mt1* and *Mt2* with an inflammatory phenotype of hippocampal astrocytes [463]. Indeed, the promoters of *MTs* show a wide presence of response elements to different factors such as antioxidant response element (ARE), metals (MRE) as well as elements of response to cytokines, including IL6, and binding sites for different transcription factors [131]. Future studies would be necessary to identify whether MTs participate in A1 or A2 polarization; however, our results suggest that MTs could have a role in the polarization of astrocytes towards a protective phenotype.

Apart from the study of the differentially expressed genes between centenarians and the other 2 groups, we completed an analysis comparing young and elderly groups that

revealed a subset of genes that were differentially expressed in the elderly. They were involved in pathways related to DNA repair, metabolism, development, synaptic signaling, ion transport, hormone regulation, protein secretion and autophagy, all of them previously associated with aging [25].

As a summary, we detected high levels of MTs in the hippocampus of centenarian individuals. Moreover, MTs are expressed in astrocytes, where we confirmed that they have a role in their viability and activity. Our results, together with the previously published information, suggests that MTs could respond to stress situations and provide protection in the aging brain. Therefore, maintenance of their high levels could be a potential anti-aging strategy.

2.3. The expression of 6 genes correlates with chronological aging in human hippocampus

We performed an additional bioinformatic analysis to unravel the molecular mechanisms that are associated with chronological aging. This analysis revealed changes in the expression of 6 genes. In particular *SMPD4*, *RASGEF1B* and *ANKRD18B* correlated positively with aging whilst the expression of *RAD23B*, *HYOU1* and *OR2A42* showed a decline in human hippocamus with age. *SMPD4* has a role in the homeostasis of membrane sphingolipids, thereby influencing membrane integrity, and ER organization and function [464]. In skeletal muscle, it mediates TNF-stimulated oxidant production and diseases associated with *SMPD4* include neurodevelopmental disorders [465]. *RASGEF1B* is a toll-like receptor-inducible Ras guanine-nucleotide exchange factor that has been associated with cancer, proliferation and inflammation pathways [466], and *ANKRD18B* has been linked fundamentally with lung cancer progression [467]. Moreover, the protein encoded by *HYOU1* is involved in protein folding and secretion in the endoplasmic reticulum [468]. Its expression is up-regulated in many diseases, including different types of cancer, endoplasmic reticulum stress-related diseases or under hypoxic conditions but the suppression is associated with apoptosis. However, little is known regarding their activity in the brain and during aging. In this regard, the alteration in the expression of the 6 genes was confirmed in both human primary fibroblasts and NHA maintained in culture. Thus, we detected higher levels of *SMPD4*, *RASGEF1B* and *ANKRD18B* whereas decreased expression of *RAD23B*, *HYOU1* and

OR2A42 in "aged" cells *in vitro*. We further addressed this issue and taking advantage of omics studies in several publicly available datasets, we detected that the expression pattern of these 6 genes was variable among the different organs and tissues of the body and that they were expressed in the human brain to a greater or lesser extent. Specifically, *SMPD4*, *RASGEF1B* and *ANKRD18B* were expressed mainly in the forebrain and the neocortex whereas *RAD23B* and *HYOU1* were expressed in the hippocampus. Accordingly, *Rad23b* and *Hyou1* showed to be expressed in the DG of mice. In addition, we observed that the expression of the 6 genes presented a homogeneous expression pattern between the different cell types of the brain. Although future experiments should be done in order to study their activity in detail, our results revealed a novel link of these genes with the biological process of aging.

2.4. RAD23B expression correlates negatively with physiological and pathological aging in human hippocampus

Among the candidate genes, the most promising one could be *RAD23B* since it showed the strongest differences at statistical level both in human and mice. This gene is involved in DNA damage repair, specifically in nucleotide excision repair (NER), a multistep process that corrects DNA alterations from endogenous oxidative stress or single-strand breaks, among others [469]. Indeed, the accumulation of DNA damage is one of the well-known hallmarks of aging [25] and it is particularly prevalent in the CNS, owing to the low DNA repair capacity in postmitotic brain tissue [470]. In addition to his role in DNA damage recognition, *RAD23B* also has an important function in protein degradation (it binds ubiquitinated substrates and the proteasome) [471] and in cell cycle control [352], which are also relevant processes in aging [25]. Notably, IHC and IF revealed that RAD23B protein levels were also lower in hippocampal neurogenic niche of aged individuals with physiological aging. In addition, our data indentified that RAD23B protein expression was even lower or totally absent in patients with AD in comparison with old or young samples, indicating that it could be a negative marker of physiological or pathological aging. Consistent with this, it has been detected that RAD23B protein inclusions are found predominantly in cortices (frontal, temporal and motor), spinal cord and hippocampal DG in a number of neurodegenerative diseases, including frontotemporal dementia, Huntington's disease, spinocerebellar ataxia type 3 and 7, fragile X associated tremor/ataxia syndrome and Parkinson's disease [472],

[473]. Our results further reinforce the link between DNA repair pathways and brain aging. In this sense, an impaired transcription of critical neural genes, a loss of neurons by apoptosis or defective neurogenesis have been proposed as a link from decreased DNA repair and persistent DNA damage to neurodegeneration [474], [475]. Moreover, different neurodegenerative diseases have been associated with deficits in DNA repair mechanisms [476]. In particular, mutations in DNA repair genes such as *BRCA1*, *ATM* or *RAD51*, have been reported in neurodegenerative diseases such as AD [477].

Following the strategy carried out in the study of MTs and given the relevance of astrocytes as a protective cell type in the brain, we studied the possible role of RAD23B and the effects of the downregulation of this gene in astrocytes. *RAD23B* silencing caused a reduction of cell growth and an increase in apoptosis and senescence, indicating that *RAD23B* could be involved in astrocyte viability and activity. Previous studies have described that DNA damage can give rise to genomic instability and induce signaling cascades leading to cell death, senescence or secretion of inflammatory cytokines, which are cellular phenotypes associated with aging [478], [479]. Additionally, elevations of the well-established marker of DNA damage gamma-H2A histone family member X (γH2AX), have also been observed in astrocytes of hippocampus and cerebral cortex of patients with AD [480], together with changes in astrocyte function [481].

In summary, our results identify a novel pattern of expression associated to chronological brain aging. In addition, we reveal a significant decrease in the expression of RAD23B in the hippocampal neurogenic niche with physiological aging that is exacerbated in AD pathology. We also completed *in vitro* studies that suggest that *RAD23B* is necessary for astrocyte viability and activity. Thus, *RAD23B* could be a good target in order to enhance DNA repair that is usually decreased during aging and it will be interesting to determine whether its restoration in the brain could have beneficial effects in physiological or pathological aging.

Conclusions

1. Whole-transcriptome analysis revealed 35 genes differentially expressed associated with frailty status. 7 genes were validated in frail individuals from 3 independent cohorts.

2. The expression of the molecular pattern associated to frailty is restored after 3 independent physical interventions together with a reversion of the frailty phenotype.

3. Maintenance of human primary myoblasts and fibroblasts *in vitro* promotes a similar pattern of expression than frail individuals.

4. A reduced pattern of 3 genes (increased *EGR1* and lower *DDX11L1* and *miR454*), correlates robustly with frailty and with clinical characteristics associated to frailty such comorbidity and polypharmacy. They represent the most promising biomarkers of frailty.

5. *miR454*, *DDX11L1* and *EGR1* are implicated in cell aging and are associated with senescence-related pathways, revealing a link between senescence and frailty. The treatment of senescent cells with senolytic compounds restores the molecular pattern identified in frailty.

6. Transcriptomic study revealed a differential gene expression pattern in the hippocampus of centenarians, characterized by high levels of metallothioneins (*MTs*) family of genes.

7. MTs are mainly expressed by astrocytes and participate in their viability and activity.

8. Transcriptome analysis identified a subset of genes differentially expressed between young and elderly individuals, involved in pathways already associated with aging such as DNA repair, metabolism, development, synaptic signaling, ion transport, hormone regulation, protein secretion and autophagy.

9. Additional computational biology analysis revealed a pattern of 6 genes correlated with chronological aging in human hippocampus. *SMPD4*, *RASGEF1B* and *ANKRD18B*

correlated positively with age whilst the expression of *RAD23B*, *HYOU1* and *OR2A42* was decreased.

10. The expression of RAD23B correlates negatively with physiological and pathological aging, and plays a role in astrocyte activity. It represents the most promising biomarker of brain aging.

References

[1] N. K. Isaev, E. v. Stelmashook, and E. E. Genrikhs, “Neurogenesis and brain aging,” Rev Neurosci, vol. 30, no. 6, pp. 573–580, Aug. 2019, doi: 10.1515/REVNEURO-2018-0084.

[2] C. López-Otín, M. A. Blasco, L. Partridge, M. Serrano, and G. Kroemer, “The hallmarks of aging,” Cell, vol. 153, no. 6, p. 1194, Jun. 2013, doi: 10.1016/J.CELL.2013.05.039.

[3] J. R. Beard, A. M. Officer, and A. K. Cassels, “The World Report on Ageing and Health,” Gerontologist, vol. 56 Suppl 2, pp. S163–S166, Apr. 2016, doi: 10.1093/GERONT/GNW037.

[4] J. R. Beard et al., “The World report on ageing and health: a policy framework for healthy ageing,” Lancet, vol. 387, no. 10033, pp. 2145–2154, May 2016, doi: 10.1016/S0140-6736(15)00516-4.

[5] J. Oeppen and J. W. Vaupel, “Demography. Broken limits to life expectancy,” Science, vol. 296, no. 5570, pp. 1029–1031, May 2002, doi: 10.1126/SCIENCE.1069675.

[6] X. Dong, B. Milholland, and J. Vijg, “Evidence for a limit to human lifespan,” Nature, vol. 538, no. 7624, pp. 257–259, 2016, doi: 10.1038/NATURE19793.

[7] Eurostat, “People in the EU - statistics on an ageing society ,” 2022.

[8] L. Partridge, J. Deelen, and P. E. Slagboom, “Facing up to the global challenges of ageing,” Nature, vol. 561, no. 7721, pp. 45–56, Sep. 2018, doi: 10.1038/S41586-018-0457-8.

[9] N. A. Bishop, T. Lu, and B. A. Yankner, “Neural mechanisms of ageing and cognitive decline,” Nature, vol. 464, no. 7288, pp. 529–535, Mar. 2010, doi: 10.1038/NATURE08983.

[10] R. A. Kohanski et al., “Reverse geroscience: how does exposure to early diseases accelerate the age-related decline in health?,” Ann N Y Acad Sci, vol. 1386, no. 1, pp. 30–44, Dec. 2016, doi: 10.1111/NYAS.13297.

[11] S. J. McLaughlin, A. M. Jette, and C. M. Connell, “An examination of healthy aging across a conceptual continuum: prevalence estimates, demographic patterns, and validity,” J Gerontol A Biol Sci Med Sci, vol. 67, no. 7, pp. 783–789, Jun. 2012, doi: 10.1093/GERONA/GLR234.

[12] D. R. Seals, J. N. Justice, and T. J. Larocca, “Physiological geroscience: targeting function to increase healthspan and achieve optimal longevity,” J Physiol, vol. 594, no. 8, pp. 2001–2024, Apr. 2016, doi: 10.1113/JPHYSIOL.2014.282665.

[13] J. P. Michel, C. Graf, and F. Ecarnot, “Individual healthy aging indices, measurements and scores,” Aging Clin Exp Res, vol. 31, no. 12, pp. 1719–1725, Dec. 2019, doi: 10.1007/S40520-019-01327-Y.

[14] S. M. A. Juan and P. A. Adlard, “Ageing and Cognition,” Subcell Biochem, vol. 91, pp. 107–122, 2019, doi: 10.1007/978-981-13-3681-2_5.

[15] G. v. Mkrtchyan et al., “ARDD 2020: from aging mechanisms to interventions,” Aging, vol. 12, no. 24, pp. 24486–24503, Dec. 2020, doi: 10.18632/AGING.202454.

[16] C. López-Otín, L. Galluzzi, J. M. P. Freije, F. Madeo, and G. Kroemer, “Metabolic Control of Longevity,” Cell, vol. 166, no. 4, pp. 802–821, Aug. 2016, doi: 10.1016/J.CELL.2016.07.031.

[17] C. López-Otín and G. Kroemer, “Hallmarks of Health,” Cell, vol. 184, no. 1, pp. 33–63, Jan. 2021, doi: 10.1016/J.CELL.2020.11.034.

[18] L. M. DeVito et al., “Extending human healthspan and longevity: a symposium report,” Ann N Y Acad Sci, vol. 1507, no. 1, pp. 70–83, Jan. 2022, doi: 10.1111/NYAS.14681.

[19] J. B. Burch et al., "Advances in geroscience: impact on healthspan and chronic disease," J Gerontol A Biol Sci Med Sci, vol. 69 Suppl 1, no. Suppl 1, 2014, doi: 10.1093/GERONA/GLU041.

[20] B. K. Kennedy et al., "Geroscience: linking aging to chronic disease," Cell, vol. 159, no. 4, pp. 709–713, Nov. 2014, doi: 10.1016/J.CELL.2014.10.039.

[21] D. R. Seals and S. Melov, "Translational geroscience: emphasizing function to achieve optimal longevity," Aging, vol. 6, no. 9, pp. 718–730, 2014, doi: 10.18632/AGING.100694.

[22] J. R. Beard and D. E. Bloom, "Towards a comprehensive public health response to population ageing," Lancet, vol. 385, no. 9968, pp. 658–661, Feb. 2015, doi: 10.1016/S0140-6736(14)61461-6.

[23] P. J. Barnes, "Mechanisms of development of multimorbidity in the elderly," Eur Respir J, vol. 45, no. 3, pp. 790–806, Mar. 2015, doi: 10.1183/09031936.00229714.

[24] I. J. Deary et al., "Age-associated cognitive decline," Br Med Bull, vol. 92, no. 1, pp. 135–152, Jan. 2009, doi: 10.1093/BMB/LDP033.

[25] C. López-Otín, M. A. Blasco, L. Partridge, M. Serrano, and G. Kroemer, "Hallmarks of aging: An expanding universe," Cell, Dec. 2022, doi: 10.1016/J.CELL.2022.11.001.

[26] T. B. L. Kirkwood, "Understanding the odd science of aging," Cell, vol. 120, no. 4, pp. 437–447, Feb. 2005, doi: 10.1016/J.CELL.2005.01.027.

[27] A. A. Moskalev et al., "The role of DNA damage and repair in aging through the prism of Koch-like criteria," Ageing Res Rev, vol. 12, no. 2, pp. 661–684, Mar. 2013, doi: 10.1016/J.ARR.2012.02.001.

[28] S. Frenk and J. Houseley, "Gene expression hallmarks of cellular ageing," Biogerontology, vol. 19, no. 6, pp. 547–566, Dec. 2018, doi: 10.1007/S10522-018-9750-Z.

[29] J. P. de Magalhães, J. Curado, and G. M. Church, "Meta-analysis of age-related gene expression profiles identifies common signatures of aging," Bioinformatics, vol. 25, no. 7, pp. 875–881, 2009, doi: 10.1093/BIOINFORMATICS/BTP073.

[30] A. Brunet and S. L. Berger, "Epigenetics of aging and aging-related disease," J Gerontol A Biol Sci Med Sci, vol. 69 Suppl 1, no. Suppl 1, 2014, doi: 10.1093/GERONA/GLU042.

[31] S. Horvath and K. Raj, "DNA methylation-based biomarkers and the epigenetic clock theory of ageing," Nat Rev Genet, vol. 19, no. 6, pp. 371–384, Jun. 2018, doi: 10.1038/S41576-018-0004-3.

[32] H. J. Jung and Y. Suh, "Circulating miRNAs in ageing and ageing-related diseases," J Genet Genomics, vol. 41, no. 9, pp. 465–472, Sep. 2014, doi: 10.1016/J.JGG.2014.07.003.

[33] T. Smith-Vikos et al., "A serum miRNA profile of human longevity: findings from the Baltimore Longitudinal Study of Aging (BLSA)," Aging, vol. 8, no. 11, pp. 2971–2987, 2016, doi: 10.18632/AGING.101106.

[34] C. López-Otín, F. Pietrocola, D. Roiz-Valle, L. Galluzzi, and G. Kroemer, "Meta-hallmarks of aging and cancer," Cell Metab, vol. 35, no. 1, pp. 12–35, Jan. 2023, doi: 10.1016/J.CMET.2022.11.001.

[35] J. Campisi and F. D'Adda Di Fagagna, "Cellular senescence: when bad things happen to good cells," Nat Rev Mol Cell Biol, vol. 8, no. 9, pp. 729–740, Sep. 2007, doi: 10.1038/NRM2233.

[36] F. Rodier and J. Campisi, “Four faces of cellular senescence,” J Cell Biol, vol. 192, no. 4, pp. 547–556, Feb. 2011, doi: 10.1083/JCB.201009094.

[37] L. Hayflick and P. S. Moorhead, “The serial cultivation of human diploid cell strains,” Exp Cell Res, vol. 25, no. 3, pp. 585–621, 1961, doi: 10.1016/0014-4827(61)90192-6.

[38] J. M. van Deursen, “The role of senescent cells in ageing,” Nature, vol. 509, no. 7501, pp. 439–446, 2014, doi: 10.1038/NATURE13193.

[39] A. Calcinotto, J. Kohli, E. Zagato, L. Pellegrini, M. Demaria, and A. Alimonti, “Cellular Senescence: Aging, Cancer, and Injury,” Physiol Rev, vol. 99, no. 2, pp. 1047–1078, Apr. 2019, doi: 10.1152/PHYSREV.00020.2018.

[40] E. Carrasco-Garcia, M. Moreno, L. Moreno-Cugnon, and A. Matheu, “Increased Arf/p53 activity in stem cells, aging and cancer,” Aging Cell, vol. 16, no. 2, pp. 219–225, Apr. 2017, doi: 10.1111/ACEL.12574.

[41] D. Muñoz-Espín and M. Serrano, “Cellular senescence: from physiology to pathology,” Nat Rev Mol Cell Biol, vol. 15, no. 7, pp. 482–496, 2014, doi: 10.1038/NRM3823.

[42] D. McHugh and J. Gil, “Senescence and aging: Causes, consequences, and therapeutic avenues,” J Cell Biol, vol. 217, no. 1, pp. 65–77, Jan. 2018, doi: 10.1083/JCB.201708092.

[43] B. Y. Lee et al., “Senescence-associated beta-galactosidase is lysosomal beta-galactosidase,” Aging Cell, vol. 5, no. 2, pp. 187–195, Apr. 2006, doi: 10.1111/J.1474-9726.2006.00199.X.

[44] A. Hernandez-Segura, J. Nehme, and M. Demaria, “Hallmarks of Cellular Senescence,” Trends Cell Biol, vol. 28, no. 6, pp. 436–453, Jun. 2018, doi: 10.1016/J.TCB.2018.02.001.

[45] S. Lopes-Paciencia, E. Saint-Germain, M. C. Rowell, A. F. Ruiz, P. Kalegari, and G. Ferbeyre, “The senescence-associated secretory phenotype and its regulation,” Cytokine, vol. 117, pp. 15–22, May 2019, doi: 10.1016/J.CYTO.2019.01.013.

[46] J. P. Coppé et al., “Senescence-associated secretory phenotypes reveal cell-nonautonomous functions of oncogenic RAS and the p53 tumor suppressor,” PLoS Biol, vol. 6, no. 12, 2008, doi: 10.1371/JOURNAL.PBIO.0060301.

[47] T. Kuilman et al., “Oncogene-induced senescence relayed by an interleukin-dependent inflammatory network,” Cell, vol. 133, no. 6, pp. 1019–1031, Jun. 2008, doi: 10.1016/J.CELL.2008.03.039.

[48] J. C. Acosta et al., “A complex secretory program orchestrated by the inflammasome controls paracrine senescence,” Nat Cell Biol, vol. 15, no. 8, pp. 978–990, Aug. 2013, doi: 10.1038/NCB2784.

[49] G. Nelson et al., “A senescent cell bystander effect: senescence-induced senescence,” Aging Cell, vol. 11, no. 2, pp. 345–349, Apr. 2012, doi: 10.1111/J.1474-9726.2012.00795.X.

[50] N. Herranz and J. Gil, “Mechanisms and functions of cellular senescence,” J Clin Invest, vol. 128, no. 4, pp. 1238–1246, Apr. 2018, doi: 10.1172/JCI95148.

[51] M. B. Schultz and D. A. Sinclair, “When stem cells grow old: phenotypes and mechanisms of stem cell aging,” Development, vol. 143, no. 1, pp. 3–14, Jan. 2016, doi: 10.1242/DEV.130633.

[52] J. Wu and J. C. Izpisua Belmonte, “Stem Cells: A Renaissance in Human Biology Research,” Cell, vol. 165, no. 7, pp. 1572–1585, Jun. 2016, doi: 10.1016/J.CELL.2016.05.043.

[53] K. Mohammad, P. Dakik, Y. Medkour, D. Mitrofanova, and V. I. Titorenko, "Quiescence Entry, Maintenance, and Exit in Adult Stem Cells," Int J Mol Sci, vol. 20, no. 9, May 2019, doi: 10.3390/IJMS20092158.

[54] S. Tümpel and K. L. Rudolph, "Quiescence: Good and Bad of Stem Cell Aging," Trends Cell Biol, vol. 29, no. 8, pp. 672–685, Aug. 2019, doi: 10.1016/J.TCB.2019.05.002.

[55] R. Ren, A. Ocampo, G. H. Liu, and J. C. Izpisua Belmonte, "Regulation of Stem Cell Aging by Metabolism and Epigenetics," Cell Metab, vol. 26, no. 3, pp. 460–474, Sep. 2017, doi: 10.1016/J.CMET.2017.07.019.

[56] J. R. Aunan, M. M. Watson, H. R. Hagland, and K. Søreide, "Molecular and biological hallmarks of ageing," Br J Surg, vol. 103, no. 2, pp. e29–e46, Jan. 2016, doi: 10.1002/BJS.10053.

[57] C. Franceschi et al., "Inflamm-aging. An evolutionary perspective on immunosenescence," Ann N Y Acad Sci, vol. 908, pp. 244–254, 2000, doi: 10.1111/J.1749-6632.2000.TB06651.X.

[58] D. Monti, R. Ostan, V. Borelli, G. Castellani, and C. Franceschi, "Inflammaging and human longevity in the omics era," Mech Ageing Dev, vol. 165, no. Pt B, pp. 129–138, Jul. 2017, doi: 10.1016/J.MAD.2016.12.008.

[59] C. Franceschi and J. Campisi, "Chronic inflammation (inflammaging) and its potential contribution to age-associated diseases," J Gerontol A Biol Sci Med Sci, vol. 69 Suppl 1, pp. S4–S9, Jun. 2014, doi: 10.1093/GERONA/GLU057.

[60] P. L. Minciullo et al., "Inflammaging and Anti-Inflammaging: The Role of Cytokines in Extreme Longevity," Arch Immunol Ther Exp (Warsz), vol. 64, no. 2, pp. 111–126, Apr. 2016, doi: 10.1007/S00005-015-0377-3.

[61] M. Puzianowska-Kuźnicka et al., "Interleukin-6 and C-reactive protein, successful aging, and mortality: the PolSenior study," Immun Ageing, vol. 13, no. 1, Jun. 2016, doi: 10.1186/S12979-016-0076-X.

[62] M. Michaud et al., "Proinflammatory cytokines, aging, and age-related diseases," J Am Med Dir Assoc, vol. 14, no. 12, pp. 877–882, 2013, doi: 10.1016/J.JAMDA.2013.05.009.

[63] A. Wikby et al., "The immune risk phenotype is associated with IL-6 in the terminal decline stage: findings from the Swedish NONA immune longitudinal study of very late life functioning," Mech Ageing Dev, vol. 127, no. 8, pp. 695–704, Aug. 2006, doi: 10.1016/J.MAD.2006.04.003.

[64] S. Giovannini et al., "Interleukin-6, C-reactive protein, and tumor necrosis factor-alpha as predictors of mortality in frail, community-living elderly individuals," J Am Geriatr Soc, vol. 59, no. 9, pp. 1679–1685, Sep. 2011, doi: 10.1111/J.1532-5415.2011.03570.X.

[65] J. N. Justice et al., "A framework for selection of blood-based biomarkers for geroscience-guided clinical trials: report from the TAME Biomarkers Workgroup," Geroscience, vol. 40, no. 5–6, pp. 419–436, Dec. 2018, doi: 10.1007/S11357-018-0042-Y.

[66] L. P. Fried et al., "Frailty in older adults: evidence for a phenotype," J Gerontol A Biol Sci Med Sci, vol. 56, no. 3, 2001, doi: 10.1093/GERONA/56.3.M146.

[67] A. Clegg, J. Young, S. Iliffe, M. O. Rikkert, and K. Rockwood, "Frailty in elderly people," Lancet, vol. 381, no. 9868, pp. 752–762, 2013, doi: 10.1016/S0140-6736(12)62167-9.

[68] J. E. Morley et al., "Frailty consensus: a call to action," J Am Med Dir Assoc, vol. 14, no. 6, pp. 392–397, 2013, doi: 10.1016/J.JAMDA.2013.03.022.

[69] L. Rodríguez-Mañas et al., “Searching for an operational definition of frailty: a Delphi method based consensus statement: the frailty operative definition-consensus conference project,” J Gerontol A Biol Sci Med Sci, vol. 68, no. 1, pp. 62–67, Jan. 2013, doi: 10.1093/GERONA/GLS119.

[70] L. Rodriguez Manas, “Determinants of Frailty and Longevity: Are They the Same Ones?,” Nestle Nutr Inst Workshop Ser, vol. 83, pp. 29–39, 2015, doi: 10.1159/000382057.

[71] M. Ruiz, C. Cefalu, and T. Reske, “Frailty syndrome in geriatric medicine,” Am J Med Sci, vol. 344, no. 5, pp. 395–398, 2012, doi: 10.1097/MAJ.0B013E318256C6AA.

[72] WHO, “World report on ageing and health. Geneva, Switzerland: World Health Organization.,” 2015.

[73] L. Rodriguez-Mañas and L. P. Fried, “Frailty in the clinical scenario,” Lancet, vol. 385, no. 9968, pp. e7–e9, Feb. 2015, doi: 10.1016/S0140-6736(14)61595-6.

[74] R. Varadhan, J. D. Walston, and K. Bandeen-Roche, “Can a Link Be Found Between Physical Resilience and Frailty in Older Adults by Studying Dynamical Systems?,” J Am Geriatr Soc, vol. 66, no. 8, pp. 1455–1458, Aug. 2018, doi: 10.1111/JGS.15409.

[75] B. Santos-Eggimann, P. Cuénoud, J. Spagnoli, and J. Junod, “Prevalence of frailty in middle-aged and older community-dwelling Europeans living in 10 countries,” J Gerontol A Biol Sci Med Sci, vol. 64, no. 6, pp. 675–681, Jun. 2009, doi: 10.1093/GERONA/GLP012.

[76] R. M. Collard, H. Boter, R. A. Schoevers, and R. C. Oude Voshaar, “Prevalence of frailty in community-dwelling older persons: a systematic review,” J Am Geriatr Soc, vol. 60, no. 8, pp. 1487–1492, Aug. 2012, doi: 10.1111/J.1532-5415.2012.04054.X.

[77] Q. L. Xue, “The frailty syndrome: definition and natural history,” Clin Geriatr Med, vol. 27, no. 1, pp. 1–15, Feb. 2011, doi: 10.1016/J.CGER.2010.08.009.

[78] F. Rodríguez-Artalejo and L. Rodríguez-Mañas, “The frailty syndrome in the public health agenda,” J Epidemiol Community Health (1978), vol. 68, no. 8, pp. 703–704, 2014, doi: 10.1136/JECH-2014-203863.

[79] M. Cesari et al., “Frailty: An Emerging Public Health Priority,” J Am Med Dir Assoc, vol. 17, no. 3, pp. 188–192, Mar. 2016, doi: 10.1016/J.JAMDA.2015.12.016.

[80] WHO, “World report on ageing and health. Geneva, Switzerland: World Health Organization.,” 2021.

[81] M. Cesari et al., “Evidence for the Domains Supporting the Construct of Intrinsic Capacity,” J Gerontol A Biol Sci Med Sci, vol. 73, no. 12, pp. 1653–1660, Nov. 2018, doi: 10.1093/GERONA/GLY011.

[82] O. Theou et al., “The effectiveness of exercise interventions for the management of frailty: a systematic review,” J Aging Res, vol. 2011, 2011, doi: 10.4061/2011/569194.

[83] M. T. E. Puts et al., “Interventions to prevent or reduce the level of frailty in community-dwelling older adults: a scoping review of the literature and international policies,” Age Ageing, vol. 46, no. 3, pp. 383–392, May 2017, doi: 10.1093/AGEING/AFW247.

[84] E. L. Cadore, L. Rodríguez-Mañas, A. Sinclair, and M. Izquierdo, “Effects of different exercise interventions on risk of falls, gait ability, and balance in physically frail older adults: a systematic review,” Rejuvenation Res, vol. 16, no. 2, pp. 105–114, Apr. 2013, doi: 10.1089/REJ.2012.1397.

[85] T. J. Hsieh et al., "Individualized home-based exercise and nutrition interventions improve frailty in older adults: a randomized controlled trial," Int J Behav Nutr Phys Act, vol. 16, no. 1, Dec. 2019, doi: 10.1186/S12966-019-0855-9.

[86] T. Ngandu et al., "A 2 year multidomain intervention of diet, exercise, cognitive training, and vascular risk monitoring versus control to prevent cognitive decline in at-risk elderly people (FINGER): a randomised controlled trial," Lancet, vol. 385, no. 9984, pp. 2255–2263, Jun. 2015, doi: 10.1016/S0140-6736(15)60461-5.

[87] R. Daniels, E. van Rossum, L. de Witte, G. I. J. M. Kempen, and W. van den Heuvel, "Interventions to prevent disability in frail community-dwelling elderly: a systematic review," BMC Health Serv Res, vol. 8, 2008, doi: 10.1186/1472-6963-8-278.

[88] R. Daniels et al., "A disability prevention programme for community-dwelling frail older persons," Clin Rehabil, vol. 25, no. 11, pp. 963–974, Nov. 2011, doi: 10.1177/0269215511410728.

[89] F. Panza et al., "Cognitive frailty: a potential target for secondary prevention of dementia," Expert Opin Drug Metab Toxicol, vol. 13, no. 10, pp. 1023–1027, Oct. 2017, doi: 10.1080/17425255.2017.1372424.

[90] T. Sugimoto et al., "Epidemiological and clinical significance of cognitive frailty: A mini review," Ageing Res Rev, vol. 44, pp. 1–7, Jul. 2018, doi: 10.1016/J.ARR.2018.03.002.

[91] S. E. Howlett, A. D. Rutenberg, and K. Rockwood, "The degree of frailty as a translational measure of health in aging," Nature Aging 2021 1:8, vol. 1, no. 8, pp. 651–665, Aug. 2021, doi: 10.1038/s43587-021-00099-3.

[92] S. Vermeiren et al., "Frailty and the Prediction of Negative Health Outcomes: A Meta-Analysis," J Am Med Dir Assoc, vol. 17, no. 12, pp. 1163.e1-1163.e17, Dec. 2016, doi: 10.1016/J.JAMDA.2016.09.010.

[93] S. A. Sternberg, A. W. Schwartz, S. Karunananthan, H. Bergman, and A. Mark Clarfield, "The identification of frailty: a systematic literature review," J Am Geriatr Soc, vol. 59, no. 11, pp. 2129–2138, Nov. 2011, doi: 10.1111/J.1532-5415.2011.03597.X.

[94] E. Dent, P. Kowal, and E. O. Hoogendijk, "Frailty measurement in research and clinical practice: A review," Eur J Intern Med, vol. 31, pp. 3–10, Jun. 2016, doi: 10.1016/J.EJIM.2016.03.007.

[95] A. B. Mitnitski, A. J. Mogilner, and K. Rockwood, "Accumulation of deficits as a proxy measure of aging," ScientificWorldJournal, vol. 1, pp. 323–336, 2001, doi: 10.1100/TSW.2001.58.

[96] K. Rockwood et al., "A global clinical measure of fitness and frailty in elderly people," CMAJ, vol. 173, no. 5, pp. 489–495, Aug. 2005, doi: 10.1503/CMAJ.050051.

[97] M. B. van Iersel and M. G. M. Olde Rikkert, "Frailty criteria give heterogeneous results when applied in clinical practice," J Am Geriatr Soc, vol. 54, no. 4, pp. 728–729, Apr. 2006, doi: 10.1111/J.1532-5415.2006.00668_14.X.

[98] G. Abellan Van Kan et al., "Gait speed at usual pace as a predictor of adverse outcomes in community-dwelling older people an International Academy on Nutrition and Aging (IANA) Task Force," J Nutr Health Aging, vol. 13, no. 10, pp. 881–889, 2009, doi: 10.1007/S12603-009-0246-Z.

[99] M. Montero-Odasso et al., “Gait velocity as a single predictor of adverse events in healthy seniors aged 75 years and older,” J Gerontol A Biol Sci Med Sci, vol. 60, no. 10, pp. 1304–1309, 2005, doi: 10.1093/GERONA/60.10.1304.

[100] N. U. I. B. Mathias S, “Balance in elderly patients: the ‘get-up and go’ test,” Arch Phys Med Rehabil, vol. 6, Jun. 1986.

[101] J. C. Wall, C. Bell, S. Campbell, and J. Davis, “The timed get-up-and-go test revisited: Measurement of the component tasks,” J Rehabil Res Dev, vol. 37, no. 1, pp. 109–114, Jan. 2000.

[102] B. DW. Mahoney FI., “Functional evaluation: the barthel index,” Md State Med J, vol. 5, Feb. 1965.

[103] J. Walston, B. Buta, and Q. L. Xue, “Frailty Screening and Interventions: Considerations for Clinical Practice,” Clin Geriatr Med, vol. 34, no. 1, pp. 25–38, Feb. 2018, doi: 10.1016/J.CGER.2017.09.004.

[104] J. M. Guralnik et al., “A short physical performance battery assessing lower extremity function: association with self-reported disability and prediction of mortality and nursing home admission,” J Gerontol, vol. 49, no. 2, 1994, doi: 10.1093/GERONJ/49.2.M85.

[105] G. A. van Kan, Y. M. Rolland, J. E. Morley, and B. Vellas, “Frailty: toward a clinical definition,” J Am Med Dir Assoc, vol. 9, no. 2, pp. 71–72, 2008, doi: 10.1016/J.JAMDA.2007.11.005.

[106] R. J. J. Gobbens, M. A. L. M. van Assen, K. G. Luijkx, M. T. Wijnen-Sponselee, and J. M. G. A. Schols, “The Tilburg Frailty Indicator: psychometric properties,” J Am Med Dir Assoc, vol. 11, no. 5, pp. 344–355, 2010, doi: 10.1016/J.JAMDA.2009.11.003.

[107] S. Studenski et al., “Clinical Global Impression of Change in Physical Frailty: development of a measure based on clinical judgment,” J Am Geriatr Soc, vol. 52, no. 9, pp. 1560–1566, Sep. 2004, doi: 10.1111/J.1532-5415.2004.52423.X.

[108] B. Vellas et al., “Looking for frailty in community-dwelling older persons: the Gérontopôle Frailty Screening Tool (GFST),” J Nutr Health Aging, vol. 17, no. 7, pp. 629–631, Aug. 2013, doi: 10.1007/S12603-013-0363-6.

[109] E. O. Hoogendijk, J. Afilalo, K. E. Ensrud, P. Kowal, G. Onder, and L. P. Fried, “Frailty: implications for clinical practice and public health,” Lancet, vol. 394, no. 10206, pp. 1365–1375, Oct. 2019, doi: 10.1016/S0140-6736(19)31786-6.

[110] J. E. Morley, “The New Geriatric Giants,” Clin Geriatr Med, vol. 33, no. 3, pp. xi–xii, Aug. 2017, doi: 10.1016/J.CGER.2017.05.001.

[111] E. Kelaiditi et al., “Cognitive frailty: rational and definition from an (I.A.N.A./I.A.G.G.) international consensus group,” J Nutr Health Aging, vol. 17, no. 9, pp. 726–734, Nov. 2013, doi: 10.1007/S12603-013-0367-2.

[112] F. Panza et al., “Cognitive Frailty: A Systematic Review of Epidemiological and Neurobiological Evidence of an Age-Related Clinical Condition,” Rejuvenation Res, vol. 18, no. 5, pp. 389–412, Oct. 2015, doi: 10.1089/REJ.2014.1637.

[113] A. J. Woods, R. A. Cohen, and M. Pahor, “Cognitive frailty: frontiers and challenges,” J Nutr Health Aging, vol. 17, no. 9, pp. 741–743, Nov. 2013, doi: 10.1007/S12603-013-0398-8.

[114] D. Facal et al., "Cognitive frailty: A conceptual systematic review and an operational proposal for future research," Maturitas, vol. 121, pp. 48–56, Mar. 2019, doi: 10.1016/J.MATURITAS.2018.12.006.

[115] T. K. Malmstrom and J. E. Morley, "Frailty and cognition: linking two common syndromes in older persons," J Nutr Health Aging, vol. 17, no. 9, pp. 723–725, Nov. 2013, doi: 10.1007/S12603-013-0395-Y.

[116] D. A. Robertson, G. M. Savva, and R. A. Kenny, "Frailty and cognitive impairment--a review of the evidence and causal mechanisms," Ageing Res Rev, vol. 12, no. 4, pp. 840–851, Sep. 2013, doi: 10.1016/J.ARR.2013.06.004.

[117] K. Strimbu and J. A. Tavel, "What are biomarkers?," Curr Opin HIV AIDS, vol. 5, no. 6, pp. 463–466, Nov. 2010, doi: 10.1097/COH.0B013E32833ED177.

[118] A. J. Atkinson et al., "Biomarkers and surrogate endpoints: preferred definitions and conceptual framework," Clin Pharmacol Ther, vol. 69, no. 3, pp. 89–95, Jan. 2001, doi: 10.1067/MCP.2001.113989.

[119] L. Rodríguez-Mañas, "Use of Biomarkers," J Frailty Aging, vol. 4, no. 3, pp. 1–4, 2015, doi: 10.14283/JFA.2015.46.

[120] A. E. Kane and D. A. Sinclair, "Frailty biomarkers in humans and rodents: Current approaches and future advances," Mech Ageing Dev, vol. 180, pp. 117–128, Jun. 2019, doi: 10.1016/J.MAD.2019.03.007.

[121] A. L. Cardoso et al., "Towards frailty biomarkers: Candidates from genes and pathways regulated in aging and age-related diseases," Ageing Res Rev, vol. 47, pp. 214–277, Nov. 2018, doi: 10.1016/J.ARR.2018.07.004.

[122] M. Álvarez-Satta et al., "Relevance of oxidative stress and inflammation in frailty based on human studies and mouse models," Aging, vol. 12, no. 10, pp. 9982–9999, May 2020, doi: 10.18632/AGING.103295.

[123] M. el Assar et al., "Frailty Is Associated With Lower Expression of Genes Involved in Cellular Response to Stress: Results From the Toledo Study for Healthy Aging," J Am Med Dir Assoc, vol. 18, no. 8, pp. 734.e1-734.e7, Aug. 2017, doi: 10.1016/J.JAMDA.2017.04.019.

[124] P. Soysal et al., "Oxidative stress and frailty: A systematic review and synthesis of the best evidence," Maturitas, vol. 99, pp. 66–72, May 2017, doi: 10.1016/J.MATURITAS.2017.01.006.

[125] J. Viña, C. Borras, and M. C. Gomez-Cabrera, "A free radical theory of frailty," Free Radic Biol Med, vol. 124, pp. 358–363, Aug. 2018, doi: 10.1016/J.FREERADBIOMED.2018.06.028.

[126] S. Leng, P. Chaves, K. Koenig, and J. Walston, "Serum interleukin-6 and hemoglobin as physiological correlates in the geriatric syndrome of frailty: a pilot study," J Am Geriatr Soc, vol. 50, no. 7, pp. 1268–1271, 2002, doi: 10.1046/J.1532-5415.2002.50315.X.

[127] J. Walston et al., "Frailty and activation of the inflammation and coagulation systems with and without clinical comorbidities: results from the Cardiovascular Health Study," Arch Intern Med, vol. 162, no. 20, pp. 2333–2341, Nov. 2002, doi: 10.1001/ARCHINTE.162.20.2333.

[128] J. I. Barzilay et al., “Insulin resistance and inflammation as precursors of frailty: the Cardiovascular Health Study,” Arch Intern Med, vol. 167, no. 7, pp. 635–641, Apr. 2007, doi: 10.1001/ARCHINTE.167.7.635.

[129] K. Darvin et al., “Plasma protein biomarkers of the geriatric syndrome of frailty,” J Gerontol A Biol Sci Med Sci, vol. 69, no. 2, pp. 182–186, 2014, doi: 10.1093/GERONA/GLT183.

[130] P. Soysal et al., “Inflammation and frailty in the elderly: A systematic review and meta-analysis,” Ageing Res Rev, vol. 31, pp. 1–8, Nov. 2016, doi: 10.1016/J.ARR.2016.08.006.

[131] L. Sargent et al., “Shared biological pathways for frailty and cognitive impairment: A systematic review,” Ageing Res Rev, vol. 47, pp. 149–158, Nov. 2018, doi: 10.1016/J.ARR.2018.08.001.

[132] Q. Ruan et al., “Emerging biomarkers and screening for cognitive frailty,” Aging Clin Exp Res, vol. 29, no. 6, pp. 1075–1086, Dec. 2017, doi: 10.1007/S40520-017-0741-8.

[133] R. S. dos S. A. Gonçalves, Á. C. C. Maciel, Y. Rolland, B. Vellas, and P. de Souto Barreto, “Frailty biomarkers under the perspective of geroscience: A narrative review,” Ageing Res Rev, vol. 81, Nov. 2022, doi: 10.1016/J.ARR.2022.101737.

[134] J. Walston et al., “The physical and biological characterization of a frail mouse model,” J Gerontol A Biol Sci Med Sci, vol. 63, no. 4, pp. 391–398, 2008, doi: 10.1093/GERONA/63.4.391.

[135] F. Ko et al., “Inflammation and mortality in a frail mouse model,” Age (Dordr), vol. 34, no. 3, pp. 705–715, Jun. 2012, doi: 10.1007/S11357-011-9269-6.

[136] G. Sikka et al., “Interleukin 10 knockout frail mice develop cardiac and vascular dysfunction with increased age,” Exp Gerontol, vol. 48, no. 2, pp. 128–135, Feb. 2013, doi: 10.1016/J.EXGER.2012.11.001.

[137] S. Nóbrega-Pereira et al., “G6PD protects from oxidative damage and improves healthspan in mice,” Nat Commun, vol. 7, Mar. 2016, doi: 10.1038/NCOMMS10894.

[138] G. Lippi et al., “Laboratory biomarkers and frailty: presentation of the FRAILOMIC initiative,” Clin Chem Lab Med, vol. 53, no. 10, pp. e253–e255, Sep. 2015, doi: 10.1515/CCLM-2015-0147.

[139] J. D. Erusalimsky et al., “In Search of ’Omics’-Based Biomarkers to Predict Risk of Frailty and Its Consequences in Older Individuals: The FRAILOMIC Initiative,” Gerontology, vol. 62, no. 2, pp. 182–190, Feb. 2016, doi: 10.1159/000435853.

[140] D. Gomez-Cabrero et al., “A robust machine learning framework to identify signatures for frailty: a nested case-control study in four aging European cohorts,” Geroscience, vol. 43, no. 3, pp. 1317–1329, Jun. 2021, doi: 10.1007/S11357-021-00334-0.

[141] C. S. Prince et al., “Frailty in middle age is associated with frailty status and race-specific changes to the transcriptome,” Aging, vol. 11, no. 15, pp. 5518–5534, Aug. 2019, doi: 10.18632/AGING.102135.

[142] M. Kameda, T. Teruya, M. Yanagida, and H. Kondoh, “Frailty markers comprise blood metabolites involved in antioxidation, cognition, and mobility,” Proc Natl Acad Sci U S A, vol. 117, no. 17, pp. 9483–9489, Apr. 2020, doi: 10.1073/PNAS.1920795117.

[143] N. J. W. Rattray et al., “Metabolic dysregulation in vitamin E and carnitine shuttle energy mechanisms associate with human frailty,” Nat Commun, vol. 10, no. 1, Dec. 2019, doi: 10.1038/S41467-019-12716-2.

[144] G. Livshits et al., "Multi-OMICS analyses of frailty and chronic widespread musculoskeletal pain suggest involvement of shared neurological pathways," Pain, vol. 159, no. 12, pp. 2565–2572, 2018, doi: 10.1097/J.PAIN.0000000000001364.

[145] E. Pujos-Guillot et al., "Identification of Pre-frailty Sub-Phenotypes in Elderly Using Metabolomics," Front Physiol, vol. 9, no. JAN, 2019, doi: 10.3389/FPHYS.2018.01903.

[146] G. Carini et al., "miRNome Profiling Detects miR-101-3p and miR-142-5p as Putative Blood Biomarkers of Frailty Syndrome," Genes (Basel), vol. 13, no. 2, Feb. 2022, doi: 10.3390/GENES13020231.

[147] B. R. Ipson, M. B. Fletcher, S. E. Espinoza, and A. L. Fisher, "Identifying Exosome-Derived MicroRNAs as Candidate Biomarkers of Frailty," J Frailty Aging, vol. 7, no. 2, pp. 100–103, Feb. 2018, doi: 10.14283/JFA.2017.45.

[148] B. Dalmasso et al., "Age-related microRNAs in older breast cancer patients: biomarker potential and evolution during adjuvant chemotherapy," BMC Cancer, vol. 18, no. 1, Oct. 2018, doi: 10.1186/S12885-018-4920-6.

[149] I. Rusanova et al., "Analysis of Plasma MicroRNAs as Predictors and Biomarkers of Aging and Frailty in Humans," Oxid Med Cell Longev, vol. 2018, 2018, doi: 10.1155/2018/7671850.

[150] I. Rusanova et al., "Involvement of plasma miRNAs, muscle miRNAs and mitochondrial miRNAs in the pathophysiology of frailty," Exp Gerontol, vol. 124, Sep. 2019, doi: 10.1016/J.EXGER.2019.110637.

[151] M. Fabbri, A. Paone, F. Calore, R. Galli, and C. M. Croce, "A new role for microRNAs, as ligands of Toll-like receptors," RNA Biol, vol. 10, no. 2, pp. 169–174, 2013, doi: 10.4161/RNA.23144.

[152] B. G. Hughes and S. Hekimi, "Many possible maximum lifespan trajectories," Nature, vol. 546, no. 7660, pp. E8–E9, Jun. 2017, doi: 10.1038/NATURE22786.

[153] E. Barbi, F. Lagona, M. Marsili, J. W. Vaupel, and K. W. Wachter, "The plateau of human mortality: Demography of longevity pioneers," Science, vol. 360, no. 6396, pp. 1459–1461, Jun. 2018, doi: 10.1126/SCIENCE.AAT3119.

[154] L. Teixeira, L. Araújo, D. Jopp, and O. Ribeiro, "Centenarians in Europe," Maturitas, vol. 104, pp. 90–95, Oct. 2017, doi: 10.1016/J.MATURITAS.2017.08.005.

[155] S. L. Andersen, P. Sebastiani, D. A. Dworkis, L. Feldman, and T. T. Perls, "Health span approximates life span among many supercentenarians: compression of morbidity at the approximate limit of life span," J Gerontol A Biol Sci Med Sci, vol. 67, no. 4, pp. 395–405, Apr. 2012, doi: 10.1093/GERONA/GLR223.

[156] J. F. Fries, "Aging, natural death, and the compression of morbidity," N Engl J Med, vol. 303, no. 3, pp. 245–250, 1980, doi: 10.1056/NEJM198007173030304.

[157] A. B. Newman et al., "Health and function of participants in the Long Life Family Study: A comparison with other cohorts," Aging, vol. 3, no. 1, pp. 63–76, 2011, doi: 10.18632/AGING.100242.

[158] P. Sebastiani and T. T. Perls, "The genetics of extreme longevity: lessons from the new England centenarian study," Front Genet, vol. 3, no. NOV, 2012, doi: 10.3389/FGENE.2012.00277.

[159] K. Ismail et al., “Compression of Morbidity Is Observed Across Cohorts with Exceptional Longevity,” J Am Geriatr Soc, vol. 64, no. 8, pp. 1583–1591, Aug. 2016, doi: 10.1111/JGS.14222.

[160] Y. Lv, C. Mao, Z. Yin, F. Li, X. Wu, and X. Shi, “Healthy Ageing and Biomarkers Cohort Study (HABCS): a cohort profile,” BMJ Open, vol. 9, no. 10, Oct. 2019, doi: 10.1136/BMJOPEN-2018-026513.

[161] J. F. Calvert, J. Hollander-Rodriguez, J. Kaye, and M. Leahy, “Dementia-free survival among centenarians: an evidence-based review,” J Gerontol A Biol Sci Med Sci, vol. 61, no. 9, pp. 951–956, 2006, doi: 10.1093/GERONA/61.9.951.

[162] A. SL, “Centenarians as Models of Resistance and Resilience to Alzheimer’s Disease and Related Dementias,” Adv Geriatr Med Res, vol. 2, no. 3, 2020, doi: 10.20900/AGMR20200018.

[163] A. Galioto et al., “Cardiovascular risk factors in centenarians,” Exp Gerontol, vol. 43, no. 2, pp. 106–113, Feb. 2008, doi: 10.1016/J.EXGER.2007.06.009.

[164] M. Suzuki, B. J. Wilcox, and C. D. Wilcox, “Implications from and for food cultures for cardiovascular disease: longevity,” Asia Pac J Clin Nutr, vol. 10, no. 2, pp. 165–171, 2001, doi: 10.1111/J.1440-6047.2001.00219.X.

[165] A. Davey et al., “Diabetes mellitus in centenarians,” J Am Geriatr Soc, vol. 60, no. 3, pp. 468–473, Mar. 2012, doi: 10.1111/J.1532-5415.2011.03836.X.

[166] N. Pavlidis, G. Stanta, and R. A. Audisio, “Cancer prevalence and mortality in centenarians: a systematic review,” Crit Rev Oncol Hematol, vol. 83, no. 1, pp. 145–152, Jul. 2012, doi: 10.1016/J.CRITREVONC.2011.09.007.

[167] M. Clerencia-Sierra et al., “Do Centenarians Die Healthier than Younger Elders? A Comparative Epidemiological Study in Spain,” J Clin Med, vol. 9, no. 5, May 2020, doi: 10.3390/JCM9051563.

[168] D. C. Willcox, B. J. Willcox, S. Shimajiri, S. Kurechi, and M. Suzuki, “Aging gracefully: a retrospective analysis of functional status in Okinawan centenarians,” Am J Geriatr Psychiatry, vol. 15, no. 3, pp. 252–256, 2007, doi: 10.1097/JGP.0B013E31803190CC.

[169] E M Gruenberg, “The failures of success,” Milbank Memorial Fund quarterly / Health and society, vol. 1, Jan. 1977.

[170] E. M. Gruenberg, “The Failures of Success,” Milbank Q, vol. 83, no. 4, p. 779, 2005, doi: 10.1111/J.1468-0009.2005.00400.X.

[171] S. J. Olshansky, M. A. Rudberg, C. K. Cassel, B. A. Carnes, and J. A. Brody, “Trading Off Longer Life for Worsening Health: The Expansion of Morbidity Hypothesis,” eweb:103205, vol. 3, no. 2, pp. 194–216, 1991, doi: 10.1177/089826439100300205.

[172] K. Andersen-Ranberg, M. Schroll, and B. Jeune, “Healthy centenarians do not exist, but autonomous centenarians do: a population-based study of morbidity among Danish centenarians,” J Am Geriatr Soc, vol. 49, no. 7, pp. 900–908, 2001, doi: 10.1046/J.1532-5415.2001.49180.X.

[173] K. Andersen-Ranberg, K. Christensen, B. Jeune, A. Skytthe, L. Vasegaard, and J. W. Vaupel, “Declining physical abilities with age: a cross-sectional study of older twins and centenarians in Denmark,” Age Ageing, vol. 28, no. 4, pp. 373–377, 1999, doi: 10.1093/AGEING/28.4.373.

[174] K. Andersen-Ranberg, L. Vasegaard, and B. Jeune, “Dementia is not inevitable: a population-based study of Danish centenarians,” J Gerontol B Psychol Sci Soc Sci, vol. 56, no. 3, 2001, doi: 10.1093/GERONB/56.3.P152.

[175] M. H. Silver, E. Jilinskaia, and T. T. Perls, “Cognitive functional status of age-confirmed centenarians in a population-based study,” J Gerontol B Psychol Sci Soc Sci, vol. 56, no. 3, 2001, doi: 10.1093/GERONB/56.3.P134.

[176] Y. Gondo et al., “Functional status of centenarians in Tokyo, Japan: developing better phenotypes of exceptional longevity,” J Gerontol A Biol Sci Med Sci, vol. 61, no. 3, pp. 305–310, 2006, doi: 10.1093/GERONA/61.3.305.

[177] J. A. Ailshire, H. Beltrán-Sánchez, and E. M. Crimmins, “Becoming centenarians: disease and functioning trajectories of older US Adults as they survive to 100,” J Gerontol A Biol Sci Med Sci, vol. 70, no. 2, pp. 193–201, Feb. 2015, doi: 10.1093/GERONA/GLU124.

[178] J. Evert, E. Lawler, H. Bogan, and T. Perls, “Morbidity profiles of centenarians: survivors, delayers, and escapers,” J Gerontol A Biol Sci Med Sci, vol. 58, no. 3, pp. 232–237, Mar. 2003, doi: 10.1093/GERONA/58.3.M232.

[179] L. Bucci et al., “Centenarians’ offspring as a model of healthy aging: a reappraisal of the data on Italian subjects and a comprehensive overview,” Aging, vol. 8, no. 3, pp. 510–519, Mar. 2016, doi: 10.18632/AGING.100912.

[180] C. Franceschi, G. Passarino, D. Mari, and D. Monti, “Centenarians as a 21st century healthy aging model: A legacy of humanity and the need for a world-wide consortium (WWC100+),” Mech Ageing Dev, vol. 165, no. Pt B, pp. 55–58, Jul. 2017, doi: 10.1016/J.MAD.2017.06.002.

[181] R. Bhardwaj, S. Amiri, D. Buchwald, and O. Amram, “Environmental Correlates of Reaching a Centenarian Age: Analysis of 144,665 Deaths in Washington State for 2011-2015,” Int J Environ Res Public Health, vol. 17, no. 8, Apr. 2020, doi: 10.3390/IJERPH17082828.

[182] R. J. Pignolo, “Exceptional Human Longevity,” Mayo Clin Proc, vol. 94, no. 1, pp. 110–124, Jan. 2019, doi: 10.1016/J.MAYOCP.2018.10.005.

[183] Z. D. Zhang et al., “Genetics of extreme human longevity to guide drug discovery for healthy ageing,” Nat Metab, vol. 2, no. 8, pp. 663–672, Aug. 2020, doi: 10.1038/S42255-020-0247-0.

[184] Y. Zeng et al., “Novel loci and pathways significantly associated with longevity,” Sci Rep, vol. 6, Feb. 2016, doi: 10.1038/SREP21243.

[185] D. Lio et al., “Laboratory parameters in centenarians of Italian ancestry,” Exp Gerontol, vol. 43, no. 2, pp. 119–122, Feb. 2008, doi: 10.1016/J.EXGER.2007.06.005.

[186] D. F. Terry et al., “Lower all-cause, cardiovascular, and cancer mortality in centenarians’ offspring,” J Am Geriatr Soc, vol. 52, no. 12, pp. 2074–2076, Dec. 2004, doi: 10.1111/J.1532-5415.2004.52561.X.

[187] E. R. Adams, V. G. Nolan, S. L. Andersen, T. T. Perls, and D. F. Terry, “Centenarian offspring: start healthier and stay healthier,” J Am Geriatr Soc, vol. 56, no. 11, pp. 2089–2092, Nov. 2008, doi: 10.1111/J.1532-5415.2008.01949.X.

[188] C. Borras et al., “Centenarians: An excellent example of resilience for successful ageing,” Mech Ageing Dev, vol. 186, Mar. 2020, doi: 10.1016/J.MAD.2019.111199.

[189] J. Deelen et al., “A meta-analysis of genome-wide association studies identifies multiple longevity genes,” Nat Commun, vol. 10, no. 1, Dec. 2019, doi: 10.1038/S41467-019-11558-2.

[190] J. Deelen et al., “Genome-wide association meta-analysis of human longevity identifies a novel locus conferring survival beyond 90 years of age,” Hum Mol Genet, vol. 23, no. 16, pp. 4420–4432, 2014, doi: 10.1093/HMG/DDU139.

[191] A. Nebel et al., “A genome-wide association study confirms APOE as the major gene influencing survival in long-lived individuals,” Mech Ageing Dev, vol. 132, no. 6–7, pp. 324–330, Jun. 2011, doi: 10.1016/J.MAD.2011.06.008.

[192] A. H. Shadyab and A. Z. LaCroix, “Genetic factors associated with longevity: a review of recent findings,” Ageing Res Rev, vol. 19, pp. 1–7, Jan. 2015, doi: 10.1016/J.ARR.2014.10.005.

[193] T. P. Cash et al., “Exome sequencing of three cases of familial exceptional longevity,” Aging Cell, vol. 13, no. 6, pp. 1087–1090, Dec. 2014, doi: 10.1111/ACEL.12261.

[194] D. Govindaraju, G. Atzmon, and N. Barzilai, “Genetics, lifestyle and longevity: Lessons from centenarians,” Appl Transl Genom, vol. 4, pp. 23–32, Mar. 2015, doi: 10.1016/J.ATG.2015.01.001.

[195] S. Dato et al., “Exploring the role of genetic variability and lifestyle in oxidative stress response for healthy aging and longevity,” Int J Mol Sci, vol. 14, no. 8, pp. 16443–16472, Aug. 2013, doi: 10.3390/IJMS140816443.

[196] K. Christensen, T. E. Johnson, and J. W. Vaupel, “The quest for genetic determinants of human longevity: challenges and insights,” Nat Rev Genet, vol. 7, no. 6, pp. 436–448, Jun. 2006, doi: 10.1038/NRG1871.

[197] M. Soerensen et al., “Evidence from case-control and longitudinal studies supports associations of genetic variation in APOE, CETP, and IL6 with human longevity,” Age (Dordr), vol. 35, no. 2, pp. 487–500, Apr. 2013, doi: 10.1007/S11357-011-9373-7.

[198] C. V. Anselmi et al., “Association of the FOXO3A locus with extreme longevity in a southern Italian centenarian study,” Rejuvenation Res, vol. 12, no. 2, pp. 95–103, Apr. 2009, doi: 10.1089/REJ.2008.0827.

[199] F. Flachsbart et al., “Association of FOXO3A variation with human longevity confirmed in German centenarians,” Proc Natl Acad Sci U S A, vol. 106, no. 8, pp. 2700–2705, Feb. 2009, doi: 10.1073/PNAS.0809594106.

[200] Y. Li et al., “Genetic association of FOXO1A and FOXO3A with longevity trait in Han Chinese populations,” Hum Mol Genet, vol. 18, no. 24, pp. 4897–4904, 2009, doi: 10.1093/HMG/DDP459.

[201] B. J. Willcox et al., “FOXO3A genotype is strongly associated with human longevity,” Proc Natl Acad Sci U S A, vol. 105, no. 37, pp. 13987–13992, Sep. 2008, doi: 10.1073/PNAS.0801030105.

[202] Y. Suh et al., “Functionally significant insulin-like growth factor I receptor mutations in centenarians,” Proc Natl Acad Sci U S A, vol. 105, no. 9, pp. 3438–3442, Mar. 2008, doi: 10.1073/PNAS.0705467105.

[203] M. Inglés et al., “Centenarians Overexpress Pluripotency-Related Genes,” J Gerontol A Biol Sci Med Sci, vol. 74, no. 9, pp. 1391–1395, Aug. 2019, doi: 10.1093/GERONA/GLY168.

[204] I. P. Trougakos, C. Petropoulou, C. Franceschi, and E. S. Gonos, "Reduced expression levels of the senescence biomarker clusterin/apolipoprotein j in lymphocytes from healthy centenarians," Ann N Y Acad Sci, vol. 1067, no. 1, pp. 294–300, 2006, doi: 10.1196/ANNALS.1354.039.

[205] C. Borras et al., "Human exceptional longevity: transcriptome from centenarians is distinct from septuagenarians and reveals a role of Bcl-xL in successful aging," Aging, vol. 8, no. 12, pp. 3185–3208, 2016, doi: 10.18632/AGING.101078.

[206] P. Sebastiani et al., "Protein signatures of centenarians and their offspring suggest centenarians age slower than other humans," Aging Cell, vol. 20, no. 2, Feb. 2021, doi: 10.1111/ACEL.13290.

[207] D. Gentilini et al., "Role of epigenetics in human aging and longevity: genome-wide DNA methylation profile in centenarians and centenarians' offspring," Age (Dordr), vol. 35, no. 5, pp. 1961–1973, Oct. 2013, doi: 10.1007/S11357-012-9463-1.

[208] S. Horvath et al., "Aging effects on DNA methylation modules in human brain and blood tissue," Genome Biol, vol. 13, no. 10, p. R97, 2012, doi: 10.1186/GB-2012-13-10-R97.

[209] S. Horvath et al., "Decreased epigenetic age of PBMCs from Italian semi-supercentenarians and their offspring," Aging, vol. 7, no. 12, pp. 1159–1170, 2015, doi: 10.18632/AGING.100861.

[210] M. Zhao et al., "Distinct epigenomes in CD4+ T cells of newborns, middle-ages and centenarians," Sci Rep, vol. 6, Dec. 2016, doi: 10.1038/SREP38411.

[211] N. Noren Hooten, K. Abdelmohsen, M. Gorospe, N. Ejiogu, A. B. Zonderman, and M. K. Evans, "microRNA expression patterns reveal differential expression of target genes with age," PLoS One, vol. 5, no. 5, 2010, doi: 10.1371/JOURNAL.PONE.0010724.

[212] A. Elsharawy et al., "Genome-wide miRNA signatures of human longevity," Aging Cell, vol. 11, no. 4, pp. 607–616, Aug. 2012, doi: 10.1111/J.1474-9726.2012.00824.X.

[213] E. Serna et al., "Centenarians, but not octogenarians, up-regulate the expression of microRNAs," Sci Rep, vol. 2, 2012, doi: 10.1038/SREP00961.

[214] C. Borrás, E. Serna, J. Gambini, M. Inglés, and J. Vina, "Centenarians maintain miRNA biogenesis pathway while it is impaired in octogenarians," Mech Ageing Dev, vol. 168, pp. 54–57, Dec. 2017, doi: 10.1016/J.MAD.2017.07.003.

[215] T. Lu et al., "REST and stress resistance in ageing and Alzheimer's disease," Nature, vol. 507, no. 7493, pp. 448–454, 2014, doi: 10.1038/NATURE13163.

[216] J. M. Zullo et al., "Regulation of lifespan by neural excitation and REST," Nature, vol. 574, no. 7778, pp. 359–364, Oct. 2019, doi: 10.1038/S41586-019-1647-8.

[217] L. T. et al., "Addendum: REST and stress resistance in ageing and Alzheimer's disease," Nature, vol. 540, no. 7633, pp. 470–470, Dec. 2016, doi: 10.1038/NATURE20579.

[218] M. Mampay and G. K. Sheridan, "REST: An epigenetic regulator of neuronal stress responses in the young and ageing brain," Front Neuroendocrinol, vol. 53, Apr. 2019, doi: 10.1016/J.YFRNE.2019.04.001.

[219] M. Kawamura et al., "Loss of nuclear REST/NRSF in aged-dopaminergic neurons in Parkinson's disease patients," Neurosci Lett, vol. 699, pp. 59–63, Apr. 2019, doi: 10.1016/J.NEULET.2019.01.042.

[220] K. A. Maldonado and K. Alsayouri, “Physiology, Brain,” StatPearls, Dec. 2021, Accessed: Jan. 17, 2023. [Online]. Available: https://www.ncbi.nlm.nih.gov/books/NBK551718/

[221] X. Jiang and J. Nardelli, “Cellular and molecular introduction to brain development,” Neurobiol Dis, vol. 92, no. Pt A, pp. 3–17, Aug. 2016, doi: 10.1016/J.NBD.2015.07.007.

[222] G. Herbet and H. Duffau, “Revisiting the Functional Anatomy of the Human Brain: Toward a Meta-Networking Theory of Cerebral Functions,” Physiol Rev, vol. 100, no. 3, pp. 1181–1228, 2020, doi: 10.1152/PHYSREV.00033.2019.

[223] J. J. Knierim, “The hippocampus,” Curr Biol, vol. 25, no. 23, pp. R1116–R1121, Dec. 2015, doi: 10.1016/J.CUB.2015.10.049.

[224] B. T. Giap, C. N. Jong, J. H. Ricker, N. K. Cullen, and R. D. Zafonte, “The hippocampus: anatomy, pathophysiology, and regenerative capacity,” J Head Trauma Rehabil, vol. 15, no. 3, pp. 875–894, 2000, doi: 10.1097/00001199-200006000-00003.

[225] R. M. Brouwer et al., “Genetic variants associated with longitudinal changes in brain structure across the lifespan,” Nat Neurosci, vol. 25, no. 4, pp. 421–432, Apr. 2022, doi: 10.1038/S41593-022-01042-4.

[226] C. S. von Bartheld, J. Bahney, and S. Herculano-Houzel, “The search for true numbers of neurons and glial cells in the human brain: A review of 150 years of cell counting,” J Comp Neurol, vol. 524, no. 18, pp. 3865–3895, Dec. 2016, doi: 10.1002/CNE.24040.

[227] S. Herculano-Houzel, “The human brain in numbers: a linearly scaled-up primate brain,” Front Hum Neurosci, vol. 3, no. NOV, Nov. 2009, doi: 10.3389/NEURO.09.031.2009.

[228] F. Paquet-Durand and G. Bicker, “Human model neurons in studies of brain cell damage and neural repair,” Curr Mol Med, vol. 7, no. 6, pp. 541–554, Aug. 2007, doi: 10.2174/156652407781695747.

[229] G. J. Duncan, S. B. Manesh, B. J. Hilton, P. Assinck, J. R. Plemel, and W. Tetzlaff, “The fate and function of oligodendrocyte progenitor cells after traumatic spinal cord injury,” Glia, vol. 68, no. 2, pp. 227–245, Feb. 2020, doi: 10.1002/GLIA.23706.

[230] S. B. Nelson, K. Sugino, and C. M. Hempel, “The problem of neuronal cell types: a physiological genomics approach,” Trends Neurosci, vol. 29, no. 6, pp. 339–345, Jun. 2006, doi: 10.1016/J.TINS.2006.05.004.

[231] T. Riedemann, “Diversity and Function of Somatostatin-Expressing Interneurons in the Cerebral Cortex,” Int J Mol Sci, vol. 20, no. 12, Jun. 2019, doi: 10.3390/IJMS20122952.

[232] L. J. Ansen-Wilson and R. J. Lipinski, “Gene-environment interactions in cortical interneuron development and dysfunction: A review of preclinical studies,” Neurotoxicology, vol. 58, pp. 120–129, Jan. 2017, doi: 10.1016/J.NEURO.2016.12.002.

[233] S. Jäkel and L. Dimou, “Glial Cells and Their Function in the Adult Brain: A Journey through the History of Their Ablation,” Front Cell Neurosci, vol. 11, Feb. 2017, doi: 10.3389/FNCEL.2017.00024.

[234] K. R. Jessen, “Glial cells,” International Journal of Biochemistry and Cell Biology, vol. 36, no. 10, pp. 1861–1867, 2004, doi: 10.1016/j.biocel.2004.02.023.

[235] G. G. Kovacs, “Cellular reactions of the central nervous system,” Handb Clin Neurol, vol. 145, pp. 13–23, 2017, doi: 10.1016/B978-0-12-802395-2.00003-1.

[236] M. Bradl and H. Lassmann, “Oligodendrocytes: biology and pathology,” Acta Neuropathol, vol. 119, no. 1, pp. 37–53, Jan. 2010, doi: 10.1007/S00401-009-0601-5.

[237] M. R. del Bigio, “Ependymal cells: biology and pathology,” Acta Neuropathol, vol. 119, no. 1, pp. 55–73, Jan. 2010, doi: 10.1007/S00401-009-0624-Y.

[238] N. A. Oberheim, X. Wang, S. Goldman, and M. Nedergaard, “Astrocytic complexity distinguishes the human brain,” Trends Neurosci, vol. 29, no. 10, pp. 547–553, Oct. 2006, doi: 10.1016/J.TINS.2006.08.004.

[239] M. R. Freeman, “Specification and morphogenesis of astrocytes,” Science, vol. 330, no. 6005, pp. 774–778, Nov. 2010, doi: 10.1126/SCIENCE.1190928.

[240] M. Santello, N. Toni, and A. Volterra, “Astrocyte function from information processing to cognition and cognitive impairment,” Nat Neurosci, vol. 22, no. 2, pp. 154–166, Feb. 2019, doi: 10.1038/S41593-018-0325-8.

[241] A. V. Molofsky and B. Deneen, “Astrocyte development: A Guide for the Perplexed,” Glia, vol. 63, no. 8, pp. 1320–1329, Aug. 2015, doi: 10.1002/GLIA.22836.

[242] F. Ginhoux and M. Prinz, “Origin of microglia: current concepts and past controversies,” Cold Spring Harb Perspect Biol, vol. 7, no. 8, Aug. 2015, doi: 10.1101/CSHPERSPECT.A020537.

[243] H. Wake, A. J. Moorhouse, and J. Nabekura, “Functions of microglia in the central nervous system--beyond the immune response,” Neuron Glia Biol, vol. 7, no. 1, pp. 47–53, Jun. 2011, doi: 10.1017/S1740925X12000063.

[244] H. J. Rippon and A. E. Bishop, “Embryonic stem cells,” Cell Prolif, vol. 37, no. 1, pp. 23–34, Feb. 2004, doi: 10.1111/J.1365-2184.2004.00298.X.

[245] P. Malatesta, I. Appolloni, and F. Calzolari, “Radial glia and neural stem cells,” Cell Tissue Res, vol. 331, no. 1, pp. 165–178, Jan. 2008, doi: 10.1007/S00441-007-0481-8.

[246] S. K. Zahr, D. R. Kaplan, and F. D. Miller, “Translating neural stem cells to neurons in the mammalian brain,” Cell Death Differ, vol. 26, no. 12, pp. 2495–2512, Dec. 2019, doi: 10.1038/S41418-019-0411-9.

[247] S. Falk and M. Götz, “Glial control of neurogenesis,” Curr Opin Neurobiol, vol. 47, pp. 188–195, Dec. 2017, doi: 10.1016/J.CONB.2017.10.025.

[248] A. J. Wagers and I. L. Weissman, “Plasticity of adult stem cells,” Cell, vol. 116, no. 5, pp. 639–648, Mar. 2004, doi: 10.1016/S0092-8674(04)00208-9.

[249] J. B. Aimone, Y. Li, S. W. Lee, G. D. Clemenson, W. Deng, and F. H. Gage, “Regulation and function of adult neurogenesis: from genes to cognition,” Physiol Rev, vol. 94, no. 4, pp. 991–1026, Oct. 2014, doi: 10.1152/PHYSREV.00004.2014.

[250] A. Borsini, P. A. Zunszain, S. Thuret, and C. M. Pariante, “The role of inflammatory cytokines as key modulators of neurogenesis,” Trends Neurosci, vol. 38, no. 3, pp. 145–157, Mar. 2015, doi: 10.1016/J.TINS.2014.12.006.

[251] J. P. Andreotti et al., “Neural stem cell niche heterogeneity,” Semin Cell Dev Biol, vol. 95, pp. 42–53, Nov. 2019, doi: 10.1016/J.SEMCDB.2019.01.005.

[252] P. Malatesta, E. Hartfuss, and M. Götz, “Isolation of radial glial cells by fluorescent-activated cell sorting reveals a neuronal lineage,” Development, vol. 127, no. 24, pp. 5253–5263, 2000, doi: 10.1242/DEV.127.24.5253.

[253] F. Doetsch, I. Caille, D. A. Lim, J. M. Garcia-Verdugo, and A. Alvarez-Buylla, “Subventricular zone astrocytes are neural stem cells in the adult mammalian brain,” Cell, vol. 97, no. 6, pp. 703–716, 1999, doi: 10.1016/S0092-8674(00)80783-7.

[254] G. L. Ming and H. Song, “Adult neurogenesis in the mammalian central nervous system,” Annu Rev Neurosci, vol. 28, pp. 223–250, 2005, doi: 10.1146/ANNUREV.NEURO.28.051804.101459.

[255] I. Smart and C. P. Leblond, “Evidence for division and transformations of neuroglia cells in the mouse brain, as derived from radioautography after injection of thymidine-H3,” Journal of Comparative Neurology, vol. 116, no. 3, pp. 349–367, Jun. 1961, doi: 10.1002/CNE.901160307.

[256] P. S. Eriksson et al., “Neurogenesis in the adult human hippocampus,” Nat Med, vol. 4, no. 11, pp. 1313–1317, Nov. 1998, doi: 10.1038/3305.

[257] A. Ernst et al., “Neurogenesis in the striatum of the adult human brain,” Cell, vol. 156, no. 5, pp. 1072–1083, Feb. 2014, doi: 10.1016/J.CELL.2014.01.044.

[258] S. S. Magavi, B. R. Leavitt, and J. D. Macklis, “Induction of neurogenesis in the neocortex of adult mice,” Nature, vol. 405, no. 6789, pp. 951–955, Jun. 2000, doi: 10.1038/35016083.

[259] J. Fares, Z. Bou Diab, S. Nabha, and Y. Fares, “Neurogenesis in the adult hippocampus: history, regulation, and prospective roles,” Int J Neurosci, vol. 129, no. 6, pp. 598–611, Jun. 2019, doi: 10.1080/00207454.2018.1545771.

[260] B. Leuner and E. Gould, “Structural plasticity and hippocampal function,” Annu Rev Psychol, vol. 61, pp. 111–140, Jan. 2010, doi: 10.1146/ANNUREV.PSYCH.093008.100359.

[261] B. Leuner, S. Mendolia-Loffredo, Y. Kozorovitskiy, D. Samburg, E. Gould, and T. J. Shors, “Learning enhances the survival of new neurons beyond the time when the hippocampus is required for memory,” J Neurosci, vol. 24, no. 34, pp. 7477–7481, Aug. 2004, doi: 10.1523/JNEUROSCI.0204-04.2004.

[262] W. Deng, J. B. Aimone, and F. H. Gage, “New neurons and new memories: how does adult hippocampal neurogenesis affect learning and memory?,” Nat Rev Neurosci, vol. 11, no. 5, pp. 339–350, May 2010, doi: 10.1038/NRN2822.

[263] M. Llorens-Martín, J. Jurado-Arjona, J. Avila, and F. Hernández, “Novel connection between newborn granule neurons and the hippocampal CA2 field,” Exp Neurol, vol. 263, pp. 285–292, Jan. 2015, doi: 10.1016/J.EXPNEUROL.2014.10.021.

[264] F. L. Hitti and S. A. Siegelbaum, “The hippocampal CA2 region is essential for social memory,” Nature, vol. 508, no. 7494, pp. 88–92, 2014, doi: 10.1038/NATURE13028.

[265] M. E. Wintzer, R. Boehringer, D. Polygalov, and T. J. McHugh, “The hippocampal CA2 ensemble is sensitive to contextual change,” J Neurosci, vol. 34, no. 8, pp. 3056–3066, 2014, doi: 10.1523/JNEUROSCI.2563-13.2014.

[266] E. C. Cope and E. Gould, “Adult Neurogenesis, Glia, and the Extracellular Matrix,” Cell Stem Cell, vol. 24, no. 5, pp. 690–705, May 2019, doi: 10.1016/J.STEM.2019.03.023.

[267] Y. Gu, S. Janoschka, and S. Ge, “Neurogenesis and hippocampal plasticity in adult brain,” Curr Top Behav Neurosci, vol. 15, pp. 31–48, Aug. 2013, doi: 10.1007/7854_2012_217.

[268] S. G. Temprana et al., "Delayed coupling to feedback inhibition during a critical period for the integration of adult-born granule cells," Neuron, vol. 85, no. 1, pp. 116–130, Jan. 2015, doi: 10.1016/J.NEURON.2014.11.023.

[269] H. D. VanGuilder and W. M. Freeman, "The hippocampal neuroproteome with aging and cognitive decline: past progress and future directions," Front Aging Neurosci, vol. 3, no. MAY, pp. 1–14, 2011, doi: 10.3389/FNAGI.2011.00008.

[270] W. Jagust, "Vulnerable neural systems and the borderland of brain aging and neurodegeneration," Neuron, vol. 77, no. 2, pp. 219–234, Jan. 2013, doi: 10.1016/J.NEURON.2013.01.002.

[271] B. P. Drayer, "Imaging of the aging brain. Part I. Normal findings," Radiology, vol. 166, no. 3, pp. 785–796, 1988, doi: 10.1148/RADIOLOGY.166.3.3277247.

[272] C. N. Harada, M. C. Natelson Love, and K. L. Triebel, "Normal cognitive aging," Clin Geriatr Med, vol. 29, no. 4, pp. 737–752, Nov. 2013, doi: 10.1016/J.CGER.2013.07.002.

[273] D. L. Murman, "The Impact of Age on Cognition," Semin Hear, vol. 36, no. 3, pp. 111–121, Aug. 2015, doi: 10.1055/S-0035-1555115.

[274] N. K. Isaev, E. E. Genrikhs, M. v. Oborina, and E. v. Stelmashook, "Accelerated aging and aging process in the brain," Rev Neurosci, vol. 29, no. 3, pp. 233–240, Mar. 2018, doi: 10.1515/REVNEURO-2017-0051.

[275] J. Azpurua and B. A. Eaton, "Neuronal epigenetics and the aging synapse," Front Cell Neurosci, vol. 9, no. MAY, May 2015, doi: 10.3389/FNCEL.2015.00208.

[276] L. E. Clarke, S. A. Liddelow, C. Chakraborty, A. E. Münch, M. Heiman, and B. A. Barres, "Normal aging induces A1-like astrocyte reactivity," Proc Natl Acad Sci U S A, vol. 115, no. 8, pp. E1896–E1905, Feb. 2018, doi: 10.1073/PNAS.1800165115/-/DCSUPPLEMENTAL.

[277] P. Navarro Negredo, R. W. Yeo, and A. Brunet, "Aging and Rejuvenation of Neural Stem Cells and Their Niches," Cell Stem Cell, vol. 27, no. 2, pp. 202–223, Aug. 2020, doi: 10.1016/J.STEM.2020.07.002.

[278] V. Capilla-Gonzalez, V. Herranz-Pérez, and J. M. García-Verdugo, "The aged brain: genesis and fate of residual progenitor cells in the subventricular zone," Front Cell Neurosci, vol. 9, no. September, Sep. 2015, doi: 10.3389/FNCEL.2015.00365.

[279] J. M. Encinas et al., "Division-coupled astrocytic differentiation and age-related depletion of neural stem cells in the adult hippocampus," Cell Stem Cell, vol. 8, no. 5, pp. 566–579, May 2011, doi: 10.1016/J.STEM.2011.03.010.

[280] N. M. B. ben Abdallah, L. Slomianka, A. L. Vyssotski, and H. P. Lipp, "Early age-related changes in adult hippocampal neurogenesis in C57 mice," Neurobiol Aging, vol. 31, no. 1, pp. 151–161, Jan. 2010, doi: 10.1016/J.NEUROBIOLAGING.2008.03.002.

[281] L. Bondolfi, F. Ermini, J. M. Long, D. K. Ingram, and M. Jucker, "Impact of age and caloric restriction on neurogenesis in the dentate gyrus of C57BL/6 mice," Neurobiol Aging, vol. 25, no. 3, pp. 333–340, 2004, doi: 10.1016/S0197-4580(03)00083-6.

[282] E. Enwere, T. Shingo, C. Gregg, H. Fujikawa, S. Ohta, and S. Weiss, "Aging results in reduced epidermal growth factor receptor signaling, diminished olfactory neurogenesis, and deficits in fine olfactory discrimination," J Neurosci, vol. 24, no. 38, pp. 8354–8365, Sep. 2004, doi: 10.1523/JNEUROSCI.2751-04.2004.

[283] J. Luo, S. B. Daniels, J. B. Lennington, R. Q. Notti, and J. C. Conover, “The aging neurogenic subventricular zone,” Aging Cell, vol. 5, no. 2, pp. 139–152, Apr. 2006, doi: 10.1111/J.1474-9726.2006.00197.X.

[284] M. Bouab, G. N. Paliouras, A. Aumont, K. Forest-Bérard, and K. J. L. Fernandes, “Aging of the subventricular zone neural stem cell niche: evidence for quiescence-associated changes between early and mid-adulthood,” Neuroscience, vol. 173, pp. 135–149, Jan. 2011, doi: 10.1016/J.NEUROSCIENCE.2010.11.032.

[285] D. M. Apple, R. Solano-Fonseca, and E. Kokovay, “Neurogenesis in the aging brain,” Biochem Pharmacol, vol. 141, pp. 77–85, Oct. 2017, doi: 10.1016/J.BCP.2017.06.116.

[286] J. T. Gonçalves, S. T. Schafer, and F. H. Gage, “Adult Neurogenesis in the Hippocampus: From Stem Cells to Behavior,” Cell, vol. 167, no. 4, pp. 897–914, Nov. 2016, doi: 10.1016/J.CELL.2016.10.021.

[287] A. J. Eisch, H. A. Cameron, J. M. Encinas, L. A. Meltzer, G. L. Ming, and L. S. Overstreet-Wadiche, “Adult neurogenesis, mental health, and mental illness: hope or hype?,” J Neurosci, vol. 28, no. 46, pp. 11785–11791, Nov. 2008, doi: 10.1523/JNEUROSCI.3798-08.2008.

[288] E. P. Moreno-Jiménez et al., “Adult hippocampal neurogenesis is abundant in neurologically healthy subjects and drops sharply in patients with Alzheimer’s disease,” Nat Med, vol. 25, no. 4, pp. 554–560, Apr. 2019, doi: 10.1038/S41591-019-0375-9.

[289] M. K. Tobin et al., “Human Hippocampal Neurogenesis Persists in Aged Adults and Alzheimer’s Disease Patients,” Cell Stem Cell, vol. 24, no. 6, pp. 974-982.e3, Jun. 2019, doi: 10.1016/J.STEM.2019.05.003.

[290] K. M. McAvoy et al., “Modulating Neuronal Competition Dynamics in the Dentate Gyrus to Rejuvenate Aging Memory Circuits,” Neuron, vol. 91, no. 6, pp. 1356–1373, Sep. 2016, doi: 10.1016/J.NEURON.2016.08.009.

[291] N. Urbán et al., “Return to quiescence of mouse neural stem cells by degradation of a proactivation protein,” Science, vol. 353, no. 6296, pp. 292–295, Jul. 2016, doi: 10.1126/SCIENCE.AAF4802.

[292] S. F. Sorrells et al., “Human hippocampal neurogenesis drops sharply in children to undetectable levels in adults,” Nature, vol. 555, no. 7696, pp. 377–381, Mar. 2018, doi: 10.1038/NATURE25975.

[293] K. L. Spalding et al., “Dynamics of hippocampal neurogenesis in adult humans,” Cell, vol. 153, no. 6, p. 1219, Jun. 2013, doi: 10.1016/J.CELL.2013.05.002.

[294] J. Altman, “Are new neurons formed in the brains of adult mammals?,” Science, vol. 135, no. 3509, pp. 1127–1128, 1962, doi: 10.1126/SCIENCE.135.3509.1127.

[295] S. A. Goldman and F. Nottebohm, “Neuronal production, migration, and differentiation in a vocal control nucleus of the adult female canary brain,” Proc Natl Acad Sci U S A, vol. 80, no. 8, pp. 2390–2394, 1983, doi: 10.1073/PNAS.80.8.2390.

[296] B. A. Reynolds and S. Weiss, “Generation of neurons and astrocytes from isolated cells of the adult mammalian central nervous system,” Science, vol. 255, no. 5052, pp. 1707–1710, 1992, doi: 10.1126/SCIENCE.1553558.

[297] F. H. Gage and S. Temple, “Neural stem cells: generating and regenerating the brain,” Neuron, vol. 80, no. 3, pp. 588–601, Oct. 2013, doi: 10.1016/J.NEURON.2013.10.037.

[298] M. Boldrini et al., "Human Hippocampal Neurogenesis Persists throughout Aging," Cell Stem Cell, vol. 22, no. 4, pp. 589-599.e5, Apr. 2018, doi: 10.1016/J.STEM.2018.03.015.

[299] G. Kempermann et al., "Human Adult Neurogenesis: Evidence and Remaining Questions," Cell Stem Cell, vol. 23, no. 1, pp. 25–30, Jul. 2018, doi: 10.1016/J.STEM.2018.04.004.

[300] A. M. Fjell and K. B. Walhovd, "Structural brain changes in aging: courses, causes and cognitive consequences," Rev Neurosci, vol. 21, no. 3, pp. 187–221, 2010, doi: 10.1515/REVNEURO.2010.21.3.187.

[301] A. T. Higgins-Chen, K. L. Thrush, and M. E. Levine, "Aging biomarkers and the brain," Semin Cell Dev Biol, vol. 116, pp. 180–193, Aug. 2021, doi: 10.1016/J.SEMCDB.2021.01.003.

[302] S. di Benedetto, L. Müller, E. Wenger, S. Düzel, and G. Pawelec, "Contribution of neuroinflammation and immunity to brain aging and the mitigating effects of physical and cognitive interventions," Neurosci Biobehav Rev, vol. 75, pp. 114–128, Apr. 2017, doi: 10.1016/J.NEUBIOREV.2017.01.044.

[303] J. Cohen and C. Torres, "Astrocyte senescence: Evidence and significance," Aging Cell, vol. 18, no. 3, Jun. 2019, doi: 10.1111/ACEL.12937.

[304] M. A. Lynch, "Age-related neuroinflammatory changes negatively impact on neuronal function," Front Aging Neurosci, vol. 1, Jan. 2010, doi: 10.3389/NEURO.24.006.2009.

[305] J. P. Godbout and R. W. Johnson, "Age and neuroinflammation: a lifetime of psychoneuroimmune consequences," Immunol Allergy Clin North Am, vol. 29, no. 2, pp. 321–337, May 2009, doi: 10.1016/J.IAC.2009.02.007.

[306] M. E. Lull and M. L. Block, "Microglial activation and chronic neurodegeneration," Neurotherapeutics, vol. 7, no. 4, pp. 354–365, Oct. 2010, doi: 10.1016/J.NURT.2010.05.014.

[307] R. Bhat et al., "Astrocyte senescence as a component of Alzheimer's disease," PLoS One, vol. 7, no. 9, Sep. 2012, doi: 10.1371/JOURNAL.PONE.0045069.

[308] D. M. Norden and J. P. Godbout, "Review: microglia of the aged brain: primed to be activated and resistant to regulation," Neuropathol Appl Neurobiol, vol. 39, no. 1, pp. 19–34, Feb. 2013, doi: 10.1111/J.1365-2990.2012.01306.X.

[309] Y. Blinkouskaya, A. Caçoilo, T. Gollamudi, S. Jalalian, and J. Weickenmeier, "Brain aging mechanisms with mechanical manifestations," Mech Ageing Dev, vol. 200, Dec. 2021, doi: 10.1016/J.MAD.2021.111575.

[310] M. P. Mattson and T. v. Arumugam, "Hallmarks of Brain Aging: Adaptive and Pathological Modification by Metabolic States," Cell Metab, vol. 27, no. 6, pp. 1176–1199, Jun. 2018, doi: 10.1016/J.CMET.2018.05.011.

[311] M. Calvo-Rodriguez and B. J. Bacskai, "Mitochondria and Calcium in Alzheimer's Disease: From Cell Signaling to Neuronal Cell Death," Trends Neurosci, vol. 44, no. 2, pp. 136–151, Feb. 2021, doi: 10.1016/J.TINS.2020.10.004.

[312] A. Grimm and A. Eckert, "Brain aging and neurodegeneration: from a mitochondrial point of view," J Neurochem, vol. 143, no. 4, pp. 418–431, Nov. 2017, doi: 10.1111/JNC.14037.

[313] J. N. Keller, K. B. Hanni, and W. R. Markesbery, "Possible involvement of proteasome inhibition in aging: implications for oxidative stress," Mech Ageing Dev, vol. 113, no. 1, pp. 61–70, Jan. 2000, doi: 10.1016/S0047-6374(99)00101-3.

[314] N. v. Bobkova et al., “Exogenous Hsp70 delays senescence and improves cognitive function in aging mice,” Proc Natl Acad Sci U S A, vol. 112, no. 52, pp. 16006–16011, Dec. 2015, doi: 10.1073/PNAS.1516131112.

[315] J. M. Hafycz, E. Strus, and N. Naidoo, “Reducing ER stress with chaperone therapy reverses sleep fragmentation and cognitive decline in aged mice,” Aging Cell, vol. 21, no. 6, Jun. 2022, doi: 10.1111/ACEL.13598.

[316] J. Auzmendi-Iriarte et al., “High levels of HDAC expression correlate with microglial aging,” Expert Opin Ther Targets, 2022, doi: 10.1080/14728222.2022.2158081.

[317] I. H. Salas, J. Burgado, and N. J. Allen, “Glia: victims or villains of the aging brain?,” Neurobiol Dis, vol. 143, Sep. 2020, doi: 10.1016/J.NBD.2020.105008.

[318] A. Diez-Ruiz, A. Bueno-Errandonea, J. Nuñez-Barrio, I. Sanchez-Martín, K. Vrotsou, and I. Vergara, “Factors associated with frailty in primary care: a prospective cohort study,” BMC Geriatr, vol. 16, no. 1, Apr. 2016, doi: 10.1186/S12877-016-0263-9.

[319] F. Rivas-Ruiz et al., “Prevalence of frailty among community-dwelling elderly persons in Spain and factors associated with it,” Eur J Gen Pract, vol. 25, no. 4, pp. 190–196, Oct. 2019, doi: 10.1080/13814788.2019.1635113.

[320] M. Machón et al., “Dietary Patterns and Their Relationship with Frailty in Functionally Independent Older Adults,” Nutrients, vol. 10, no. 4, Apr. 2018, doi: 10.3390/NU10040406.

[321] G. Fernández-Eulate et al., “Blood Markers in Healthy-Aged Nonagenarians: A Combination of High Telomere Length and Low Amyloidβ Are Strongly Associated With Healthy Aging in the Oldest Old,” Front Aging Neurosci, vol. 10, Nov. 2018, doi: 10.3389/FNAGI.2018.00380.

[322] E. Carrasco-Garcia et al., “SOX2 expression diminishes with ageing in several tissues in mice and humans,” Mech Ageing Dev, vol. 177, pp. 30–36, Jan. 2019, doi: 10.1016/J.MAD.2018.03.008.

[323] M. Moreno-Valladares et al., “CD8+ T cells are increased in the subventricular zone with physiological and pathological aging,” Aging Cell, vol. 19, no. 9, Sep. 2020, doi: 10.1111/ACEL.13198.

[324] M. Moreno-Valladares et al., “CD8+ T cells are present at low levels in the white matter with physiological and pathological aging,” Aging, vol. 12, no. 19, pp. 18928–18939, Oct. 2020, doi: 10.18632/AGING.104043.

[325] J. A. Miller et al., “Neuropathological and transcriptomic characteristics of the aged brain,” Elife, vol. 6, Nov. 2017, doi: 10.7554/ELIFE.31126.

[326] M. Olah et al., “A transcriptomic atlas of aged human microglia,” Nat Commun, vol. 9, no. 1, Dec. 2018, doi: 10.1038/S41467-018-02926-5.

[327] E. S. Lein et al., “Genome-wide atlas of gene expression in the adult mouse brain,” Nature, vol. 445, no. 7124, pp. 168–176, Jan. 2007, doi: 10.1038/NATURE05453.

[328] S. Brenner, “The genetics of Caenorhabditis elegans,” Genetics, vol. 77, no. 1, pp. 71–94, May 1974, doi: 10.1093/GENETICS/77.1.71.

[329] R. S. Kamath, M. Martinez-Campos, P. Zipperlen, A. G. Fraser, and J. Ahringer, “Effectiveness of specific RNA-mediated interference through ingested double-stranded

RNA in Caenorhabditis elegans," Genome Biol, vol. 2, no. 1, p. research0002.1, 2001, doi: 10.1186/GB-2000-2-1-RESEARCH0002.

[330] J. Schindelin et al., "Fiji: an open-source platform for biological-image analysis," Nat Methods, vol. 9, no. 7, pp. 676–682, Jul. 2012, doi: 10.1038/NMETH.2019.

[331] T. Wu et al., "clusterProfiler 4.0: A universal enrichment tool for interpreting omics data," Innovation (Cambridge (Mass.)), vol. 2, no. 3, Aug. 2021, doi: 10.1016/J.XINN.2021.100141.

[332] H. Mi, A. Muruganujan, D. Ebert, X. Huang, and P. D. Thomas, "PANTHER version 14: more genomes, a new PANTHER GO-slim and improvements in enrichment analysis tools," Nucleic Acids Res, vol. 47, no. D1, pp. D419–D426, Jan. 2019, doi: 10.1093/NAR/GKY1038.

[333] J. Tigges et al., "The hallmarks of fibroblast ageing," Mech Ageing Dev, vol. 138, no. 1, pp. 26–44, 2014, doi: 10.1016/J.MAD.2014.03.004.

[334] D. Y. Zhu et al., "MiR-454 promotes the progression of human non-small cell lung cancer and directly targets PTEN," Biomed Pharmacother, vol. 81, pp. 79–85, Jul. 2016, doi: 10.1016/J.BIOPHA.2016.03.029.

[335] B. Fang, J. Zhu, Y. Wang, F. Geng, and G. Li, "MiR-454 inhibited cell proliferation of human glioblastoma cells by suppressing PDK1 expression," Biomed Pharmacother, vol. 75, pp. 148–152, Oct. 2015, doi: 10.1016/J.BIOPHA.2015.07.029.

[336] Y. Song, Q. Guo, S. Gao, and K. Hua, "miR-454-3p promotes proliferation and induces apoptosis in human cervical cancer cells by targeting TRIM3," Biochem Biophys Res Commun, vol. 516, no. 3, pp. 872–879, Aug. 2019, doi: 10.1016/J.BBRC.2019.06.126.

[337] V. Costa et al., "DDX11L: a novel transcript family emerging from human subtelomeric regions," BMC Genomics, vol. 10, May 2009, doi: 10.1186/1471-2164-10-250.

[338] Y. R. Lee, M. Chen, and P. P. Pandolfi, "The functions and regulation of the PTEN tumour suppressor: new modes and prospects," Nat Rev Mol Cell Biol, vol. 19, no. 9, pp. 547–562, Sep. 2018, doi: 10.1038/S41580-018-0015-0.

[339] Q. Xu et al., "Targeting amphiregulin (AREG) derived from senescent stromal cells diminishes cancer resistance and averts programmed cell death 1 ligand (PD-L1)-mediated immunosuppression," Aging Cell, vol. 18, no. 6, Dec. 2019, doi: 10.1111/ACEL.13027.

[340] M. Das et al., "Suppression of p53-dependent senescence by the JNK signal transduction pathway," Proc Natl Acad Sci U S A, vol. 104, no. 40, pp. 15759–15764, Oct. 2007, doi: 10.1073/PNAS.0707782104.

[341] H. Miyahara et al., "[Local control after radiation therapy for T1N0M0 glottic carcinoma]," Nihon Jibiinkoka Gakkai Kaiho, vol. 92, no. 3, pp. 414–419, 1989, doi: 10.3950/JIBIINKOKA.92.414.

[342] R. Kumari and P. Jat, "Mechanisms of Cellular Senescence: Cell Cycle Arrest and Senescence Associated Secretory Phenotype," Front Cell Dev Biol, vol. 9, Mar. 2021, doi: 10.3389/FCELL.2021.645593.

[343] J. Chang et al., "Clearance of senescent cells by ABT263 rejuvenates aged hematopoietic stem cells in mice," Nat Med, vol. 22, no. 1, pp. 78–83, Jan. 2016, doi: 10.1038/NM.4010.

[344] Y. Zhu et al., "Identification of a novel senolytic agent, navitoclax, targeting the Bcl-2 family of anti-apoptotic factors," Aging Cell, vol. 15, no. 3, pp. 428–435, Jun. 2016, doi: 10.1111/ACEL.12445.

[345] Y. Zhu et al., “The Achilles’ heel of senescent cells: from transcriptome to senolytic drugs,” Aging Cell, vol. 14, no. 4, pp. 644–658, 2015, doi: 10.1111/ACEL.12344.

[346] P. Deloron et al., “Serological reactivity to the ring-infected erythrocyte surface antigen and circumsporozoite protein in gravid and nulligravid women infected with Plasmodium falciparum,” Trans R Soc Trop Med Hyg, vol. 83, no. 1, pp. 58–62, 1989, doi: 10.1016/0035-9203(89)90705-0.

[347] J. G. Izant and J. R. McIntosh, “Microtubule-associated proteins: a monoclonal antibody to MAP2 binds to differentiated neurons,” Proc Natl Acad Sci U S A, vol. 77, no. 8, pp. 4741–4745, 1980, doi: 10.1073/PNAS.77.8.4741.

[348] O. von Bohlen Und Halbach, “Immunohistological markers for staging neurogenesis in adult hippocampus,” Cell Tissue Res, vol. 329, no. 3, pp. 409–420, Sep. 2007, doi: 10.1007/S00441-007-0432-4.

[349] M. K. Lee, J. B. Tuttle, L. I. Rebhun, D. W. Cleveland, and A. Frankfurter, “The expression and posttranslational modification of a neuron-specific beta-tubulin isotype during chick embryogenesis,” Cell Motil Cytoskeleton, vol. 17, no. 2, pp. 118–132, 1990, doi: 10.1002/CM.970170207.

[350] E. E. Geisert and A. Frankfurter, “The neuronal response to injury as visualized by immunostaining of class III beta-tubulin in the rat,” Neurosci Lett, vol. 102, no. 2–3, pp. 137–141, Jul. 1989, doi: 10.1016/0304-3940(89)90068-2.

[351] A. M. Jurga, M. Paleczna, J. Kadluczka, and K. Z. Kuter, “Beyond the GFAP-Astrocyte Protein Markers in the Brain,” Biomolecules, vol. 11, no. 9, Sep. 2021, doi: 10.3390/BIOM11091361.

[352] M. Yokoi and F. Hanaoka, “Two mammalian homologs of yeast Rad23, HR23A and HR23B, as multifunctional proteins,” Gene, vol. 597, pp. 1–9, Jan. 2017, doi: 10.1016/J.GENE.2016.10.027.

[353] T. Flatt and L. Partridge, “Horizons in the evolution of aging,” BMC Biol, vol. 16, no. 1, Aug. 2018, doi: 10.1186/S12915-018-0562-Z.

[354] J. Viña, A. Salvador-Pascual, F. J. Tarazona-Santabalbina, L. Rodriguez-Mañas, and M. C. Gomez-Cabrera, “Exercise training as a drug to treat age associated frailty,” Free Radic Biol Med, vol. 98, pp. 159–164, Sep. 2016, doi: 10.1016/J.FREERADBIOMED.2016.03.024.

[355] R. Calvani et al., “Biomarkers for physical frailty and sarcopenia: state of the science and future developments,” J Cachexia Sarcopenia Muscle, vol. 6, no. 4, pp. 278–286, Dec. 2015, doi: 10.1002/JCSM.12051.

[356] R. J. J. Gobbens, J. M. G. A. Schols, and M. A. L. M. van Assen, “Exploring the efficiency of the Tilburg Frailty Indicator: a review,” Clin Interv Aging, vol. 12, pp. 1739–1752, Oct. 2017, doi: 10.2147/CIA.S130686.

[357] I. Vergara et al., “Description of frail older people profiles according to four screening tools applied in primary care settings: a cross sectional analysis,” BMC Geriatr, vol. 19, no. 1, Dec. 2019, doi: 10.1186/S12877-019-1354-1.

[358] B. Hsu et al., “Cross-Sectional and Longitudinal Relationships Between Inflammatory Biomarkers and Frailty in Community-dwelling Older Men: The Concord Health and Ageing in Men Project,” J Gerontol A Biol Sci Med Sci, vol. 74, no. 6, pp. 835–841, May 2019, doi: 10.1093/GERONA/GLX142.

[359] J. Vina et al., "Pharmacological properties of physical exercise in the elderly," Curr Pharm Des, vol. 20, no. 18, pp. 3019–3029, May 2014, doi: 10.2174/13816128113196660704.

[360] C. Rezola-Pardo et al., "Effects of multicomponent and dual-task exercise on falls in nursing homes: The AgeingOn Dual-Task study," Maturitas, vol. 164, pp. 15–22, Oct. 2022, doi: 10.1016/J.MATURITAS.2022.06.006.

[361] H. Arrieta et al., "Effects of an individualized and progressive multicomponent exercise program on blood pressure, cardiorespiratory fitness, and body composition in long-term care residents: Randomized controlled trial," Geriatr Nurs, vol. 45, pp. 77–84, May 2022, doi: 10.1016/J.GERINURSE.2022.03.005.

[362] C. Rezola-Pardo et al., "Comparison Between Multicomponent Exercise and Walking Interventions in Long-Term Nursing Homes: A Randomized Controlled Trial," Gerontologist, vol. 60, no. 7, pp. 1364–1373, Oct. 2020, doi: 10.1093/GERONT/GNZ177.

[363] C. Rezola-Pardo et al., "Comparison between multicomponent and simultaneous dual-task exercise interventions in long-term nursing home residents: the Ageing-ONDUAL-TASK randomized controlled study," Age Ageing, vol. 48, no. 6, pp. 817–823, Nov. 2019, doi: 10.1093/AGEING/AFZ105.

[364] H. Arrieta et al., "The impact of physical exercise on cognitive and affective functions and serum levels of brain-derived neurotrophic factor in nursing home residents: A randomized controlled trial," Maturitas, vol. 131, pp. 72–77, Jan. 2020, doi: 10.1016/J.MATURITAS.2019.10.014.

[365] B. Davies, F. García, I. Ara, F. R. Artalejo, L. Rodriguez-Mañas, and S. Walter, "Relationship Between Sarcopenia and Frailty in the Toledo Study of Healthy Aging: A Population Based Cross-Sectional Study," J Am Med Dir Assoc, vol. 19, no. 4, pp. 282–286, Apr. 2018, doi: 10.1016/J.JAMDA.2017.09.014.

[366] M. Cesari, F. Landi, B. Vellas, R. Bernabei, and E. Marzetti, "Sarcopenia and physical frailty: two sides of the same coin," Front Aging Neurosci, vol. 6, no. JUL, 2014, doi: 10.3389/FNAGI.2014.00192.

[367] A. Mitnitski et al., "Age-related frailty and its association with biological markers of ageing," BMC Med, vol. 13, no. 1, Jul. 2015, doi: 10.1186/S12916-015-0400-X.

[368] F. Pellicano et al., "hsa-mir183/EGR1-mediated regulation of E2F1 is required for CML stem/progenitor cell survival," Blood, vol. 131, no. 14, pp. 1532–1544, Apr. 2018, doi: 10.1182/BLOOD-2017-05-783845.

[369] T. E. Kimura et al., "Inhibition of Egr1 expression underlies the anti-mitogenic effects of cAMP in vascular smooth muscle cells," J Mol Cell Cardiol, vol. 72, no. 100, pp. 9–19, 2014, doi: 10.1016/J.YJMCC.2014.02.001.

[370] C. Liu, V. M. Rangnekar, E. Adamson, and D. Mercola, "Suppression of growth and transformation and induction of apoptosis by EGR-1.," Cancer Gene Ther, vol. 5, no. 1, pp. 3–28, Jan. 1998, Accessed: Jan. 18, 2023. [Online]. Available: https://europepmc.org/article/med/9476963

[371] C. S. Riedel, B. Georg, H. L. Jørgensen, J. Hannibal, and J. Fahrenkrug, "Mice Lacking EGR1 Have Impaired Clock Gene (BMAL1) Oscillation, Locomotor Activity, and Body Temperature," J Mol Neurosci, vol. 64, no. 1, pp. 9–19, Jan. 2018, doi: 10.1007/S12031-017-0996-8.

[372] S. F. Yan et al., “Egr-1, a master switch coordinating upregulation of divergent gene families underlying ischemic stress,” Nat Med, vol. 6, no. 12, pp. 1355–1361, 2000, doi: 10.1038/82168.

[373] V. Baron, E. D. Adamson, A. Calogero, G. Ragona, and D. Mercola, “The transcription factor Egr1 is a direct regulator of multiple tumor suppressors including TGFbeta1, PTEN, p53, and fibronectin,” Cancer Gene Ther, vol. 13, no. 2, pp. 115–124, Feb. 2006, doi: 10.1038/SJ.CGT.7700896.

[374] F. Duclot and M. Kabbaj, “The Role of Early Growth Response 1 (EGR1) in Brain Plasticity and Neuropsychiatric Disorders,” Front Behav Neurosci, vol. 11, Mar. 2017, doi: 10.3389/FNBEH.2017.00035.

[375] Y. Zwang, M. Oren, and Y. Yarden, “Consistency test of the cell cycle: roles for p53 and EGR1,” Cancer Res, vol. 72, no. 5, pp. 1051–1054, Mar. 2012, doi: 10.1158/0008-5472.CAN-11-3382.

[376] J. C. Acosta et al., “Chemokine signaling via the CXCR2 receptor reinforces senescence,” Cell, vol. 133, no. 6, pp. 1006–1018, Jun. 2008, doi: 10.1016/J.CELL.2008.03.038.

[377] A. Freund, C. K. Patil, and J. Campisi, “p38MAPK is a novel DNA damage response-independent regulator of the senescence-associated secretory phenotype,” EMBO J, vol. 30, no. 8, pp. 1536–1548, Apr. 2011, doi: 10.1038/EMBOJ.2011.69.

[378] Y. Sun et al., “Treatment-induced damage to the tumor microenvironment promotes prostate cancer therapy resistance through WNT16B,” Nat Med, vol. 18, no. 9, pp. 1359–1368, Sep. 2012, doi: 10.1038/NM.2890.

[379] C. Anerillas, K. Abdelmohsen, and M. Gorospe, “Regulation of senescence traits by MAPKs,” Geroscience, vol. 42, no. 2, pp. 397–408, Apr. 2020, doi: 10.1007/S11357-020-00183-3.

[380] K. Inoue and E. A. Fry, “Tumor suppression by the EGR1, DMP1, ARF, p53, and PTEN Network,” Cancer Invest, vol. 36, no. 9–10, pp. 520–536, Nov. 2018, doi: 10.1080/07357907.2018.1533965.

[381] H. Ko, J. M. Kim, S. J. Kim, S. H. Shim, C. H. Ha, and H. I. Chang, “Induction of apoptosis by genipin inhibits cell proliferation in AGS human gastric cancer cells via Egr1/p21 signaling pathway,” Bioorg Med Chem Lett, vol. 25, no. 19, pp. 4191–4196, Oct. 2015, doi: 10.1016/J.BMCL.2015.08.005.

[382] L. Yuan, P. Mu, B. Huang, H. Li, H. Mu, and Y. Deng, “EGR1 is essential for deoxynivalenol-induced G2/M cell cycle arrest in HepG2 cells via the ATF3ΔZip2a/2b-EGR1-p21 pathway,” Toxicol Lett, vol. 299, pp. 95–103, Dec. 2018, doi: 10.1016/J.TOXLET.2018.09.012.

[383] D. J. Baker, R. L. Weaver, and J. M. VanDeursen, “p21 both attenuates and drives senescence and aging in BubR1 progeroid mice,” Cell Rep, vol. 3, no. 4, pp. 1164–1174, Apr. 2013, doi: 10.1016/J.CELREP.2013.03.028.

[384] Y.-S. Cong, W. E. Wright, and J. W. Shay, “Human telomerase and its regulation,” Microbiol Mol Biol Rev, vol. 66, no. 3, pp. 407–425, Sep. 2002, doi: 10.1128/MMBR.66.3.407-425.2002.

[385] J. N. Justice et al., “Cellular Senescence Biomarker p16INK4a+ Cell Burden in Thigh Adipose is Associated With Poor Physical Function in Older Women,” J Gerontol A Biol Sci Med Sci, vol. 73, no. 7, pp. 939–945, Jun. 2018, doi: 10.1093/GERONA/GLX134.

[386] L. Ma, G. Sha, Y. Zhang, and Y. Li, "Elevated serum IL-6 and adiponectin levels are associated with frailty and physical function in Chinese older adults," Clin Interv Aging, vol. 13, pp. 2013–2020, 2018, doi: 10.2147/CIA.S180934.

[387] H. Y. Lai, H. T. Chang, Y. L. Lee, and S. J. Hwang, "Association between inflammatory markers and frailty in institutionalized older men," Maturitas, vol. 79, no. 3, pp. 329–333, Nov. 2014, doi: 10.1016/J.MATURITAS.2014.07.014.

[388] W. J. Lee, L. K. Chen, C. K. Liang, L. N. Peng, S. T. Chiou, and P. Chou, "Soluble ICAM-1, Independent of IL-6, Is Associated with Prevalent Frailty in Community-Dwelling Elderly Taiwanese People," PLoS One, vol. 11, no. 6, Jun. 2016, doi: 10.1371/JOURNAL.PONE.0157877.

[389] W. Semmarath et al., "The Association between Frailty Indicators and Blood-Based Biomarkers in Early-Old Community Dwellers of Thailand," Int J Environ Res Public Health, vol. 16, no. 18, Sep. 2019, doi: 10.3390/IJERPH16183457.

[390] J. Collerton et al., "Frailty and the role of inflammation, immunosenescence and cellular ageing in the very old: cross-sectional findings from the Newcastle 85+ Study," Mech Ageing Dev, vol. 133, no. 6, pp. 456–466, Jun. 2012, doi: 10.1016/J.MAD.2012.05.005.

[391] B. G. Childs et al., "Senescent cells: an emerging target for diseases of ageing," Nat Rev Drug Discov, vol. 16, no. 10, pp. 718–735, Oct. 2017, doi: 10.1038/NRD.2017.116.

[392] S. He and N. E. Sharpless, "Senescence in Health and Disease," Cell, vol. 169, no. 6, pp. 1000–1011, Jun. 2017, doi: 10.1016/J.CELL.2017.05.015.

[393] D. J. Baker et al., "Clearance of p16Ink4a-positive senescent cells delays ageing-associated disorders," Nature, vol. 479, no. 7372, pp. 232–236, Nov. 2011, doi: 10.1038/NATURE10600.

[394] M. P. Baar et al., "Targeted Apoptosis of Senescent Cells Restores Tissue Homeostasis in Response to Chemotoxicity and Aging," Cell, vol. 169, no. 1, pp. 132-147.e16, Mar. 2017, doi: 10.1016/J.CELL.2017.02.031.

[395] M. Xu et al., "Senolytics improve physical function and increase lifespan in old age," Nat Med, vol. 24, no. 8, pp. 1246–1256, Aug. 2018, doi: 10.1038/S41591-018-0092-9.

[396] M. García-Puga et al., "Senescence plays a role in myotonic dystrophy type 1," JCI Insight, vol. 7, no. 19, Oct. 2022, doi: 10.1172/JCI.INSIGHT.159357.

[397] J. N. Justice et al., "Senolytics in idiopathic pulmonary fibrosis: Results from a first-in-human, open-label, pilot study," EBioMedicine, vol. 40, pp. 554–563, Feb. 2019, doi: 10.1016/J.EBIOM.2018.12.052.

[398] L. T. J. Hickson et al., "Senolytics decrease senescent cells in humans: Preliminary report from a clinical trial of Dasatinib plus Quercetin in individuals with diabetic kidney disease," EBioMedicine, vol. 47, pp. 446–456, Sep. 2019, doi: 10.1016/J.EBIOM.2019.08.069.

[399] D. Marcos-Pérez, A. Saenz-Antoñanzas, and A. Matheu, "Centenarians as models of healthy aging: Example of REST," Ageing Res Rev, vol. 70, Sep. 2021, doi: 10.1016/J.ARR.2021.101392.

[400] W. Chowanadisai, "Comparative genomic analysis of slc39a12/ZIP12: insight into a zinc transporter required for vertebrate nervous system development," PLoS One, vol. 9, no. 11, Nov. 2014, doi: 10.1371/JOURNAL.PONE.0111535.

[401] W. Chowanadisai, D. M. Graham, C. L. Keen, R. B. Rucker, and M. A. Messerli, “Neurulation and neurite extension require the zinc transporter ZIP12 (slc39a12),” Proc Natl Acad Sci U S A, vol. 110, no. 24, pp. 9903–9908, Jun. 2013, doi: 10.1073/PNAS.1222142110.

[402] E. Scarr et al., “Increased cortical expression of the zinc transporter SLC39A12 suggests a breakdown in zinc cellular homeostasis as part of the pathophysiology of schizophrenia,” NPJ Schizophr, vol. 2, Mar. 2016, doi: 10.1038/NPJSCHZ.2016.2.

[403] M. Bly, “Examination of the zinc transporter gene, SLC39A12,” Schizophr Res, vol. 81, no. 2–3, pp. 321–322, Jan. 2006, doi: 10.1016/J.SCHRES.2005.07.039.

[404] N. Krumm et al., “Excess of rare, inherited truncating mutations in autism,” Nat Genet, vol. 47, no. 6, pp. 582–588, May 2015, doi: 10.1038/NG.3303.

[405] P. Babula et al., “Mammalian metallothioneins: properties and functions,” Metallomics, vol. 4, no. 8, pp. 739–750, Aug. 2012, doi: 10.1039/C2MT20081C.

[406] M. Nordberg and G. F. Nordberg, “Toxicological aspects of metallothionein.,” Cell Mol Biol (Noisy-le-grand), vol. 46, no. 2, pp. 451–463, Mar. 2000, Accessed: Jan. 18, 2023. [Online]. Available: https://europepmc.org/article/MED/10774933

[407] W. R. Swindell, “Metallothionein and the biology of aging,” Ageing Res Rev, vol. 10, no. 1, pp. 132–145, Jan. 2011, doi: 10.1016/J.ARR.2010.09.007.

[408] J. W. Asmussen, M. L. von Sperling, and M. Penkowa, “Intraneuronal signaling pathways of metallothionein,” J Neurosci Res, vol. 87, no. 13, pp. 2926–2936, Oct. 2009, doi: 10.1002/JNR.22118.

[409] J. Y. Koh and S. J. Lee, “Metallothionein-3 as a multifunctional player in the control of cellular processes and diseases,” Mol Brain, vol. 13, no. 1, Aug. 2020, doi: 10.1186/S13041-020-00654-W.

[410] M. Dutsch-Wicherek, J. Sikora, and R. Tomaszewska, “The possible biological role of metallothionein in apoptosis,” Front Biosci, vol. 13, no. 11, pp. 4029–4038, 2008, doi: 10.2741/2991.

[411] J. H. Kim, Y. P. Nam, S. M. Jeon, H. S. Han, and K. Suk, “Amyloid neurotoxicity is attenuated by metallothionein: dual mechanisms at work,” J Neurochem, vol. 121, no. 5, pp. 751–762, Jun. 2012, doi: 10.1111/J.1471-4159.2012.07725.X.

[412] M. Ebadi and S. Sharma, “Metallothioneins 1 and 2 attenuate peroxynitrite-induced oxidative stress in Parkinson disease,” Exp Biol Med (Maywood), vol. 231, no. 9, pp. 1576–1583, 2006, doi: 10.1177/153537020623100919.

[413] J. Hidalgo, M. Aschner, P. Zatta, and M. Vašák, “Roles of the metallothionein family of proteins in the central nervous system,” Brain Res Bull, vol. 55, no. 2, pp. 133–145, May 2001, doi: 10.1016/S0361-9230(01)00452-X.

[414] T. Kimura and T. Kambe, “The Functions of Metallothionein and ZIP and ZnT Transporters: An Overview and Perspective,” Int J Mol Sci, vol. 17, no. 3, Mar. 2016, doi: 10.3390/IJMS17030336.

[415] T. T. Ngu and M. J. Stillman, “Metalation of metallothioneins,” IUBMB Life, vol. 61, no. 4, pp. 438–446, 2009, doi: 10.1002/IUB.182.

[416] D. Juárez-Rebollar, C. Rios, C. Nava-Ruíz, and M. Méndez-Armenta, “Metallothionein in Brain Disorders,” Oxid Med Cell Longev, vol. 2017, 2017, doi: 10.1155/2017/5828056.

[417] J. Bousleiman et al., "Function of Metallothionein-3 in Neuronal Cells: Do Metal Ions Alter Expression Levels of MT3?," Int J Mol Sci, vol. 18, no. 6, Jun. 2017, doi: 10.3390/IJMS18061133.

[418] R. Giacconi et al., "Zinc-Induced Metallothionein in Centenarian Offspring From a Large European Population: The MARK-AGE Project," J Gerontol A Biol Sci Med Sci, vol. 73, no. 6, pp. 745–753, May 2018, doi: 10.1093/GERONA/GLX192.

[419] S. D. Gower-Winter and C. W. Levenson, "Zinc in the central nervous system: From molecules to behavior," Biofactors, vol. 38, no. 3, pp. 186–193, May 2012, doi: 10.1002/BIOF.1012.

[420] S. D. Portbury and P. A. Adlard, "Zinc Signal in Brain Diseases," Int J Mol Sci, vol. 18, no. 12, Dec. 2017, doi: 10.3390/IJMS18122506.

[421] S. M. Hancock, D. I. Finkelstein, and P. A. Adlard, "Glia and zinc in ageing and Alzheimer's disease: a mechanism for cognitive decline?," Front Aging Neurosci, vol. 6, no. JUN, 2014, doi: 10.3389/FNAGI.2014.00137.

[422] T. Kambe, T. Tsuji, A. Hashimoto, and N. Itsumura, "The Physiological, Biochemical, and Molecular Roles of Zinc Transporters in Zinc Homeostasis and Metabolism," Physiol Rev, vol. 95, no. 3, pp. 749–784, Jul. 2015, doi: 10.1152/PHYSREV.00035.2014.

[423] E. Mocchegiani et al., "Zinc homeostasis in aging: two elusive faces of the same 'metal,'" Rejuvenation Res, vol. 9, no. 2, pp. 351–354, Jun. 2006, doi: 10.1089/REJ.2006.9.351.

[424] D. H. Linkous et al., "Evidence that the ZNT3 protein controls the total amount of elemental zinc in synaptic vesicles," J Histochem Cytochem, vol. 56, no. 1, pp. 3–6, Jan. 2008, doi: 10.1369/JHC.6A7035.2007.

[425] T. Saito et al., "Deficiencies of hippocampal Zn and ZnT3 accelerate brain aging of Rat," Biochem Biophys Res Commun, vol. 279, no. 2, pp. 505–511, Dec. 2000, doi: 10.1006/BBRC.2000.3946.

[426] T. J. da Rocha et al., "The effects of interactions between selenium and zinc serum concentration and SEP15 and SLC30A3 gene polymorphisms on memory scores in a population of mature and elderly adults," Genes Nutr, vol. 9, no. 1, Jan. 2014, doi: 10.1007/S12263-013-0377-Z.

[427] P. A. Adlard, J. M. Parncutt, D. I. Finkelstein, and A. I. Bush, "Cognitive loss in zinc transporter-3 knock-out mice: a phenocopy for the synaptic and memory deficits of Alzheimer's disease?," J Neurosci, vol. 30, no. 5, pp. 1631–1636, Feb. 2010, doi: 10.1523/JNEUROSCI.5255-09.2010.

[428] O. M. Ijomone, C. W. Ifenatuoha, O. M. Aluko, O. K. Ijomone, and M. Aschner, "The aging brain: impact of heavy metal neurotoxicity," Crit Rev Toxicol, vol. 50, no. 9, pp. 801–814, 2020, doi: 10.1080/10408444.2020.1838441.

[429] K. A. Walker, N. Basisty, D. M. Wilson, and L. Ferrucci, "Connecting aging biology and inflammation in the omics era," J Clin Invest, vol. 132, no. 14, Jul. 2022, doi: 10.1172/JCI158448.

[430] E. D. Levin, C. Perraut, N. Pollard, and J. H. Freedman, "Metallothionein expression and neurocognitive function in mice," Physiol Behav, vol. 87, no. 3, pp. 513–518, Mar. 2006, doi: 10.1016/J.PHYSBEH.2005.11.014.

[431] J. Carrasco et al., “Role of metallothionein-III following central nervous system damage,” Neurobiol Dis, vol. 13, no. 1, pp. 22–36, 2003, doi: 10.1016/S0969-9961(03)00015-9.

[432] N. Thirumoorthy, A. Shyam Sunder, K. T. Manisenthil Kumar, M. Senthil kumar, G. N. K. Ganesh, and M. Chatterjee, “A review of metallothionein isoforms and their role in pathophysiology,” World J Surg Oncol, vol. 9, May 2011, doi: 10.1186/1477-7819-9-54.

[433] M. Malavolta and K. Pabis, “Elevated metallothionein expression in long-lived species,” Aging, vol. 14, no. 1, pp. 1–3, 2022, doi: 10.18632/AGING.203831.

[434] E. C. Carlson et al., “Podocyte-specific overexpression of metallothionein mitigates diabetic complications in the glomerular filtration barrier and glomerular histoarchitecture: a transmission electron microscopy stereometric analysis,” Diabetes Metab Res Rev, vol. 29, no. 2, pp. 113–124, Feb. 2013, doi: 10.1002/DMRR.2342.

[435] W. Sun et al., “Zinc rescue of Akt2 gene deletion-linked murine cardiac dysfunction and pathological changes is metallothionein-dependent,” J Mol Cell Cardiol, vol. 74, pp. 88–97, 2014, doi: 10.1016/J.YJMCC.2014.04.023.

[436] K. Inoue et al., “Role of metallothionein in coagulatory disturbance and systemic inflammation induced by lipopolysaccharide in mice,” FASEB J, vol. 20, no. 3, pp. 533–535, Mar. 2006, doi: 10.1096/FJ.05-3864FJE.

[437] M. Higashimoto et al., “Preventive effects of metallothionein against DNA and lipid metabolic damages in dyslipidemic mice under repeated mild stress,” J Med Invest, vol. 60, no. 3–4, pp. 240–248, 2013, doi: 10.2152/JMI.60.240.

[438] M. Malavolta et al., “Survival study of metallothionein-1 transgenic mice and respective controls (C57BL/6J): influence of a zinc-enriched environment,” Rejuvenation Res, vol. 15, no. 2, pp. 140–143, Apr. 2012, doi: 10.1089/REJ.2011.1261.

[439] X. Yang et al., “Metallothionein prolongs survival and antagonizes senescence-associated cardiomyocyte diastolic dysfunction: role of oxidative stress,” FASEB J, vol. 20, no. 7, pp. 1024–1026, May 2006, doi: 10.1096/FJ.05-5288FJE.

[440] D. BARSYTE, D. A. LOVEJOY, and G. J. LITHGOW, “Longevity and heavy metal resistance in daf-2 and age-1 long-lived mutants of Caenorhabditis elegans,” FASEB J, vol. 15, no. 3, pp. 627–634, Mar. 2001, doi: 10.1096/FJ.99-0966COM.

[441] Y. Kadota et al., “Deficiency of metallothionein-1 and -2 genes shortens the lifespan of the 129/Sv mouse strain,” Exp Gerontol, vol. 66, pp. 21–24, Jun. 2015, doi: 10.1016/J.EXGER.2015.04.007.

[442] C. Cipriano et al., “Polymorphisms in MT1a gene coding region are associated with longevity in Italian Central female population,” Biogerontology, vol. 7, no. 5–6, pp. 357–365, Oct. 2006, doi: 10.1007/S10522-006-9050-X.

[443] M. Karlsson et al., “A single-cell type transcriptomics map of human tissues,” Sci Adv, vol. 7, no. 31, Jul. 2021, doi: 10.1126/SCIADV.ABH2169.

[444] J. Hidalgo, “Metallothioneins and brain injury: What transgenic mice tell us,” Environ Health Prev Med, vol. 9, no. 3, pp. 87–94, May 2004, doi: 10.1007/BF02898066.

[445] M. van Lookeren Campagne et al., “Evidence for a protective role of metallothionein-1 in focal cerebral ischemia,” Proc Natl Acad Sci U S A, vol. 96, no. 22, pp. 12870–12875, Oct. 1999, doi: 10.1073/PNAS.96.22.12870.

[446] G. Trendelenburg et al., "Serial analysis of gene expression identifies metallothionein-II as major neuroprotective gene in mouse focal cerebral ischemia," J Neurosci, vol. 22, no. 14, pp. 5879–5888, Jul. 2002, doi: 10.1523/JNEUROSCI.22-14-05879.2002.

[447] M. Penkowa, J. Carrasco, M. Giralt, T. Moos, and J. Hidalgo, "CNS wound healing is severely depressed in metallothionein I- and II-deficient mice," J Neurosci, vol. 19, no. 7, pp. 2535–2545, Apr. 1999, doi: 10.1523/JNEUROSCI.19-07-02535.1999.

[448] G. M. C. J. H. H. H. J. Penkowa M, "Impaired inflammatory response and increased oxidative stress and neurodegeneration after brain injury in interleukin-6-deficient mice.," Glia, vol. 32, no. 3, pp. 271–285, Dec. 2000.

[449] M. Penkowa, "Metallothioneins are multipurpose neuroprotectants during brain pathology," FEBS J, vol. 273, no. 9, pp. 1857–1870, May 2006, doi: 10.1111/J.1742-4658.2006.05207.X.

[450] M. Penkowa and J. Hidalgo, "Metallothionein treatment reduces proinflammatory cytokines IL-6 and TNF-alpha and apoptotic cell death during experimental autoimmune encephalomyelitis (EAE)," Exp Neurol, vol. 170, no. 1, pp. 1–14, 2001, doi: 10.1006/EXNR.2001.7675.

[451] S. J. Lee, B. R. Seo, and J. Y. Koh, "Metallothionein-3 modulates the amyloid β endocytosis of astrocytes through its effects on actin polymerization," Mol Brain, vol. 8, no. 1, Dec. 2015, doi: 10.1186/S13041-015-0173-3.

[452] C. B. Poulsen et al., "Brain response to traumatic brain injury in wild-type and interleukin-6 knockout mice: a microarray analysis," J Neurochem, vol. 92, no. 2, pp. 417–432, Jan. 2005, doi: 10.1111/J.1471-4159.2004.02877.X.

[453] M. Penkowa et al., "Metallothionein-I overexpression alters brain inflammation and stimulates brain repair in transgenic mice with astrocyte-targeted interleukin-6 expression," Glia, vol. 42, no. 3, pp. 287–306, May 2003, doi: 10.1002/GLIA.10208.

[454] J. Hernández, A. Molinero, I. L. Campbell, and J. Hidalgo, "Transgenic expression of interleukin 6 in the central nervous system regulates brain metallothionein-I and -III expression in mice," Molecular Brain Research, vol. 48, no. 1, pp. 125–131, Aug. 1997, doi: 10.1016/S0169-328X(97)00087-9.

[455] J. Carrasco, J. Hernandez, B. Gonzalez, I. L. Campbell, and J. Hidalgo, "Localization of metallothionein-I and -III expression in the CNS of transgenic mice with astrocyte-targeted expression of interleukin 6," Exp Neurol, vol. 153, no. 2, pp. 184–194, 1998, doi: 10.1006/EXNR.1998.6861.

[456] J. Carrasco, M. Giralt, M. Penkowa, A. K. Stalder, I. L. Campbell, and J. Hidalgo, "Metallothioneins are upregulated in symptomatic mice with astrocyte-targeted expression of tumor necrosis factor-alpha," Exp Neurol, vol. 163, no. 1, pp. 46–54, 2000, doi: 10.1006/EXNR.1999.7335.

[457] U. Wilhelmsson et al., "Redefining the concept of reactive astrocytes as cells that remain within their unique domains upon reaction to injury," Proc Natl Acad Sci U S A, vol. 103, no. 46, pp. 17513–17518, Nov. 2006, doi: 10.1073/PNAS.0602841103.

[458] C. Scuderi, C. Stecca, A. Iacomino, and L. Steardo, "Role of astrocytes in major neurological disorders: the evidence and implications," IUBMB Life, vol. 65, no. 12, pp. 957–961, Dec. 2013, doi: 10.1002/IUB.1223.

[459] F. Giovannoni and F. J. Quintana, “The Role of Astrocytes in CNS Inflammation,” Trends Immunol, vol. 41, no. 9, pp. 805–819, Sep. 2020, doi: 10.1016/J.IT.2020.07.007.

[460] L. Lange Canhos et al., “Repetitive injury and absence of monocytes promote astrocyte self-renewal and neurological recovery,” Glia, vol. 69, no. 1, pp. 165–181, Jan. 2021, doi: 10.1002/GLIA.23893.

[461] M. v. Sofroniew, “Astrocyte Reactivity: Subtypes, States, and Functions in CNS Innate Immunity,” Trends Immunol, vol. 41, no. 9, pp. 758–770, Sep. 2020, doi: 10.1016/J.IT.2020.07.004.

[462] C. Escartin et al., “Reactive astrocyte nomenclature, definitions, and future directions,” Nat Neurosci, vol. 24, no. 3, pp. 312–325, Mar. 2021, doi: 10.1038/S41593-020-00783-4.

[463] N. Habib et al., “Div-Seq: Single-nucleus RNA-Seq reveals dynamics of rare adult newborn neurons,” Science, vol. 353, no. 6302, pp. 925–928, Aug. 2016, doi: 10.1126/SCIENCE.AAD7038.

[464] O. Krut, K. Wiegmann, H. Kashkar, B. Yazdanpanah, and M. Krönke, “Novel tumor necrosis factor-responsive mammalian neutral sphingomyelinase-3 is a C-tail-anchored protein,” J Biol Chem, vol. 281, no. 19, pp. 13784–13793, May 2006, doi: 10.1074/JBC.M511306200.

[465] C. A. Corcoran, Q. He, S. Ponnusamy, B. Ogretmen, Y. Huang, and M. S. Sheikh, “Neutral sphingomyelinase-3 is a DNA damage and nongenotoxic stress-regulated gene that is deregulated in human malignancies,” Mol Cancer Res, vol. 6, no. 5, pp. 795–807, May 2008, doi: 10.1158/1541-7786.MCR-07-2097.

[466] W. A. Andrade et al., “Early endosome localization and activity of RasGEF1b, a toll-like receptor-inducible Ras guanine-nucleotide exchange factor,” Genes Immun, vol. 11, no. 6, pp. 447–457, Sep. 2010, doi: 10.1038/GENE.2009.107.

[467] W. bin Liu et al., “Epigenetic regulation of ANKRD18B in lung cancer,” Mol Carcinog, vol. 54, no. 4, pp. 312–321, Apr. 2015, doi: 10.1002/MC.22101.

[468] S. Rao et al., “Biological Function of HYOU1 in Tumors and Other Diseases,” Onco Targets Ther, vol. 14, pp. 1727–1735, 2021, doi: 10.2147/OTT.S297332.

[469] S. Katiyar and W. J. Lennarz, “Studies on the intracellular localization of hHR23B,” Biochem Biophys Res Commun, vol. 337, no. 4, pp. 1296–1300, Dec. 2005, doi: 10.1016/J.BBRC.2005.09.192.

[470] L. Narciso et al., “The Response to Oxidative DNA Damage in Neurons: Mechanisms and Disease,” Neural Plast, vol. 2016, 2016, doi: 10.1155/2016/3619274.

[471] L. Chen and K. Madura, “Evidence for distinct functions for human DNA repair factors hHR23A and hHR23B,” FEBS Lett, vol. 580, no. 14, pp. 3401–3408, Jun. 2006, doi: 10.1016/J.FEBSLET.2006.05.012.

[472] F. W. Riemslagh et al., “HR23B pathology preferentially co-localizes with p62, pTDP-43 and poly-GA in C9ORF72-linked frontotemporal dementia and amyotrophic lateral sclerosis,” Acta Neuropathol Commun, vol. 7, no. 1, p. 39, Mar. 2019, doi: 10.1186/S40478-019-0694-6.

[473] S. Bergink et al., “The DNA repair-ubiquitin-associated HR23 proteins are constituents of neuronal inclusions in specific neurodegenerative disorders without hampering DNA repair,” Neurobiol Dis, vol. 23, no. 3, pp. 708–716, Sep. 2006, doi: 10.1016/J.NBD.2006.06.005.

[474] K. H. Tse and K. Herrup, "DNA damage in the oligodendrocyte lineage and its role in brain aging," Mech Ageing Dev, vol. 161, no. Pt A, pp. 37–50, Jan. 2017, doi: 10.1016/J.MAD.2016.05.006.

[475] R. R. Laposa and J. E. Cleaver, "DNA repair on the brain," Proc Natl Acad Sci U S A, vol. 98, no. 23, pp. 12860–12862, Nov. 2001, doi: 10.1073/PNAS.241519498.

[476] H. L. Wang, S. Lautrup, D. Caponio, J. Zhang, and E. F. Fang, "DNA Damage-Induced Neurodegeneration in Accelerated Ageing and Alzheimer's Disease," Int J Mol Sci, vol. 22, no. 13, Jul. 2021, doi: 10.3390/IJMS22136748.

[477] X. Lin et al., "Contributions of DNA Damage to Alzheimer's Disease," Int J Mol Sci, vol. 21, no. 5, Mar. 2020, doi: 10.3390/IJMS21051666.

[478] F. Rodier et al., "Persistent DNA damage signalling triggers senescence-associated inflammatory cytokine secretion," Nat Cell Biol, vol. 11, no. 8, pp. 973–979, 2009, doi: 10.1038/NCB1909.

[479] G. C.-N. Wong and K. H.-M. Chow, "DNA Damage Response-Associated Cell Cycle Re-Entry and Neuronal Senescence in Brain Aging and Alzheimer's Disease," J Alzheimers Dis, pp. 1–23, Jul. 2022, doi: 10.3233/JAD-220203.

[480] N. H. Myung et al., "Evidence of DNA damage in Alzheimer disease: phosphorylation of histone H2AX in astrocytes," Age (Dordr), vol. 30, no. 4, pp. 209–215, Dec. 2008, doi: 10.1007/S11357-008-9050-7.

[481] R. E. González-Reyes, M. O. Nava-Mesa, K. Vargas-Sánchez, D. Ariza-Salamanca, and L. Mora-Muñoz, "Involvement of Astrocytes in Alzheimer's Disease from a Neuroinflammatory and Oxidative Stress Perspective," Front Mol Neurosci, vol. 10, Dec. 2017, doi: 10.3389/FNMOL.2017.00427.

Appendix

Appendix 1

Tables of the diferentially expressed genes between young, elderly and centenarian individuals in human hippocampus

Table A1. Genes up-regulated in the transcriptome analysis of centenarian vs. old hippocampus samples.

Gene symbol	Gene name	Fold Change	p-value
RASSF4	Ras association (RalGDS/AF-6) domain family member 4	2,57	0,000
MT1M	metallothionein 1M	3,41	0,000
ATP13A4	ATPase type 13A4	2,36	0,000
LRP4	LDL receptor related protein 4	2,44	0,000
LRRC8A	leucine rich repeat containing 8 family, member A	2,28	0,000
SLC25A18	solute carrier family 25, member 18	2,21	0,000
MT1E	metallothionein 1E	4,01	0,000
LRP6	LDL receptor related protein 6	2,02	0,000
CHD9	chromodomain helicase DNA binding protein 9	2,46	0,000
HEPACAM	hepatic and glial cell adhesion molecule	2,92	0,000
LGI4	leucine-rich repeat LGI family, member 4	2,72	0,000
MT1X	metallothionein 1X	4,22	0,000
ARHGAP31	Rho GTPase activating protein 31	2,74	0,000
MT1F	metallothionein 1F	3,1	0,001
FXYD1	FXYD domain containing ion transport regulator 1	5,83	0,001
PDGFRB	platelet-derived growth factor receptor, beta polypeptide	2,58	0,001
OPTN	optineurin	2,48	0,001
METTL7A	methyltransferase like 7A	4,71	0,001
MT1A	metallothionein 1A	2,58	0,001
TFCP2	transcription factor CP2	2,04	0,001
TPCN1	two pore segment channel 1	2,6	0,001
RAPGEF3	Rap guanine nucleotide exchange factor 3	2,27	0,001
ADCY2	adenylate cyclase 2	2,93	0,002
GPR75	G protein-coupled receptor 75	2,62	0,002
CTDSP1	CTD small phosphatase 1	3,08	0,002
GPR37L1	G protein-coupled receptor 37 like 1	2,52	0,002
SLC2A5	solute carrier family 2, member 5	2,65	0,002
SLC39A12	solute carrier family 39, member 12	2,65	0,002
ADGRG1	adhesion G protein-coupled receptor G1	3,61	0,002
CNTFR	ciliary neurotrophic factor receptor	3,18	0,002
HTRA1	HtrA serine peptidase 1	3,45	0,002
P3H2	prolyl 3-hydroxylase 2	4,13	0,002
ROCK1	Rho-associated, coiled-coil containing protein kinase 1	2,03	0,002
PHYHD1	phytanoyl-CoA dioxygenase domain containing 1	2,02	0,002
TNS2	tensin 2	2,01	0,002
MED12	mediator complex subunit 12	2,84	0,003

Table A1 (continued). Genes up-regulated in the transcriptome analysis of centenarian vs. old hippocampus samples.

Gene symbol	Gene name	Fold Change	p-value
ALMS1	Alstrom syndrome protein 1	2,21	0,003
USP1	ubiquitin specific peptidase 1	2,17	0,003
DCHS2	dachsous cadherin-related 2	2,06	0,003
CABLES1	Cdk5 and Abl enzyme substrate 1	2,89	0,003
CLASP2	cytoplasmic linker associated protein 2	2,4	0,003
OPHN1	oligophrenin 1	2,05	0,004
SNTA1	syntrophin, alpha 1	2,11	0,004
ACACB	acetyl-CoA carboxylase beta	2,81	0,004
MERTK	MER proto-oncogene, tyrosine kinase	2,71	0,004
MT1G	metallothionein 1G	2,00	0,004
TP53BP2	tumor protein p53 binding protein 2	3,26	0,005
MAPRE1	microtubule-associated protein, RP/EB family, member 1	2,17	0,005
NPL	N-acetylneuraminate pyruvate lyase	3,22	0,005
TMEM176A	transmembrane protein 176A	2,14	0,005
TCF7L2	transcription factor 7-like 2 (T-cell specific, HMG-box)	2,52	0,006
IGFBP7	insulin like growth factor binding protein 7	3,46	0,006
PADI2	peptidyl arginine deiminase, type II	2,78	0,006
HOMEZ	homeobox and leucine zipper encoding	2,15	0,006
SLC14A1	solute carrier family 14, member 1	5,00	0,006
PAPLN	papilin, proteoglycan-like sulfated glycoprotein	3,49	0,006
PMS1	PMS1 homolog 1, mismatch repair system component	2,07	0,006
ADIRF	adipogenesis regulatory factor	2,71	0,006
PSD2	pleckstrin and Sec7 domain containing 2	2,02	0,006
GLUL	glutamate-ammonia ligase	2,16	0,007
MGLL	monoglyceride lipase	2,71	0,007
PRDX6	peroxiredoxin 6	2,32	0,007
TYRO3	TYRO3 protein tyrosine kinase	2,28	0,007
KCNN3	potassium channel, subfamily N alpha, member 3	3,27	0,007
STON2	stonin 2	2,51	0,007
PLXNB3	plexin B3	2,33	0,008
MT1L	metallothionein 1L	2,36	0,008
PNRC1	proline-rich nuclear receptor coactivator 1	2,38	0,008
CYP4V2	cytochrome P450, family 4, subfamily V, polypeptide 2	2,2	0,009
GJA1	gap junction protein alpha 1	3,34	0,009
EFHD1	EF-hand domain family member D1	2,11	0,009
MT1B	metallothionein 1B	2,22	0,011
CPM	carboxypeptidase M	2,13	0,011
SORL1	sortilin related receptor 1	2,35	0,011
FAT1	FAT atypical cadherin 1	2,46	0,011
STOM	stomatin	2,06	0,011
LIMCH1	LIM and calponin homology domains 1	2,03	0,011
SEC14L1	SEC14-like lipid binding 1	2,69	0,011
WASF2	WAS protein family, member 2	2,29	0,011
SEPN1	selenoprotein N, 1	2,13	0,012
CAPN2	calpain 2, (m/II) large subunit	2,14	0,012

Table A1 (continued). Genes up-regulated in the transcriptome analysis of centenarian vs. old hippocampus samples.

Gene symbol	Gene name	Fold Change	p-value
ARHGEF4	Rho guanine nucleotide exchange factor 4	2,19	0,012
PFKFB3	6-phosphofructo-2-kinase/fructose-2,6-biphosphatase 3	3,06	0,012
RGCC	regulator of cell cycle	2,3	0,012
ZNRF3	zinc and ring finger 3	2,27	0,013
TMEM259	transmembrane protein 259	2,5	0,013
WIF1	WNT inhibitory factor 1	2,64	0,013
TPD52L1	tumor protein D52-like 1	2,64	0,013
FERMT2	fermitin family member 2	2,54	0,013
AMOT	angiomotin	2,48	0,013
PREX1	phosphatidylinositol-3,4,5-trisphosphate Rac exchange factor 1	2,29	0,013
HSDL2	hydroxysteroid dehydrogenase like 2	2,49	0,014
CHST11	carbohydrate sulfotransferase 11	2,22	0,014
HEPN1	hepatocellular carcinoma, down-regulated 1	2,74	0,014
PTCH1	patched 1	2,37	0,014
MDM4	MDM4, p53 regulator	2,14	0,015
KLF10	Kruppel-like factor 10	2,12	0,015
PAX6	paired box 6	3,02	0,015
LOC101929372	uncharacterized LOC101929372	2,69	0,015
CHPT1	choline phosphotransferase 1	2,85	0,016
AHCYL1	adenosylhomocysteinase like 1	2,44	0,016
PPP1R1B	protein phosphatase 1, regulatory subunit 1B	3,01	0,017
SHANK1	SH3 and multiple ankyrin repeat domains 1	2,17	0,017
TRPS1	trichorhinophalangeal syndrome I	2,22	0,017
ALG6	ALG6, alpha-1,3-glucosyltransferase	2,63	0,017
TAF15	TATA-box binding protein associated factor 15	2,36	0,018
GPRC5B	G protein-coupled receptor, class C, group 5, member B	2,78	0,018
GRAMD3	GRAM domain containing 3	2,47	0,018
ENG	endoglin	2,46	0,018
NEK11	NIMA-related kinase 11	2,00	0,019
CTSH	cathepsin H	2,94	0,019
GSTM5	glutathione S-transferase mu 5	2,83	0,021
DOCK7	dedicator of cytokinesis 7	2,1	0,021
PROX1	prospero homeobox 1	2,99	0,021
TBX3	T-box 3	2,84	0,021
PITPNC1	phosphatidylinositol transfer protein, cytoplasmic 1	2,3	0,021
GOLIM4	golgi integral membrane protein 4	2,58	0,021
SLC16A1	solute carrier family 16, member 1	2,51	0,021
XPNPEP3	X-prolyl aminopeptidase 3, mitochondrial	2,06	0,022
KCNJ10	potassium channel, inwardly rectifying subfamily J, member 10	2,69	0,022
GYS1	glycogen synthase 1	2,05	0,022
ATP1B2	ATPase, Na+/K+ transporting, beta 2 polypeptide	3,15	0,022
ETNPPL	ethanolamine-phosphate phospho-lyase	2,33	0,023
HBA1	hemoglobin, alpha 1	3,98	0,023
ARHGAP24	Rho GTPase activating protein 24	2,04	0,023
PDK4	pyruvate dehydrogenase kinase, isozyme 4	3,8	0,023

Table A1 (continued). Genes up-regulated in the transcriptome analysis of centenarian vs. old hippocampus samples.

Gene symbol	Gene name	Fold Change	p-value
FAM198B	family with sequence similarity 198, member B	2,86	0,023
STAT3	signal transducer and activator of transcription 3	2,07	0,023
MRAS	muscle RAS oncogene homolog	2,02	0,024
EZR	ezrin	3,00	0,024
ZNF462	zinc finger protein 462	2,02	0,024
RFTN2	raftlin family member 2	2,27	0,025
PECAM1	platelet/endothelial cell adhesion molecule 1	2,22	0,025
GNA12	guanine nucleotide binding protein alpha 12	2,1	0,025
CLDN5	claudin 5	3,17	0,026
ING3	inhibitor of growth family member 3	2,29	0,026
TXNIP	thioredoxin interacting protein	2,46	0,026
HRSP12	heat-responsive protein 12	2,42	0,027
NPAS3	neuronal PAS domain protein 3	2,00	0,027
GIMAP7	GTPase, IMAP family member 7	2,06	0,028
TNKS	tankyrase, TRF1-interacting ankyrin-related ADP-ribose polymerase	2,18	0,028
PARP4	poly(ADP-ribose) polymerase family member 4	2,02	0,031
HBA2	hemoglobin, alpha 2	2,52	0,031
KCNJ16	potassium channel, inwardly rectifying subfamily J, member 16	2,03	0,032
NFKBIA	nuclear factor of kappa light polypeptide gene enhancer in B-cells inhibitor, alpha	3,08	0,033
FAXDC2	fatty acid hydroxylase domain containing 2	2,88	0,033
BMP2K	BMP2 inducible kinase	2,13	0,033
RANBP3L	RAN binding protein 3-like	4,23	0,034
BAMBI	BMP and activin membrane-bound inhibitor	2,33	0,034
S100A1	S100 calcium binding protein A1	2,26	0,034
EPS15	epidermal growth factor receptor pathway substrate 15	2,61	0,035
GRAMD1C	GRAM domain containing 1C	2,12	0,035
POLR2G	polymerase II polypeptide G	2,06	0,035
AAMDC	adipogenesis associated, Mth938 domain containing	2,45	0,036
MLXIP	MLX interacting protein	2,35	0,036
ARRDC3	arrestin domain containing 3	2,25	0,036
MTSS1L	metastasis suppressor 1-like	2,05	0,036
RPS6KA2	ribosomal protein S6 kinase, 90kDa, polypeptide 2	2,11	0,036
MECOM	MDS1 and EVI1 complex locus	2,01	0,037
EPAS1	endothelial PAS domain protein 1	3,33	0,037
CCNB1IP1	cyclin B1 interacting protein 1	2,7	0,038
ATP11C	ATPase, class VI, type 11C	2,45	0,038
NT5DC2	5-nucleotidase domain containing 2	2,44	0,038
EPHX1	epoxide hydrolase 1, microsomal	2,51	0,039
AGT	angiotensinogen	2,29	0,041
MT3	metallothionein 3	5,69	0,041
WFS1	Wolfram syndrome 1 (wolframin)	2,06	0,041
ITGB4	integrin beta 4	2,29	0,041
PCDHG	protocadherin gamma	2,28	0,041
FAM177B	family with sequence similarity 177, member B	2,43	0,041

Table A1 (continued). Genes up-regulated in the transcriptome analysis of centenarian vs. old hippocampus samples.

Gene symbol	Gene name	Fold Change	p-value
NOTCH2NL	notch 2 N-terminal like	3,6	0,041
SDC4	syndecan 4	2,31	0,041
NUDT6	nudix hydrolase 6	2,64	0,042
PLPP3	phospholipid phosphatase 3	3,26	0,043
PODXL	podocalyxin-like	2,02	0,043
ZFP36L1	ZFP36 ring finger protein-like 1	3,5	0,044
CD58	CD58 molecule	2,71	0,044
SFMBT2	Scm-like with four mbt domains 2	2,24	0,045
CST3	cystatin C	2,15	0,045
PLEKHG1	pleckstrin homology domain containing, family G member 1	2,16	0,045
PYGL	glycogen phosphorylase L	2,22	0,045
SLC16A1	solute carrier family 16, member 1	2,06	0,046
RUBCN	RUN and cysteine-rich domain containing, Beclin 1-interacting protein	2,65	0,046
LHX2	LIM homeobox 2	2,42	0,047
RBBP8	retinoblastoma binding protein 8	2,05	0,047
SAFB2	scaffold attachment factor B2	2,08	0,047
BID	BH3 interacting domain death agonist	2,1	0,047
SLC2A1	solute carrier family 2, member 1	4,03	0,047
LHFP	lipoma HMGIC fusion partner	2,25	0,048
GMNN	geminin DNA replication inhibitor	2,05	0,049

Table A2. Genes down-regulated in the transcriptome analysis of centenarian vs. old hippocampus samples.

Gene symbol	Gene name	Fold Change	p-value
POGZ	pogo transposable element derived with ZNF domain	-2,58	0,001
CCBE1	collagen and calcium binding EGF domains 1	-2,31	0,001
TDO2	tryptophan 2,3-dioxygenase	-2,06	0,001
PSMD13	proteasome 26S subunit, non-ATPase 13	-2,8	0,002
SPINK1	serine peptidase inhibitor, Kazal type 1	-2,04	0,002
PDS5B	PDS5 cohesin associated factor B	-2,11	0,003
SLC38A6	solute carrier family 38, member 6	-3,39	0,003
TRMT6	tRNA methyltransferase 6	-2,16	0,003
CD274	CD274 molecule	-2,79	0,004
TRPC5	transient receptor potential cation channel, subfamily C, member 5	-2,27	0,005
AREG	amphiregulin	-2,43	0,005
CHN2	chimerin 2	-2,02	0,005
ABCD2	ATP binding cassette subfamily D, member 2	-2,52	0,005
ARPP21	cAMP regulated phosphoprotein 21	-2,22	0,006
C3orf49	chromosome 3 open reading frame 49	-2,47	0,006
PANK1	pantothenate kinase 1	-2,04	0,007
SHCBP1	SHC SH2-domain binding protein 1	-2,42	0,008

Table A2 (continued). Genes down-regulated in the transcriptome analysis of centenarian vs. old hippocampus samples.

Gene symbol	Gene name	Fold Change	p-value
PRG1	p53-responsive gene 1	-2,08	0,009
CLLU1OS	chronic lymphocytic leukemia up-regulated 1 opposite strand	-2,05	0,009
HCP5	HLA complex P5	-2,03	0,011
UTS2	urotensin 2	-2,01	0,011
TRPV2	transient receptor potential cation channel, subfamily V, member 2	-2,08	0,011
ADAT2	adenosine deaminase, tRNA-specific 2	-2,08	0,011
DEFB106A	defensin, beta 106A	-2,1	0,011
GBP3	guanylate Binding Protein 3	-2,29	0,011
PLCZ1	phospholipase C, zeta 1	-2,12	0,011
MAP1B	microtubule associated protein 1B	-2,14	0,012
OR4D1	olfactory receptor, family 4, subfamily D, member 1	-2,13	0,013
ZNF442	zinc finger protein 442	-2,09	0,013
PKP4	plakophilin 4	-2,02	0,017
PTPN20	protein tyrosine phosphatase, non-receptor type 20	-2,15	0,017
CLUL1	clusterin-like 1	-2,64	0,017
F11	coagulation factor XI	-2,24	0,017
PCDH11X	protocadherin 11 X-linked	-2,11	0,017
RPIA	ribose 5-phosphate isomerase A	-2,00	0,018
SLC12A5	solute carrier family 12, member 5	-2,12	0,018
KLHL11	kelch-like family member 11	-2,06	0,018
TBPL1	TBP-like 1	-2,69	0,019
CHI3L2	chitinase 3-like 2	-3,35	0,020
FAM19A1	family with sequence similarity 19, member A1	-2,17	0,021
POLR2M	RNA polymerase II subunit M	-2,12	0,021
OR4C11	olfactory receptor, family 4, subfamily C, member 11	-2,35	0,022
PROS1	protein S	-2,24	0,023
OR51G1	olfactory receptor, family 51, subfamily G, member 1	-2,36	0,024
DEFB126	defensin, beta 126	-2,01	0,024
TRPC7	transient receptor potential cation channel, subfamily C, member 7	-2,04	0,024
HELB	helicase (DNA) B	-2,04	0,027
PFDN4	prefoldin subunit 4	-2,38	0,029
RNF17	ring finger protein 17	-2,45	0,031
EDDM3A	epididymal protein 3A	-2,22	0,031
TNNC1	troponin C type 1	-2,14	0,031
PRKG2	protein kinase, cGMP-dependent, type II	-2,03	0,031
TSPAN13	tetraspanin 13	-2,76	0,035
FAM151B	family with sequence similarity 151 member B	-2,83	0,036
LRRC28	leucine rich repeat containing 28	-2,5	0,037
LOC643802	u3 small nucleolar ribonucleoprotein protein MPP10-like	-2,01	0,038
FRG1BP	FSHD region gene 1 family member B	-2,62	0,041
CLC	Charcot-Leyden crystal galectin	-2,02	0,042
TRPC4	transient receptor potential cation channel, subfamily C, member 4	-2,1	0,043
LAMA1	laminin, alpha 1	-2,07	0,043
GPRASP2	G protein-coupled receptor associated sorting protein 2	-2,05	0,043

Table A2 (continued). Genes down-regulated in the transcriptome analysis of centenarian vs. old hippocampus samples.

Gene symbol	Gene name	Fold Change	p-value
ZNF705G	zinc finger protein 705G	-2,45	0,043
SEMA3E	sema domain, immunoglobulin domain, secreted 3E	-2,34	0,044
SULT4A1	sulfotransferase family 4A member 1	-2,1	0,045
PATE2	prostate and testis expressed 2	-2,16	0,046

Table A3. Genes up-regulated in the transcriptome analysis of centenarian vs. young hippocampus samples.

Gene symbol	Gene name	Fold Change	p-value
FASTKD3	FAST kinase domains 3	2,44	5,33E-05
ANKRD18B	ankyrin repeat domain 18B	4,53	0,000
RASGEF1B	RasGEF domain family member 1B	2,77	0,000
CCDC84	coiled-coil domain containing 84	4,07	0,000
LOC101929372	uncharacterized LOC101929372	3,02	0,001
FAM177B	family with sequence similarity 177, member B	3,68	0,001
CXorf57	chromosome X open reading frame 57	2,25	0,002
RASSF4	Ras association domain family member 4	2,17	0,002
PLXNB3	plexin B3	3,68	0,002
GPR37L1	G protein-coupled receptor 37 like 1	2,83	0,003
PADI2	peptidyl arginine deiminase, type II	4,01	0,003
LRRC1	leucine rich repeat containing 1	2,11	0,003
PREX1	phosphatidylinositol-3,4,5-trisphosphate Rac exchange factor 1	3,61	0,004
SLC48A1	solute carrier family 48 (heme transporter), member 1	2,00	0,004
CHI3L1	chitinase 3-like 1	3,11	0,004
CPB2	carboxypeptidase B2	2,25	0,004
ARAP2	ArfGAP with RhoGAP domain, ankyrin repeat and PH domain 2	2,63	0,004
SLC25A18	solute carrier family 25, member 18	2,10	0,005
GPRC5B	G protein-coupled receptor, class C, group 5, member B	3,41	0,005
LRIG1	leucine rich repeats and immunoglobulin like domains 1	2,59	0,005
HEPACAM	hepatic and glial cell adhesion molecule	3,05	0,005
KCNJ16	potassium channel, inwardly rectifying subfamily J, member 16	2,82	0,007
ADGRG1	adhesion G protein-coupled receptor G1	3,65	0,008
TPD52L1	tumor protein D52-like 1	3,90	0,008
SLC35B2	solute carrier family 35, member B2	2,14	0,009
CA1	carbonic anhydrase I	2,36	0,009
SLC2A5	solute carrier family 2, member 5	2,78	0,009
C17orf62	chromosome 17 open reading frame 62	2,70	0,009
MAOB	monoamine oxidase B	2,32	0,011
ADCY2	adenylate cyclase 2	2,62	0,011
GPR75	G protein-coupled receptor 75	2,43	0,011
CHD9	chromodomain helicase DNA binding protein 9	2,30	0,011

Table A3 (continued). Genes up-regulated in the transcriptome analysis of centenarian vs. young hippocampus samples.

Gene symbol	Gene name	Fold Change	p-value
PHYHD1	phytanoyl-CoA dioxygenase domain containing 1	2,15	0,011
FCGR3B	Fc fragment of IgG, low affinity IIIb	3,15	0,011
ZGRF1	zinc finger, GRF-type containing 1	2,33	0,011
RGS12	regulator of G-protein signaling 12	2,54	0,012
CYP2R1	cytochrome P450, family 2, subfamily R, polypeptide 1	2,56	0,012
NPL	N-acetylneuraminate pyruvate lyase	3,87	0,012
RARRES3	retinoic acid receptor responder 3	3,55	0,014
HHATL	hedgehog acyltransferase-like	2,41	0,014
LGI4	leucine-rich repeat LGI family, member 4	3,81	0,014
TRIM9	tripartite motif containing 9	2,35	0,015
HTRA1	HtrA serine peptidase 1	3,37	0,015
AK1	adenylate kinase 1	2,21	0,015
P3H2	prolyl 3-hydroxylase 2	2,79	0,015
SPARCL1	SPARC like 1	2,06	0,015
IGSF11	immunoglobulin superfamily, member 11	2,30	0,016
GRIA4	glutamate receptor, ionotropic, AMPA 4	4,70	0,016
PCBP4	poly(rC) binding protein 4	2,06	0,016
RABGEF1	RAB guanine nucleotide exchange factor 1	2,20	0,017
SORL1	sortilin-related receptor, L(DLR class) A repeats containing	2,48	0,017
GIMAP7	GTPase, IMAP family member 7	2,34	0,017
ATF6B	activating transcription factor 6 beta	2,16	0,018
SERPINB9	serpin peptidase inhibitor, member 9	2,05	0,018
CAPN2	calpain 2	2,23	0,018
KATNIP	katanin interacting protein	2,66	0,019
TFRC	transferrin receptor	2,30	0,021
ITPKB	inositol-trisphosphate 3-kinase B	2,22	0,021
METTL7A	methyltransferase like 7A	4,44	0,021
RRAGC	Ras related GTP binding C	3,01	0,021
KLHL32	kelch-like family member 32	2,13	0,021
ZDHHC11B	zinc finger, DHHC-type containing 11B	4,60	0,021
CP	ceruloplasmin	3,32	0,021
LIFR	leukemia inhibitory factor receptor alpha	2,03	0,021
EFEMP1	EGF containing fibulin-like extracellular matrix protein 1	3,77	0,021
TYRO3	TYRO3 protein tyrosine kinase	2,20	0,021
ZFHX4	zinc finger homeobox 4	2,15	0,021
ART3	ADP-ribosyltransferase 3	2,44	0,022
MT1F	metallothionein 1F	3,21	0,022
NPC1	Niemann-Pick disease, type C1	3,32	0,023
KCNN3	potassium channel, calcium activated intermediate/small conductance subfamily N alpha, member 3	3,25	0,023
KCNJ10	potassium channel, inwardly rectifying subfamily J, member 10	3,25	0,023
C7orf49	chromosome 7 open reading frame 49	2,57	0,024
APLNR	apelin receptor	3,33	0,024
LGI3	leucine-rich repeat LGI family, member 3	2,88	0,024
MTUS1	microtubule associated tumor suppressor 1	2,01	0,025

Table A3 (continued). Genes up-regulated in the transcriptome analysis of centenarian vs. young hippocampus samples.

Gene symbol	Gene name	Fold Change	p-value
TP53BP2	tumor protein p53 binding protein 2	3,18	0,026
IGFBP7	insulin like growth factor binding protein 7	4,00	0,026
PFKFB3	6-phosphofructo-2-kinase/fructose-2,6-biphosphatase 3	3,68	0,028
LRIG1	leucine rich repeats and immunoglobulin like domains 1	2,98	0,028
RPS6KA1	ribosomal protein S6 kinase, polypeptide 1	2,34	0,029
EFHD1	EF-hand domain family member D1	2,53	0,029
MYCT1	myc target 1	2,11	0,031
OPTN	optineurin	2,06	0,031
NDUFAF6	NADH dehydrogenase (ubiquinone) complex I, assembly factor 6	2,15	0,031
ALG6	ALG6, alpha-1,3-glucosyltransferase	2,55	0,031
SLCO2B1	solute carrier organic anion transporter family, member 2B1	3,50	0,031
DPYSL2	dihydropyrimidinase-like 2	2,12	0,031
BMP2K	BMP2 inducible kinase	2,43	0,031
SLC14A1	solute carrier family 14, member 1	2,97	0,032
GJA1	gap junction protein alpha 1	2,90	0,032
STX16-NPEPL1	STX16-NPEPL1 readthrough (NMD candidate)	2,01	0,033
TOB2	transducer of ERBB2, 2	2,09	0,033
MT1E	metallothionein 1E	2,82	0,034
CCDC88A	coiled-coil domain containing 88A	2,00	0,035
LIG4	ligase IV, DNA, ATP-dependent	2,03	0,035
FRYL	FRY like transcription coactivator	2,30	0,037
IL1RL1	interleukin 1 receptor-like 1	5,86	0,037
SCRG1	stimulator of chondrogenesis 1	2,63	0,037
MT1L	metallothionein 1L	2,13	0,038
PROX1	prospero homeobox 1	3,83	0,038
IL13RA1	interleukin 13 receptor, alpha 1	2,23	0,039
BAZ2B	bromodomain adjacent to zinc finger domain 2B	2,22	0,039
BRICD5	BRICHOS domain containing 5	2,19	0,039
CLASP2	cytoplasmic linker associated protein 2	2,20	0,041
GRID2	glutamate receptor, ionotropic, delta 2	2,54	0,041
ARAP2	ArfGAP with RhoGAP domain, ankyrin repeat and PH domain 2	2,07	0,041
STON2	stonin 2	2,56	0,042
ZDHHC9	zinc finger, DHHC-type containing 9	2,50	0,042
SUSD2	sushi domain containing 2	2,04	0,042
CSNK1E	casein kinase 1, epsilon	2,25	0,042
SERPINA3	serpin peptidase inhibitor, clade A, member 3	8,34	0,043
TRPS1	trichorhinophalangeal syndrome I	2,44	0,043
MAL	mal, T-cell differentiation protein	2,79	0,043
PTTG2	pituitary tumor-transforming 2	2,02	0,044
ADIRF	adipogenesis regulatory factor	3,46	0,044
LEAP2	liver expressed antimicrobial peptide 2	2,54	0,044
MT1C	metallothionein 1C	2,82	0,044
WFS1	Wolfram syndrome 1 (wolframin)	2,12	0,044
TMPRSS5	transmembrane protease, serine 5	2,53	0,045

Table A3 (continued). Genes up-regulated in the transcriptome analysis of centenarian vs. young hippocampus samples.

Gene symbol	Gene name	Fold Change	p-value
MT1X	metallothionein 1X	3,76	0,045
ALMS1	Alstrom syndrome protein 1	2,11	0,045
MT1G	metallothionein 1G	2,39	0,046
MT1B	metallothionein 1B	2,62	0,046
STOM	stomatin	2,15	0,047
ZDHHC11	zinc finger, DHHC-type containing 11	2,07	0,047
MAP3K12	mitogen-activated protein kinase kinase kinase 12	2,04	0,047
EFHC2	EF-hand domain (C-terminal) containing 2	2,21	0,047
MS4A7	membrane-spanning 4-domains, subfamily A, member 7	2,19	0,047
RGCC	regulator of cell cycle	2,35	0,048
WIF1	WNT inhibitory factor 1	2,45	0,048
CHST11	carbohydrate sulfotransferase 11	2,29	0,049
PLLP	plasmolipin	2,16	0,049
CD34	CD34 molecule	2,18	0,049
HEY2	hes-related family bHLH transcription factor with YRPW motif 2	2,49	0,049

Table A4. Genes down-regulated in the transcriptome analysis of centenarian vs. young hippocampus samples.

Gene symbol	Gene name	Fold Change	p-value
PANK1	pantothenate kinase 1	-3,60	0,001
ZNF432	zinc finger protein 432	-2,46	0,001
FOXP1	forkhead box P1	-2,84	0,002
TP63	tumor protein p63	-2,08	0,002
F11	coagulation factor XI	-2,82	0,003
PNLDC1	poly(A)-specific ribonuclease (PARN)-like domain containing 1	-2,00	0,004
SPTLC3	serine palmitoyltransferase, long chain base subunit 3	-6,63	0,004
SUFU	SUFU negative regulator of hedgehog signaling	-2,02	0,005
CDON	cell adhesion associated, oncogene regulated	-2,34	0,005
NIPAL2	NIPA-like domain containing 2	-2,48	0,006
SLC38A6	solute carrier family 38, member 6	-2,41	0,006
CCDC36	coiled-coil domain containing 36	-2,16	0,007
SPRY3	sprouty RTK signaling antagonist 3	-2,10	0,009
SPRY3	sprouty RTK signaling antagonist 3	-2,10	0,009
CRY2	cryptochrome circadian regulator 2	-2,27	0,009
NARS	asparaginyl-tRNA synthetase	-2,33	0,009
SWI5	SWI5 homologous recombination repair protein	-2,22	0,009
TMEM246	transmembrane protein 246	-2,75	0,011
LOXHD1	lipoxygenase homology domains 1	-2,08	0,011
OSR1	odd-skipped related transciption factor 1	-2,05	0,011

Table A4 (continued). Genes down-regulated in the transcriptome analysis of centenarian vs. young hippocampus samples.

Gene symbol	Gene name	Fold Change	p-value
SLIT2	slit guidance ligand 2	-2,30	0,011
SERPINF1	serpin peptidase inhibitor, clade F (alpha-2 antiplasmin, pigment epithelium derived factor), member 1	-3,02	0,012
GREB1	growth regulation by estrogen in breast cancer 1	-2,38	0,012
PTGDR	prostaglandin D2 receptor	-2,13	0,013
ERGIC2	ERGIC and golgi 2	-2,11	0,014
GALNT14	polypeptide N-acetylgalactosaminyltransferase 14	-2,41	0,014
EPGN	epithelial mitogen	-2,21	0,015
POGZ	pogo transposable element derived with ZNF domain	-2,15	0,015
TPMT	thiopurine S-methyltransferase	-2,95	0,015
SLC5A5	solute carrier family 5, member 5	-2,00	0,015
CRYZ	crystallin zeta	-2,13	0,0161
CTSK	cathepsin K	-2,42	0,017
MAP2K6	mitogen-activated protein kinase kinase 6	-2,29	0,018
HYOU1	hypoxia up-regulated 1	-2,28	0,021
CHRNA6	cholinergic receptor, nicotinic alpha 6	-2,33	0,021
ARSG	arylsulfatase G	-2,22	0,026
GOLGA6L22	golgin A6 family-like 22	-2,04	0,027
FKBP4	FK506 binding protein 4	-2,53	0,027
NNAT	neuronatin	-3,88	0,028
DIO2	deiodinase, iodothyronine, type II	-2,00	0,028
DNAJA1	DnaJ (Hsp40) homolog, subfamily A, member 1	-2,24	0,028
RNF17	ring finger protein 17	-2,45	0,029
UHRF2	ubiquitin-like with PHD and ring finger domains 2	-2,05	0,031
ZBTB10	zinc finger and BTB domain containing 10	-2,75	0,031
EFEMP2	EGF containing fibulin-like extracellular matrix protein 2	-2,21	0,032
HTT	huntingtin	-2,30	0,033
GPRC5A	G protein-coupled receptor, class C, group 5, member A	-2,13	0,033
LNX2	ligand of numb-protein X 2	-2,14	0,033
SSTR2	somatostatin receptor 2	-3,39	0,033
DFNA5	deafness, autosomal dominant 5	-3,10	0,035
GALK2	galactokinase 2	-2,13	0,036
PDK3	pyruvate dehydrogenase kinase, isozyme 3	-2,52	0,037
SLC22A6	solute carrier family 22 (organic anion transporter), member 6	-2,29	0,037
SLC25A30	solute carrier family 25, member 30	-2,06	0,037
ULK1	unc-51 like autophagy activating kinase 1	-2,26	0,038
LAMA1	laminin, alpha 1	-2,15	0,038
HSPH1	heat shock 105kDa/110kDa protein 1	-2,23	0,039
EXT1	exostosin glycosyltransferase 1	-2,38	0,041
UAP1	UDP-N-acetylglucosamine pyrophosphorylase 1	-2,18	0,041
CD83	CD83 molecule	-2,02	0,043
TSPAN18	tetraspanin 18	-9,20	0,043
ANGPT4	angiopoietin 4	-2,01	0,045
PPM1G	protein phosphatase, Mg2+/Mn2+ dependent, 1G	-2,23	0,046
C9orf72	chromosome 9 open reading frame 72	-2,25	0,046

Table A4 (continued). Genes down-regulated in the transcriptome analysis of centenarian vs. young hippocampus samples.

Gene symbol	Gene name	Fold Change	p-value
GOLGA6L6	golgin A6 family-like 6	-2,06	0,046
PTGR1	prostaglandin reductase 1	-2,38	0,046
LAMB1	laminin, beta 1	-2,19	0,047
FAM134A	family with sequence similarity 134, member A	-2,90	0,047
TBPL1	TBP-like 1	-3,95	0,048
MPP6	membrane protein, palmitoylated 6	-3,95	0,048
NREP	neuronal regeneration related protein	-2,65	0,048
GCKR	glucokinase regulator	-2,10	0,049
KLF5	Kruppel-like factor 5	-2,41	0,049
ZFPM2	zinc finger protein, FOG family member 2	-3,36	0,049

Table A5. Genes up-regulated in the transcriptome analysis of old vs. young human hippocampus samples.

Gene symbol	Gene name	Fold Change	p-value
ANKRD18B	ankyrin repeat domain 18B	2,45	0,001
ANKRD19P	ankyrin repeat domain 19, pseudogene	2,20	0,001
CHI3L1	chitinase 3-like 1 (cartilage glycoprotein-39)	2,27	0,002
TMEM167A	Transmembrane Protein 167A	2,45	0,002
GPR63	G protein-coupled receptor 63	2,20	0,004
SERPINA3	serpin peptidase inhibitor, clade A member 3	7,25	0,006
ANKRD30B	ankyrin repeat domain 30B	3,34	0,007
MRAP2	melanocortin 2 receptor accessory protein 2	4,32	0,009
CERCAM	cerebral endothelial cell adhesion molecule	3,73	0,009
FAR2P1	fatty acyl-CoA reductase 2 pseudogene 1	2,33	0,010
CHI3L2	chitinase 3-like 2	3,80	0,010
COL24A1	collagen, type XXIV, alpha 1	3,01	0,014
HSD11B1	hydroxysteroid (11-beta) dehydrogenase 1	2,31	0,016
MS4A6A	membrane-spanning 4-domains, subfamily A, member 6A	2,71	0,016
ZNF419	zinc finger protein 419	2,19	0,021
PLEKHH1	pleckstrin homology domain containing, family H member 1	4,17	0,024
KCNAB1	potassium Voltage-Gated Channel Subfamily A Regulatory Beta Subunit 1	2,01	0,024
DLGAP1	DLG Associated Protein 1	2,28	0,025
CCDC84	coiled-coil domain containing 84	2,06	0,026
ARPP21	CAMP Regulated Phosphoprotein 21	2,21	0,026
CAPN3	calpain 3	3,68	0,032
GRIA4	glutamate receptor, ionotropic, AMPA 4	2,40	0,032
FAM45A	non-classical DENN domain protein	2,95	0,033
CES4A	carboxylesterase 4A	2,49	0,034
PDE1C	phosphodiesterase 1C, calmodulin-dependent 70kDa	2,67	0,042
BEST1	bestrophin 1	2,32	0,044
MOG	myelin oligodendrocyte glycoprotein	3,12	0,047
LGI3	leucine-rich repeat LGI family, member 3	2,04	0,049

Table A6. Genes down-regulated in the transcriptome analysis of old vs. young human hippocampus samples.

Gene symbol	Gene name	Fold Change	p-value
GRK4	G protein-coupled receptor kinase 4	-2,11	0,000
EYA1	EYA transcriptional coactivator and phosphatase 1	-2,76	0,000
RAD21	RAD21 cohesin complex component	-2,12	0,001
SWI5	SWI5 homologous recombination repair protein	-2,02	0,002
FYCO1	FYVE and coiled-coil domain containing 1	-2,07	0,003
OSR1	odd-skipped related transciption factor 1	-2,17	0,003
SLC26A2	solute carrier family 26 (anion exchanger), member 2	-2,02	0,004
APCDD1	adenomatosis polyposis coli down-regulated 1	-2,10	0,004
FBXO32	F-box protein 32	-2,02	0,005
RAP1B	RAP1B, member of RAS oncogene family	-2,87	0,006
MPP6	membrane protein, palmitoylated 6	-3,36	0,007
DCHS1	dachsous cadherin-related 1	-2,07	0,007
CHRNA6	cholinergic receptor, nicotinic alpha 6	-2,06	0,008
SPTLC3	serine palmitoyltransferase, long chain base subunit 3	-2,35	0,009
TSPAN18	tetraspanin 18	-8,82	0,009
CDON	cell adhesion associated, oncogene regulated	-2,05	0,009
GPCPD1	glycerophosphocholine phosphodiesterase 1	-2,05	0,009
HIST1H2BD	histone cluster 1, H2bd	-2,14	0,011
SSTR2	somatostatin receptor 2	-2,56	0,012
GJB6	gap junction protein beta 6	-2,37	0,012
THSD4	thrombospondin type 1 domain containing 4	-2,03	0,012
IFT81	intraflagellar transport 81	-2,12	0,013
PPP1R1B	protein phosphatase 1, regulatory (inhibitor) subunit 1B	-2,99	0,015
SPINT2	serine peptidase inhibitor, Kunitz type, 2	-2,10	0,016
KLF5	Kruppel-like factor 5 (intestinal)	-2,12	0,019
LPAR3	lysophosphatidic acid receptor 3	-2,32	0,019
CREM	cAMP responsive element modulator	-2,74	0,020
SLC47A1	solute carrier family 47 (multidrug and toxin extrusion), member 1	-5,49	0,020
BZW1	basic leucine zipper and W2 domains 1	-2,10	0,021
ZBTB10	zinc finger and BTB domain containing 10	-2,02	0,024
KCNJ13	potassium channel, inwardly rectifying subfamily J, member 13	-2,22	0,026
SERPINF1	serpin peptidase inhibitor, clade F, member 1	-2,12	0,027
FUNDC2	FUN14 domain containing 2	-2,17	0,027
MTIF2	mitochondrial translational initiation factor 2	-2,16	0,028
SLC22A8	solute carrier family 22 (organic anion transporter), member 8	-3,12	0,030
ZIC1	Zic family member 1	-2,80	0,031
EFEMP2	EGF containing fibulin-like extracellular matrix protein 2	-2,29	0,032
MDGA2	MAM domain containing glycosylphosphatidylinositol anchor 2	-2,05	0,036
POMGNT2	protein O-linked mannose N-acetylglucosaminyltransferase 2	-2,23	0,039
AKR1C1	aldo-keto reductase family 1, member C1	-2,33	0,039
HLF	hepatic leukemia factor	-2,12	0,039
EPHX1	epoxide hydrolase 1, microsomal (xenobiotic)	-2,80	0,039
NNAT	neuronatin	-3,33	0,042
NIPAL2	NIPA-like domain containing 2	-2,38	0,047
DGCR6	Homo sapiens DiGeorge syndrome critical region gene 6	-2,15	0,048

Publications

1. Auzmendi-Iriarte J, Moreno-Cugnon L, **Saenz-Antoñanzas A**, Grassi D, de Pancorbo MM, Arevalo MA, Wood IC, Matheu A (2022). High levels of HDAC expression correlate with microglial aging. *Expert Opin Ther Targets*. 2022 Dec 15;1-12. doi: 10.1080/14728222.2022.2158081.

2. García-Puga M*, **Saenz-Antoñanzas A***, Gerenu G, Arrieta A, Fernandez-Torron R, Zulaica M, Saenz A, Elizazu J, Nogales-Gadea G, Araúzo-Bravo MJ, Lopez de Munain A, Matheu A (2022). Senescence plays a role in Myotonic Dystrophy type 1. *JCI Insight*. 2022 Aug 30:e159357. doi: 10.1172/jci.insight.159357. *authors contributed equally to this work and should be considered as co-first authors.

3. Aldaz P, Martín-Martín N, **Saenz-Antoñanzas A**, Carrasco-Garcia E, Álvarez-Satta M, Elúa-Pinín A, MPollard S, HLawrie C, Moreno-Valladares M, Samprón N, Hench J, Lovell-Badge R, Carracedo A, Matheu A (2022). High SOX9 Maintains Glioma Stem Cell Activity through a Regulatory Loop Involving STAT3 and PML. *Int J Mol Sci.* 2022 Apr 19;23(9):4511. doi: 10.3390/ijms23094511.

4. García-Puga M, **Saenz-Antoñanzas A**, Matheu A, López de Munain A (2022). Targeting Myotonic Dystrophy Type 1 with Metformin. *Int J Mol Sci.* 2022 Mar 7;23(5):2901. doi: 10.3390/ijms23052901. (Review).

5. Auzmendi-Iriarte J, Otaegi-Ugartemendia M, Carrasco-Garcia E, Azkargorta M, Diaz A, **Saenz-Antoñanzas A**, Andermatten JA, García-Puga M, Garcia I, Elua-Pinin A, Ruiz I, Samprón N, Elortza F, Cuervo AM , Matheu A (2022). Chaperone-mediated autophagy controls proteomic and transcriptomic pathways to maintain glioma stem cell activity. *Cancer Res.* 2022 Feb 7;canres.2161.2021. doi: 10.1158/0008-5472.CAN-21-2161.

6. Marcos-Pérez D, **Saenz-Antoñanzas A**, Matheu A (2021). Centenarians as models of healthy aging: Example of REST. *Ageing Res Rev.* 2021 Jun 14:101392. doi: 10.1016/j.arr.2021.101392.

7. **Saenz-Antoñanzas A**, Moncho-Amor V, Auzmendi-Iriarte J, Elua-Pinin A, Rizzoti K, Lovell-Badge R, Matheu A (2021). CRISPR/Cas9 deletion of SOX2 Regulatory Region 2 (SRR2)

decreases SOX2 malignant activity in glioblastoma. *Cancers*. 2021 Mar 29;13(7):1574. doi: 10.3390/cancers13071574.

8. Moreno-Valladares M, Silva TM, Garcés JP, **Saenz-Antoñanzas A**, Moreno-Cugnon L, Álvarez-Satta M, Matheu A (2020). CD8+ T cells are present at low levels in the white matter with physiological and pathological aging. *Aging*. 2020 Oct 13;12(19):18928-18941. doi: 10.18632/aging.104043.

9. Moreno-Valladares M, Moreno-Cugnon L, Silva TM, Garcés JP, **Saenz-Antoñanzas A**, Álvarez-Satta M, Matheu A (2020). $CD8^+$ T cells are increased in the subventricular zone with physiological and pathological aging. *Aging cell*. 2020 Aug 1;e13198. doi: 10.1111/acel.13198.

10. Auzmendi-Iriarte J, **Saenz-Antoñanzas A**, Mikelez-Alonso I, Carrasco-Garcia E, Tellaetxe-Abete M, Lawrie CH, Nicolás Sampron N, Cortajarena AL, Matheu A (2020). Characterization of a new small-molecule inhibitor of HDAC6 in glioblastoma. *Cell Death and Disease*. 2020 Jun 2:11(6):417. doi: 10.1038/s41419-020-2586-x.

11. Álvarez-Satta M, Berna-Erro A, Carrasco-Garcia E, Alberro A, **Saenz-Antoñanzas A**, Vergara V, Otaegui D, Matheu A (2020). Relevance of Oxidative Stress and Inflammation in Frailty Based on Human Studies and Mouse Models. *Aging*. 2020 May 27;12. doi: 10.18632/aging.103295. (Review).

12. García-Puga M, **Saenz-Antoñanzas A**, Fernández-Torrón R, Munain AL, Matheu A (2019). Myotonic Dystrophy type 1 cells display impaired metabolism and mitochondrial dysfunction that are reversed by metformin. *Aging*. 2020 Apr 8;12(7):6260-6275. doi: 10.18632/aging.103022.

13. Aldaz P*, Otaegi-Ugartemendia M*, **Saenz-Antoñanzas A**, Garcia-Puga M, Moreno-Valladares M, Flores JM, Gerovska D, Arauzo-Bravo MJ, Samprón N, Matheu A, Carrasco-Garcia E (2020). SOX9 promotes tumor progression through the axis BMI1-p21CIP. *Scientific Reports*. 2020 Jan 15;10(1):357. doi: 10.1038/s41598-019-57047-w. *authors contributed equally to this work and should be considered as co-first authors.

14. **Saenz-Antoñanzas A**, Auzmendi-Iriarte J, Carrasco-Garcia E, Moreno-Cugnon L, Ruiz I, Villanua J, Egaña L, Otaegui D, Samprón N, Matheu A (2019). Liquid Biopsy in Glioblastoma: Opportunities, Applications and Challenges. *Cancers*. 2019 Jul 5;11(7). doi:10.3390/cancers11070950. (Review).

15. Torres-Bayona S, Aldaz P, Auzmendi-Iriarte J, **Saenz-Antoñanzas A**, Garcia I, Arrazola M, Gerovska D, Undabeitia J, Querejeta A, Egaña L, Villanúa J, Ruiz I, Sarasqueta C, Urculo E, Araúzo-Bravo MJ, Huarte M, Samprón N, Matheu A (2018). PR-LncRNA signature regulates glioma cell activity through expression of SOX factors. *Scientific Reports*. 2018 Aug 24;8(1):12746. doi: 10.1038/s41598-018-30836-5

16. De la Rosa J*, **Saenz-Antoñanzas A***, Shahi MH, Meléndez B, Rey JA, Castresana JS (2016). Lamininadherent versus suspension-non-adherent cell culture conditions for the isolation of cancer stem cells in the DAOY medulloblastoma cell line. *Tumor Biology*. 2016 Sep;37(9):12359-12370. doi: 10.1007/s13277-016-5119-6 *authors contributed equally to this work and should be considered as co-first authors